**Universidade de Lisboa**

**Faculdade de Medicina de Lisboa**

# Molecular features of glycine-mediated neurotransmission in rat brain

**Rita Isabel Pedro Aroeira**

**Doutoramento em Ciências Biomédicas**

**Especialidade em Neurociências**

**2014**

# Universidade de Lisboa

## Faculdade de Medicina de Lisboa



# Molecular features of glycine-mediated neurotransmission in rat brain


**Rita Isabel Pedro Aroeira**

Tese orientada pela Doutora Cláudia Valente e
Professora Doutora Ana Maria Sebastião


**Doutoramento em Ciências Biomédicas**
**Especialidade em Neurociências**

**A impressão desta dissertação foi aprovada pelo Conselho Científico da Faculdade de Medicina de Lisboa em reunião de 28 de Outubro de 2014.**

The experimental work herein described was performed at Instituto de Medicina Molecular – Faculdade de Medicina da Universidade de Lisboa, under the supervision of Dr. Cláudia Valente and Prof. Ana Maria Sebastião.

## Publications:

The scientific content of the present thesis has been included in the publication of the following original articles:

**Aroeira R.I.**, Ribeiro J.A., Sebastião A.M. and Valente C.A. (2011) "Age-related changes of glycine receptor at the rat hippocampus: from the embryo to the adult". J. Neurochem. 118, 339-353.

**Aroeira R.I.**, Sebastião A.M. and Valente C.A. (2014) "GlyT1 and GlyT2 in brain astrocytes: expression, distribution and function". Brain Struct. Funct. 219(3):817-30.

**Aroeira R.I.**, Sebastião A.M. and Valente C.A. (2014) "BDNF, via truncated TrkB receptor, modulates GlyT1 and GlyT2 in astrocytes". Submitted – under review

**Aroeira R.I.**, Sebastião A.M. and Valente C.A. (2014) "BDNF modulates glycine uptake in brain nerve terminals by decreasing GlyT2 membrane insertion". Submitted – under review

## Table of contents:

# Figure Index:

# Table Index:

## Acknowledgements:

Em primeiro lugar gostaria de agradecer aos meus orientadores, Doutora Cláudia Valente de Castro e Professora Doutora Ana Sebastião. À Doutora Cláudia Valente por todos os ensinamentos, paciência, conselhos e amizade. À Professora Doutora Ana Sebastião pela sua disponibilidade e por todos os ensinamentos e esclarecimentos. Gostaria também de expressar os meus agradecimentos ao Professor Doutor Joaquim Alexandre Ribeiro por me ter recebido no seu laboratório ainda como estudante de mestrado.

Queria também agradecer a todos os colegas de laboratório que ao longo destes anos contribuíram para o bom ambiente que se vive no laboratório e com quem partilhei experiências, discussões científicas, bons e maus momentos. Gostaria ainda de expressar os meus agradecimentos à Alexandra, à Cristina e à Elvira por toda a ajuda, disponibilidade e amizade e ao Sr. João por toda a assistência na manipulação dos animais.
Uma palavra de agradecimento também ao Diogo, à Vânia e ao André com quem percorri este percurso e com quem, muitas vezes, partilhei as mesmas dúvidas.

Gostaria ainda de deixar uma mensagem de agradecimento à Sandra e à Sara que mais do que colegas se tornaram amigas, conselheiras e confidentes.

E porque a vida profissional se cruzou com a vida pessoal, muito obrigada André, pela paciência, incentivos, apoio e boa disposição.
Um agradecimento também muito especial à minha família, especialmente à minha mãe, por todo o apoio incondicional, conselhos e compreensão.

Gostaria também de agradecer a todos os colegas do Instituto de Medicina Molecular, em especial a todos os membros da Comissão de Estudantes de Doutoramento por terem contribuído para um ambiente extremamente agradável em todas as actividades desenvolvidas e por me terem proporcionado momentos inesquecíveis.

Um obrigado muito especial à Unidade de Bioimagem do Instituto de Medicina Molecular por toda a formação e esclarecimentos aquando do uso dos microscópios, em particular ao Dr. José Rino (Lisboa) pela ajuda na quantificação das imagens obtidas. Agradeço também

à Dra. Sandra Vaz (Lisboa) por toda a ajuda na optimização das experiências com os transportadores de glicina.
Agradeço também ao Dr. Bruno Gasnier (Paris), ao Dr. Manuel Miranda-Arango (Texas) e ao Dr. Louis Reichardt (Califórnia) que gentilmente doaram os anticorpos que reconhecem o VIAAT, o GlyT1/GlyT2 e o p75 NTR, respectivamente, ao Dr. Tiago Outeiro (Lisboa) que amavelmente cedeu a sequência de *primers* utilizados para a amplificação da β-actina, ao Dr. Eero Castrén (Helsínquia) que disponibilizou os *primers* para o TrkB-FL e o TrkB-T1 e à *Regeneron Pharmaceuticals* por ter cedido o BDNF.

Por fim, gostaria de agradecer às instituições envolvidas neste trabalho, ao Instituto de Medicina Molecular por me ter acolhido e à Fundação para a Ciência e a Tecnologia (FCT) por me ter financiado a Bolsa de Doutoramento (SFRH/BD/62831/2009).

## Abbreviation list:

**AC -** associational commissural pathway

**aCSF** - artificial cerebrospinal fluid

**Akt -** protein kinase B

**AMPA -** α-amino-3-hydroxy-5-methyl-4-isoxazolepropionic acid

**ANOVA** - analysis of variance

**APS -** ammonium persulfate

**ATP -** adenosine-5'-triphosphate

**BDNF -** brain-derived neurotrophic factor

**BSA -** bovine serum albumin

**CaM -** calmodulin

**CaMK II/IV -** calmodulin-dependent protein kinase II/IV

**cAMP** - Cyclic adenosine monophosphate

**CA 1-4 -** cornu ammonis 1 – 4

**cDNA -** complementary DNA

**CLC2 -** voltage-gated chloride channel 2

**CNS -** central nervous system

**CREB -** cAMP response element-binding protein

**Ct** - threshold cycle

**DAG -** diacylglycerol

**DAPI -** 4',6-diamidino-2-phenylindole

**DG -** dentate gyrus

**DIV** - days *in vitro*

**DMEM** - Dulbecco's Modified Eagles medium

**DNA -** deoxyribonucleic acid

**dNTP** - deoxynucleotide

**DTT -** dithiothreitol

**EC -** entorhinal cortex

**EDTA -** ethylenediamine tetraacetic acid

**EEA1** - early endosome antigen 1

**FBS** - fetal bovine serum

**5-HT3** - serotonin type 3 receptor

**GABA -** gamma-amino butyric acid

**$GABA_AR$ -** $GABA_A$ receptor

**GAT -** GABA transporters

**GAT-1** - GABA transporter 1

**GAT-3** - GABA transporter 3

**GCS -** glycine cleavage system

**GFAP** - glial fibrillary acidic protein

**Glu -** glutamate

**Gly -** glycine

**GlyR -** glycine receptors

**GlyT -** glycine transporters

**GlyT1 -** glycine transporters 1

**GlyT2 -** glycine transporters 2

**GTP -** guanosine-5'-triphosphate

**HEPES** - N-2-hydroxyethylpiperazine-N'-2-ethanesulfonic acid

**Hf -** hippocampal fissure

**HRP -** horseradish peroxidise

**IP3 -** inositol 1,4,5-triphosphate

**KA -** kainic acid

**KCC2 -** $K^+$-$Cl^-$ cotransporter 2

**KHR** - Krebs-Henseleit-Ringer solution

**$K_m$** - affinity constant by Michaelis-Menton model

**LPP -** lateral perforant pathway

**LTP** - long-term potentiation

**MAPK -** mitogen-activated protein kinase

**MAP2 -** microtubule-associated protein 2

**MF -** mossy fibers

**MPP -** medial perforant pathway

**mRNA -** messenger ribonucleic acid

**nAChR** - nicotinic acetylcholine receptor

**Nbea** - neurobeachin

**NF-kB** - nuclear factor-kB

**NGF -** nerve growth factor

**NKCC1 -** $Na^+$-$K^+$-$2Cl^-$ cotransporter 1

**NMDA -** N-Methyl-D-aspartate

**NP40 -** nonyl phenoxylpolyethoxylethanol

**NT-3 -** neurotrophin-3

**NT-4 -** neurotrophin-4

**P –** postnatal

**PAK -** p21-activated kinases

**PBS -** phosphate buffered saline

**PCR -** polymerase chain reaction

**PDL** - poly-D-lysine hydrobromide

**PFA -** paraformaldehyde

**PI3K -** phosphatidylinositol 3-kinase

**PIP2 -** phosphatidylinositol 4,5-bisphosphate

**PKC -** protein kinase C

**PLC -** phospholipase C

**PP -** perforant pathway

**PVDF** - polyvinylidene difluoride

**PMSF** - phenylmethylsulfonyl fluoride

**PTK** - protein tyrosine kinase

**p75 NTR -** p75 pan-neurotrophin receptor

**qPCR** - quantitative PCR

**RhoGDI1 -** rho-GDP dissociation inhibitor 1

**RIPA -** radioimmunoprecipitation assay buffer

**RNA -** ribonucleic acid

**ROCK -** rho-associated protein kinase

**RT** - room temperature

**RT-PCR -** reverse transcriptase polymerase chain reaction

**Sb –** subiculum

**SC -** schaffer collateral pathway

**SDS -** sodium dodecyl sulfate

**SDS-PAGE -** sodium dodecyl sulfate polyacrylamide gel electrophoresis

**SEM** - standard error of the mean

**Sg -** stratum granulosum

**Shc -** Src homology 2/α-collagen-related protein

**S.luc -** stratum lucidum

**Sm -** stratum moleculare

**SNARE -** soluble NSF (N-ethylmaleimide-sensitive fusion protein) attachment receptor

**So -** stratum oriens

**Sp -** stratum pyramidale

**Sr -** stratum radiatum

**SSV -** small synaptic vesicles

**TAE -** Tris-acetate-EDTA

**TBS-T -** tris buffered saline Tween-20

**TEMED -** N,N,N',N'- tetramethylethylenediamine

**TLE -** temporal lobe epilepsy

**TM1-4 -** transmembrane 1 – 4

**Trk -** tropomyosin-related kinase

**TrkA -** tropomyosin-related kinase A

**TrkB -** tropomyosin-related kinase B

**TrkC -** tropomyosin-related kinase C

**TrkB-FL –** full-length tropomyosin-related kinase B isoform

**TrkB-T1 –** truncated 1 tropomyosin-related kinase B isoform

**TrkB-T2 –** truncated 2 tropomyosin-related kinase B isoform

**TrkB-T-Shc –** truncated tropomyosin-related kinase B isoform that contain a Shc binding site

**Ulip6 -** Unc-33-like protein

**VDCC -** voltage-dependent calcium channel

**vGluT1** - vesicular glutamate transporter 1

**VIAAT -** vesicular inhibitory amino acid transporter

$\mathbf{V_{max}}$ - maximal velocity of transport

**Vps35 -** vacuolar protein sorting 35

**WHO -** World Health Organization

## Abstract:

Glycine, an inhibitory neurotransmitter in central nervous system, binds to its high affinity post-synaptic glycine receptors (GlyR). GlyR are pentameric channels, composed of several subunits (α1, α2, α3 and β). Termination of glycine-mediated synaptic activity occurs through removal of neurotransmitter from extracellular space, and is mediated by two glycine transporters (GlyT), GlyT1 and GlyT2. It is widely accepted that GlyT1 is mainly expressed in astrocytes, while GlyT2 is predominantly expressed in glycinergic pre-synaptic nerve terminals.

Brain-derived neurotrophic factor (BDNF) is a neurotrophin that activates its high affinity tropomyosin-related kinase B (TrkB) receptor, which includes full length (TrkB-FL) and truncated (TrkB-T1/T2) isoforms.

Throughout this work the key players of glycinergic neurotransmission were studied in the three components which comprise the tripartite synapse in rat brain. GlyR localization and subunit composition were assessed in the post-synaptic neurons, GlyT2 expression was evaluated in pre-synaptic nerve terminals and GlyT1 and GlyT2 expression and localization was examined in astrocytes.

In order to evaluate if GlyT are functional, [$^3$H]glycine uptake experiments were performed with selective inhibitors, Org-24598 and ALX-1393, for GlyT1 and GlyT2, respectively. Additionally, the BDNF effect upon glycine uptake mediated by GlyT in rat cortical cultured astrocytes and in hippocampal pre-synaptic nerve terminals was analyzed. Moreover, the signaling pathways involved in the BDNF effect were evaluated through a pharmacological approach.

Immunofluorescence assays in brain slices showed a predominance of extrasynaptic GlyR and an alteration in synaptic GlyR composition. At P7, post-synaptic receptors are mainly GlyR α2/β. In mature hippocampus (P21) synaptic GlyR decrease and are composed by α1/β subunits. Furthermore, extrasynaptic α2/α3-containing GlyR become predominant.

It was also demonstrated that hippocampal pre-synaptic nerve terminals express GlyT2. Quantitative PCR indicated that GlyT1 and GlyT2 transcripts are expressed in cultured astrocytes and immunofluorescence analysis corroborated these results since GlyT1 and GlyT2 were detected in astrocytes, both in culture and in brain slices.

By [$^3$H]glycine uptake assays, GlyT2 in pre-synaptic nerve terminals and both GlyT1 and GlyT2 in astrocytes, were shown to be functional.

It was also reported that BDNF decreases glycine uptake, mediated by GlyT, causing similar $K_m$ values and a lower $V_{max}$, in both astrocytes and pre-synaptic nerve terminals. In astrocytes BDNF acts through TrkB-T1 receptors, promoting GlyT internalization through a Rho-GTPase-dependent mechanism. In pre-synaptic nerve terminals the BDNF effect is due to the activation of the TrkB-FL receptors and the subsequent intracellular cascades, namely PLC, Akt and MAPK pathways, leading to the inhibition of GlyT2 insertion in the plasma membrane.

This work irrefutably confirms the occurrence of glycinergic synapses in the brain. It was shown the predominance of extrasynaptic GlyR, which suggests a role for slow tonic glycinergic neurotransmission, as well as the expression of functional GlyT1 and GlyT2 in astrocytes and GlyT2 in nerve terminals. In addition, it was described that GlyT1 and GlyT2 are modulated by BDNF.

In conclusion, this work provides new insights about glycinergic neurotransmission in brain.

Keywords: glycine, glycine receptor, glycine transporters, brain, BDNF, TrkB receptor.

## Resumo:

A glicina, um neurotransmissor inibitório do sistema nervoso central, actua através da ligação aos seus receptores de elevada afinidade localizados na membrana pós-sináptica, os receptores de glicina. Os receptores de glicina são canais pentaméricos, compostos por várias subunidades (α1, α2, α3 e β). A terminação da actividade sináptica mediada pela glicina ocorre através da remoção do neurotransmissor do espaço extracelular, e é mediada por dois transportadores de glicina, GlyT1 (*glycine transporter 1*) e GlyT2 (*glycine transporter 2*). É aceite pela comunidade científica que o GlyT1 é maioritariamente expresso em astrócitos enquanto o GlyT2 é predominantemente expresso em terminais glicinérgicos.

BDNF (*brain-derived neurotrophic factor*) é uma neurotrofina que activa os seus receptores de elevada afinidade, denominados TrkB (*tropomyosin-related kinase B*), que inclui as isoformas completa (TrkB-FL - *TrkB full length*) e truncada (TrkB-T1/T2).

Durante este trabalho, foram estudados os elementos principais da sinapse glicinérgica nos três componentes que constituem a sinapse tripartida no cérebro de rato. A localização do receptor de glicina e a sua composição ao nível das subunidades foram investigadas em neurónios pós-sinápticos, a expressão do GlyT2 foi avaliada em terminais de neurónios pré-sinápticos e a expressão e localização do GlyT1 e do GlyT2 foram analisadas em astrócitos.

Para avaliar se os transportadores de glicina são funcionais, foram realizadas experiências de recaptação da [$^3$H]glicina com inibidores selectivos, o Org-24598 e o ALX-1393, do GlyT1 e do GlyT2, respectivamente. Foi igualmente analisado o efeito do BDNF na recaptação de glicina mediada pelos seus transportadores em culturas primárias de astrócitos de córtex de rato e em terminais de neurónios pré-sinápticos. Além disso, as vias de sinalização envolvidas no efeito do BDNF foram avaliadas através de uma abordagem farmacológica.

Ensaios de imunofluorescência em fatias de cérebro mostraram a predominância do receptor de glicina extrasináptico e alterações na composição do receptor de glicina sináptico. A P7, os receptores pós-sinápticos são maioritariamente constituídos por subunidades α2/β. No hipocampo de um animal mais maduro (P21) o número de receptores de glicina sinápticos diminui e são compostos por subunidades α1/β. Deste

modo, os receptores de glicina extrasinápticos compostos pelas subunidades α2/α3 tornam-se predominantes.

Foi também demonstrado que os terminais de neurónios pré-sinápticos de hipocampo expressam o GlyT2. Experiências de PCR quantitativo indicam que os transcritos que codificam para o GlyT1 e o GlyT2 são expressos em culturas primárias de astrócitos sendo que, uma análise por imunofluorescência corrobora estes resultados, pois o GlyT1 e o GlyT2 foram também detectados em astrócitos, quer em culturas primárias quer em fatias de cérebro.

Através dos ensaios de recaptação da [$^3$H]glicina, foi demostrado que o GlyT2 em terminais de neurónios pré-sinápticos, e ambos os transportadores (GlyT1 e GlyT2) em astrócitos, são funcionais.

Foi ainda descrito que o BDNF diminui a recaptação de glicina mediada pelos seus transportadores que, na presença de BDNF, apresentam valores semelhantes de $K_m$ e uma diminuição no valor de $V_{max}$, tanto em astrócitos como em terminais de neurónios pré-sinápticos. Em astrócitos, o BDNF actua através da ligação aos seus receptores truncados TrkB-T1, promovendo a internalização do GlyT1 e do GlyT2 através de um mecanismo dependente de Rho-GTPases. Em terminais de neurónios pré-sinápticos, o efeito do BDNF ocorre devido à activação dos receptores TrkB-FL e das subsequentes vias de sinalização intracelulares, nomeadamente a PLC, a Akt e a MAPK, originando a inibição da inserção do GlyT2 na membrana plasmática.

Este trabalho confirma a existência de sinapses glicinérgicas no cérebro, pois foi mostrada a predominância do receptor de glicina nas regiões extrasinápticas, o que sugere que a glicina pode ser importante para a neurotransmissão tónica, assim como a presença de GlyT1 e GlyT2 em astrócitos e a expressão de GlyT2 nos neurónios pré-sinápticos. Foi ainda investigada a modelação dos transportadores de glicina pelo BDNF.

Em conclusão, este trabalho proporciona uma nova visão sobre a transmissão glicinérgica no cérebro.

Palavras-chave: glicina, receptor de glicina, transportadores de glicina, cérebro, BDNF, receptor TrkB.

# 1. Introduction

## 1.1. The Nervous System

The nervous system can be divided in central nervous system (CNS), composed by the brain and spinal cord, and the peripheral nervous system that contains the autonomic nervous system and the somatic nervous system (Zigmond 1999).

At the cellular level, the nervous system is composed by different types of neurons and also by non-neuronal cells that are called glial cells, which include the astrocytes, oligodendrocytes, microglia and Schwann cells. Astrocytes, oligodendrocytes and microglia are present in the CNS, while the Schwann cells can be found in the peripheral nervous system (Zigmond 1999).

Despite the fact that the human brain contains about 90% of glial cells and only 10% of neurons, the different types of glial cells interact with neurons, having specific and important roles in the CNS (Figure 1.1.). Microglia cells are the immune cells of the CNS and control brain infections. During CNS maturation, microglia cells, through phagocytosis, are also important to remove the inappropriate synaptic connections and ensure the correct neuronal development. Furthermore, microglia is activated during many neurological diseases. Oligodendrocytes and Schwann cells are the responsible for the myelin production, which enwrap axons, contributing to a rapid propagation of the electrical impulses and, consequently to a fast communication between neurons. Astrocytes are important cells in the CNS given that they communicate closely with neurons, and contribute to brain homeostasis through the release of several substances (gliotransmitters). Additionally, astrocytes, which are connected to adjacent astrocytes by gap junctions, are able to propagate information through large distances by the generation of intracellular calcium ($Ca^{2+}$) waves (Allen & Barres 2009).

Neurons are considered the vital cells of the nervous system and they can communicate through the generation and propagation of electrochemical signals that will originate the release, by exocytosis, of chemical molecules, called the neurotransmitters. The neurotransmitters are released to the synaptic cleft and are used to amplify and modulate signals between two cells (Dumoulin *et al.* 1999).

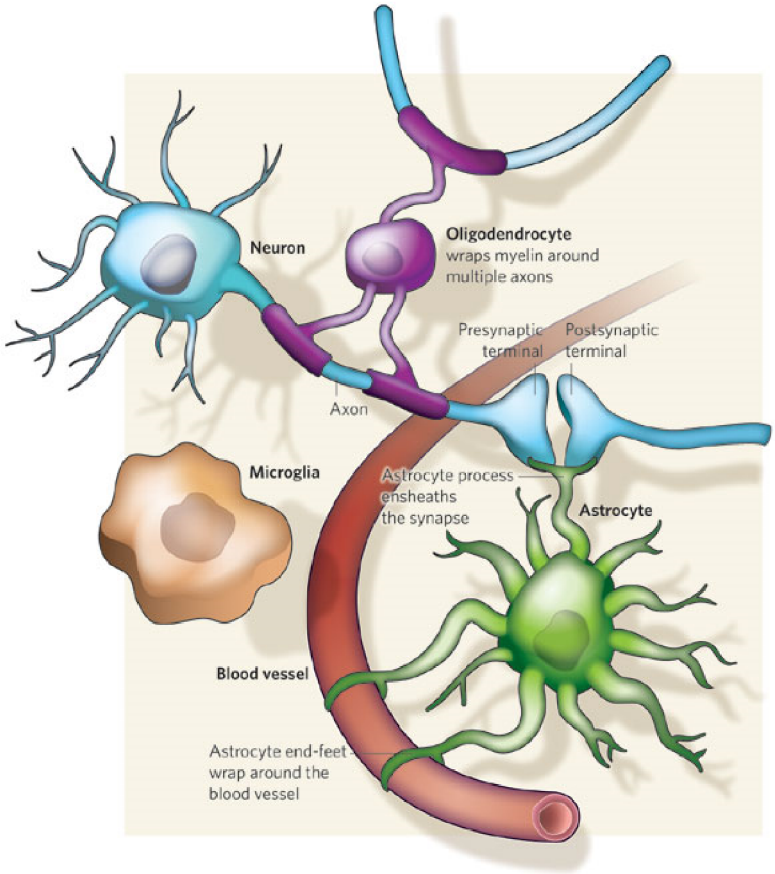


**Figure 1.1. - Interactions between glia cells and neurons.** Different types of glia cells (microglia, oligodendrocytes and astrocytes) interact with neurons and with the surrounding blood vessels. Microglia are responsible for maintaining the brain without damages or infections. Oligodendrocytes wrap myelin around axons to increase the velocity of neuronal transmission. Astrocytes are enriched in long processes that wrap blood vessels and synapses (Allen & Barres 2009).

The main functions of the CNS are the coordination of all the muscular activity and organs movement, by initiating and finalizing stimulus and actions, existing always an equilibrium between the excitatory and inhibitory actions to maintain the normal functioning (Zigmond 1999).

The inhibitory neurotransmission of the CNS is mediated by GABA (gamma-amino butyric acid) and glycine. While GABA is considered the main inhibitory neurotransmitter in the brain, glycine is described as the major inhibitory neurotransmitter in spinal cord and brainstem. By other hand, the excitatory neurotransmission in the brain occurs due to glutamate and aspartate actions (Siegel 1989).

## 1.2. The tripartite synapse

Classically, astrocytes are considered supportive cells that merely provide the optimal environment for neuronal functions. However in the last decade, new information has emerged that support the concept that astrocytes are the third element of a structure known as "tripartite synapse", which proposes that the synapse is composed by the typically pre- and post-synaptic neurons as well as the associated astrocyte (Figure. 1.2.). This model proposes that astrocytes are able to closely interact with neurons, by having projections that envelops the synapse and thus, control the synaptic activity, through a bidirectional communication with neurons (Araque *et al.* 1999, Perea *et al.* 2009).

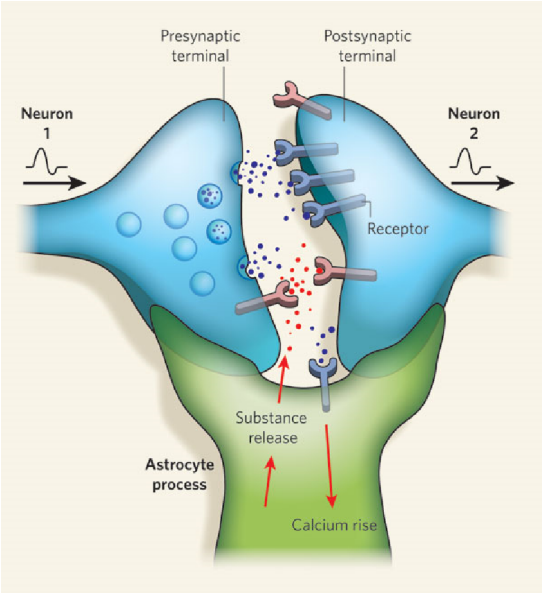


**Figure 1.2. - Representation of the tripartite synapse.** The neurotransmitters are released from the presynaptic nerve terminal and can act in receptors present in the membrane of astrocytes, leading to an increase in intracellular calcium ions in the astrocytes. This will lead to the release of several substances (gliotransmitters), such as ATP (adenosine-5'-triphosphate), glutamate and serine, which will have feedback actions on neurons to modulate the neuronal activity and the synapse formation (Allen & Barres 2009).

Astrocytes play a pivotal role in brain homeostasis through several cooperative metabolic processes that they establish with neurons, such as energy supply and neurotransmitter recycling functions (Allaman *et al.* 2011). At the synapse, astrocytes can be stimulated by released neurotransmitters, which cause intracellular $Ca^{2+}$ elevations, and trigger gliotransmitters release (such as ATP (adenosine-5'-triphosphate), D-serine and glutamate), that in turn regulate synaptic transmission and plasticity (Hamilton & Attwell 2010). By

other hand, astrocytes express in their membrane neurotransmitters transporters that are responsible for stopping neurotransmitters action, since they are able to transport the neurotransmitters from the extracellular space to the intracellular space. Consequently, the neurotransmitters levels in the synaptic cleft decrease and they are not able to bind to their receptors (Allen & Barres 2009). Thus, astrocytes are able to modulate synaptic activity both by the neurotransmitters uptake and by the gliotransmitters release.

There are two types of astrocytes with different morphology and distribution in the CNS: the protoplasmic and the fibrous (Figure 1.3.). The protoplasmic (type I) are localized in the grey matter, have generally a stellate shape, irregular contours, extremely long and branching processes with a globoid distribution that go just to one direction and are frequently closed to cell bodies and synapses. The fibrous (type II) are found in white matter, present regular contours, many filaments and extended processes in all the directions, which origin an association with neuronal axons (Andriezen 1893, Sofroniew & Vinters 2010).

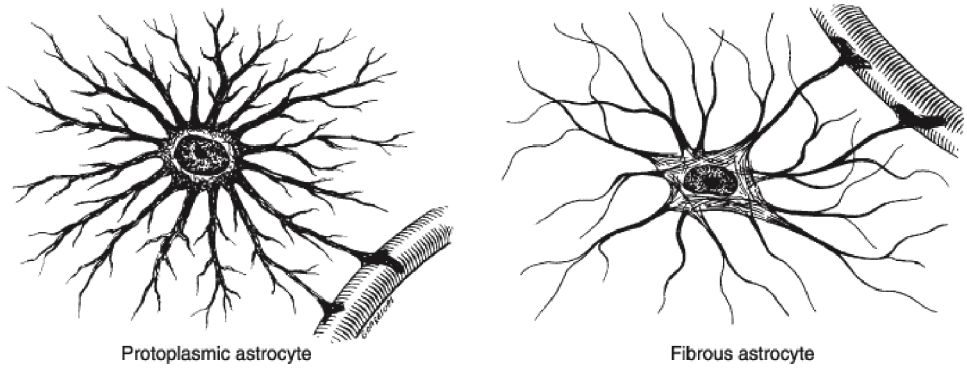


**Figure 1.3. - Representation of the two types of astrocytes present in the central nervous system: the protoplasmic and the fibrous.** The protoplasmic astrocytes present a more stellate shape, irregular contours and extremely long and branching processes while the fibrous astrocytes have regular contours, many filaments and extended processes (Adapted from Ganong 2012).

## 1.3. Glycine

Glycine is a non essential amino acid with a very simple structure (Nelson 2000). In the CNS glycine has a dual role: it is an inhibitory neurotransmitter, mainly in the spinal cord and brainstem (Siegel 1989) and it is also a co-agonist of the excitatory neurotransmission,

by potentiating the NMDA (N-Methyl-D-aspartate) receptors response (Johnson & Ascher 1987).

Glycine can participate in several metabolic processes and the majority of glycine found in the brain is synthesized from serine through the serine hydroxymethyltransferase enzyme (EC 2.1.2.1) (Figure 1.4.).

However, the enzyme activity can not be used to identify which neurons synthesize and release glycine, since glycine synthesis is constant in several areas and it can not be correlated with the existence of glycinergic neurons (Siegel 1989).

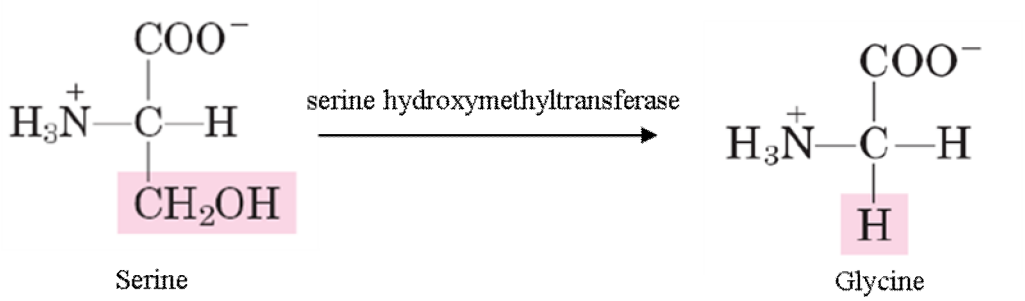


**Figure 1.4. – Glycine synthesis from serine through the serine hydroxymethyltransferase enzyme.** Both the structural formulas (serine and glycine) show the ionization state that predominates at pH 7.0. The unshaded structure is common to all the amino acids, while the portions shaded correspond to the amino acids R groups (Nelson 2000).

### 1.3.1. Glycine in the pre-synaptic nerve terminal

In the pre-synaptic nerve terminals glycine can be packaged in synaptic vesicles through VIAAT (vesicular inhibitory amino acid transporter) (57 kDa) (Sagne *et al.* 1997) (Figure 1.5.), making VIAAT a good marker of inhibitory pre-synaptic terminals (Legendre 2001). By other hand, the glycine transport to the synaptic vesicles is dependent of proton pumps that originate electrochemical gradients by transporting protons from the cytosol to the vesicles lumen, making them more acidic. These pumps use ATP hydrolysis as energy source, being called vacuolar-type $H^+$-ATPase (Figure 1.5.) (Dumoulin *et al.* 1999).

This ATPase is essential for VIAAT to work properly, since it is necessary the exchange of protons, present in vesicles lumen, for glycine (Sagne *et al.* 1997). However, VIAAT it is not specific for glycine, it is a common vesicular transporter for both glycine and GABA,

being present in pure glycinergic terminals, pure GABAergic terminals and also in mixed terminals, which release both GABA and glycine (Dumoulin *et al.* 1999).

The VIAAT ability to transport GABA or glycine is related to the neurotransmitter concentration in the cytosol. This depends of the synthesis pathways and of the specific transporter activity expressed in the pre-synaptic membrane (Dumoulin *et al.* 1999, revised in Legendre 2001).

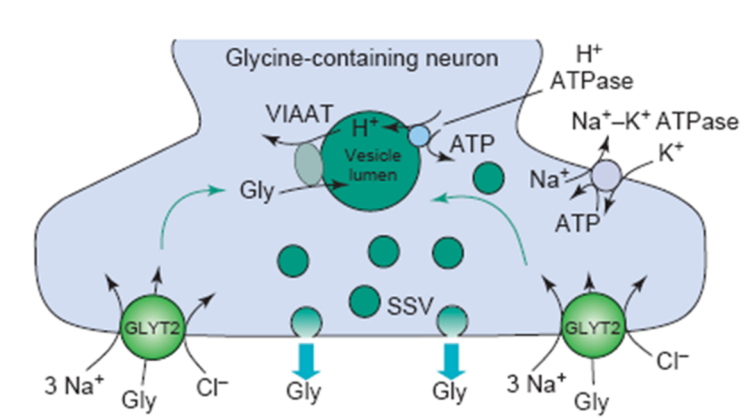


**Figure 1.5. - The glycinergic pre-synaptic nerve terminals.** The vesicular inhibitory amino acid transporter (VIAAT) uptakes glycine (Gly) from the cytosol to the small synaptic vesicles (SSV) in exchange of protons. This transport is driven by a proton gradient preserved by the vacuolar $H^+$-ATPase. After the action potential and the entrance of calcium ions, the synaptic vesicles fuse with the plasma membrane and release glycine to the synaptic cleft. Glycine can be transported again to the pre-synaptic terminal by $Na^+$-$Cl^-$-dependent glycine transporter (GlyT2) located in the membrane of the pre-synaptic nerve terminals. GlyT2 increases glycine concentrations in the cytosol providing substrate to VIAAT (Aragon & Lopez-Corcuera 2005).

Once the neurotransmitter is inside the synaptic vesicles, it is guided to the pre-synaptic membrane forming vesicle pools docked to the cell membrane. This orientation is conducted by a group of proteins called synapsins, which interact with the microtubules, and also by the action of a specific family of GTPases, the Rab proteins, which hydrolyze GTP (guanosine-5'-triphosphate) (Purves 2008).

The synaptic vesicles are anchored to the pre-synaptic membrane by the formation of a protein complex, usually called SNARE (soluble NSF (N-ethylmaleimide-sensitive fusion protein) attachment receptor) complex. The SNARE complex is composed by membrane proteins from the synaptic vesicles and also from the pre-synaptic nerve terminal. Thus, the synaptic vesicles are already primed before the complete fusion occurs. The priming is an initial step that organizes the synaptic vesicles, so that they are able to quickly fuse with

the membrane in response to the action potential (Purves 2008). When an action potential occurs, the pre-synaptic membrane depolarizes, which generates alterations in the membrane potential and consequently, the opening of the voltage dependent $Ca^{2+}$ ions channels allowing the entry of $Ca^{2+}$ ions into the cell. The $Ca^{2+}$ ions will bind to the $Ca^{2+}$-binding synaptic vesicle protein synaptotagmin, which catalyze the vesicles fusion with the nerve terminal membrane. Therefore, the fusion pore is formed, which leads to the extrusion of the vesicle content to the synaptic cleft (Purves 2008).

Once in the synaptic cleft, the neurotransmitter, and in the particular case of glycinergic synapses (Figure 1.6.), glycine can bind to its particular receptors expressed in the membrane of the post-synaptic neurons and cause an inhibition of the system (Dumoulin *et al.* 1999). By other hand, glycine can activate its specific transporters localized in the membrane of astrocytes or in the membrane of the pre-synaptic nerve terminals.

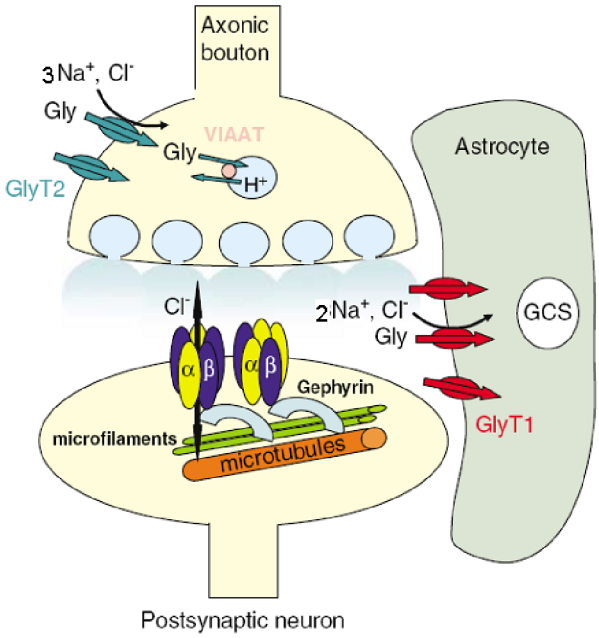


**Figure 1.6. – The glycinergic synapse.** Pre-synaptic glycine (Gly) is packaged into synaptic vesicles through vesicular inhibitory amino acid transporter (VIAAT). Glycine receptors (GlyR) are represented as pentamers of stoichiometry 3α:2β and also the more recent stoichiometry 2α:3β. The receptors, through the β subunit, are anchored to gephyrin and therefore to the microfilaments and microtubules. By other hand, glycine can be transported by GlyT1 to astrocytes, where it will be hydrolysed by the glycine cleavage system (GCS), or by GlyT2 to the pre-synaptic nerve terminal being available to be re-packaged into synaptic vesicles (Bowery & Smart 2006).

### 1.3.2. Glycine Transporters

At glycinergic synapses, termination of glycine-mediated synaptic activity occurs through removal of the neurotransmitter from the synaptic cleft, by specific glycine transporters (GlyT) present in the plasma membrane of pre-synaptic nerve endings and of astrocytes (Eulenburg *et al.* 2005), being responsible for the regulation of glycine concentration in the extracellular space (Vandenberg *et al.* 2007).

Until now two GlyT have been identified, glycine transporter 1 (GlyT1) (Guastella *et al.* 1992) and glycine transporter 2 (GlyT2) (Liu *et al.* 1992), sharing about 50% of amino acid sequence homology but displaying different pharmacology (Dohi *et al.* 2009). GlyT1 and GlyT2 share a common transmembrane topology with twelve transmembrane domains (TM1-12) and with amino and carboxyl terminals in the intracellular space, although the amino terminal of GlyT2 is longer than the one of GlyT1. In the extracellular space there is a large loop between TM3 and TM4 with residues susceptible to N-glycosylation, which is important for the intracellular trafficking to the plasma membrane (Eulenburg *et al.* 2005). Both GlyT1 (Figure 1.7.A) and GlyT2 (Figure 1.7.B) can be present in several isoforms generated by alternative splicing and the use of alternative promoters (Adams *et al.* 1995, Ebihara *et al.* 2004). GlyT1 isoforms can differ both in the amino terminal (a,b,c) and in the carboxyl terminal (d,e), while GlyT2 isoforms vary only in the amino terminal (a,b,c) (Eulenburg *et al.* 2005).

GlyT ensure the glycine transporter to the cell by a symport system with sodium ions ($Na^+$) and chloride ions ($Cl^-$) (Zafra *et al.* 1995, Roux & Supplisson 2000). GlyT1 is responsible for the transporter of glycine, together with two $Na^+$ ions and only one $Cl^-$ ion, to astrocytes (Roux & Supplisson 2000), where glycine can be hydrolysed by an efficient glycine cleavage system (GCS) composed by several enzymes (Sato *et al.* 1991). By other hand, GlyT2 requires three $Na^+$ ions and one $Cl^-$ ion to be co-transported with glycine (Roux & Supplisson 2000) (Figure 1.6.).

Both GlyT1 and GlyT2 are strongly expressed in caudal regions of the brain and in spinal cord (Zafra *et al.* 1995). Additionally, by *in situ* hybridization, GlyT1 expression was detected in most brain areas, while GlyT2 was mostly observed in spinal cord and brainstem (Borowsky *et al.* 1993), being present in a lesser extent in the brain than GlyT1 (Jursky & Nelson 1996). Recently, GlyT2 was detected in hippocampal interneurons (Danglot *et al.* 2004). Furthermore, GlyT2 protein distribution reproduces the distribution of glycine receptors (GlyR), the postsynaptic component of the glycinergic synapse (Jursky

*et al.* 1994, Jursky & Nelson 1995, Zafra *et al.* 1995), being considered a reliable marker for glycinergic nerve terminals (Poyatos *et al.* 1997).

An analysis of GlyT expression and activity in spinal cord at different developmental stages described that at birth, GlyT1 is the predominant GlyT, being responsible for the majority of glycine uptake. However, after the postnatal day 10, GlyT2 expression and activity increase and in adulthood both GlyT1 and GlyT2 have a similarly contribution to glycine uptake (Lall *et al.* 2012).

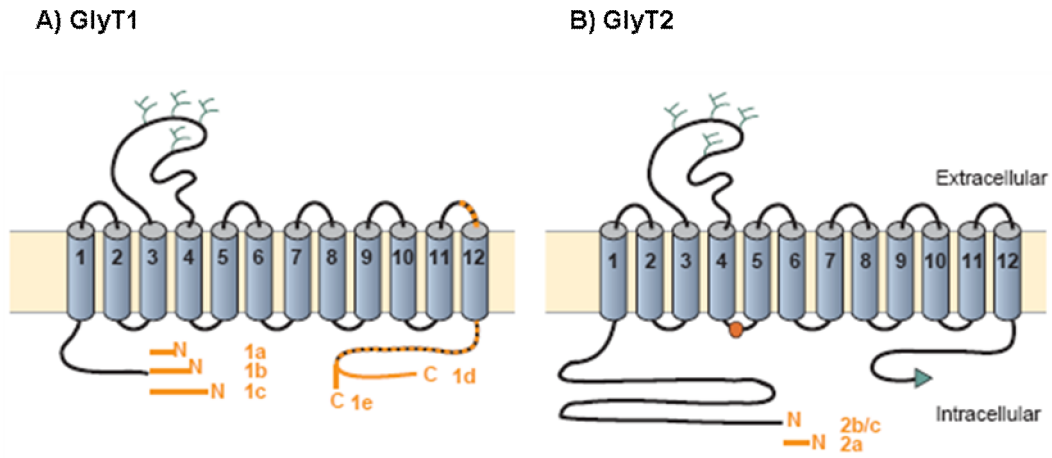


**Figure 1.7. – Membrane topology of GlyT1 (A) and GlyT2 (B).** Glycine transporters (GlyT) have twelve transmembrane domains with amino and carboxyl terminals in the intracellular space. The different splice variants are indicated in orange. For GlyT1, three isoforms in the amino terminal (a,b,c) and two in the carboxyl terminal (d,e) have been described. The dashed line represents the shorter GlyT1e isoform, identified only in bovine. For GlyT2, three isoforms of the amino terminal (a,b,c) were discovered. N-glycosylation in the large extracellular loop is indicated in green (Eulenburg et al. 2005).

It is worldwide accepted that GlyT1 is mainly expressed in astrocytes, while GlyT2 is predominantly expressed in glycinergic nerve terminals (Eulenburg *et al.* 2005). However, the expression of GlyT2 in glial cells has been described in cerebellum (Zafra *et al.* 1995), in cortical oligodendrocyte progenitor cells (Belachew *et al.* 2000) and, recently, in purified preparations of mouse spinal cord astrocyte-derived subcellular particles, named gliosomes (Raiteri *et al.* 2008). Whether GlyT2 is also present in brain astrocytes, where glycinergic transmission represents a minor proportion of the inhibitory transmission is still unknown.

It was already elucidated that GlyT have important and opposite functions in the glycinergic synapses according to its localization. In the rat striatum it was already

described that the blockade of GlyT1 increased the extrasynaptic glycine concentration (Nagy *et al.* 2010). Moreover, in GlyT1 knock-out mice, the accumulation of glycine in the synaptic cleft leads to a critical reinforcement of inhibitory neurotransmission and, consequently, to numerous motor and respiratory insufficiencies, culminating with the animals' dead during the first postnatal day (Gomeza *et al.* 2003a). By other hand, GlyT2-deficient mice present a reduction of presynaptic glycine release and therefore a reduction in glycinergic inhibition, which origins a severe motor deficit characterized by muscular rigidity, tremor and strong convulsions, and culminates with the animals' dead throughout the second postnatal week (Gomeza *et al.* 2003b). These symptoms are very similar to the ones described in human hyperekplexia, being GlyT2 involved in some forms of this disease (Gomeza *et al.* 2003b).

The data obtained with the knock-out mice are consistent with the complementary functions attributed to GlyT. Glial GlyT1 ensures the removal of glycine from the synaptic cleft leading to the termination of glycine mediated neurotransmission, while neuronal GlyT2 ensures the refilling of presynaptic vesicles of glycinergic neurons (Gomeza *et al.* 2003a, Gomeza *et al.* 2003b).

In addition, GlyT1 is also present in glutamatergic neurons and regulates the concentration of glycine at excitatory synapses containing NMDA receptors, known to require glycine as a co-agonist (Smith *et al.* 1992, Eulenburg *et al.* 2005). By other hand, glycine levels in the glutamatergic synapses can increase due to a phenomenon called spillover, which occurs when the glycine released from the adjacent inhibitory synapses escapes from the synaptic cleft and potentiates the NMDA receptors currents (Ahmadi *et al.* 2003). Moreover, GlyT1 inhibition increases extracellular glycine concentration, potentiating the NMDA receptors response (Bradaia *et al.* 2004, Martina *et al.* 2004). However, it was described that high concentrations of glycine can prime NMDA receptors internalization (Nong *et al.* 2003), being a protective mechanism to avoid the excessive neuronal excitability.

Therefore, GlyT1 mediates both the clearance of glycine from the synaptic cleft of inhibitory synapses and participates in the regulation of glycine concentration at excitatory synapses (Figure 1.8.).

Furthermore, both GlyT1 and GlyT2 can reverse. GlyT1 reverse the glycine transport upon depolarization of the astrocytic membrane or if the extracellular glycine levels are low due to GlyT2 activation, which leads to an increase in the extracellular glycine levels (in inhibitory and in excitatory synapses), indicating an unusual mechanism for extracellular glycine accumulation (Roux & Supplisson 2000). GlyT2 can reverse and consequently

transport glycine from the cytosol to the extracellular space in specific conditions, namely when the presynaptic terminals were superfused with veratridine (Romei *et al.* 2011), an alkaloid that prevents the inactivation of the $Na^+$ channels, leading to an increase of $Na^+$ influx and consequently of the cytosolic $Na^+$ levels (Ulbricht 1998).

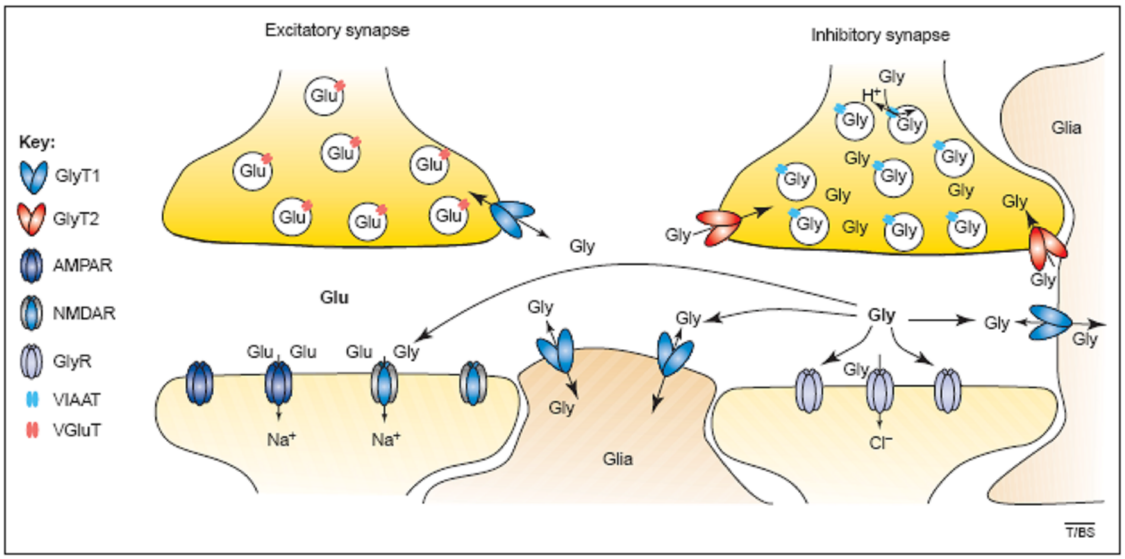


**Figure 1.8. – Localization of glycine transporters at excitatory and inhibitory synapses.** At inhibitory synapses, glycine (Gly) is transported to the synaptic vesicles through the vesicular inhibitory amino acid transporter (VIAAT) and then is released to the synaptic cleft. Glycine will bind to the glycine receptors (GlyR) localized in the post-synaptic membrane. Glycine can also be transported by the glycine transporter 1 (GlyT1) to the astrocytes or can be transported by the glycine transporter 2 (GlyT2) to the pre-synaptic nerve terminal, where can be transported again to the synaptic vesicles. At excitatory synapses, glycine that might derived from neighbouring inhibitory synapses, can act as a co-agonist of post-synaptic glutamate (Glu) NMDA (N-Methyl-D-aspartate) receptor, while the glutamate AMPA (α-amino-3-hydroxy-5-methyl-4-isoxazolepropionic acid) receptor requires only glutamate. The pre-synaptic excitatory terminals also express GlyT1 to regulate glycine extracellular levels in excitatory synapses (Eulenburg et al. 2005).

Moreover, the localization of GlyT2 in the pre-synaptic membrane can be modulated, since it was already described that membrane depolarization with the consequent influx of $Ca^{2+}$ leads to an increase of the GlyT2 number into the neuronal plasma membrane. Furthermore, GlyT2 physically interacts with syntaxin 1A, a pre-synaptic protein, which is also involved in the $Ca^{2+}$-dependent GlyT2 insertion in the membrane (Geerlings *et al.* 2001). By other hand, in the presence of sustained $Ca^{2+}$ influx, GlyT2 is removed from the cell membrane due to protein kinase C (PKC) activation (Fornes *et al.* 2004) or due to the

interactions with other GlyT2-binding proteins, like Unc-33-like protein (Ulip)6, a member of the collapsin response mediator protein family (Horiuchi *et al.* 2005).
In addition, GlyT1 can be phosphorylated by PKC at serine and/or threonine residues, modulating the GlyT1 expression in the cellular membrane (Vargas-Medrano *et al.* 2011).
GlyT are often regarded as important therapeutic targets, since they can be modulated by specific drugs, which can lead to an increase of the glycine concentration in the synaptic cleft, enhancing the inhibitory action of glycine (Guastella *et al.* 1992).

### 1.3.3. Glycine Receptor

Up to now, only one type of receptor is known for glycine, the ionotrophic GlyR, which are mainly involved in the phasic neurotransmission that occurs at the synaptic level (revised in Bowery & Smart 2006).
GlyR belong to the Cys-loop ligand-gated ion channel superfamily of receptors, which also includes nicotinic acetylcholine receptors (nAChR), serotonin type 3 receptors (5-HT3), and the closely related $GABA_A$ receptors ($GABA_AR$) (revised in Jensen *et al.* 2005).
GlyR are composed of five protein subunits that form a pentameric channel (Figure 1.9.) (Langosch *et al.* 1988) permeable to $Cl^-$ ions. Glycine binds to GlyR leading to the opening of the channel and the consequent influx of $Cl^-$ ion, which causes the hyperpolarization of the membrane and the inhibition of the synaptic neurotransmission (Young-Pearse *et al.* 2006).
Each one of the five subunits is composed by proteins with four transmembrane domains (TM1-4) and with amino and carboxyl terminals in the extracellular space. The amino terminal is larger than the carboxyl terminal (Figure 1.9.) and contains four conserved cystein residues that form a disulfide bond, which gives the name to this family. In the cytoplasm there is a short connection between TM1 and TM2 and a large loop between TM3 and TM4 (Kirsch 2006). This loop is important to GlyR anchoring at the synapses and to the trafficking to and from the membrane, as well as being susceptible to post-translation modifications like phosphorylation by kinases (revised in Bowery & Smart 2006). TM2 is the main responsible for pore formation (Figure 1.9.) (revised in Jensen *et al.* 2005).

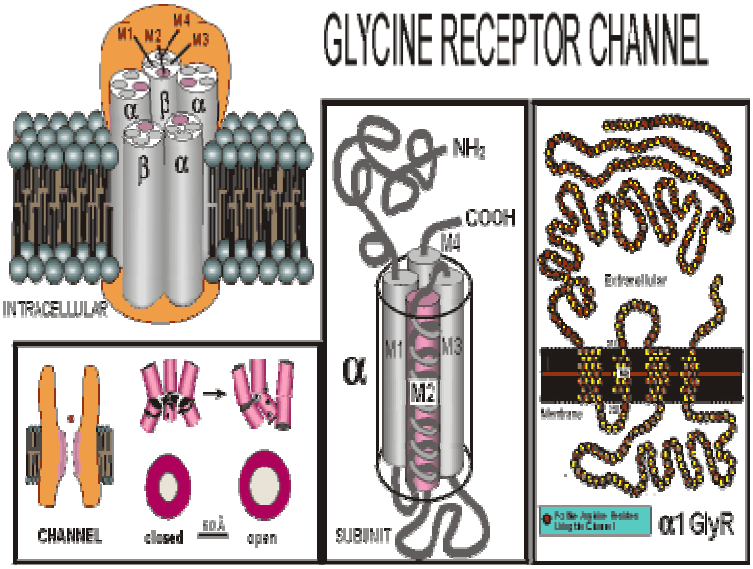


**Figure 1.9. – Schematic representation of the glycine receptor.** The pentameric struture and mechanism for glycine receptors (GlyR) channel opening is here elucidated. The struture and amino acid composition of the GlyR alpha 1 subunit as well as its membrane topology is revealed. It is possible to observe the four transmembrane domains (TM1-4), the amino and carboxyl terminals in the extracellular space and also a large intracellular loop between TM3 and TM4. (Adapted from www.biophysics.org.au/About/index.html).

GlyR are composed by alpha (α) and beta (β) subunits with approximately, 48 and 58 kDa, respectively (revised in Bowery & Smart 2006). All α subunits present high sequence identity (>80%), while the β subunit exhibits significant sequence differences when compared to the α subunits (<50%) (revised in Dutertre *et al.* 2012). During many years it was thought that GlyR were composed by three α subunits and two β subunits (3α:2β) (Kuhse *et al.* 1993). However, it was already reveal that GlyR can also be composed by two α subunits and three β subunits (2α:3β), which can have implications for GlyR function and pharmacology (Grudzinska *et al.* 2005). This stoichiometry was recently confirmed by atomic force microscopy, which suggests a β-α-β-α-β subunit arrangement (Yang *et al.* 2012).

Several gene variants of α subunits (α1, α2, α3 and α4) have been described, while for β subunit only one gene was described. All the α subunits are able to form functional homomeric receptors whereas the β subunit can only form functional GyR when it is co-assembled with α subunits, forming heteromeric GlyR (revised in Bowery & Smart 2006). The diversity in GlyR subunits can additionally be achieved by alternative splicing (revised in Kirsch 2006). For instance, the α1 subunit can exist in two isoforms: α1 and $\alpha1_{INS}$ that

contains an additional small amino acid sequence in the large loop between TM3 and TM4 (Malosio *et al.* 1991a). The α2 subunit splice variants α2A and α2B present a different amino terminal caused by a dual amino acid substitution (Kuhse *et al.* 1991), which causes different agonist sensitivity presenting the α2B isoform a higher agonist potency (Miller *et al.* 2004). Regarding the α3 subunit, similar to what happens for α1 subunit, two splicing isoforms, α3S and α3L with more 15 amino acids in the loop between TM3 and TM4, were already described (Nikolic *et al.* 1998). In addition, it was reported a α3 isoform, α3P185L, originated by an amino acid substitution and with increased agonist potency (Meier *et al.* 2005).

The α1 (48 kDa) and α2 (49 kDa) subunits are considered essential and are largely expressed in the nervous system. However, their expression is highly regulated and varies with the development and with the organ, which origins alterations in the GlyR physiology and pharmacology (Takahashi *et al.* 1992, revised in Lynch 2009).

α3 and α4 subunits are considered rare subunits and thus, not so relevant to glycine-mediated synaptic activity. Nevertheless, it was already demonstrated that α3 subunit has an important role in spinal cord, namely in prostaglandin-mediated inflammatory pain sensitization (Harvey *et al.* 2004). Additionally, it was recently show that this subunit is expressed in brain, namely in the hippocampus (Eichler *et al.* 2009).

The β subunit is largely expressed in the nervous system, but its expression pattern can not be correlated with α subunits expression. This may suggest other functions for this subunit, since by itself it is unable to form homomeric GlyR (Grenningloh *et al.* 1990, revised in Bowery & Smart 2006).

Despite the main function of β subunit, which is to ensure the anchoring to gephyrin (Figure 1.6.) (Meyer *et al.* 1995), it was recently reported that the β subunit can interact with the trafficking proteins Vacuolar Protein Sorting 35 (Vps35) and Neurobeachin (Nbea) (del Pino *et al.* 2011).

Gephyrin is a cytoplasmic post-synaptic protein (93 kDa) necessary for synaptic localization of GlyR (Kirsch *et al.* 1991). Actually, GlyR were the firsts neurotransmitters receptors described by immunohistochemistry to cluster in the postsynaptic sites (Triller *et al.* 1985), facing GABA-containing nerve terminals, which suggested the existence of synapses where GABA and glycine coexist (Triller *et al.* 1987).

The accumulation of GlyR in post-synaptic membranes can be achieved as a two-step process. First, it is necessary the gephyrin independent formation of GlyR clusters that freely diffuse for all the plasmatic membrane (Meier *et al.* 2000), and that, in a matter of

seconds, are able to bind to gephyrin (Meier *et al.* 2001). Second, gephyrin interacts with cytoskeleton proteins, and anchors GlyR to the post-synaptic membrane (Figure 1.6.) (Kirsch *et al.* 1991). The interaction between GlyR β subunit and gephyrin is reversible and highly dynamic (Meier *et al.* 2001), regulating the GlyR lateral diffusion and consequently, the number of GlyR in the post-synaptic membrane. This is a consequence of the equilibrium between the pools of stabilized GlyR in the post-synaptic areas and the freely diffused ones that can be activated by neurotransmitter spillover from the synaptic cleft (Meier *et al.* 2001, revised in Fritschy *et al.* 2008). In fact, the GlyR lateral diffusion between synaptic and extrasynaptic sites has been elegantly tracked using imaging techniques (Dahan *et al.* 2003).

The modulation of GlyR localization in the post-synaptic sites and in the extrasynaptic areas can be achieved by changing the GlyR β subunit and gephyrin interaction capacity, through, for example, post-translation modifications. Recently, it was identified a PKC phosphorylation site in the cytoplasmic domain of the β subunit (residue S403). When this residue is phosphorylated β subunit and gephyrin binding affinity decreases, which causes a reduction of synaptic GlyR and an increased GlyR expression in extrasynaptic sites (Specht *et al.* 2011).

Additionally, it was already described that $Ca^{2+}$ ions increase GlyR levels in the synapses by decreasing the lateral diffusion in the membrane, which corroborate the PKC involvement in the regulation of the GlyR diffusion properties, since this enzyme is dependent of $Ca^{2+}$ ions (Levi *et al.* 2008).

However, besides the involvement of PKC in GlyR localization within the membrane, it was previously shown that PKC can modulate the direct function of GlyR. By whole-cell studies, it was demonstrated that PKC activation facilitates the GlyR current, while PKC inhibitors decrease GlyR function (Schonrock & Bormann 1995). Moreover, the phosphorylation of the β subunit (residue Y413) by protein tyrosine kinase (PTK) also increases GlyR function (Caraiscos *et al.* 2002).

Although post-synaptic GlyR are the most abundant ones, several studies indicated the presence of GlyR in the pre-synaptic nerve terminals. Pre-synaptic GlyR were described firstly in the calyceal synapse of the medial nucleus of the trapezoid body (Turecek & Trussell 2001) and later in the spinal cord (Jeong *et al.* 2003). Although these pre-synaptic GlyR are functional, several differences were described in relation to post-synaptic ones: the pre-synaptic GlyR trigger a weakly depolarizing $Cl^-$ current, which activates $Ca^{2+}$

channels, potentiating neurotransmitters release (Turecek & Trussell 2001, Jeong *et al.* 2003) and are composed only by α1 subunits, presenting an homomeric composition, contrasting with heteromeric post-synaptic GlyR (Jeong *et al.* 2003, Hruskova *et al.* 2012). More recently, it was found not only the presence of pre-synaptic GlyR in the excitatory nerve terminals of the hippocampus (Eichler *et al.* 2009, Lee *et al.* 2009), but also that their activation causes a depolarization of the glutamatergic neurons facilitating glutamate release (Lee *et al.* 2009). However, hippocampal pre-synaptic GlyR have a lower affinity for glycine and their expression decrease during development (Kubota *et al.* 2010).

## 1.4. Pharmacology of GlyR and GlyT

### 1.4.1. GlyR Pharmacology

The main agonists of GlyR are glycine, β-alanine and taurine, in a potency descending order (Lewis *et al.* 2003). The agonists binding site of GlyR was found to be in the interface between the α1 and β subunits, in the case of the heteromeric GlyR (Grudzinska *et al.* 2005). By other hand, GABA was also described as a weak partial agonist of GlyR, since it is able to potentiate the glycine-mediated GlyR activation (Lu *et al.* 2008).

The well-known, specific and potent antagonist of GlyR is the plant alkaloid strychnine (Curtis *et al.* 1968, Young & Snyder 1973) that exerts its action through the binding to α1 subunit (Ruiz-Gomez *et al.* 1990). However, this binding can be blocked by glycine, which suggests an association between the agonist binding sites and the antagonist binding sites (Graham *et al.* 1983).

The other GlyR antagonist is picrotoxin, which is also used as an antagonist of $GABA_AR$, being this receptor more sensitive to picrotoxin that GlyR. One of the important features of this antagonist is that it is able to discriminate between homomeric and heteromeric GlyR, being more potent in homomeric ones, due to the resistance conferred by the β subunit (Pribilla *et al.* 1992). In hippocampus, it was already shown that picrotoxin only partially reduced GlyR-mediated currents, which proposes the expression of both homomeric and heteromeric GlyR (Chattipakorn & McMahon 2002).

Thus, agonists and antagonists are able to bind to GlyR, involving highly conserved residues of two adjacent subunits. In the case of the homomeric GlyR, it is possible that the agonist/antagonist binds to any of the five α-α interfaces, while for the heteromeric GlyR

the binding occurs through the α-β interfaces. The possible pharmacology of the β-β interfaces is still unknown and controversial (Grudzinska *et al.* 2005, revised in Betz & Laube 2006). Actually, the regions where the agonist and antagonist bind are also used by several compounds that are able to modulate GlyR like zinc ions ($Zn^{2+}$), anesthetics, alcohols, steroids and also endogenous cannabinoids, such as anandamide and 2-arachidonylglycerol (revised in Lynch 2004, revised in Dutertre *et al.* 2012).

### 1.4.2 GlyT Pharmacology

GlyT1 can be specifically blocked by sarcosine-based inhibitors, like Org 24598, leading to an accumulation of glycine in the extracellular space (Dohi *et al.* 2009). However, it has to be noted that by inhibiting GlyT1, the glycine levels in the vicinity of the NMDA receptors are also being regulated. This may be relevant in situations of hypoglutamatergic functions that can be related with schizophrenia or depression (Tsai *et al.* 2004, Gomeza *et al.* 2006).

The GlyT2 inhibitors are not as explored as the GlyT1 inhibitors. Nevertheless, GlyT2 actions were described to be inhibited by ALX 1393 (Xu *et al.* 2005, Luccini & Raiteri 2007) or amoxapine (Nunez *et al.* 2000).

GlyT inhibitors are used in models of neuropathic pain, since GlyT is very important to regulate the pain-mediated neurotransmission in the spinal cord, where glycinergic neurotransmission is abundant (Dohi *et al.* 2009).

## 1.5. Glycinergic neurotransmission over development – depolarization vs hyperpolarization

In immature neurons, both $GABA_AR$ and GlyR activation cause membrane depolarization instead of membrane hyperpolarization observed in mature neurons. This depolarization mediated by GABA or glycine occurs before the establishment of the glutamatergic activity. Therefore, there is a period in the early development where GlyR have excitatory actions and then, over time, change to an inhibitory role (revised in Ben-Ari 2002).

This modification is related with the change of $Cl^-$ ion intracellular concentration, which is dependent on the action of two ion transporters that determine the direction of $Cl^-$

electrochemical gradient. One promotes the influx of $Cl^-$ ions with both the $Na^+$ ions and the potassium ions ($K^+$) and is denominated of $Na^+$-$K^+$-$2Cl^-$ cotransporter 1 (NKCC1). The other transporter is the $K^+$-$Cl^-$ cotransporter 2 (KCC2) that is the responsible for the $Cl^-$ ions efflux with the co-transport of the $K^+$ ions (Delpire 2000).

NKCC1 is highly expressed at birth and during the first postnatal week, and its expression declines with development (Plotkin *et al.* 1997), whereas KCC2 is weakly expressed at birth and its expression increases over time (Clayton *et al.* 1998). The differentiated expression of these ion transporters is responsible for the decrease in $Cl^-$ ion intracellular concentration observed during development and also for the directional change in $Cl^-$ ion currents through GlyR (Delpire 2000). Consequently, in immature neurons, glycine and GABA, through the activation of the corresponding ligand-gated ion channel, cause membrane depolarization and exert an excitatory action (Figure 1.10.A) (Flint *et al.* 1998).

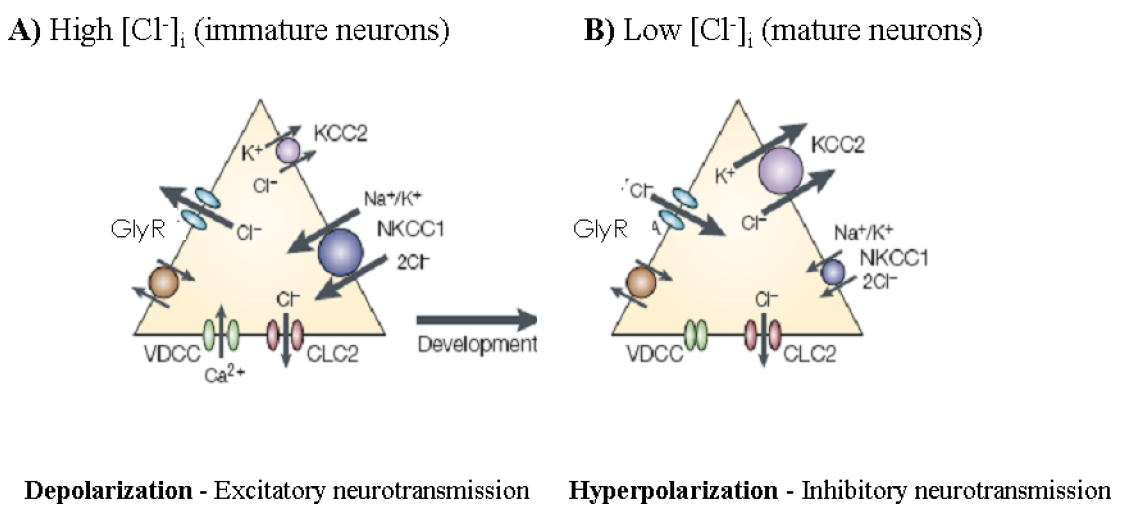


**Figure 1.10. – Schematic representation of the expression of NKCC1 and KCC2 in immature (A) and mature (B) neurons and the consequent changes in $Cl^-$ gradients. (A)** In immature neurons the expression of NKCC1 ($Na^+$-$K^+$-$2Cl^-$ cotransporter 1) is predominant and the intracellular concentration of $Cl^-$ ($[Cl^-]i$) is high. Glycine receptors (GlyR) activation generates an efflux of $Cl^-$ and a neuronal excitation. **(B)** In mature neurons the expression of KCC2 ($K^+$-$Cl^-$ cotransporter 2) is predominant and the $[Cl^-]i$ is low. GlyR activation will lead to a $Cl^-$ influx and a neuronal inhibition. CLC2 (voltage-gated chloride channel 2); VDCC (voltage-dependent calcium channel) (Adapted from Ben-Ari 2002).

By other hand, in mature neurons, GlyR and $GABA_AR$ activation originates $Cl^-$ ion influx, which leads to a hyperpolarization of the cells and to an inhibition of the system (Figure 1.10.B) (revised in Ben-Ari 2002).

In the hippocampus this shift is described to occur during the second postnatal week (Ben-Ari *et al.* 1989, Ito & Cherubini 1991).

### 1.5.1. Glycine receptor composition in spinal cord – changes over development

In the CNS, GlyR are highly expressed in the spinal cord and brainstem. However, GlyR were already detected in thalamus, hypothalamus, cerebellum, cortex and hippocampus, being also expressed in retina (revised in Lynch 2004).

Due to the very important role of glycine-mediated synaptic activity in spinal cord, where glycine is the main inhibitory neurotransmitter, GlyR have been extremely well characterized in this tissue, at mRNA (messenger ribonucleic acid) and protein levels.

Over development there is an alteration in the subunit composition of GlyR. In immature spinal cord neurons it is consensual that α2 is the abundant isoform, and GlyR are mostly α2 homomeric. The α1 subunit dominates in mature spinal cord neurons in association with β subunit forming αβ heteromeric receptors (Becker *et al.* 1988).

Later on, a study of the GlyR subunits mRNA, by *in situ* hybridization, showed that in immature neurons (embryonic) the α2 subunit has a high expression level, which decreases after birth. Contrastingly, the α1 and β subunits mRNAs expression is low in immature neurons, increasing after birth (Malosio *et al.* 1991b), which is in accordance with the protein expression analyzed.

This switch in GlyR subunit composition is completed by around postnatal day 20. However, this temporal window originates the co-existence of several subunits and consequently, implies a mixture of receptor isoforms. Originally, it was thought that this switch was complete at adulthood and that the α2 subunit was no longer present, but now there are evidences that the α2 subunit is still expressed in mature neurons of the auditory brainstem (Piechotta *et al.* 2001). The localization of the homomeric and the heteromeric GlyR are not identical, since the heteromeric GlyR are composed by α and β subunits, allowing the binding to gephyrin (Meyer *et al.* 1995), which is crucial to the anchoring of GlyR in the synaptic membrane. The homomeric GlyR freely diffuse throughout the plasmatic membrane being considered extrasynaptic receptors (Sola *et al.* 2004).

The synaptic GlyR are mainly responsible for a fast and phasic neurotransmission while the extrasynaptic GlyR are involved in the slow and tonic modulation of the neuronal activity (Muller *et al.* 2008).

## 1.6. Glycinergic neurotransmission in the hippocampus

In the hippocampus, where GABA is the main inhibitory neurotransmitter, the role of glycine as a neurotransmitter has been disregarded. In this brain region, the dual role of glycine as an inhibitory neurotransmitter and as an agonist of the excitatory NMDA receptors, increasing inhibition and potentiating excitation, respectively, is particularly relevant due to the hippocampal network.

Despite the presence of GABAergic synapses in the hippocampus, it was detected by immonohistochemical assays that GABAergic interneurons contain glycine and express GlyT2, suggesting the existence of mixed synapses, which release both GABA and glycine (Danglot *et al.* 2004, Song *et al.* 2006), as already described in spinal cord neurons (Jonas *et al.* 1998). However, a small portion of cells only release glycine, being denominated of pure glycinergic neurons (Danglot *et al.* 2004, Song *et al.* 2006).

Glycine levels decrease from the embryonic stage until young adulthood, contrary to what happens for GABA. It was already documented that in the mouse embryonic brain glycine levels are 3-4 fold higher than GABA, while in the brain of 3-4 weeks old animals glycine concentration is about 2.6 fold lower than GABA. However, the most abundant neurotransmitter in the embryonic brain is taurine, an agonist of GlyR (Benitez-Diaz *et al.* 2003, revised in Avila *et al.* 2013a).

The glycine concentration in the cytosol of the presynaptic neurons vary between 20 and 40 mM, whereas the extracellular levels of glycine are around 0.1-0.2 μM at non stimulated conditions, being able to reach the mM range after the neuronal stimulation (Dohi *et al.* 2009). In the extrasynaptic region, glycine levels are described to be 100-1000 lower than in the synaptic ones (revised in Harsing & Matyus 2013).

In the last years, GlyR expression in the hippocampus has been established using electrophysiological (Chattipakorn & McMahon 2002), immunocytochemical (Brackmann *et al.* 2004, Levi *et al.* 2004, Meier & Grantyn 2004), immunohistochemical (Danglot *et al.* 2004) and *in situ* hybridization approaches (Malosio *et al.* 1991b). At the cellular level, GlyR expression in the hippocampus was detected in pyramidal cells and in interneurons (Song *et al.* 2006), being 5-6 times lower than in the spinal cord and around 2-3 times lower than $GABA_AR$ (Danglot *et al.* 2004).

It was described the expression of GlyR composed by α2 and β subunits in embryonic neurons (Malosio *et al.* 1991b). Moreover, it was recently established that, in the immature brain, the activation of homomeric GlyRα2 in interneurons, leads to the opening of

voltage-gated $Ca^{2+}$ channels and to the consequent increase of intracellular $Ca^{2+}$ levels, which promotes neuronal migration (Avila *et al.* 2013b).

Nevertheless, the GlyR composition in the adult hippocampus seems to be different that the one found in the spinal cord. *In situ* hybridization studies showed that the transcripts for α2, α3 and β subunits were present in the mature hippocampal neurons, which is different from the subunit composition found in the spinal cord mature neurons, where GlyR are mainly composed by α1 and β subunits (Malosio *et al.* 1991b). Actually, it was demonstrated that α3 subunit exist in the brain as two splice variants, α3L and α3K, being the α3L not only the predominant splice variant in the brain but the one that preferentially associates with the glutamatergic nerve endings (Eichler *et al.* 2009).

Over the brain development, the presence of GlyR α2 subunit seems to be important in both immature and mature neurons. To test this hypothesis, it was generated a mouse model with the deletion of this gene by knock out (Young-Pearse *et al.* 2006). Although no morphological or molecular changes were observed in the nervous system, electrophysiology studies showed that these animals do not respond to glycine. However, after P7, glycine is already able to induce a electrophysiological response, which can be explain by a compensatory expression of others GlyR subunits after this stage (Young-Pearse *et al.* 2006).

In hippocampal neurons, as described in spinal cord neurons, was shown the presence of both homomeric GlyR, composed only by α subunits, in extrasynaptic sites and also heteromeric GlyR, composed by α and β subunits, expressed in the post-synaptic membrane (Chattipakorn & McMahon 2002). However, several evidences suggest that most GlyR are homomeric with an extrasynaptic localization, mediating tonic inhibition (Chattipakorn & McMahon 2002, Mori *et al.* 2002, Zhang *et al.* 2008, revised in Xu & Gong 2010).

### 1.6.1. Hippocampus

The hippocampus is a small structure of the limbic system buried deep within the medial temporal lobe of the brain. This region is composed by many millions of neurons organized into a network very different from what is found elsewhere in the nervous system. The hippocampus is very important in learning and memory processes and is also the focus of many clinical studies, since it is involved in some neurological conditions such

as epilepsy or Alzheimer's disease. The physiologic and pathologic characteristics of the hippocampus attracted the scientist's interest and it is, nowadays, one of the cerebral structures more studied in the world (Andersen 2007).

The mammals have two hippocampi, one in each cerebral hemisphere, which have a characteristic curve shape allowing an easy localization and identification. This shape is very similar to a seahorse, which originates his name (from Greek hippos – horse and kampi – curved) (Andersen 2007).

The hippocampus is a heterogenic structure since it is composed by several cells types, compact cell layers and nerve terminals. It is composed by two layers of cortical tissue, binding between them, and formed by two types of cells: the granular cells of the dentate gyrus (DG) and the pyramidal cells of the *cornu ammonis* (CA) areas. The CA region is usually divided in four areas, identified as CA1-4, being the CA1 area localized closely to the cortex and the CA4 the area that directly get in touch with the DG cells. Closely to the CA1 region exists a specific structure called the subiculum (Andersen 2007).

Besides pyramidal and granular cells, other neuronal cell type exists in the hippocampus, the interneurons. Interneurons are a very heterogeneous group of neurons that are found in all hippocampal layers and are immunoreactive for GABAergic markers, so most are thought to be GABAergic neurons (Andersen 2007).

Going into detail on the hippocampus laminar organization, three layers can be found in the entire CA region (Figure 1.11.A). The main layer is the *stratum pyramidale* that is tightly packed in CA1 and more loosely packed in CA2 and CA3, and contains the majority of neuronal cell bodies. These pyramidal neurons are glutamatergic and have predominantly excitatory actions through glutamate release. Adjacent to *stratum pyramidale*, in the external site of the hippocampus, there is a layer called *stratum oriens*. This layer contains several basal dendrites of the pyramidal neurons and some interneurons. Above the *stratum pyramidale*, in the internal side, is the *stratum radiatum*. This layer contains several axons and dendrites that pass through this layer to communicate with others hippocampal regions. Similarly to what happens for *stratum oriens*, *stratum radiatum* contains a variety of interneurons (Andersen 2007).

The DG also has a highly organized structure with several layers (Figure 1.11.A). The major layer of this area is the *stratum granulosum*, where the majority of the neuronal cell bodies are localized. Close to this layer, there is another one, called *stratum moleculare*. The *stratum moleculare* includes several neuronal axons, as well as numerous

interneurons. In the internal side of the *stratum granulosum* there is a region called *hilus*, where some interneurons and synaptic terminals are localized (Andersen 2007).

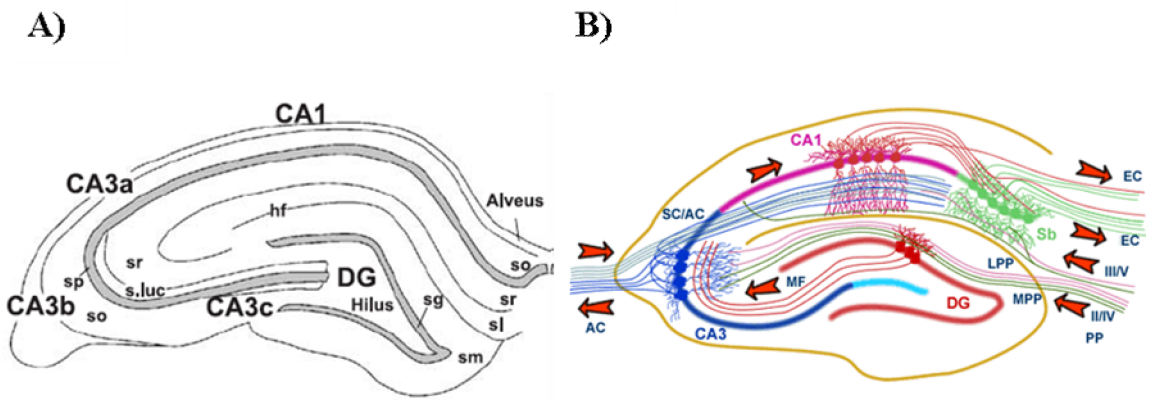


**Figure 1.11. – Diagram of the principal layers and pathways in hippocampus. (A)** Representation of a hippocampal coronal slice with the main regions highlighted (Danglot et al. 2004). **(B)** The hippocampal network. The perforant pathway (PP) starts in the entorhinal cortex (EC) forming connections with the dentate gyrus (DG) and *Cornu Ammonis* 3 (CA3). The DG communicates with the CA3 neurons via the mossy fibers (MF). CA3 send axons to *Cornu Ammonis* 1 (CA1) through the Schaffer Collateral Pathway (SC), as well as to CA1 neurons in the contralateral hippocampus via the associational commissural (AC) pathways. Finally, CA1 cells can also receive inputs from PP and send axons to the subiculum (Sb), which in turn send the main hippocampal output back to the EC, forming a loop. (Adapted from http://www.bristol.ac.uk/synaptic/pathways/).
AC (Associational Commissural Pathway); CA1 – CA3 (*Cornu Ammonis* 1 – 3); DG (Dentate Gyrus); EC (Entorhinal Cortex); Hf (Hippocampal Fissure); LPP (Lateral Perforant Pathway); MF (Mossy Fibers); MPP (Medial Perforant Pathway); PP (Perforant Pathway); Sb (Subiculum); SC (Schaffer Collateral); Sg (*stratum granulosum*); S.luc (*stratum lucidum*); Sm (*stratum moleculare*); So (*stratum oriens*); Sp (*stratum pyramidale*); Sr (*stratum radiatum*).

In the hippocampus there is a group of unidirectional pathways, where the most important are the *Perforant Pathway*, the *Mossy Fiber Pathway* and the *Schaffer Collateral Pathway* (Figure 1.11.B).

The *Perforant Pathway* can be divided in lateral and medial pathway and begins in the Entorhinal Cortex (EC) layer II, projecting connections to the DG and CA3. This pathway is the main responsible for the inputs to the hippocampus. Additionally, the EC layer III communicates directly with the CA1 neurons (Andersen 2007).

By other hand, the DG granule neurons communicate with the CA3 pyramidal cells through the *Mossy Fiber Pathway*. Furthermore, the CA3 neurons can project axons to the CA1 region forming the *Schaffer Collateral Pathway,* one of the most known and studied

hippocampal pathways. On the other hand, CA1 cells in the contralateral hippocampus receive inputs from CA3 through the *Associational Commisural Pathway* (Andersen 2007).
The CA1 neurons can also receive inputs from the *Perforant Pathway* and can also communicate with the subiculum, which project axons to the EC, forming a loop. This pathway is the major output of the hippocampus (Andersen 2007).

It is relatively easy to recognize the diverse regions of the hippocampus. However, to compare the two principal cell types of the same animal and between different animals, it is necessary to have into account that the brains have to be carefully oriented (Palkovits 1988).
The hippocampus is one of the brain regions more susceptible to epileptiform activity. Nevertheless, it is not known if it is the abnormal alterations in the hippocampus that cause epilepsy or if it is the epileptic activity that damages the hippocampus (Andersen 2007).

## 1.7. Glycinergic neurotransmission and neuronal diseases

There are several signs that the glycine-mediated neurotransmission can have important roles in movement disorders like hyperekplexia and epilepsy (Brackmann *et al.* 2004).
Hyperekplexia is a genetic neuromotor disorder that manifests through an exaggerated startle response to unexpected visual, auditory or tactile stimulus (Dutertre *et al.* 2012).
There are several gene mutations affecting glycinergic neurotransmission that cause hyperekplexia (Davies *et al.* 2010). Mutations in the loop between TM2 and TM3 of GLRA1, the gene that encodes for GlyR α1 subunit (Rajendra *et al.* 1994), in the β subunit (Rees *et al.* 2002, James *et al.* 2013), in gephyrin (Rees *et al.* 2003) and also in GlyT2 (Gomeza *et al.* 2003b, Harvey *et al.* 2008) were already described.
These GlyR mutations can have several consequences that ultimately lead to a reduction of GlyR sensitivity to glycine and a reduction of the GlyR ability to conduct $Cl^-$ ions, which originate a decrease of the number of functional GlyR in the plasma membrane (Lynch 2004).
By other hand, several evidences have emerged showing that components of glycinergic synapses play pivotal roles in epilepsy (see for example Cherubini *et al.* 1981, Kirchner *et al.* 2003, Eichler *et al.* 2008). Epilepsy is a brain disorder characterized by recurrent

seizures caused by excessive electrical discharges (Simonato *et al.* 2006). Glycinergic neurotransmission can be seen as an alternative way of controlling the excessive neuronal activity, since work *in vivo* has demonstrated that exogenous glycine application depresses seizure activity in an animal model of epilepsy (Cherubini *et al.* 1981) and potentiates the anticonvulsant effects of $GABA_AR$ agonists (Seiler & Sarhan 1984). In the hippocampus, exogenous application of glycine suppressed neuronal hyperexcitability in the dentate gyrus, by a strychnine-dependent way (Chattipakorn & McMahon 2003). It was also shown that GlyR agonists could act as anticonvulsants in hippocampus (Kirchner *et al.* 2003) and GlyT1 inhibition, with the consequent accumulation of glycine in the synaptic cleft, was able to reduce seizures in this brain area (Zhang *et al.* 2008). These observations, together with the recent discovery that patients with temporal lobe epilepsy (TLE) show an increased GlyR expression in the hippocampus (Eichler *et al.* 2008), suggest an important role for glycine and GlyR-mediated neurotransmission in this brain area, as well as a potential target within the context of epilepsy.

### 1.7.1. Epilepsy

Epilepsy is a neurological disease that affects the CNS. It is described as the brain propensity to have seizures, an abnormal electric discharge, which can cause involuntary body contractions and uncontrolled convulsions, being sometimes accompanied by consciousness loss (Andersen 2007). It affects around 50 million people worldwide and nearly 80% of epilepsy cases are found in developing countries (data from World Health Organization (WHO) – in September 2014).

Epilepsy causes can be genetic or acquired. Several mutations that can lead to epileptic syndromes were described, including mutations in the subunits of $Na^+$, $K^+$, $Ca^{2+}$ channels and in several genes involved in GABAergic neurotransmission namely in GABA synthesis, in the control of GABA levels and in genes that codify for the GABA receptors subunits (Noebels 2003). By other hand, acquired epilepsy can be caused by a brain tumour, a stroke with brain hypoxia, a brain infection, head trauma, etc. These actions will initiate a cascade of cellular events that can lead to seizures development and to epilepsy progress (Simonato *et al.* 2006).

Seizures are the neurological consequences of hyperexcitability and hypersynchronized electric activity in the brain and can be caused by an insufficiency in inhibitory

neurotransmission or by an increase in excitatory neurotransmission (Delpire 2000). The seizures can be split into two types: partial (or focal) seizures, when seizures occur in a specific area of the brain and generalized seizures, arising simultaneously throughout the cortex, representing 40 and 50% of seizures, respectively (10% are unclassifiable) (Andersen 2007).

Nowadays, the therapy used for epilepsy acts on essential functions of the CNS (GABAergic neurotransmission, $Ca^{2+}$ channels and $Na^{+}$ channels) and frequently causes undesirable side effects due to their roles in hippocampal synaptic activities. Furthermore, near 30% (data from WHO – in September 2014) of the cases remain refractory to available pharmacotherapy, for which the only solution is surgery. So, an alternative pharmacologic therapy urges to be found. A new therapy based on inhibitory glycinergic transmission, less crucial than GABAergic transmission in the hippocampus, could prove useful and with less side effects.

Epilepsy can be divided in several syndromes, which have different pathophysiologies and mechanisms. One of those syndromes is TLE that represents approximately 60% of all partial epilepsies, being the most frequent type of focal epilepsies (Andersen 2007). In TLE the seizure focus is localized in the mesial temporal lobe, a region that includes the hippocampus and the entorhinal cortex, causing a deep neurodegeneration in these areas and subsequently a proliferation of astrocytes and microglia (Haglid *et al.* 1994).

## 1.8. Neurothrophins

Until now, there are four types of neurotrophins characterized in mammals: the nerve growth factor (NGF), the brain-derived neurotrophic factor (BDNF), the neurotrophin-3 (NT-3) and neurotrophin-4 (NT-4). The first neurotrophin to be discovered and isolated was NGF in the early 1950s by Levi-Montalcini and Cohen (Levi-Montalcini & Hamburger 1951, Cohen *et al.* 1954) and for that discovery they won the Nobel Prize in Physiology or Medicine in 1986. Only in 1982, Barde and co-workers isolated a second type of neurotrophin, from the pig brain, the BDNF (Barde *et al.* 1982). Afterwards, other neurotrophins have been identified in mammals, namely NT-3 (Phillips *et al.* 1990) and NT-4 (Ibanez *et al.* 1993), which are very similar in sequence and structure (Hallbook 1999).

The neurotrophins are proteins involved in the regulation of neuronal growth, survival and differentiation (Blum & Konnerth 2005). They are synthesized by neurons and also by non-neuronal cells in the form of precursor proteins, pre-pro-neurotrophins. Following the removal of a signal peptide localized at the N-terminal, the pro-neurotrophin is obtained and is able to form homodimers in the endoplasmic reticulum. After that, the pro-neurotrophin can be cleaved, originating the mature neurotrophin, or can be released by the cell in an unprocessed form (Seidah *et al.* 1996, Bartkowska *et al.* 2010). Once in the extracellular space, the pro-neurotrophin will be the target of extracellular proteases that will cleave it in order to achieve the mature form (Pang *et al.* 2004). The mature neurotrophins can then act in a paracrine or autocrine mode, being important regulators of several processes of the CNS, including the control of neurotransmitter release (Bartkowska *et al.* 2010). The cells can release neurotrophins by two ways: 1) a regulated pathway, that occurs when neurotrophins are secreted in response to a stimuli and 2) a constitutive pathway, which happens when neurotrophins are spontaneously secreted (Blum & Konnerth 2005).

### 1.8.1. Neurotrophins Receptors

The neurotrophins can activate two different families of receptors, the tropomyosin-related kinase (Trk) receptors, which belong to the tyrosine kinase family of receptors, and the p75 pan-neurotrophin receptor (p75 NTR) (Patapoutian & Reichardt 2001, Roux & Barker 2002, Binder & Scharfman 2004). Only the mature forms and not the pro-forms of the neurotrophins are able to activate the Trk receptors, while the p75 NTR can be activated by all neurotrophins, including the pro-forms, with high affinity, and the mature ones, with low affinity (Figure 1.12.) (Lee *et al.* 2001). Therefore, the biological role of neurotrophins is regulated by the proteolytic cleavage, since the pro-neurotrophins mainly activate the p75 NTR, promoting cell death by apoptosis, while the neurotrophins predominantly activate Trk receptors supporting cell survival (Lee *et al.* 2001).

The p75 NTR is a member of the tumour necrosis factor receptor superfamily and has a similar low affinity for all the neurotrophins. This receptor has an extracellular region susceptible to glycosylation, a transmembrane domain and a short intracellular region lacking intrinsic catalytic activity (Chao & Hempstead 1995, Binder & Scharfman 2004). Although with no catalytic activity, p75 NTR binds to adaptor proteins, modulating several

neuronal signalling pathways, like nuclear factor-kB (NF-kB), jun kinase and RhoA pathways (Reichardt 2006). Additionally, p75 NTR is also present in astrocytes, where it regulates the cell cycle and have no effects in apoptosis (Cragnolini *et al.* 2009, Cragnolini *et al.* 2012). However, in general, when Trk receptors are activated the p75 NTR-mediated signalling is suppressed (Patapoutian & Reichardt 2001).

Regarding the Trk receptors, three types of high affinity Trk receptors, which specifically recognize a different neurotrophin, were already described. Namely, tropomyosin-related kinase A (TrkA) recognizes NGF, tropomyosin-related kinase B (TrkB) binds BDNF and NT-4/5 while tropomyosin-related kinase C (TrkC) is activated by NT-3 (Figure 1.12.) (Bartkowska *et al.* 2010). Moreover, NT-3 can also bind to TrkA and TrkB with low affinity and in some cellular conditions (Patapoutian & Reichardt 2001).

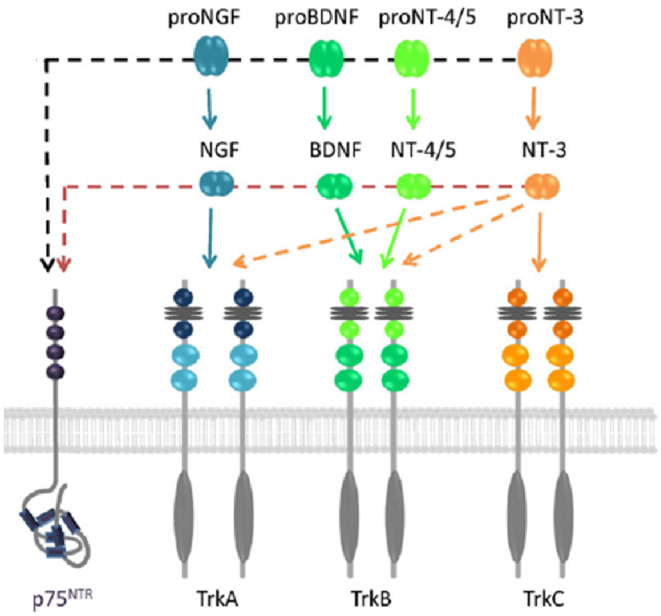


**Figure 1.12. – Neurotrophins receptors specificity.** All the pro-neurotrophins and the neurotrophins can bind to p75 pan-neurotrophin receptor (P75 NTR), with high and low affinity, respectively. The tropomyosin-related kinase (Trk) receptors can only be activated by the mature forms: nerve growth factor (NGF) activates TrkA, brain-derived neurotrophic factor (BDNF) and neurotrophin-4/5 (NT-4/5) bind to TrkB and neurotrophin-3 (NT-3) activates predominantly TrkC (Hondermarck 2012).

The TrkB receptors include full length (TrkB-FL), truncated receptors 1 (TrkB-T1) and 2 (TrkB-T2), and truncated receptors that contain a Shc (Src homology 2/α-collagen-related

protein) binding site (TrkB-T-Shc), which can be obtain by alternative splicing (Klein *et al.* 1990, Stoilov *et al.* 2002).

The TrkB-FL is composed by an extracellular ligand binding domain, a transmembrane domain and a tyrosine kinase intracellular domain with several tyrosine residues susceptible to phosphorylation. By other hand, the truncated isoforms have an extracellular domain 100% homologous with TrkB-FL, but have a small cytoplasmic domain lacking the kinase domain (Figure 1.13.) (Middlemas *et al.* 1991, Shelton *et al.* 1995, Stoilov *et al.* 2002). The TrkB-T1 and TrkB-T2 isoforms differ in the intracellular domain's length, having 23 and 21 amino acids, respectively (Klein *et al.* 1990, Middlemas *et al.* 1991). The TrkB-T-Shc is predominantly expressed in the human brain and has an exclusive intracellular domain with a Shc binding site (Stoilov *et al.* 2002).

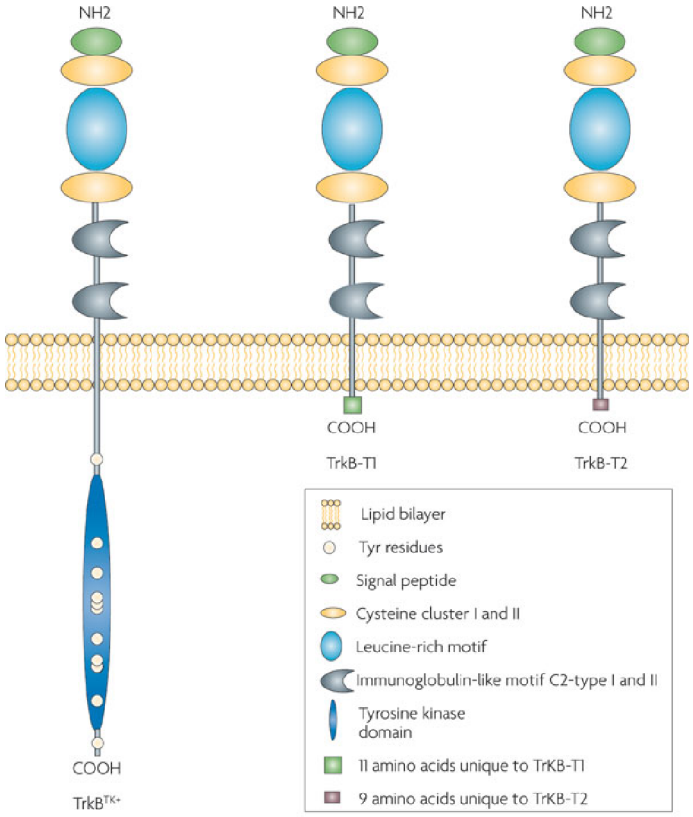


**Figure 1.13. – Different isoforms of TrkB receptors obtained by alternative splicing.** The extracellular and the transmembrane domains are common to all tropomyosin-related kinase B (TrkB) isoforms. The TrkB full length (TrkB-FL – also known as TrkB$^{TK+}$) has an intracellular tyrosine kinase domain, whereas both the TrkB truncated receptors 1/2 (TrkB-T1/2) lack this region, having only a small cytoplasmic domain (Minichiello 2009).

BDNF-binding to TrkB-FL receptors induces receptor dimerization and autophosphorylation of tyrosine residues in the intracellular kinase domain, which activates several signalling cascades (Figure 1.14.), namely, the phospholipase C-γ (PLC-γ) / PKC, phosphatidylinositol-3 kinase (PI3K) / protein kinase B (Akt) and mitogen-activated protein kinase (MAPK) pathways, which crosstalk between them (Blum & Konnerth 2005, Sebastiao *et al.* 2011).

The phosphorylation of tyrosine residues creates large intracellular signalling complexes. In detail (Figure 1.14.), tyrosine phosphorylation in the position 515 (Y515) originates the binding site for the adaptor proteins Shc. By one hand, this will lead to the activation of PI3K and Akt and by other to the increase in Ras GTPase and MAPK activities. The activation of the Akt pathway increases mainly the neuronal survival and the activation of the MAPK pathway enhances the neuronal survival, differentiation and growth. Nevertheless, the tyrosine 816 (Y816) phosphorylation catalyzes the formation of the binding site for PLCγ, initiating the subsequent downstream pathway. This leads to the generation of inositol 1,4,5-triphosphate (IP3) and diacylglycerol (DAG), which are involved in the release of $Ca^{2+}$ from intracellular stores and activation of $Ca^{2+}$ and DAG-regulated protein kinases, with implications in synaptic transmission and plasticity (Huang & Reichardt 2003, Reichardt 2006). Moreover, these three main pathways can activate the calmodulin-dependent protein kinase II/IV (CaMK II/IV), which will phosphorylate the cyclic adenosine monophosphate (cAMP) response element-binding protein (CREB), which is a transcription factor that will modulate gene transcription (Patapoutian & Reichardt 2001).

The expression of the TrkB-T isoforms reduces the response to BDNF mediated by TrkB-FL. Either it acts as a dominant-negative receptor by inhibiting the homodimerization of the TrkB-FL receptors and the consequent intracellular signaling cascades, through the formation of TrkB-FL / TrkB-T heterodimers, (Eide *et al.* 1996), or by binding BDNF, preventing its diffusion and causing its internalization (Biffo *et al.* 1995). Thus, in the brain, three types of TrkB dimers were already detected: TrkB-FL homodimers, TrkB-T homodimers and TrkB-FL/TrkB-T heterodimers (Ohira *et al.* 2001).

A similar expression of TrkB-FL and TrkB-T isoforms was described in primary neuronal cultures, while in primary cultures of astrocytes TrkB-T are more expressed than the TrkB-FL. Moreover, as the astrocytes differentiate, from 4 days to 14 days in culture, it is possible to observe a decrease, both at the mRNA and at the protein levels, of the TrkB-FL

receptors while the TrkB-T isoforms are consistently the predominant TrkB receptors (Climent *et al.* 2000).

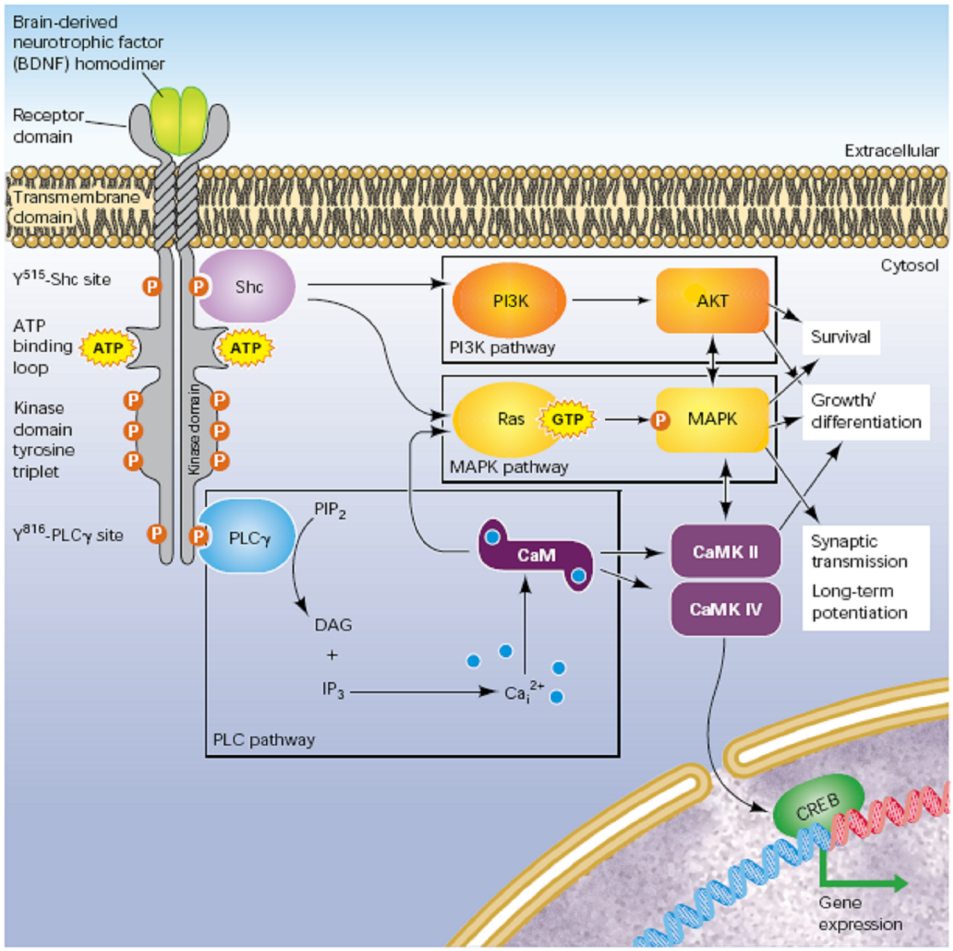


**Figure 1.14. – Binding of BDNF to TrkB receptor and activation of the downstream signalling pathways.** Brain-derived neurotrophic factor (BDNF) induces tropomyosin-related kinase B (TrkB) receptor dimerization and autophosphorylation of tyrosine residues in the intracellular kinase domain. Phosphorylation of tyrosine in the position 515 (Y515) creates the binding site for Shc (Src homology 2/α-collagen-related protein), whereas phosphorylation of tyrosine 816 (Y816) forms the adaptor site for the phospholipase C (PLCγ). The activation of intracellular signaling pathways mediate effects of BDNF on cell survival, growth, differentiation, synaptic transmission, long-term potentiation and gene expression (Blum & Konnerth 2005).

Akt (protein kinase B); ATP (adenosine-5'-triphosphate); $Ca_i^{2+}$ (intracellular calcium ions); CaM (calmodulin); CaMK II/IV (calmodulin-dependent protein kinase II/IV); CREB (cyclic adenosine monophosphate (cAMP) response element-binding protein); DAG (diacylglycerol); GTP (guanosine-5'-triphosphate); IP3 (inositol 1,4,5-trisphosphate); MAPK (mitogen-activated protein kinase); PIP2 (phosphatidylinositol 4,5-bisphosphate); PI3K (phosphatidylinositol 3-kinase).

TrkB-T isoforms don't have the intracellular kinase domain (Blum & Konnerth 2005, Sebastiao *et al.* 2011). However, TrkB-T receptors, in which the TrkB-T1 is the most studied, can also activate signalling pathways. It was described that TrkB-T receptors are able to mediate BDNF-evoked $Ca^{2+}$ signalling in glia cells (Figure 1.15.) (Rose *et al.* 2003). These authors confirmed that astrocytes mainly express the TrkB-T1 isoform and that the BDNF-dependent $Ca^{2+}$ release is mediated by the activation of PLC. Additionally, it was demonstrated that TrkB-T1 induces filopodia and neurite outgrowth (Yacoubian & Lo 2000), controls the morphology and cytoskeletal changes of astrocytes (Ohira *et al.* 2005a, Ohira *et al.* 2007) and glioma cells (Ohira *et al.* 2006), stimulates PKC through G protein activation (Cheng *et al.* 2007) and regulates Rho GTPase activity (Ohira *et al.* 2005a) (Figure 1.15.). This modulation of Rho GTPases activity occurs through the interaction between TrkB-FL and Rho GDP dissociation inhibitor (RhoGDI1) (Ohira *et al.* 2005a). When BDNF binds to TrkB-T1, this interaction is lost and RhoGDI1 is available to bind and inhibit RhoGTPases, which regulate Rho-associated protein kinase (ROCK) and MAPK pathways (Ohira *et al.* 2006). Additionally, it was discovered that TrkB-T1 receptors interact with other proteins with an unknown function like truncated-TrkB interacting protein (TTIP) (Kryl & Barker 2000), which suggests that TrkB-T1 receptors might interact with other still unidentified molecules (Rose *et al.* 2003, Fenner 2012). Taking into account all the TrkB-T1 functions described above, TrkB-T1 is an important receptor able to activate signalling pathways and to regulate cellular processes (Fenner 2012).

### 1.8.2. BDNF actions in the synapse

BDNF can exert its action through the activation of TrkB receptors leading to the triggering of several intracellular pathways, which promote neuronal differentiation, survival and growth (Blum & Konnerth 2005).

In the specific case of hippocampus, where it is known that BDNF has a high expression (Conner *et al.* 1997), it was described that stimulation inducing long-term potentiation (LTP) increases BDNF mRNA levels (Patterson *et al.* 1992) and that the synaptic activity causes the release of BDNF. This BDNF is then prone to act on populations of pre- and/or post-synaptic TrkB receptors, modulating neuronal activity and plasticity (Andersen 2007). BDNF can also regulate the expression and localization of several synaptic proteins, like

synaptogamin, syntaxin or synapsin I, during the process of synaptic vesicle formation and fusion with the plasmatic membrane (Fenner 2012).

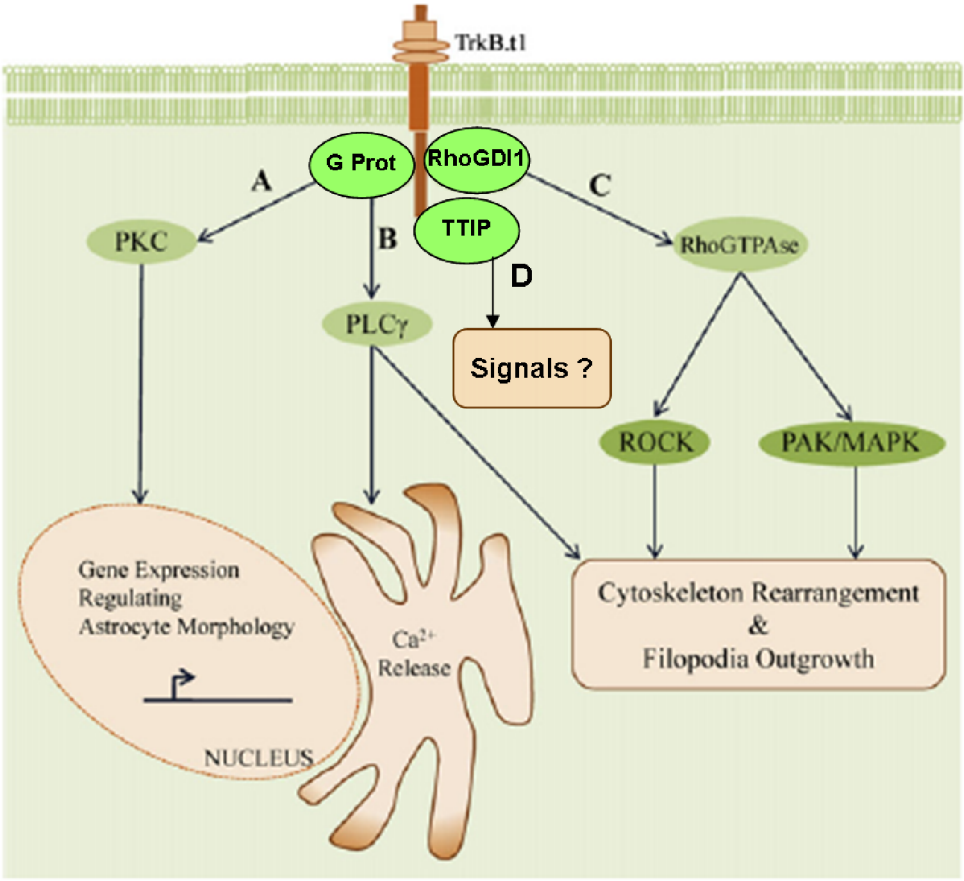


**Figure 1.15. – TrkB-T1 intracellular signalling pathways in astrocytes. (A)** Truncated 1 tropomyosin-related kinase isoforms (TrkB-T1) can stimulate the protein kinase C (PKC) signalling pathway, through G proteins (G Prot) activation. This will induce gene expression that will drive stem cells to adopt a glial cell phenotype, causing a rearrangement of the astrocyte morphology. **(B)** The G protein's activation can also stimulate phospholipase C (PLCγ), which will increase the calcium ions ($Ca^{2+}$) release from internal stores and cytoskeleton rearrangement. **(C)** TrkB-T1 can bind to Rho-GDP dissociation inhibitor 1 (RhoGDI1) and regulate RhoGTPase activity, which can lead to cytoskeleton rearrangement and filopodia output. **(D)** TTIP (truncated TrkB-interacting protein) can also bind to TrkB-T1 but their downstream signals are not completely understood (Adapted from Fenner 2012).
MAPK (mitogen-activated protein kinase); PAK (p21-activated kinases); ROCK (Rho-associated protein kinase).

BDNF, acting through TrkB-FL, has fast actions on hippocampal synapses leading to the facilitation of synaptic activity (Diogenes *et al.* 2004) and to the increase of glutamate

receptors levels in the post-synaptic neuronal membrane, namely NMDA (Caldeira *et al.* 2007b) and AMPA (α-amino-3-hydroxy-5-methyl-4-isoxazolepropionic acid) (Caldeira *et al.* 2007a). By other hand, BDNF can also modulate the pre-synaptic components, by enhancing pre-synaptic glutamate release (Lessmann & Heumann 1998, Canas *et al.* 2004) and inhibiting GABA release (Canas *et al.* 2004). Moreover, it was shown that BDNF reduces the GABAergic synaptic neurotransmission (Tanaka *et al.* 1997) and increases GABA uptake by enhancing the number of membrane GABA transporters (GAT) in primary cultures of astrocytes (Vaz *et al.* 2011). It also decreases GABA uptake in rat hippocampal nerve terminals (Vaz *et al.* 2008).

In general, BDNF seems to potentiate excitatory synapses and restrain inhibitory (specifically GABAergic) synapses (revised in Binder & Scharfman 2004).

### 1.8.3. BDNF and epilepsy

There are several evidences that epileptiform activity increases the hippocampal BDNF expression both at mRNA (Mudo *et al.* 1996) and protein levels (Rudge *et al.* 1998), which suggests that BDNF increases epileptogenesis (McNamara & Scharfman 2012). Furthermore, in heterozygotes (BDNF +/-) mice, in which only one functional copy of BDNF gene is present, the kindling development is markedly delayed, since these mice developed seizures around two times later than the wild-type mice (BDNF +/+) (Kokaia *et al.* 1995). In fact, after seizures the heterozygotes mice present lower levels of BDNF mRNA compared to wild-type animals (Kokaia *et al.* 1995). Furthermore, animals that overexpress BDNF and that were afterwards injected with kainic acid (KA) showed increased seizures severity (Croll *et al.* 1999). In accordance with this, in the pilocarpine model, perfusion of BDNF decreases the latent period and enhances the seizures severity (Scharfman *et al.* 2002).

In addition, both the inhibition of TrkB receptor (Binder *et al.* 1999b) and the conditional deletion of TrkB receptor (He *et al.* 2004) reduces the kindling development.

However, in mice that overexpress the neuronal TrkB-FL receptor, and consequently have an increase in TrkB-FL signalling, there is an increase in epileptogenesis induced by KA (Heinrich *et al.* 2011). Additionally, in mice that overexpress the neuronal TrkB-T1 receptor, which is a dominant negative receptor of TrkB-FL receptor originating a decrease

of TrkB-FL signalling, a reduction of the seizures severity (Lahteinen *et al.* 2002) and of epileptogenesis in KA model were detected (Heinrich *et al.* 2011).

Moreover, after KA-induced seizures it was detected a transient increase in phospho-TrkB receptor expression, which is directly related to the activation of TrkB receptor (Binder *et al.* 1999a). All together, these results indicate that BDNF expression and TrkB receptors activation increase after seizures, which will contribute to epileptogenesis (Binder *et al.* 2001).

By other hand, chronic perfusion of BDNF blocked the kindling development, which suggests a protective role of BDNF in seizures generation (Larmet *et al.* 1995). These controversial results can be explained by the discovery that the previous exposure of neurons to BDNF, in culture and in the rat adult brain, originates a decrease in TrkB receptor expression, caused by BDNF desensitization (Frank *et al.* 1996, Binder *et al.* 2001). Nevertheless, the injection of a viral vector expressing fibroblast growth factor-2 and BDNF in a lesioned hippocampus, three days after the pilocarpine-induced status epileptic, increases neurogenesis but decreases epileptogenesis. Thus, at this stage, which can be comparable to a potential therapeutic approach (after the epileptic episode), BDNF is thought to act as a repair agent and helping to control the disease progression and leading to an unexpected analysis of the pathological hallmarks. Nevertheless, the opposite BDNF effect observed in epileptogenesis can be related to the different phases of the disease (Paradiso *et al.* 2009).

Based on the above, the relationship between BDNF and epilepsy is still contradictory and controversial and seems to be related to the temporal context.

## 2. Aims

The main focus of this work was to investigate the key players of glycine-mediated neurotransmission in rat hippocampus, in the three components that comprise the tripartite synapse.

The work was therefore divided in three specific goals:

1) - Explore GlyR in the post-synaptic neurons

- Analysis of GlyR localization,
- Study of GlyR subunit composition;

2) - Investigate GlyT1 and GlyT2 in astrocytes

- Assessment of GlyT1 and GlyT2 expression, localization and function,
- Evaluation of the BDNF effect upon glycine uptake mediated by GlyT1 and GlyT2;

3) - Examine GlyT2 in the presynaptic neurons

- Description of GlyT2 expression and function,
- Evaluation of the BDNF action in GlyT2-mediated glycine uptake.

# 3. Techniques

## 3.1. Primary cultures of astrocytes

The technique which directly isolate the cells from an animal allowing them to grow under controlled conditions and outside of their natural environment is commonly called primary cell culture, being used in laboratories from all over the world.

The concept behind this technique started to be developed more than 100 years ago by Ross Granville Harrison, an influent embryologist who successfully cultured frog spinal tissue maintaining the cells alive up to 4 weeks, being a pioneer in tissue culture (Harrison 1912, Gahwiler 1999). However, it was only in 1972 that the first monolayer of primary cultures of brain astrocytes was described (Booher & Sensenbrenner 1972), being the protocol used nowadays very similar to the one described by Booher and Sensenbrenner or with the modifications introduced some years after (McCarthy & de Vellis 1980).

During the time in culture, the glial cells divide, differentiate, acquire characteristics of their original tissue, and finally die. Neurons are not capable of dividing, but they can differentiate. However, these cells have limited lifespan, since cells become senescence due to alterations in molecular and cellular structure, causing disruption in their metabolism and leading to the end of cell cycle (Lange *et al.* 2012).

Primary culture of astrocytes is a relatively simple method that can be very useful to analyze cell development and function, since it is possible to obtain astrocytic-enriched cultures without a significant presence of other cell types, which is very useful to the study of astrocytes in an independent environment. However, this characteristic is also seen as a disadvantage since primary cultures of astrocytes lack the cells' heterogeneity present in the nervous tissue and consequently the interaction between the different cell types (Lange *et al.* 2012).

The optimal animal age to prepare primary cultures of astrocytes is when the astrogenesis peak takes place, which is after the peak of neurogenesis and before the peak of oligodendrogenesis. In rodents, this time window occurs from 2-3 days prenatal to 2-3 days postnatal (Saura 2007).

### 3.2. Isolated presynaptic nerve terminals (synaptosomes)

The neuronal presynaptic terminal can be isolated originating a structure commonly called synaptosomes. Synaptosomes were initially isolated to identify the subcellular compartment in which acetylcholine is synthesized and to which is bound (Hebb & Whittaker 1958). After that, Whittaker demonstrated by electron microscopy that the fraction separated by differential and density gradients centrifugations, enriched in acetylcholine, consisted almost entirely of nerve endings (Gray & Whittaker 1962), which he called synaptosomes in order to compare them with other subcellular organelles (Whittaker *et al.* 1964).

The synaptosomes are obtained by homogenization of the tissue under isotonic conditions, followed by further isolation through several differential centrifugations. This procedure will lead to the detachment of the nerve terminals from the axon and to the reseal of the plasma membrane surrounding the nerve terminals, creating the synaptosomes. These structures are osmotically sensitive and can contain numerous synaptic vesicles, some larger dense-core vesicles and at least one mitochondrion, retaining the morphological characteristics and chemical properties of the nerve terminals. However, after the isolation process, it is many times observed that synaptosomes retain a small portion of the attached post-synaptic membrane, the one facing the active zone (Bai & Witzmann 2007, Nicholls 2010) .

Nowadays, synaptosomes are widely used as an *in vitro* model to study the uptake, storage and release of several neurotransmitters since they contain all the required molecular machinery, providing an alternative model to others tissue preparations to study membrane properties (Bai & Witzmann 2007, Nicholls 2010).

### 3.3. PCR

The polymerase chain reaction (PCR) based technique revolutionized the molecular biology since it allowed the *in vitro* amplification of DNA (deoxyribonucleic acid) segments, having as a starting point a very small amount of DNA. This technique was developed by Kary Mullis (Mullis 1990) in 1983 and for that he received the Nobel Prize in Chemistry in 1993.

The PCR is based in an enzymatic amplification of specific DNA sequences using two small sequences of oligonucleotides (named forward and reverse primers) that flank the DNA segment to be amplified. The primers must complement opposite DNA strands so that after annealing, their 3' ends in effect face each other (Strachan 2004).

The PCR procedure has three steps, which are usually repeated many times in a cyclic manner (Figure 3.1.): denaturation, annealing and extension. The denaturation consists in heating the reaction to 93-95ºC causing the melting of the original double-stranded DNA sample and originating two single DNA strands. The annealing is the step where the binding of the primers to their complementary DNA sequences occurs, flanking the DNA regions to be amplified. It takes place at low temperatures (50-70ºC), depending of the primers melting temperature. In the extension phase, the enzyme DNA polymerase (EC 2.7.7.7) elongates the new DNA strand by base complementary at temperatures between 70 and 75ºC (Strachan 2004).

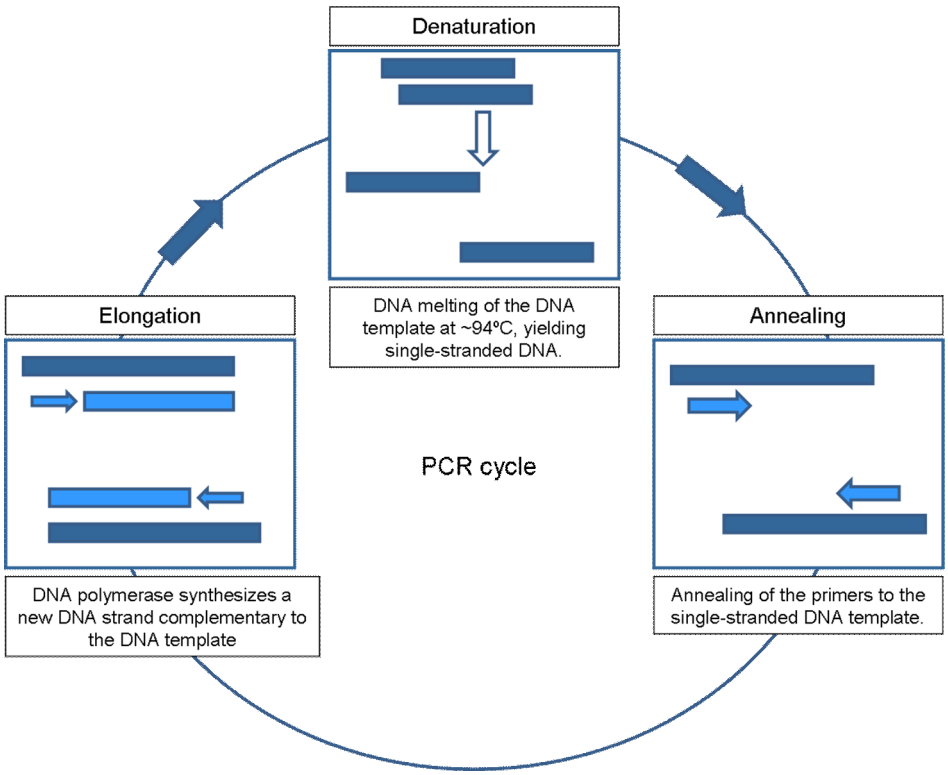


**Figure 3.1. - Schematic representation of a PCR cycle.** Each PCR cycle involves three steps: DNA denaturation, annealing and elongation. DNA (deoxyribonucleic acid); PCR (polymerase chain reaction). (Wilson 2005).

The extension products of one primer provide a template for the other primer in a subsequent cycle, so each successive cycle essentially doubles the amount of DNA. This results in the exponential accumulation of the specific target fragment by approximately $2^n$, where n is the number of cycles. However, with the increase in the number of cycles, a plateau effect occurs, which can be caused by the reagents' degradation or reduction and by the inhibition of DNA polymerase through the accumulation of DNA products (Sambrook 2001).

The original PCR technique has led to the development of several PCR variants. One of these variants is the reverse transcriptase polymerase chain reaction (RT-PCR), which is very useful to analyze mRNA and consequently, DNA coding sequences. This technique starts with the mRNA, which is later on transcribed into its complementary DNA (cDNA). Then, the cDNA will be amplified using the quantitative PCR (qPCR). The qPCR is another PCR variant and is used to detect and quantify the DNA in real time using fluorescent probes, allowing the analysis of gene expression (Wilson 2005).

### 3.4. Immunofluorescence techniques

Immunofluorescence techniques were based in the pioneer work developed by Albert Coons (Coons & Kaplan 1950) and it makes use of the interaction between the protein of interest (antigen) and the antibody that specifically recognizes it. This technique uses the capability of targeting antibodies with fluorophores, which can be detected by a fluorescence microscope, allowing the visualization of the target protein and its consequent localization in a specific area. Moreover, fluorescence microscopy can be used together with confocal microscopy (Harlow 1999).

Immunofluorescence can be applied to several types of preparations such as tissue sections and cultured cells. It can also be employed in *in vivo* studies using organisms genetically modified that express the protein of interest coupled to a fluorescent protein. Additionally, immunofluorescence can be used in combination with other fluorescent dyes, namely DAPI (4',6-diamidino-2-phenylindole) that will bind to DNA (Strachan 2004) allowing the visualization of the cell nucleus.

To detect the protein of interest, two types of immunofluorescence protocols can be used: direct and indirect. The direct method uses a primary antibody labelled with a fluorophore, while the indirect method makes use of an unlabeled primary antibody and a fluorophore-

coupled secondary one, which recognizes the primary antibody (Polak 1997, Harlow 1999).

The limitations of immunofluorescence include the photobleaching, which is the loss of fluorophore activity due to excessive light exposure, and the autofluorescence, which is many times related to the type of fixation used (Harlow 1999).

### 3.5. Western Blot

The western blot is a technique widely used in molecular biology laboratories. It was developed by Harry Towbin (Towbin *et al.* 1979) and Neal Burnette, who give the name to the technique (Burnette 1981). This technique, as happens in immunofluorescence, is based in the specific interaction between the protein of interest (antigen) and the antibody. It is commonly used to detect a specific protein in a tissue homogenate or in a cell extract (Harlow 1999).

The western blot procedure can be divided in three steps: protein separation by gel electrophoresis, protein transfer to a solid support and finally protein detection. There are many variants of this technique, but the most common type of gel electrophoresis is the electrophoresis in denaturant conditions, frequently known as SDS-PAGE (sodium dodecyl sulfate polyacrylamide gel electrophoresis). This technique uses polyacrylamide gels and separates the proteins of the sample by their molecular weight and thus the smaller proteins migrate faster than the bigger ones (Harlow 1999). After the separation, proteins are transferred by electroblotting to a solid support, typically nitrocellulose or polyvinylidene difluoride (PVDF) membranes, which are then labelled with the antibodies against the protein of interest. The membranes are an exact copy of the gel where the proteins were firstly separated. Due to their high affinity for proteins, membranes are usually blocked with a protein-enriched solution to avoid the non-specific binding of antibodies (Harlow 1999). Finally, the proteins are visualized using a primary antibody that specifically recognizes the protein in study, in this case, in a denatured state. As described for the immunofluorescence assays, it is also possible to have the primary antibody labelled (direct method), but it is more common to have a secondary antibody, which will recognize the primary one, linked to an enzyme (indirect method). The enzymatic reactions are the most common type of labelling and can either catalyze a colorimetric or a chemiluminescent reaction. In the first case, when the enzyme interacts with the

appropriate substrate, occurs the formation of a colourful product, whereas in the chemiluminescent method the enzyme-substrate interaction gives rise to a luminescent product. In the case of the chemiluminescent method, the enzyme most regularly used is the horseradish peroxidase (HRP) (EC 1.11.1.7). HRP, in the presence of hydrogen peroxide, catalyses the oxidation of luminol to 3-aminophthalate. The reaction is accompanied by the emission of light at 425 nm which can be captured with an X-ray film, indicating where the HRP-labelled antibody has bound to the primary antibody and consequently to the target protein (Harlow 1999).

# 4. Materials and Methods

## 4.1. Animals

Sprague-Dawley rats, either male or female, were obtained from Harlan (Barcelona, Spain). All experimental procedures were in accordance with the current Portuguese Laws and with the European Union Directive (2010/63/EU) on the protection of animals used for experimental and other scientific purposes. All the experimental work was performed in order to minimize animal suffering and to use the minimum number of animals.

## 4.2. Reagents and Drugs

Unless stated otherwise all reagents were purchased from Sigma (St. Louis, MO, USA). All culture media and supplements were from Gibco (Gibco, Paisley, UK). [$^3$H]glycine (specific activity 44.7 Ci/mmol) was acquired from PerkinElmer (Waltham, MA, USA). Org24598, a specific GlyT1 inhibitor (Brown *et al.* 2001), ALX1393 (Luccini & Raiteri 2007) and amoxapine (Nunez *et al.* 2000), two specific GlyT2 inhibitors, were also purchased from Sigma. Monensin and dynasore, inhibitors of the transporter recycling and of the dynamin/clathrin-dependent endocytosis, respectively, as well as Toxin B from *Clostridium difficile* were also purchased from Sigma. BDNF was kindly supplied by Regeneron Pharmaceuticals (Tarrytown, NY). K252a was obtained from Calbiochem (Billerica, MA, USA). LY294002 and U0126 were achieved from Ascent (Weston-Super-Mare, UK), while U73122 was purchased from Tocris (Bristol, UK). BAPTA-AM (Bis(2-aminophenoxy)ethane-N,N,N′,N′-tetraacetate) was obtained from Molecular Probes (Eugene, OR, USA).

## 4.3. Biological samples extraction

Except otherwise indicated, pregnant females with 18 days of gestation (E18 embryos), animals at postnatal day (P)0 – P21 (P0, P3, P7, P14 and P21) and adult rats (4 or 9 weeks

old) were deeply anesthetized with 2-bromo-2-chloro-1,1,1-trifluoroethane and sacrificed by decapitation. The procedure followed for the animals that were intracardially perfused is explained in detail in subsection "4.9. Tissue fixation".
All the procedures relative to the extraction and preparation of biological samples were made, whenever possible, in ice or with cold solutions, to decrease the temperature and consequently, reduce the cell metabolism and inhibit the action of proteases and ribonucleases.

#### 4.3.1. Spinal cord extraction

The animal (P21) body was placed with the ventral surface facing down. A scissor was introduced in the animal neck and a cut was performed in his skin throughout the entire dorsal region. The dorsal muscles were displaced, exposing the vertebral column, which was carefully open with a small scissor to reveal the spinal cord. The spinal cord was then extracted by cutting the spinal nerves and the spinal meninges. Finally, the blood vessels were removed to completely isolate the spinal cord. The spinal cord was quickly placed in ice cold phosphate buffered saline (PBS) (137 mM NaCl, 2.7 mM KCl, 8 mM $Na_2HPO_4.2H_2O$ and 1.5 mM $KH_2PO_4$, pH 7.4).

#### 4.3.2. Brain extraction

The animal head was placed with the ventral surface facing down and the skin at the top of the head was cut, exposing the skull. First, a scissor was introduced in the *foramen magnum* and by pressuring against the occipital bone to maintain the cerebral tissue intact, the occipital bone was cut and the cerebellum was revealed (Figure 4.1.A). Subsequently, a cut was performed in the sagittal suture between the two parietal bones until the bregma region (Figure 4.1.B). The two parietal bones were gently pulled to the side, exposing the brain, which was carefully lifted with a spatula. The optic and the trigeminal nerves were cut, the brain was removed (Figure 4.1.C) (Palkovits 1983) and quickly placed in ice cold PBS.
To study the prenatal phase, the E18 embryos were dissected in ice cold PBS, and the procedure for brain and hippocampus extraction was similar to the one described above.

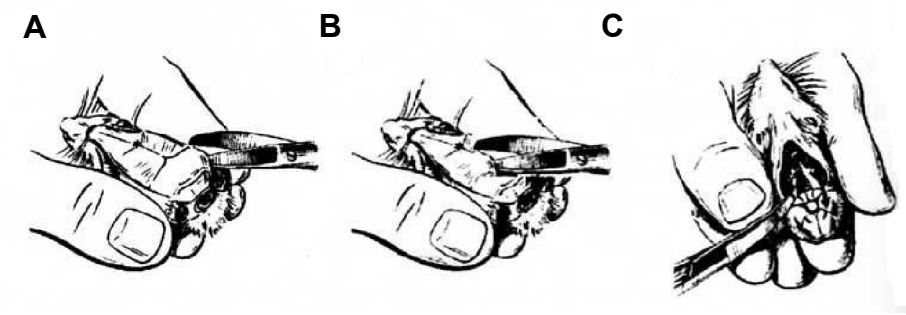


**Figure 4.1. – Rat brain extraction. (A)** – Introduction of a scissor in the foramen magnum to cut the occipital bone. **(B)** – Cut from the saggital suture to the bregma to split the parietal bones. **(C)** – Cut of the trigeminal nerves and extraction of the brain. (Adapted from Palkovits 1983).

### 4.3.3. Hippocampus extraction

The cerebellum was discarded and a cut along the *midline* of the *corpus callosum* was performed to partially split the two cerebral hemispheres, which were positioned with the medial surface facing up. Using small spatulas, the neocortex that is covering the hippocampus was slightly pulled (as indicated by arrows in Figure 4.2.A) and the hippocampus was revealed. Then, with the help of spatulas and tweezers, the hippocampus was lifted and pulled (as indicated by arrows in Figure 4.2.B) until completely cut off (Figure 4.2.C). After meninges and blood vessels removal the hippocampus was isolated (Shahar 1989) and quickly placed in ice cold PBS.

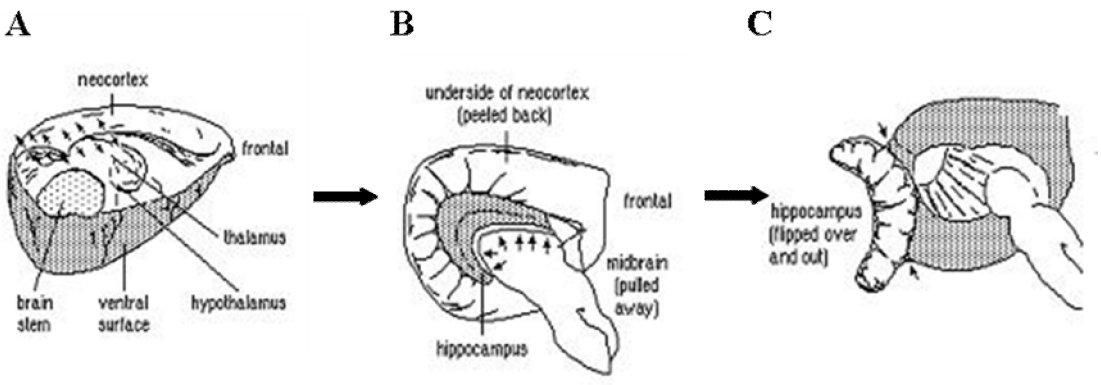


**Figure 4.2. – Hippocampal extraction from rat brain. (A)** – Removal of the neocortex to expose the hippocampus. **(B)** – Beginning of the hippocampus extraction by lifting and pulling it. **(C)** – Total isolation of the hippocampus from the remaining brain. (Adapted from Palkovits 1983).

### 4.3.4. Primary cultures of astrocytes

Astrocytes-enriched cultures were prepared from the cerebral cortex of newborn rat pups (0-2 days old), as reported (Biber *et al.* 1997, Vaz *et al.* 2011). Briefly, the animals were sacrificed by decapitation and the brain was quickly dissected in ice cold PBS. Following meninges and white matter removal, the cerebral cortex was isolated. Cells were vigorously dissociated in 4.5 g/l glucose Dulbecco's Modified Eagles Medium (DMEM) supplemented with 10% fetal bovine serum (FBS) and 1% antibiotic/antimycotic, filtered through a 230 µm cell strainer and centrifuged at 200 g for 10 minutes at room temperature (RT). The pellet was ressuspended in 4.5 g/l glucose DMEM, filtered through a 70 µm cell strainer (BD Falcon, NJ, USA) and centrifuged again. Cells were seeded into 60 mm dishes for western blot and qPCR. For immunocytochemistry assays, cells were plated on poly-D-lysine hydrobromide (PDL) (10 µg/ml)-coated coverslips at a density of 100 000 cells/well. For uptake assays cells were seeded in 24-well plates. Cultures were maintained in an incubator with a humidified atmosphere (5% $CO_2$) at 37°C for 3-4 weeks and medium was renewed twice a week.
In order to further purify the cultures from any contaminating microglia cells (McCarthy & de Vellis 1980, Gabryel *et al.* 2002, Gingras *et al.* 2007, Du *et al.* 2010), the plates were shaken overnight on an orbital shaker at 300 rpm at 9 days *in vitro* (DIV).

### 4.3.5. Synaptosomes preparation

The 4-weeks animals were deeply anesthetized and decapitated. The brain was quickly removed into ice-cold continuously oxygenated (95%$O_2$ and 5% $CO_2$) artificial cerebrospinal fluid (aCSF) (124 mM NaCl, 3 mM KCl, 1.2 mM $NaH_2PO_4$, 25 mM $NaHCO_3$, 2 mM $CaCl_2$, 1 mM $MgSO_4$ and 10 mM glucose, pH 7.4). The hippocampi and the entorhinal cortex were dissected out and added to 5 ml of a chilled sucrose solution (0.32 M in 1 mM EDTA (ethylenediaminetetraacetic acid), 10 mM HEPES (N-2-hydroxyethylpiperazine-N'-2-ethanesulfonic acid) and 1 mg/ml bovine serum albumin (BSA), pH 7.40). After homogenization at 4ºC, a first centrifugation (1000 g, 10 min, 4ºC) (Heraeus sepatech – Biofuge 28RS centrifuge) step was performed. The supernatant was collected and centrifuged for a second time (14000 g, 12 min, 4ºC). The pellet, which corresponds to the membrane fraction, was collected and ressuspended in 3 ml Percoll

solution (Percoll 45% (v/v) in Krebs-Henseleit-Ringer (KHR) solution: 140 mM NaCl, 1 mM EDTA, 10 mM HEPES, 5 mM KCl and 5 mM glucose, pH 7.40). This mixture was centrifuged again (14 000 g, 2 min, 4ºC) and the top layer, which is the synaptosomal fraction, was removed, washed with KHR and centrifuged (14000 g, 2 min, 4ºC) for two times. The pellet, which comprised the synaptosomal fraction, was ressuspended in chilled Krebs-HEPES solution (10 mM glucose, 125 mM NaCl, 3 mM KCl, 1.2 mM $MgSO_4$, 1 mM $NaH_2PO_4$, 1.5 mM $CaCl_2$ and 10 mM HEPES, pH 7.4) and kept at 4ºC. Soluble protein was quantified according with the Bradford method (Bradford 1976).

### 4.4. Western Blot

- Hippocampi and spinal cords were isolated and washed in cold PBS, homogenized and solubilised in radioimmunoprecipitation assay (RIPA) buffer (50 mM Tris base pH 8, 1 mM EDTA, 0.1% sodium dodecyl sulfate (SDS), 150 mM NaCl and 1% NP40), supplemented with protease inhibitors (Complete Mini-EDTA free from Roche, Mannheim, Germany), using a Potter homogenizer. The unsolubilized material was removed by centrifugation (11000 x g, 10 min, 4ºC).

- In the case of astrocytes, the lysates were obtained at 10, 18 and 24 DIV. The astrocytes were incubated in lysis buffer (50 mM Tris base pH 8, 5 mM EDTA, 150 mM NaCl, 1% NP40 and 10% glycerol), supplemented with protease inhibitors (Complete Mini-EDTA free from Roche) and 1 mM phenylmethylsulfonyl fluoride (PMSF), on ice during 15 min. The cells were detached from the plate with a cell scraper and the suspension was collected. A centrifugation (11000 x g, 10 min, 4ºC) was used to remove the unsolubilized material.

- The synaptosomes-enriched fractions were maintained in the absence or presence of BDNF (30 ng/ml) and solubilised with lysis buffer (50 mM Tris base pH 8, 5 mM EDTA, 150 mM NaCl and 10% glycerol), supplemented with protease inhibitors (Complete Mini-EDTA free from Roche) and 1 mM PMSF, on ice during 15 min. The unsolubilized material was removed by centrifugation (11000 x g, 10 min, 4ºC).

Soluble protein was quantified with Bio-Rad DC reagent (Peterson 1979) according to the manufacturer's guidelines (Bio-Rad DC Protein Assay from Bio-Rad, Hercules, CA, USA) using BSA as a control sample to perform a calibration curve.

The samples were denatured in the presence of a loading buffer (70 mM Tris pH 6,8, 6% glycerol, 2% SDS, 120 mM dithiothreitol (DTT) and 0,0024% bromephenol blue) at 100ºC during 10 min.

Proteins and protein size markers (Precision Plus Protein Standards from Bio-Rad) were separated on a vertical and discontinuous SDS-PAGE. The samples were applied in a 5% stacking gel (125 mM Tris/HCl pH 6.8, 5% acrylamide, 0.1% SDS, 0.1% N,N,N',N'-tetramethylethylenediamine (TEMED) and 0.1% ammonium persulfate (APS)) and separated in a 10% resolving gel (380 mM Tris/HCl pH 8.8, 10% acrylamide, 0.1% SDS, 0.04% TEMED and 0.1% APS) in the presence of the electrophoresis buffer (12,5 mM Tris base, 96 mM glycine and 0,1% SDS).

After electrophoresis, samples were transferred to a nitrocellulose membrane by electroblotting and blocked with 5% nonfat powder milk in TBS-T (20 mM Tris base, 137 mM NaCl and 0.1% Tween-20) during 1h at RT. In the case of the anti-Akt, anti-phospho Akt, anti-p44/p42 MAPK, anti-phospho p44/p42 MAPK, anti-PLC-γ1 and anti-phospho PLC-γ1 antibodies, samples were transferred to PVDF membranes and the blocking was performed with 5% bovine serum albumin in TBS-T (20 mM Tris base, 137 mM NaCl and 0.1% Tween-20) during 1h at RT.

Following the incubation with the primary antibodies, diluted in 3% BSA in TBS-T (20 mM Tris base, 137 mM NaCl and 0.1% Tween-20), overnight at 4ºC, membranes were incubated with the HRP (EC 1.11.1.7)-conjugated secondary antibodies diluted in 5% nonfat powder milk in TBS-T (20 mM Tris base, 137 mM NaCl and 0.1% Tween-20) for 1 h at RT.

Immunoreactions were visualized with the ECL chemiluminescence detection system (Amersham-ECL Western Blotting Detection Reagents from GE Healthcare, Buckinghamshire, UK). The integrated intensity of each band was calculated using computer assisted-densitometry with ImageJ software 1.44b (http://rsbweb.nih.gov/ij/).

### 4.5. RNA preparation

RNA (ribonucleic acid) was isolated from rat hippocampus and spinal cord homogenates (GE Healthcare RNAspin Mini RNA Isolation Kit), as well as from astrocytes-enriched

cultures. Total RNA integrity was confirmed by gel electrophoresis and quantified in the Nanodrop (ND-1000 Spectrophotometer).

For electrophoresis RNA samples were prepared in loading buffer (60% (v/v) glycerol and 0.3% bromophenol blue) and separated in a 3% agarose gel in TAE (Tris-acetate-EDTA) (20 mM acetic acid, 40 mM Tris base and 1 mM EDTA) pH 8, with 0,4 μg/ml of ethidium bromide. The RNA bands were visualized with a transiluminator (Vilber Lourmat) and photographed with a digital camera (Kodak).

3 μg of total RNA (in 20 μl) was used to synthesize the first-strand cDNA with the SuperScript II Reverse Transcriptase (EC 2.7.7.49, Invitrogen, Carlsbad, CA, USA) according to the manufacturer's guidelines (SuperScript First Strand Synthesis Systems for RT-PCR from Invitrogen). The reaction mixture (50 mM Tris-HCl, pH 8.3, 75 mM KCl and 3 mM $MgCl_2$) included 2.5 ng/μl of random primers, 0.5 mM of each dNTP (deoxynucleotide) (Promega, Madison, WI, USA), 0.01 M of DTT (kit SuperScript First Strand - Invitrogen) and 100U of the reverse transcriptase enzyme (EC 2.7.7.49) (SuperScript II - Invitrogen).

The reactions were carried out in a thermocycler (MyCycler – Bio-Rad) with a profile comprising: 65ºC during 5 min, 25ºC during 2 min, 25ºC during 10 min, 42ºC during 60 min and, finally, 72ºC during 20 min.

### 4.6. RT-PCR

cDNA was amplified in a PCR reaction containing 0.8 μM of each oligonucleotide primer (Invitrogen), 0.05 mM of each dNTP, 1 mM $MgCl_2$ (Promega) and 0.2 units of Taq DNA polymerase (EC 2.7.7.7, Promega). The thermocycler (MyCycler – Bio-Rad, Hercules, CA, USA) profile was 2 min at 94°C, 25-40 cycles with 30 s at 94°C, 90 s at 60°C and 60 s at 72°C followed by a final elongation step of 15 min at 72°C. PCR products and DNA size markers (Hyperladder I from Bioline, London, UK) were separated in a 2% agarose gel in TAE with 0.4 μl/ml ethidium bromide and specific bands were detected with a digital camera (Kodak).

To ensure that product amplification did not arise from genomic DNA, PCR reactions using cDNA synthesized in the absence of reverse transcriptase were also prepared.

## 4.7. qPCR

cDNA was amplified in a PCR reaction containing SYBR Green Master Mix (Applied Biosystems, Foster City, CA, USA) and 0.2 µM of each specific gene primers. The reactions were performed in a Rotor-Gene 6000 real-time rotary analyzer thermocycler (Corbett Life Science, Hilden, Germany) with a PCR profile comprising an initial denaturation for 2 min at 94°C, 50 cycles with 30 s at 94°C, 90 s at 60°C and 60 s at 72°C for GlyR subunits and GlyT genes, followed by a melting curve to assess the specificity of the reactions. The PCR conditions for TrkB genes also included an initial denaturation step for 2 min at 94°C, 50 cycles with 15 s at 94°C, 30 s at 60°C and 30 s at 72°C and, finally, a melting curve to confirm the reactions specificity. The threshold cycle (Ct) and the melting curves were acquired with Rotor-Gene 6000 Software 1.7 (Corbett Life Science).

To determine the relationship between Ct and mRNA levels, calibration curves with 5-fold sequential dilutions of a cDNA with known concentration per each gene were performed. The calibration curves were created by plotting Ct *vs* the log concentration of cDNA, i.e. Ct *vs* log cDNA (ng/µl), which allowed the calculation of cDNA initial concentration for each gene at each developmental stage. These curves also permit to determine PCR efficiency needed for the relative quantification by comparative Pfaffl method (Pfaffl 2001). The relative qPCR establishes the cDNA expression level by normalization with an internal control gene. Normalization of target gene expression is useful in order to compensate sample-to-sample and run-to-run variations and to ensure the experimental reliability. β-actin was used as a reference gene for normalization. For each gene, replica reactions were performed and the mean of the two reactions was used to calculate the corresponding expression level. Two types of negative controls, “no reverse transcription” and “no template”, were run with samples.

All the oligonucleotides primers used in this work were acquired from Invitrogen except the primers for TrkB-FL and for TrkB-T1, which were gently supplied by Dr. Eero Castrén, Helsinki, Finland.

## 4.8. Oligonucleotides

The primers for GlyRα1 and GlyRα3 subunits and also for GlyT2 were designed using the OligoAnalyzer 3.1, provided by Integrated DNA Technologies (Coralville, IA, USA). The

mRNA sequences from *Rattus norvegicus* was obtained from the GenBank sequence database of the National Center for Biotechnology Information (http://www.ncbi.nlm.nih.gov/).

A complete description of the oligonucleotides used in this work is shown in table 4.4. (subsection "4.17. Drugs, antibodies and primers").

### 4.9. Tissue fixation

For immunohistochemistry studies E18, P0 and P7 brains, as well as P21 spinal cords, were isolated as described above and fixed in 4% paraformaldehyde (PFA) in PBS for 1 week at RT. A shorter (48h) fixation time was assayed, but it did not allowed proper fixation of non-superficial brain areas, including the hippocampus. For P14 onwards, brain immersion in 4% PFA for 1 week was not enough for appropriate fixation of deep brain structures, and therefore a fixation step by perfusion was carried out. Several days before the perfusion protocol, the animals were manipulated daily to avoid possible stress effects in the results. At the day of the experiment the rats were deeply anesthetized with pentobarbital (Hikma, London, UK) (60 mg/kg body weight, intraperitoneal injection) and placed with the ventral side of the body facing up and with their forelimbs immobilized. A cut in the skin that covers the thoracic cavity was made, exhibiting the sternum. An incision was performed, to open the thoracic cavity, and the diaphragm was cut (Figure 4.3.A). Then, a rib retractor was used, revealing the lungs, the heart and the big blood vessels. Afterwards, a cannula, which was connected to the perfusion system, was introduced in the left ventricle of the animal heart (Figure 4.3.B), to ensure that the perfused solution goes to the brain through the aorta. Additionally, a small hole in the right atrium was made. The peristaltic pump (Miniplus 3 – Gilson) was turned on at a constant velocity (~13.3 ml/min) and the animal was intracardially perfused with PBS to clean the blood vessels, then with 0.5% heparin in PBS (5000 U.I. / ml) (B. Braun, Melsungen, Germany) to avoid the coagulation, and finally fixed with 4% PFA in PBS as described by others (Danglot *et al.* 2004, Muller *et al.* 2006).

After perfusion, brains were removed and further post-fixed by immersion in 4% PFA for 1 week at RT. Thus, fixation time was made comparable between all developmental stages and possible discrepancies (antibodies reactivity, and consequently, labelling pattern) which might arise from different fixation protocols were minimised.

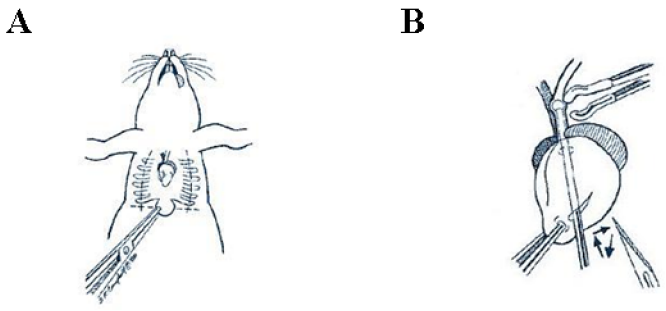


**Figure 4.3. – Schematic representation of intracardial perfusion. (A)** – A cut along the sternum was made to exhibit the thoracic cavity. **(B)** – A cannula was introduced into the left ventricle of the animal heart (Adapted from www.neuroscienceassociates.com/perf-protocol.htm).

## 4.10. Tissue preparation for immunohistochemistry

The tissues (brain and spinal cord) were placed in the appropriate cassette (Roth) for paraffin embedding, which was achieved using an automatic tissue processor (Leica TP 1020). The process consists in tissue dehydration, using progressively more concentrated ethanol baths (70% (AGA), 95% (AGA) and 100% (Panreac)), followed by a xylene (VWR) immersion to remove the ethanol and finally molten paraffin (Merck, Whitehouse Station, NJ, USA), which replaced the xylene. Afterwards, the tissue embedding into paraffin blocks was performed and coronal sections of spinal cord and brain (5 µm thickness) were cut using a microtome (Leica RM 2145, Germany). Brain slices were obtained in an area corresponding to the stereotaxic coordinates (relative to bregma) between -5.20 and -5.60 mm (Paxinos 1998). Slices were collected in proper glass slides (Superfrost Plus - Thermo-Scientific, Waltham, MA) and placed in a 60ºC water bath during some seconds, followed by an incubation at 70ºC during 30 min. After that, the slices were deparaffinized using xylene, ethanol at decreasing concentrations (100%, 95% and 70%) and finally water. Subsequently, the antigen recovery was performed with boric acid (0.02 M $H_3BO_3$ in 2 mM NaOH, pH 7) for 15 min at 95-100ºC. The slices were then preserved in PBS.

### 4.11. Immunohistochemistry

After PBS removal, slices were permeabilized (1% Triton X-100, 0.1% gelatin in PBS for mAb4a, VIAAT, vesicular glutamate transporter 1 (vGluT1) and microtubule-associated protein 2 (MAP2) labelling and 1% Triton X-100, 10% FBS in PBS for GlyR α1, GlyR α2, GlyR α3, gephyrin, GlyT1, GlyT2, glial fibrillary acidic protein (GFAP) for 10 min. For GlyR labelling with mAb4a, sections were subsequently immersed in methanol for 10 min at -20ºC and washed with PBS. After blocking (0.25% gelatin in PBS for mAb4a, VIAAT, vGluT1 and MAP2 labelling and 10% FBS in PBS for GlyR α1, GlyR α2, GlyR α3, gephyrin, GlyT1, GlyT2, GFAP labelling) slices were incubated with the primary antibodies (prepared in the blocking solution), overnight at 4ºC, and with the fluorescent-labelled secondary antibodies for 2h at RT. Nuclei were stained with DAPI (Sigma, St. Louis, MO, USA, 1:15000) and the sections were mounted in Mowiol (Sigma).

### 4.12. Immunocytochemistry

For immunocytochemistry assays, cultured cells were fixed in 4% PFA in PBS for 15 min at RT, at 10, 18 and 24 DIV. In the synaptosomes analysis, synaptosomes (20 µg of protein) were placed onto 10 µg/ml PDL pre-treated coverslips, maintained during 3h at 37ºC in a humidified atmosphere (5% $CO_2$) and fixed in 4% PFA in PBS for 15 min at RT.
After fixation, cells were permeabilized (0.1% Triton X-100 in PBS) for 10 min and blocked (10% FBS in PBS with 0.05% Tween-20) for 1 hour. After blocking, cells were incubated with the primary antibodies, 4ºC overnight, and subsequently with the fluorescent-labeled secondary antibodies for 1h at RT. Autofluorescence was removed with 50 mM $CuSO_4$ in 50 mM ammonium acetate buffer, pH 5 (adapted from Schnell *et al.* 1999) for 30 min. Nuclei were stained with DAPI (1:20000), except in the case of the synaptosomes immunoreactions, and the preparations were mounted in Mowiol.
In all immunofluorescence assays, specificity and absence of antibody cross-reaction were confirmed by omission of the primary antibodies.

## 4.13. Imaging analysis

The images were acquired with a frame size of 2048 x 2048 pixels on an inverted confocal laser scanning microscope (Zeiss LSM 510 META, Germany) using a PlanApochromat 63x oil-immersion objective (Zeiss, Germany) with a numerical aperture of 1.40 (pixel size: 100 x 100 nm). DAPI fluorescence was detected with a 405 nm diode laser (30 mW nominal output) and a BP 420-480 nm filter. Alexa Fluor 488 fluorescence was detected using the 488 nm line of an Argon laser (45 mW nominal output) and a BP 500-550 nm filter. Alexa Fluor 568 was detected using a 561 nm DPSS laser (15 mW nominal output) and a LP 615 nm filter. The pinhole aperture was adjusted in each channel to achieve the same optical slice thickness for all channels (0.7 μm). For each group of triple labelling, all images were taken using the same excitation and acquisition settings for each channel. Fluorochromes were excited sequentially with multi-track frame imaging to eliminate any potential bleed-through. Images were obtained in DG, CA3 and CA1 hippocampal regions corresponding to the following stereotaxic coordinates (relative to the bregma): for DG lateral 2.5-3 mm and depth 3.8 mm; for CA3 lateral 4 mm and depth 7 mm and finally, for CA1 lateral 4 mm and depth 3 mm (Paxinos 1998).

### 4.13.1. Quantitative analysis

Quantitative analysis was performed using in-house masks developed for ImageJ software. For quantification of synaptic GlyR from immunohistochemistry images of mAb4a and VIAAT double staining, binary masks were created for both GlyR (red) and VIAAT (green) images using the same cut-off intensity threshold value for each staining, defined as the minimum intensity corresponding to specific staining above background values. GlyR and VIAAT were identified in each binary mask image using the Particle Analyzer function of ImageJ. For VIAAT apposition quantification, GlyR binary mask was dilated by 1 pixel (~ 100 nm) all around. This value was chosen since distance between pre- and postsynaptic cell membranes is 20-40 nm (Kandel *et al.*, 2000). GlyR clusters were considered synaptic if there was at least one pixel corresponding to a VIAAT puncta in the dilated GlyR mask. The percentage of synaptic GlyR clusters was then calculated from the total number of detected GlyR clusters.

Since mAb4a antibody recognizes all α subunits, another quantitative analysis was performed in immunohistochemistry images obtained from double staining of GlyR subunit specific antibody and gephyrin. The purpose was to evaluate co-localization rather than apposition so the GlyR binary mask dilation step was skipped in this analysis. Each staining in a double labelling image (GlyR subunit and gephyrin) was therefore subjected to the same intensity threshold cut-off, binary mask generation and particle analysis detection to identify clusters of GlyR and gephyrin. GlyR clusters were now considered synaptic if they had at least one pixel co-localized with gephyrin clusters. The results were presented as a percentage of synaptic GlyR from the total number of detected GlyR clusters. The same mask was used to evaluate co-localization between GlyR and glutamatergic nerve endings in immunohistochemistry images obtained from double staining of GlyR and vGluT1. In this case, GlyR were considered present in a glutamatergic bouton if it had at least one pixel co-localizing with vGluT1. The results were presented as the percentage of GlyR-containing glutamatergic boutons over GlyR total number.

Another quantitative analysis was carried out to determine the co-localization between GlyT1/GlyT2 and early endosome antigen 1 (EEA1). Briefly, each staining of the double image was subjected to the same intensity threshold cut-off value to identify GlyT and EEA1 immunolabelling. GlyT was considered to be present in endosomes if they had at least one pixel co-localized with EEA1. The results represented the percentage of endossomatic GlyT over GlyT total number and were calculated from cell counts in four independent fields of each coverslip, using three coverslips per condition, from three/four independent cultures. Images panels were prepared using Illustrator (Adobe Systems, San Jose, CA, USA).

### 4.14. [$^3$H] Glycine uptake assays in astrocytes

Glycine uptake analysis was performed in 21-24 DIV confluent astrocytes. Cells were pre-incubated in serum-free 1 g/l glucose DMEM during 3h in the optimal atmosphere (5% $CO_2$, 37°C). This step was followed by medium exchange to new serum-free 1 g/l glucose DMEM containing GlyT specific inhibitors and cells were further incubated for 20 min

(except otherwise specified). In control experiments cells were kept in the presence of serum-free 1 g/l glucose DMEM without any added drug.

The [$^3$H]glycine transport was initiated by the addition of several [$^3$H]glycine concentrations in KHR transport buffer (containing in mM: 137 NaCl, 5.4 KCl, 1.8 $CaCl_2 \cdot 2H_2O$, 1.2 $MgSO_4$ and 10 HEPES, pH 7.40) for 2 min. For the subsequent experiments, a [$^3$H]glycine concentration value similar to the $K_m$ determined for GlyT1 and GlyT2, 50 μM and 1800 μM, respectively, was chosen. Uptake was stopped by washing the cells twice with ice cold stop buffer (containing in mM: 137 NaCl and 10 HEPES, pH 7.40). Cells were subsequently solubilized with lysis buffer (100 mM NaOH and 0.1% SDS) at 37ºC for 1 hour and scraped from the plates.

Protein concentration was quantified using Bio-Rad DC protein assay (Hercules, CA, USA) (Peterson 1979). The amount of [$^3$H]glycine taken up by astrocytes was quantified by liquid scintillation counting (MicroBeta Trilux from PerkinElmer).

The specific transport mediated by GlyT1 or GlyT2 was calculated as the difference between the [$^3$H]glycine uptake in the absence (total transport) and in the presence (unspecific transport) of the GlyT1 inhibitor, Org 24598 (10 μM), or GlyT2 inhibitors, ALX 1393 (200 nM) and amoxapine (1 μM), except when otherwise indicated.

The calculation of the kinetic constants $K_m$ (affinity constant by Michaelis-Menton model, which described the relationship between the reaction rate and the ligand concentration of a protein) and $V_{max}$ (maximal velocity of transport) was achieved using GraphPad Prism software (San Diego, CA, USA) by means of non linear regression analysis.

In BDNF experiments, BDNF was added to astrocytes 5 min before the addition of [$^3$H]glycine. The BDNF effect in [$^3$H]glycine uptake was expressed as percentage of the control value in the same experiment and under the same experimental conditions. When the influence of any drug on the BDNF-modulation was analyzed, that drug was added to the astrocytes 15 min before the addition of BDNF (except otherwise indicated).

### 4.15. [$^3$H] Glycine uptake assays in synaptosomes

To determine the saturation curves for GlyT2, the synaptosomal fraction (0.5 mg/ml of protein) in Krebs-HEPES solution was incubated at 37ºC for 20 min in the presence or in the absence of the GlyT2 inhibitor, ALX (200 nM). [$^3$H]glycine uptake was initiated by the

addition of several [$^3$H]glycine concentrations in Krebs-HEPES solution. For the following experiments with several drugs, we used a [$^3$H]glycine concentration value similar to the $K_m$ achieved for GlyT2, namely, 1.0 mM. Uptake was stopped after 1 min by washing the cells twice with 5 ml ice-cold Krebs-HEPES solution followed by low pressure filtration through 1.2 μm filters (Millipore, Glass Fibre Prefilters). The filters were analysed by liquid scintillation counting (Tri-Carb 2900 TR from PerkinElmer).

GlyT2-mediated transport was calculated as the difference between the [$^3$H]glycine uptake in the absence (total transport) and in the presence (unspecific transport) of the GlyT2 inhibitor, ALX 1393 (200 nM).

The calculation of the kinetic constants $K_m$ and $V_{max}$ was achieved using GraphPad Prism software by means of non linear regression analysis.

In the case of BDNF studies, BDNF was added to the synaptosomes 5 min before the addition of [$^3$H]glycine. The BDNF effect in [$^3$H]glycine uptake was expressed as percentage of the control value in the same experiment and under the same experimental conditions. When the influence of any drug on the BDNF effect was tested, the synaptosomes were pre-incubated with that drug 15 min before the BDNF incubation.

### 4.16. Statistical analysis

All values are present in mean ± standard error of the mean (SEM) to test for statistical significance.

Comparisons between two conditions were made using student's t-test, while multiple comparisons were performed using one way analysis of variance (ANOVA) followed by Bonferroni's multiple comparison test.

The values of p-value $< 0.05$ were considered to represent statistically significant differences.

### 4.17. Drugs, antibodies and primers

**Table 4.1.** – Drugs used in the experimental work.

| Drugs | Function | Supplier | Working Concentration |
|---|---|---|---|
| **ALX1393** O-[(2-Benzyloxyphenyl-3-flurophenyl)methyl]-L-serine | GlyT2 inhibitor | Sigma | 200 nM |
| **Amoxapine** | GlyT2 inhibitor | Sigma | 1 µM |
| **BAPTA-AM** 1,2-bis(o-aminophenoxy)ethane-N,N,N',N'-tetraacetic acid | $Ca^{2+}$ chelator | Molecular Probes | 10 µM |
| **Dynasore** | Dynamin/clathrin-dependent endocytosis inhibitor | Sigma | 70 µM |
| **K252a** | Tyrosine kinase inhibitors | Calbiochem | 0.1 µM |
| **LY294002** (2-(4-Morpholinyl)-8-phenyl-1(4H)-benzopyran-4-one) | PI3K Inhibitor | Ascent | 10 µM |
| **Monensin** | Transporter recycling inhibitor | Sigma | 25 µM |
| **Org24598** R-(−)-N-Methyl-N-[3-[(4-trifluoromethyl)phenoxy]-3-phenyl-propyl]glycine | GlyT1 inhibitor | Sigma | 10 µM |
| **U0126** (1,4-Diamino-2,3-dicyano-1,4-bis(2-aminophenylthio)butadiene) | MAPK Inhibitor | Ascent | 10 µM |
| **U73122** (1-[6-[[(17b)-3-methoxyestra-1,3,5(10)-trien-17-yl]amino]hexyl]-1H-pyrrole-2,5-dione) | PLC Inhibitor | Tocris | 3 µM |
| **Toxin B** from *Clostridium difficile* | Rho GTPase Inhibitor | Sigma | 10 ng/ml |

**Table 4.2.** – Primary antibodies used in the experimental work.

| Primary Antibodies | Supplier | Dilution | Technique |
|---|---|---|---|
| Rabbit polyclonal anti-β-actin | Abcam | 1:10000 | WB |
| Mouse monoclonal anti-Akt1 | Santa Cruz | 1:1500 | WB |
| Rabbit anti-phospho-Akt | Cell Signaling | 1:1500 | WB |
| Mouse monoclonal anti-EEA1 | BD Biosciences | 1:500 | IF |
| Rabbit polyclonal anti-gephyrin | Synaptic Systems | 1:250 | IF |
| Mouse monoclonal mAb7a anti-gephyrin | Synaptic Systems | 1:250 | IF |
| Mouse monoclonal GA5 anti-GFAP | Millipore | 1:500 | IF |
| Rabbit polyclonal anti-GFAP | Sigma | 1:500 | IF |
| Mouse monoclonal mAb4a anti-GlyR | Synaptic Systems | 1:250 | WB |
| | | 1:500 | IF |
| Mouse monoclonal mAb2b anti-GlyRα1 | Synaptic Systems | 1:250 | IF |
| Rabbit polyclonal H-50 anti-GlyRα2 | Santa Cruz | 1:250 | IF |
| Rabbit polyclonal anti-GlyRα3 | Millipore | 1:250 | IF |
| Rabbit polyclonal anti-GlyT1 | Provided by Dr. Manuel Miranda-Arango, U.S.A. | 1:1000 | WB |
| Rabbit polyclonal anti-GlyT1 | Alpha Diagnostic Intl. Inc | 1:20 | IF |
| Rabbit polyclonal anti-GlyT2 | Provided by Dr. Manuel Miranda-Arango, U.S.A. | 1:1000 | WB |
| Rabbit polyclonal anti-GlyT2 | Alpha Diagnostic Intl. Inc | 1:20 | IF |
| Mouse monoclonal AP20 anti-MAP2 | Chemicon | 1:500 | IF |
| Rabbit anti-p44/p42 MAPK | Cell Signaling | 1:6000 | WB |
| Rabbit anti-phospho p44/p42 MAPK | Cell Signaling | 1:3000 | WB |
| Mouse monoclonal anti-PLC-γ1 | Santa Cruz | 1:1500 | WB |
| Rabbit anti-phospho-PLC-γ1 | Cell Signaling | 1:1500 | WB |
| REX anti-p75 NTR | Provided by Dr. Louis Reichardt, U.S.A. | (50 μg/ml) | Uptake |
| Mouse IgG1 anti-TrkB | BD Biosciences | 1:1000 | WB |
| Rabbit anti-phospho-Trk (pTyr-490) | Cell Signaling | 1:1000 | WB |
| Rabbit polyclonal anti-α-tubulin | Abcam | 1:5000 | WB |
| Rabbit polyclonal anti-vGluT1 | Synaptic Systems | 1:1000 | IF |

Abbreviations: IF, immunofluorescence; WB, western blot.

**Table 4.3.** – Secondary antibodies used in the experimental work.

| Secondary Antibodies | Supplier | Dilution | Technique |
|---|---|---|---|
| Goat anti-mouse IgG-HRP | Santa Cruz | 1:5000 | WB |
| Goat anti-rabbit IgG-HRP | Santa Cruz | 1:5000 | WB |
| Goat anti-mouse-Alexa F488 | Invitrogen | 1:400 | IF |
| Goat anti-mouse-Alexa F568 | Invitrogen | 1:400 | IF |
| Goat anti-rabbit-Alexa F488 | Invitrogen | 1:400 | IF |
| Goat anti-rabbit-Alexa F568 | Invitrogen | 1:400 | IF |

Abbreviations: IF, immunofluorescence; WB, western blot.

**Table 4.4.** – Primers used in qPCR.

| Gene | Primer sequence (5' - 3') | Source | Fragment (bp) |
|---|---|---|---|
| β-actin | Forward: AGCCATGTACGTAGCCATCC<br>Reverse: CTCTCAGCTGTGGTGGTGAA | Sequence provided by Dr.Tiago Outeiro, Lisbon | 228 |
| GlyRα1 | Forward: ACTCTGCGATTCTACCTTTGG<br>Reverse: ATATTCATTGTAGGCGAGACGG | Designed with OligoAnalyzer 3.1 | 300 |
| GlyRα2 | Forward: CAGAGTTCAGGTTCCAGGG<br>Reverse: TCCACAAACTTCTTCTTGATAG | Heck *et al.*, 1996 | 330 |
| GlyRα3 | Forward: GTGAGACACTTTCGGACACTAC<br>Reverse: GATGGGTCGAGGTCTAATGAATC | Designed with OligoAnalyzer 3.1 | 353 |
| GlyRβ | Forward: CTGTTCATATCAAGCACTTTGC<br>Reverse: GGGATGACAGGCTTGGCAG | Heck *et al.*, 1996 | 223 |
| GlyT1 | Forward: CTGGAGGCTGTATGTGCTGA<br>Reverse: GATGACGAAGCCAGCATAGA | Barker et al. 1999 | 439 |
| GlyT2 | Forward: TCCGTCCTCATAGCCATCTA<br>Reverse: TCACTCCCGCTGACAAATG | Designed with OligoAnalyzer 3.1 | 278 |
| TrkB-FL | Forward: GTGATGCTGCTTCTGCTCAA<br>Reverse: CCTCCGAAGAAGACGGAGTG | Supplied by Dr. Eero Castrén, Finland | 142 |
| TrkB-T1 | Forward: TAAGATCCCCCTGGATGGGTAG<br>Reverse: AAGCAGCACTTCCTGGGATA | Supplied by Dr. Eero Castrén, Finland | 126 |
| TrkB-T2 | Forward: CGGGAGCATCTCTCGGTCT<br>Reverse: TCCACTTAAGAAGCAAAATAAGC | Rose et al., 2003 | 152 |

# 5. Results

## 5.1. GlyR are expressed in the rat hippocampus over several developmental stages

*Rita Aroeira has written the draft and performed all the experimental work.*
*The work presented in this section was published (Aroeira et al. 2011).*

### 5.1.1. Rationale

Glycine mediates inhibitory transmission via ionotropic GlyR, which predominate in the spinal cord and brainstem (Bowery & Smart 2006). GlyR are pentameric channels permeable to $Cl^-$ ions, composed by two different subunits, α and β (Langosch *et al.* 1988). Several variants of α subunits (α1, α2, α3 and α4) have been described (Bowery & Smart 2006). In immature spinal cord neurons, GlyR are mostly homomeric receptors composed by α2 (49 kDa). The α1 (48 kDa) subunit dominates in mature spinal cord neurons in association with β (58 kDa) subunit forming αβ heteromeric receptors (Becker *et al.* 1988). The β subunit is essential for the anchoring to gephyrin (Bowery & Smart 2006), a cytoplasmic protein necessary for synaptic localization of GlyR (Kirsch *et al.* 1991).
GlyR expression in the hippocampus has been recognized through electrophysiological (Chattipakorn & McMahon 2002), immunocytochemical (Brackmann *et al.* 2004, Levi *et al.* 2004, Meier & Grantyn 2004), immunohistochemical (Danglot *et al.* 2004) and in situ hybridization approaches (Malosio *et al.* 1991b). However, detailed information on the expression of these receptors, their subunit composition and subcellular localization in the hippocampus is still missing. Thus, a spatial characterization of GlyR in the rat hippocampus over several developmental stages, late embryonic stage (E18) to 9-weeks after birth, both at mRNA and protein level, was performed.

### 5.1.2. GlyR have a developmentally regulated expression in rat hippocampus

To assess total GlyR protein expression in rat hippocampus at different stages of development, a GlyR specific antibody (mAb4a), which has been fully characterized (Pfeiffer *et al.* 1984), was used for western blot analysis. GlyR expression in the hippocampus was evaluated at a late embryonic stage (E18), at P0 up to weaning (P3, P7,

P14 and P21) and then in young adult (9 weeks-old) rats. In all ages studied, mAb4a antibody identified a single band of 48-49 kDa, which corresponds to the molecular weight of GlyRα subunits (Figure 5.1.A). For comparison and internal control, spinal cord homogenates were also analysed. In this case, 14 times less protein was loaded and a very intense band was detected with mAb4a (Figure 5.1.A), which is in agreement with GlyR high expression in caudal regions of the CNS. No other band was detected indicating high mAb4a specificity for GlyRα subunits.

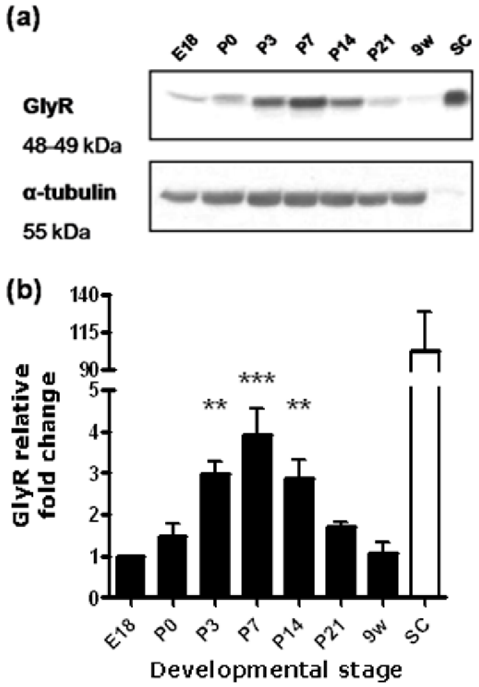


**Figure 5.1. - Expression of GlyR in rat hippocampus at different developmental stages. (A)** Western blot analysis of GlyR (48-49 kDa) and α-tubulin (55 kDa) in rat hippocampal (70 µg) and spinal cord homogenates (5 µg). α-tubulin was used as a loading control. The immunoreactive bands were detected on a 12% SDS-PAGE using mAb4a GlyR antibody. Homogenates were obtained from embryonic to 9 weeks-old rat hippocampus (E18, P0, P3, P7, P14, P21 and 9 weeks) and P21 spinal cord (SC). **(B)** Densitometry analysis of western blots (n=5). The graph shows the ratio of GlyR immunoreactivity and α-tubulin normalized to E18. All values are mean ± SEM. **p<0.01, ***p<0.001 as compared with E18 (one way ANOVA followed by Bonferroni's Multiple Comparison test).

Densitometry analysis of western blots (Figure 5.1.B) revealed a 3-5 fold-increase in the expression of GlyR from the embryonic stage (E18) to seven days postnatal (P7) (n=5, ***p<0.001). From P14 on, GlyR expression levels started to decrease, although at P14,

expression was kept significantly higher than the one detected at E18 (n=5, **p<0.01). However, and as expected, GlyR expression in hippocampus is much lower than in spinal cord. These data reveal a clear developmentally regulated expression of GlyR in rat hippocampus and is in agreement with the expression pattern reported for presynaptic GlyR in hippocampal mossy fibers, using electrophysiological recordings (Kubota *et al.* 2010).

### 5.1.3. Extraction of total RNA and analysis of their integrity

To analyze the mRNA expression of the principal GlyR subunits namely, α1, α2, α3 and β, in rat hippocampus from E18 to post-natal stages, variants of the PCR technique were used. A spinal cord sample obtained from a P21 rat was used as the positive control.
The first step was the extraction of total RNA from hippocampal and spinal cord samples. Since the analysis of the ribosomal RNA (80% of the total RNA) reflects the quality of the whole RNA, it is possible to evaluate the RNA integrity and quality by gel electrophoresis. The RNA samples analyzed, presented two bands, a higher one that correspond to the 28S ribosomal RNA and a lower one, less intense, that indicate the presence of 18S ribosomal RNA (Figure 5.2.). It is also possible to note the absence of bands with a lower mass, consequence of RNA degradation, and bands with a higher mass, indicative of contamination with genomic DNA. Thus, the isolated RNA was considered highly pure.

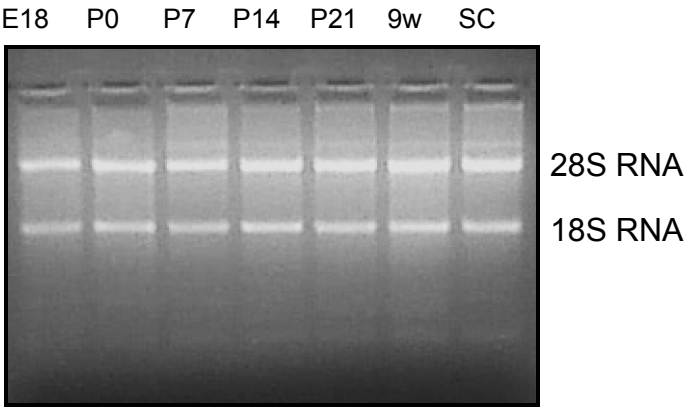


**Figure 5.2. – Analysis of total RNA integrity isolated from rat hippocampus and spinal cord.** 3% agarose gel of total RNA obtained from the hippocampus of rat embryos with 18 days of gestation (E18), day of birth (P0), seven (P7), fourteen (P14) and twenty-one (P21) days after birth and with 9 weeks old (9w). Spinal cord (SC) was isolated from a P21 rat.

### 5.1.4. GlyR subunits mRNA are expressed in rat hippocampus

mRNA expression of the main GlyR subunits namely, α1, α2, α3 and β, in rat hippocampus from E18 to post-natal stages, was studied by RT-PCR (Figure 5.3.A) with specific oligonucleotide primers. No PCR products were detected using cDNA synthesized in the absence of reverse transcriptase (-RT wells), which ensured that amplification did not arise from contaminating genomic DNA. These primers were also used in qPCR and no signal amplification was detected in the negative controls, which indicated absence of genomic DNA, external contamination or other factors that could originate a non-specific increase in the fluorescence signal. Reaction specificity was further evaluated in all assays by a melting curve (Figure 5.4.).

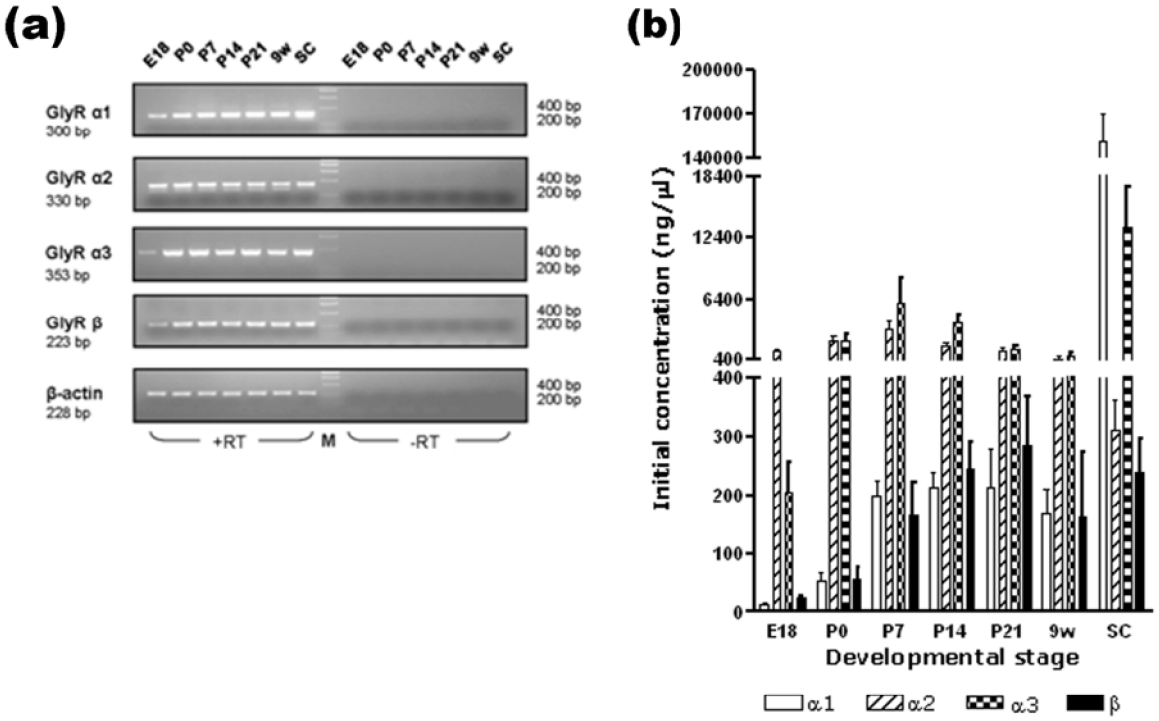


**Figure 5.3. - Expression of GlyR subunit mRNAs in rat hippocampus at different developmental stages (E18, P0, P7, P14, P21 and 9 weeks) and spinal cord (SC). (A)** Reverse Transcriptase – PCR analysis of GlyR subunits (α1, α2, α3 and β) and β-actin in rat hippocampus. PCR products were detected on a 2% agarose gel. β-actin was used as a loading control. No PCR products were obtained using cDNA synthesized in the absence of reverse transcriptase (-RT wells). **(B)** Changes in initial concentration of GlyR subunits transcripts (α1, α2, α3 and β) in rat hippocampus.

The initial concentration of each transcript (GlyR subunits mRNA α1, α2, α3 and β) at each developmental stage is showed in Figure 5.3.B and the relative changes of each GlyR subunit mRNA, evaluated by relative qPCR, are shown in Figure 5.5. It is clear that the proportion of GlyR subunits mRNA in hippocampus changes over development, but there is always a predominance of α2 and α3 over α1 and β subunits mRNA (Figure 5.3.B). This indicates that, in hippocampal neurons, GlyR are mainly composed of α2 and α3 subunits, while spinal cord neurons have a prevalence of GlyRα1, as reported by others (Malosio *et al.* 1991b).

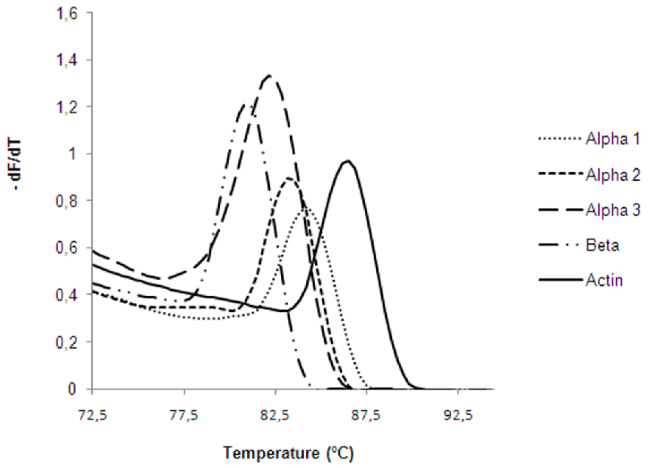


**Figure 5.4. - Melting curves of GlyR subunits (α1, α2, α3 and β) and β-actin transcripts analyzed by qPCR.** The graph represent the first derivate of raw fluorescence plotted against an increase in temperature. The single melting peak obtain for each curve indicates that a single PCR product is being amplified in these samples.

GlyRα1 mRNA expression was very low at E18, but progressively increased during the first postnatal weeks (up to 20-30 fold), reaching a plateau level from P14 onwards (Figure 5.5.A). β mRNA subunit expression pattern (Figure 5.5.D) was similar to that of α1, but the increase in expression over development (about 10-fold from E18 to P14) was lower than the one observed in GlyRα1 mRNA expression. GlyRα2 expression was high in samples from early postnatal stages (P0 and P7); at P7, α2 mRNA levels increased by 1.8-fold from those detected at E18. From P14 on, GlyRα2 expression slightly decreased but even in adult rats (9-weeks old), α2 levels were not significantly lower ($P>0.05$) than those detectable at E18 (Figure 5.5.B), in clear contrast with what has been reported for adult spinal cord neurons (Malosio *et al.* 1991b). GlyRα3 mRNA levels were low at E18 and greatly increased (up to 20-30 fold) from E18 to P7 (Figure 5.5.C). From P14 onwards,

GlyRα3 mRNA expression decreased as happens for GlyRα2 mRNA. However, in adult rats, GlyRα3 mRNA expression was still 8-fold higher than at E18, being about the same as detected at P0.

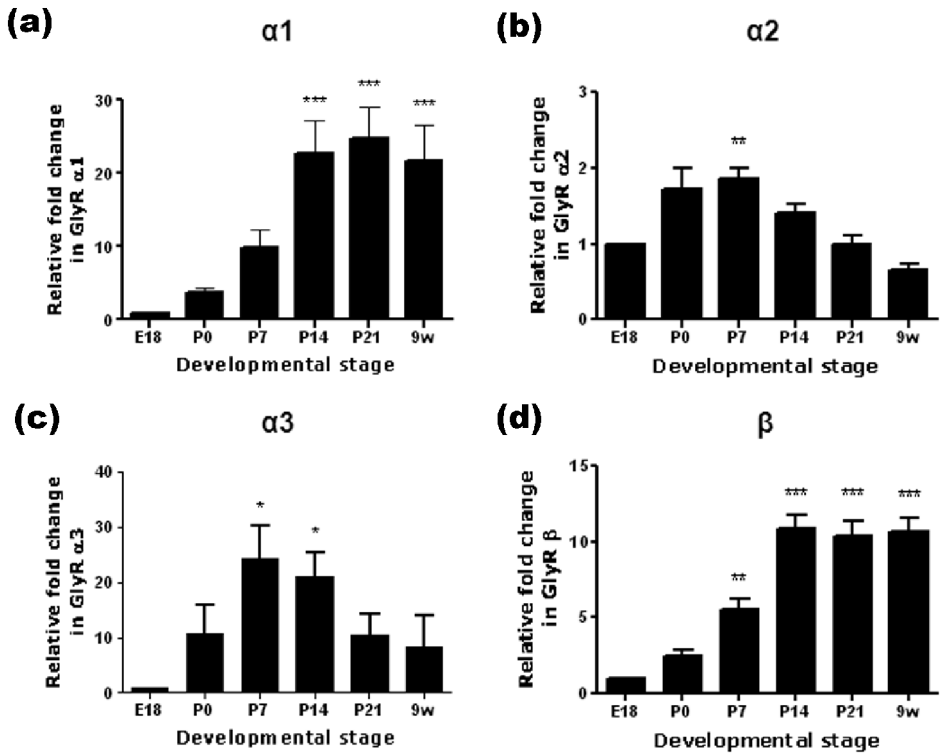


**Figure 5.5. - Composition analysis of GlyR subunit mRNAs in rat hippocampus at different developmental stages (E18, P0, P7, P14, P21 and 9 weeks) by relative qPCR. (A-D)** Changes in GlyR subunits (α1, α2, α3 and β) mRNA expression levels. All values are mean ± SEM. *p<0.05, **p<0.01, ***p<0.001 comparing with E18, (n=4, one way ANOVA followed by Bonferroni's Multiple Comparison Test). Genes are indicated on top of each graph. Note the differences in scale between panels.

### 5.1.5. Subcellular localization of GlyR and VIAAT in rat hippocampus

Analyses of coronal brain slices (5 µm) labelled with the nuclear marker DAPI revealed that at E18 it is not yet possible to distinguish between the main hippocampal areas and only the Ammon's horn is macroscopically delineated (Figure 5.6.). At P7 it is already possible to completely identify the major hippocampal areas, namely DG, CA1 and CA3. At this stage it is possible to distinguish pyramidal cell nuclei in the *stratum pyramidale* of CA1/CA3 as well as granular cells distributed in *stratum granulosum* of DG. Interneurons

in the *stratum radiatum* of CA1/CA3 areas and in the *stratum moleculare* of DG can also be visualized.

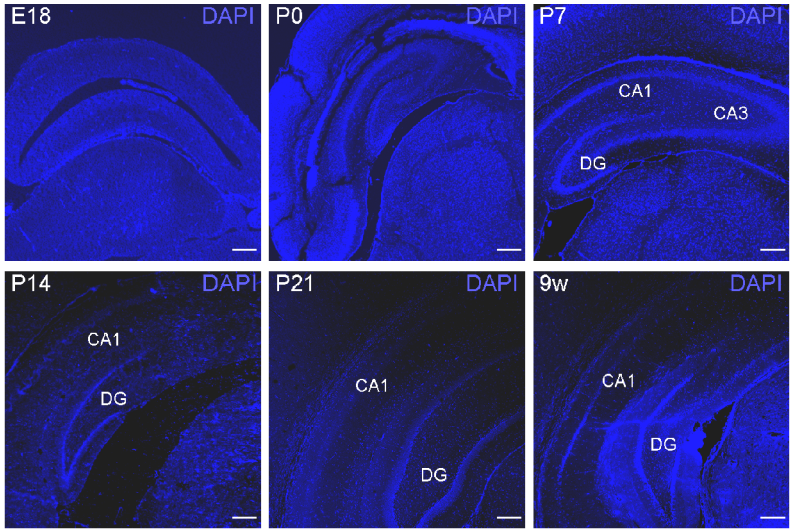


**Figure 5.6. - Hippocampal cytoarchitecture changes over the developmental stages studied: E18, P0, P7, P14, P21 and 9 weeks-old rats.** Nuclei were stained with DAPI. Confocal images were acquired with a 5X objective. Scale bars, 200 µm. Dentate Gyrus (DG); *Cornus Ammonis* 1 and 3 (CA1 and CA3).

GlyR subcellular localization in the rat hippocampus was investigated by confocal immunohistochemistry analysis of coronal brain slices (5 µm). Presynaptic glycine and/or GABA are packaged into synaptic vesicles via the common neurotransmitter transporter VIAAT, which is therefore located in both GABAergic and glycinergic terminals and can be used as a marker of all inhibitory presynaptic boutons, either GABAergic, glycinergic or mixed (Dumoulin *et al.* 1999). Therefore, a double staining with mAb4a and VIAAT antibodies, together with DAPI, allowed the identification of synaptic and extrasynaptic GlyR (Figure 5.7. and Figure 5.8.) localized in dendritic or cell bodies rich layers. A positive control was performed in slices from mature spinal cord in the same conditions (Figure 5.14.). In the absence of the primary antibodies no staining was observed (Figure 5.15.) and therefore no autofluorescence signaling had to be taken into account.

The confocal images of each hippocampal area (DG, CA1 and CA3) were obtained from the delineated regions indicated in Figure 5.7.A. In order to have a full characterization of GlyR expression within each area, each image covered two layers, one layer rich in cell bodies of pyramidal cells (*stratum granulosum* of DG and *stratum pyramidale* of

CA1/CA3), and one layer rich in dendrites and cell bodies of interneurons (*stratum moleculare* of DG and *stratum radiatum* of CA1/CA3).

In the embryonic stage (E18), both mAb4a and VIAAT antibodies perfectly delineate the cell body (Figure 5.7.B). At this stage it was not observed any juxtaposed mAb4a and VIAAT immunolabelling, which is an indicator of no synapse formation. At the neonatal stage (P0), GlyR clusters immunolabelling is mainly surrounding the cell body of granular and pyramidal cells, as well as the cell bodies of some interneurons (Figure 5.7.C1-C3), while VIAAT is restricted to the dendritic layers, namely *stratum moleculare* of DG and *stratum radiatum* of CA1/CA3, being strongly expressed close to the cell bodies of interneurons. However, at this stage a few synaptic GlyR are already detected in all hippocampal areas (Table 5.1.), but with a higher proportion in DG.

At P7, somatic GlyR expression, in granular and pyramidal cells, decreases and immunolabelling starts to be detected in the dendritic layers of the hippocampus (Figure 5.7.C4-C6). At this stage GlyR clusters also delineate the soma of interneurons in *stratum moleculare* and *stratum radiatum* areas of the hippocampus, as indicated by arrowheads in Fig 5.7.C4a, C5a and C6a. Several inhibitory GlyR-containing synapses can be detected at P7 (arrows in Fig 5.7.C4a, C5a and C6a), with a prevalence in DG (Table 5.1.). These synapses, identified by the close apposition of GlyR and VIAAT labelling were found in dendrites and facing the soma of some interneurons. Synaptic GlyR were restricted to the postsynaptic densities, since it was not observed a full co-localization between GlyR and VIAAT. Instead, it was noticed a typical pre/postsynaptic apposition between VIAAT and GlyR clusters, as previously observed in the spinal cord (Dumoulin *et al.* 1999).

At P14, it was detected less mAb4a labelling around the cell body of pyramidal cells in *stratum granulosum* of DG and *stratum pyramidale* of CA1/CA3, than in the previous developmental stages. On the other hand, at this stage, the number of GlyR-containing synapses was high (Table 5.1.), being possible to distinguish many GlyR immunoreactive clusters apposed to VIAAT-positive boutons (arrows in Figure 5.8.A1a to A3a). Some GlyR clusters were spread along all dendritic regions, but not apposed to VIAAT-positive terminals therefore representing extrasynaptic GlyR (arrowheads in Figure 5.8.A1a to A3a). At this stage, VIAAT immunoreactivity was found in the cell body layers of DG and CA1/CA3 regions, as well as in the dendrites rich layers of these regions.

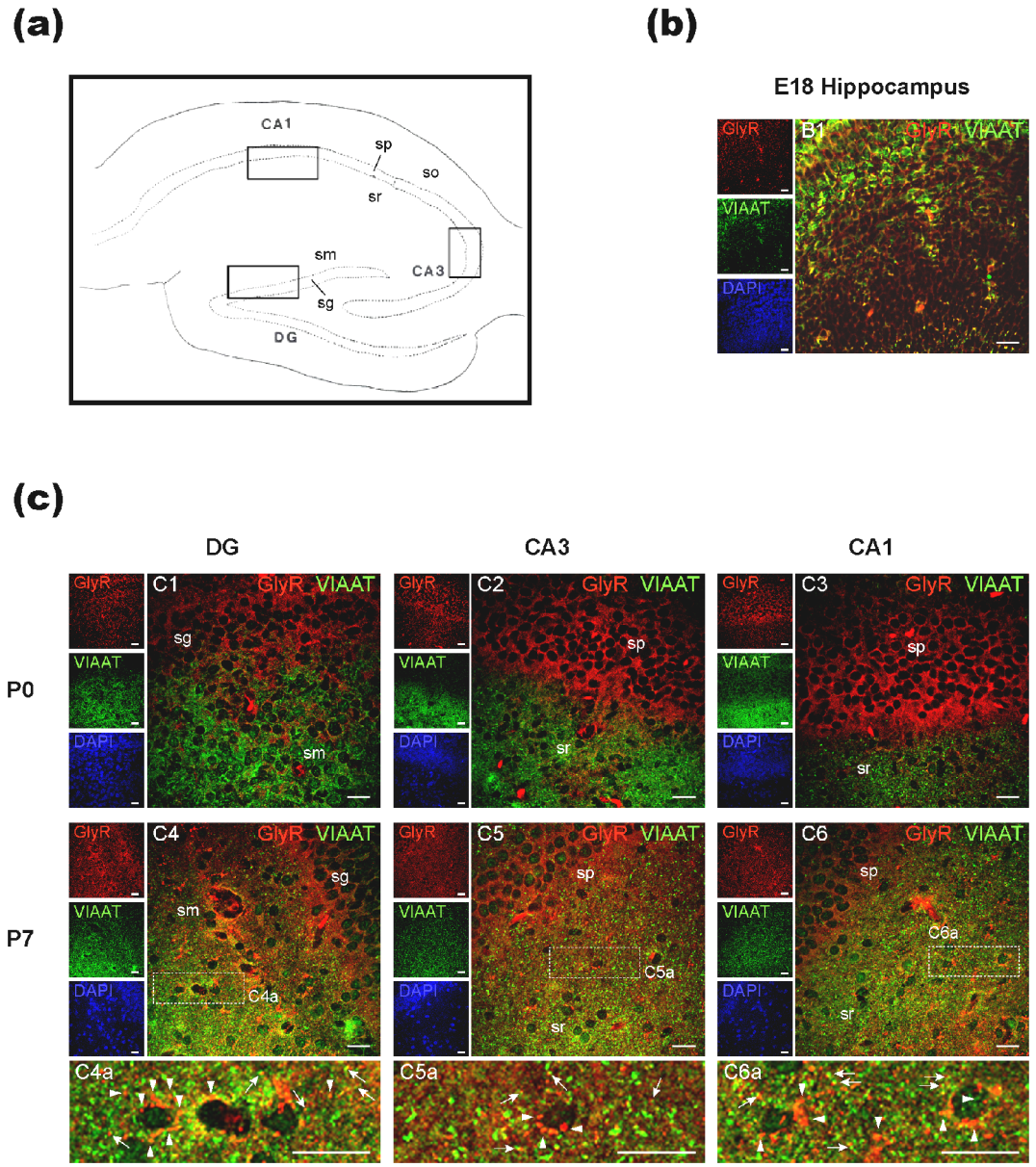


**Figure 5.7. - Synaptic and extrasynaptic localization of GlyR at early developmental stages. (A)** Representation of the hippocampus (adapted from Andersen 2007). The areas enclosed by the boxes show the regions where the confocal images were taken, namely Dentate Gyrus (DG) and *Cornus Ammonis* 1 and 3 (CA1 and CA3). Double detection of GlyR and VIAAT in rat hippocampus by confocal microscopy: **(B)** E18, **(C)** DG, CA3 and CA1 regions at P0 (C1-C3) and P7 (C4-C6). Panels (C4a-C6a) are magnifications of the boxed windows. The primary antibodies used were mouse monoclonal mab4a antibody anti-GlyR and rabbit polyclonal antibody anti-VIAAT. Small left panels represent each labelling alone: GlyR immunoreactivity is red and VIAAT containing terminals are green. Nuclei were stained with DAPI. Postsynaptic GlyR apposed to VIAAT positive terminals are indicated by arrows. Arrowheads point to GlyR extrasynaptic homomeric clusters. Confocal images were acquired with a 63X oil-immersion objective. Scale bars, 20 µm. sg, *stratum granulosum*; sm, *stratum moleculare*; so, *stratum oriens*; sp, *stratum pyramidale*; sr, *stratum radiatum*.

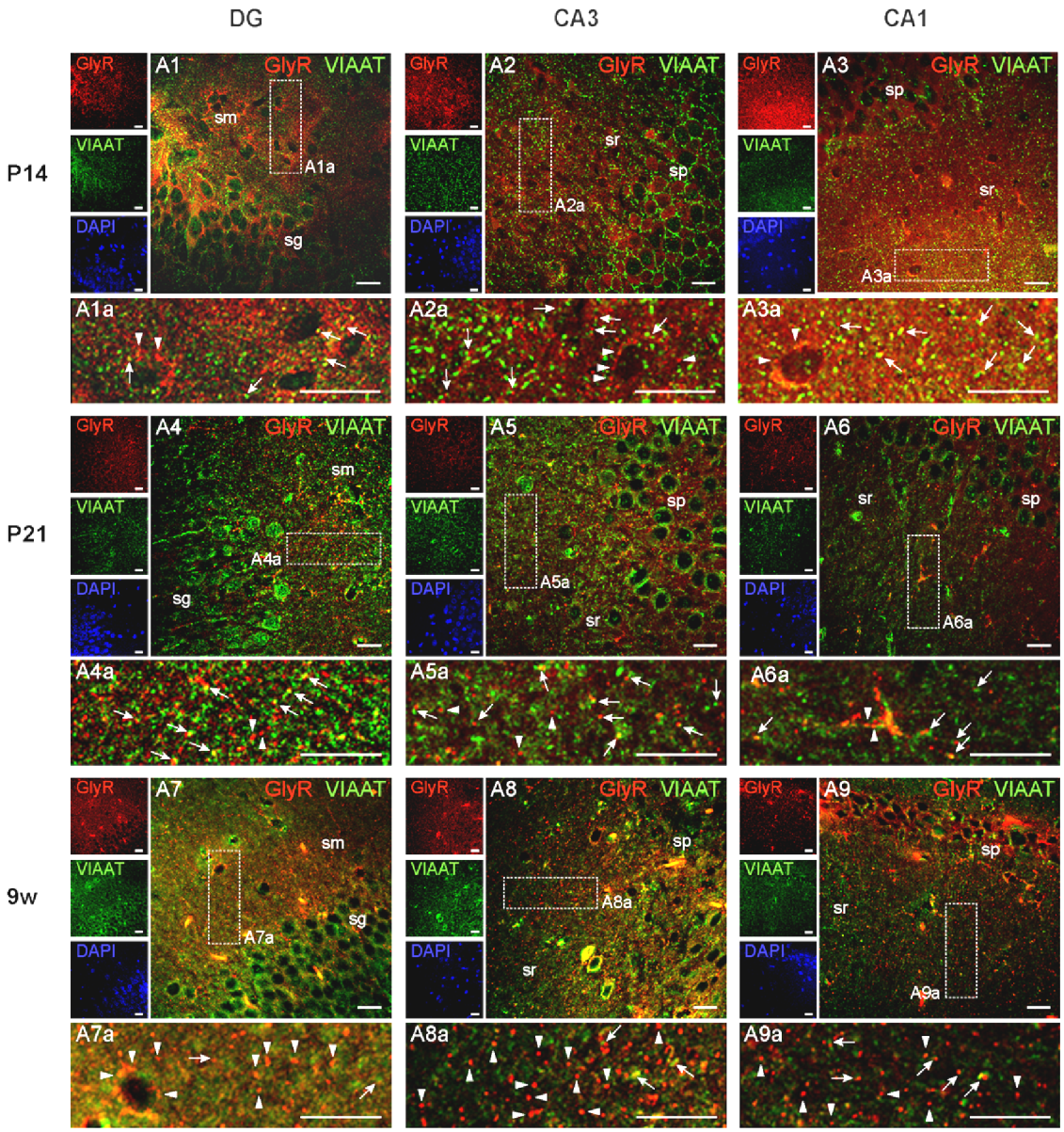


**Figure 5.8. - Synaptic and extrasynaptic localization of GlyR at late developmental stages.** Double detection of GlyR and VIAAT in rat hippocampus by confocal microscopy in Dentate Gyrus (DG) and *Cornus Ammonis* 1 and 3 (CA1 and CA3) regions at P14 (A1-A3), P21 (A4-A6) and 9-weeks old (A7-A9). Panels (A1a-A9a) are magnifications of the boxed windows. The primary antibodies used were mouse monoclonal mab4a antibody anti-GlyR and rabbit polyclonal antibody anti-VIAAT. Small left panels represent each labelling alone: GlyR immunoreactivity is red and VIAAT containing terminals are green. Nuclei were stained with DAPI. Arrows indicate GlyR-containing synapses. Arrowheads point to GlyR extrasynaptic homomeric clusters. Confocal images were acquired with a 63X oil-immersion objective. Scale bars, 20 µm sg, *stratum granulosum*; sm, *stratum moleculare*; so, *stratum oriens*; sp, *stratum pyramidale*; sr, *stratum radiatum*.

At P21 and 9-weeks old rats (Figure 5.8.A4 to A9), the DG *stratum moleculare* and the CA1/CA3 *stratum radiatum* are full with extrasynaptic GlyR clusters (arrowheads in Figure 5.8.A4a to A9a). In fact, the amount of synaptic GlyR (arrows in Figure 5.8.A4a to A9a) is decreased (Table 5.1.). VIAAT-immunoreactivity is widely spread within all dendritic regions but not predominantly apposed to GlyR clusters. These VIAAT clusters label GABAergic terminals, as reported by others (Dumoulin *et al.* 1999), which are abundant in the adult hippocampus.

**Table 5.1. -** Quantitative analysis of synaptic GlyR in rat hippocampal areas, Dentate Gyrus (DG) and *Cornus Ammonis* 1 and 3 (CA1 and CA3), and in spinal cord (SC), as achieved by juxtaposition of VIAAT and mAb4a immunolabelling.

| | **DG** | | **CA3** | | **CA1** | | **SC** | |
|---|---|---|---|---|---|---|---|---|
| | Synaptic GlyR (%) | n | Synaptic GlyR (%) | n | Synaptic GlyR (%) | n | Synaptic GlyR (%) | n |
| **P0** | 7.3 ± 1.8 | 17786 | 2.4 ± 0.9 | 20943 | 1.9 ± 1.3 | 18847 | - | - |
| **P7** | 15.9 ± 8.1 | 15222 | 14.8 ± 9.9 | 13142 | 14.6 ± 7.7 | 23996 | - | - |
| **P14** | 19.1 ± 7.9 | 18426 | 15.9 ± 6.7 | 17883 | 14.4 ± 8.1 | 21552 | - | - |
| **P21** | 7.8 ± 3.0 | 17128 | 7.3 ± 2.1 | 20269 | 7.1 ± 4.0 | 15122 | 30.3 ± 1.7 | 37754 |
| **9w** | 6.7 ± 2.4 | 20481 | 5.8 ± 2.4 | 21707 | 3.8 ± 1.7 | 18009 | - | - |

Slices were immunolabelled with mouse monoclonal mab4a antibody anti-glycine receptor (GlyR) and rabbit polyclonal antibody anti-vesicular inhibitory amino acid transporter (VIAAT). The results represent the percentage of GlyR (mean ± SEM) with a synaptic localization. In each case, the total number (n = 100%) of counted GlyR are indicated.

### 5.1.6. Subcellular localization of GlyR subunits and gephyrin in rat hippocampus

Gephyrin, a cytoplasmic protein, is the core molecule for anchoring and stabilizing GlyR and $GABA_AR$ at inhibitory postsynaptic sites (Kirsch *et al.* 1993, Meier *et al.* 2001, Fritschy *et al.* 2008). Gephyrin, through binding to the β subunit, recruits GlyR to the

postsynaptic membrane and therefore inhibitory GlyR-containing synapses always co-localize with gephyrin (Kirsch *et al.* 1991).

Hence, a double staining of GlyR subunits (GlyRα1, α2 and α3) and gephyrin, together with DAPI, was used to evaluate the subunit composition of GlyR in synaptic and extrasynaptic GlyR, in both immature (P7) and mature neurons (P21).

The double staining of each of the GlyRα subunits and the cytoplasmic postsynaptic protein gephyrin show a predominance of extrasynaptic GlyR, which do not co-localize with gephyrin, in rat hippocampus (Figures 5.9., 5.10. and 5.11., Table 5.2.), in accordance with what was observed with the double labelling of mAb4a and VIAAT antibodies. At early postnatal stages (P7), GlyRα1 (Figure 5.9.A1-A3) and GlyRα2 (Figure 5.10.A1-A3) immunoreactivity was found in both dendritic and cell body rich layers. At this stage it is possible to detect extrasynaptic α1/α2-containing GlyR (open/mid-open arrowheads in Figure 5.9.A1a-A3a and Figure 5.10.A1a-A3a) that do not co-localize with gephyrin and a few synaptic GlyR that contain mostly α2 subunits (open/mid-open arrows in Figure 5.10.A1a-A3a). Quantitative analysis of synaptic GlyR confirms a higher proportion of GlyRα2 in all hippocampal subregions (Figure 5.12.A-C). GlyRα3 (Figure 5.11.A1-A3) surrounds the cell body of granular cells in *stratum granulosum* of DG and pyramidal cells in *stratum pyramidale* of CA1/CA3, being hardly detected at inhibitory synapses (open/mid-open arrows in Figure 5.11.A1a-A3a, Table 5.2.).

In the mature hippocampus (P21), GlyRα1 (Figure 5.9.A4-A6) and GlyRα2 (Figure 5.10.A4-A6) immunoreactivity is high in the dendritic regions of DG and CA areas, with a preponderance of GlyRα2 in the *stratum moleculare* of DG. In this area, extrasynaptic GlyRα2 perfectly delineates several dendrites (mid-open arrowheads in Figure 5.10.A4a). Some extrasynaptic GlyRα1 can also be observed (open/mid-open arrowheads in Figure 5.9.A4a). On the other hand, GlyRα3 (Figure 5.11.A4-A6) is still confined to the cell body containing layers. Nevertheless, at P21, GlyRα3 immunofluorescence is greatly increased in the dendritic regions of all hippocampal areas (mid-open arrowheads in Figure 5.11.A4a-A6a) as compared with the one found at P7. In mature neurons, the quantitative analysis (Figure 5.12.A-C) points to a significant (***$p<0.001$) decrease in synaptic GlyRα2 in all hippocampal areas. Therefore, at this stage the α subunit of the few synaptic GlyR are predominantly α1 (Figure 5.12., Table 5.2.). Furthermore, the expression of α2 and α3 transcripts is high (Figure 5.3.), which is in accordance with the occurrence of many extrasynaptic α2/ α3-containing GlyR in mature hippocampal neurons.

As a control spinal cord mature neurons were evaluated and it was confirmed (Figure 5.14.B3) that synaptic GlyR are mainly GlyRα1 (Figure 5.12.D).

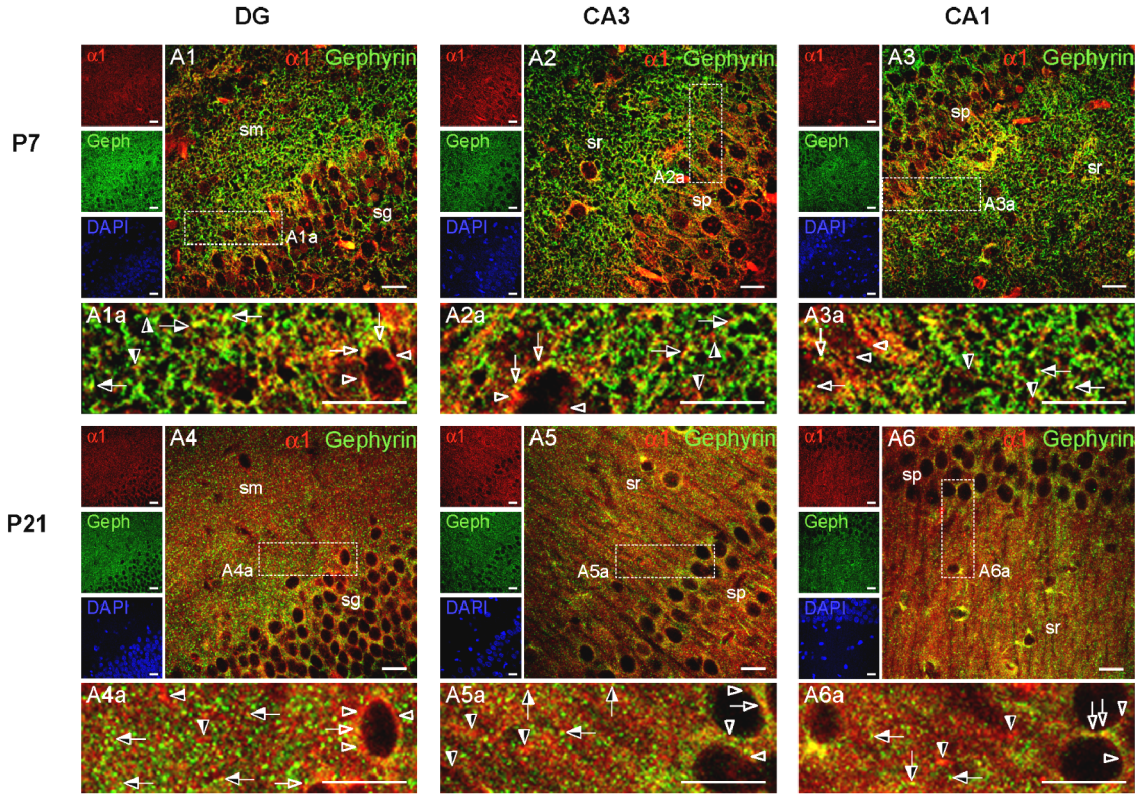


**Figure 5.9. - Synaptic and extrasynaptic localization of GlyRα1 subunit.** Double detection of GlyRα1 and gephyrin in rat hippocampus by confocal microscopy, in Dentate Gyrus (DG) and *Cornus Ammonis* 1 and 3 (CA1 and CA3) regions, at P7 (A1-A3) and P21 (A4-A6). Panels A1a-A6a are magnifications of the boxed windows. The primary antibodies used were mouse monoclonal mAb2b antibody anti-GlyRα1 and rabbit polyclonal antibody anti-gephyrin. Small left panels represent each labelling alone: red for GlyRα1 and green for gephyrin. Nuclei were stained with DAPI. Examples of extrasynaptic GlyRα1 with a somatic localization (open arrowheads), extrasynaptic GlyRα1 with a dendritic localization (mid-open arrowheads), synaptic GlyRα1 with a somatic localization (open arrows) and synaptic GlyRα1 with a dendritic localization (mid-open arrows) are indicated in the magnified panels. Confocal images were acquired with a 63X oil-immersion objective. Scale bars, 20 µm. sg, *stratum granulosum*; sm, *stratum moleculare*; sp, *stratum pyramidale*; sr, *stratum radiatum*.

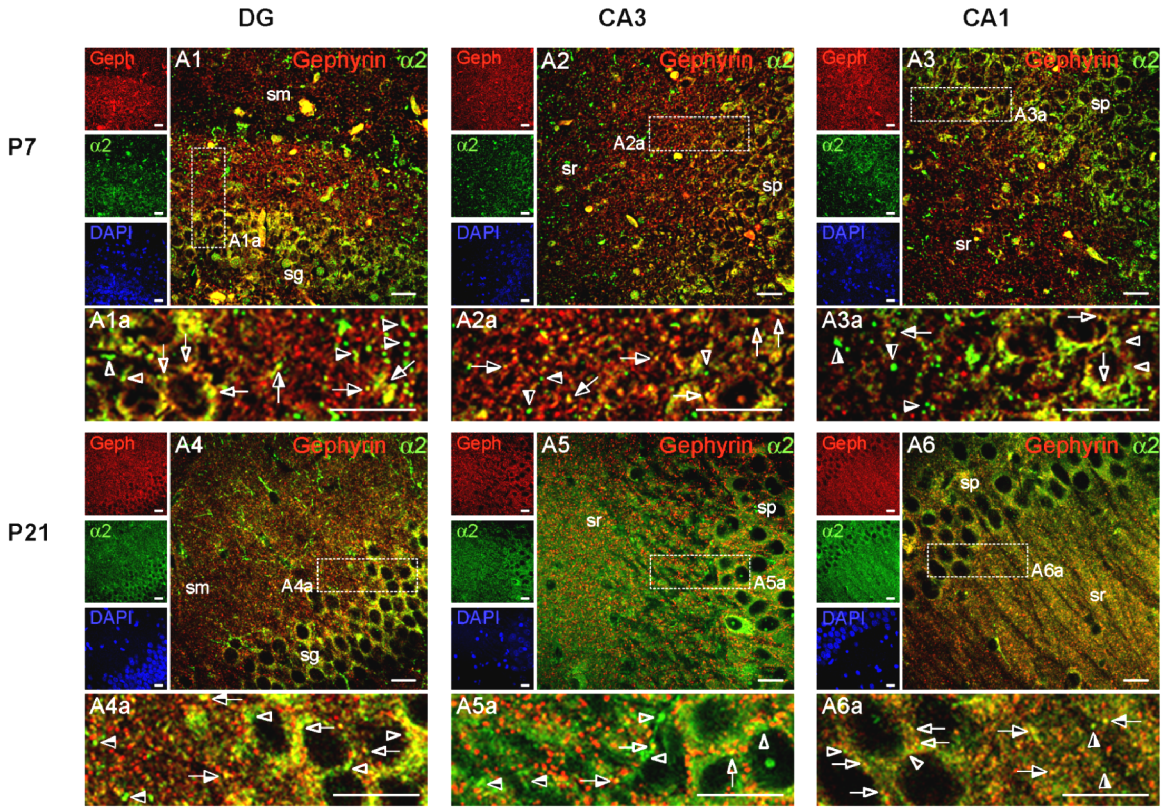


**Figure 5.10. - Synaptic and extrasynaptic localization of GlyRα2 subunit.** Double detection of GlyRα2 and gephyrin in rat hippocampus by confocal microscopy in Dentate Gyrus (DG) and *Cornus Ammonis* 1 and 3 (CA1 and CA3) regions of the hippocampus at P7 (A1-A3) and P21 (A4-A6). Panels A1a-A6a are magnifications of the boxed windows. The primary antibodies used were rabbit polyclonal antibody anti-GlyRα2 and mouse monoclonal antibody anti-gephyrin. Small left panels represent each labelling alone: red for Gephyrin and green for GlyRα2. Nuclei were stained with DAPI. Examples of extrasynaptic GlyRα2 with a somatic localization (open arrowheads), extrasynaptic GlyRα2 with a dendritic localization (mid-open arrowheads), synaptic GlyRα2 with a somatic localization (open arrows) and synaptic GlyRα2 with a dendritic localization (mid-open arrows) are indicated in the magnified panels. Confocal images were acquired with a 63X oil-immersion objective. Scale bars, 20 µm. sg, *stratum granulosum*; sm, *stratum moleculare*; sp, *stratum pyramidale*; sr, *stratum radiatum*.

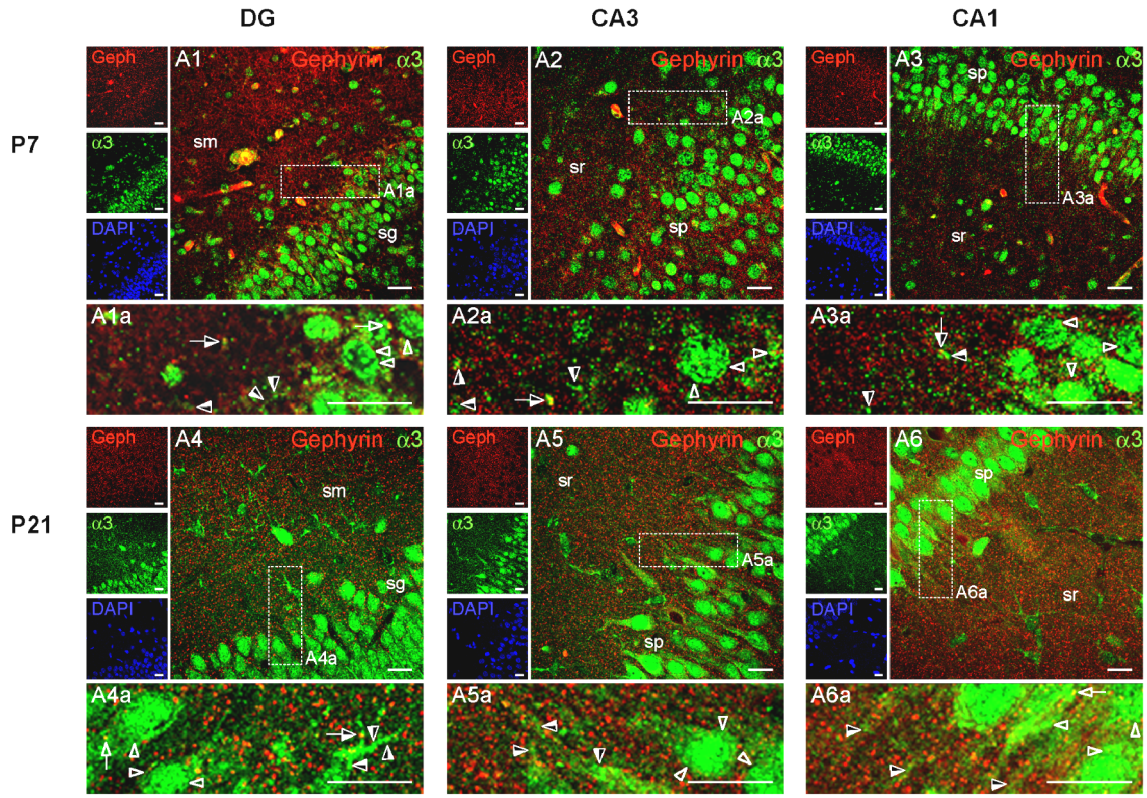


**Figure 5.11. - Synaptic and extrasynaptic localization of GlyRα3 subunit.** Double detection of GlyRα3 and gephyrin in rat hippocampus by confocal microscopy in Dentate Gyrus (DG) and *Cornus Ammonis* 1 and 3 (CA1 and CA3) regions of the hippocampus at P7 (A1-A3) and P21 (A4-A6). Panels A1a-A6a are magnifications of the boxed windows. The primary antibodies used were rabbit polyclonal antibody anti-GlyRα3 and mouse monoclonal antibody anti-gephyrin. Small left panels represent each labelling alone: red for Gephyrin and green for GlyRα3. Nuclei were stained with DAPI. Examples of extrasynaptic GlyRα3 with a somatic localization (open arrowheads), extrasynaptic GlyRα3 with a dendritic localization (mid-open arrowheads), synaptic GlyRα3 with a somatic localization (open arrows) and synaptic GlyRα3 with a dendritic localization (mid-open arrows) are indicated in the magnified panels. Confocal images were acquired with a 63x oil-immersion objective. Scale bars, 20 µm. sg, *stratum granulosum*; sm, *stratum moleculare*; sp, *stratum pyramidale*; sr, *stratum radiatum*.

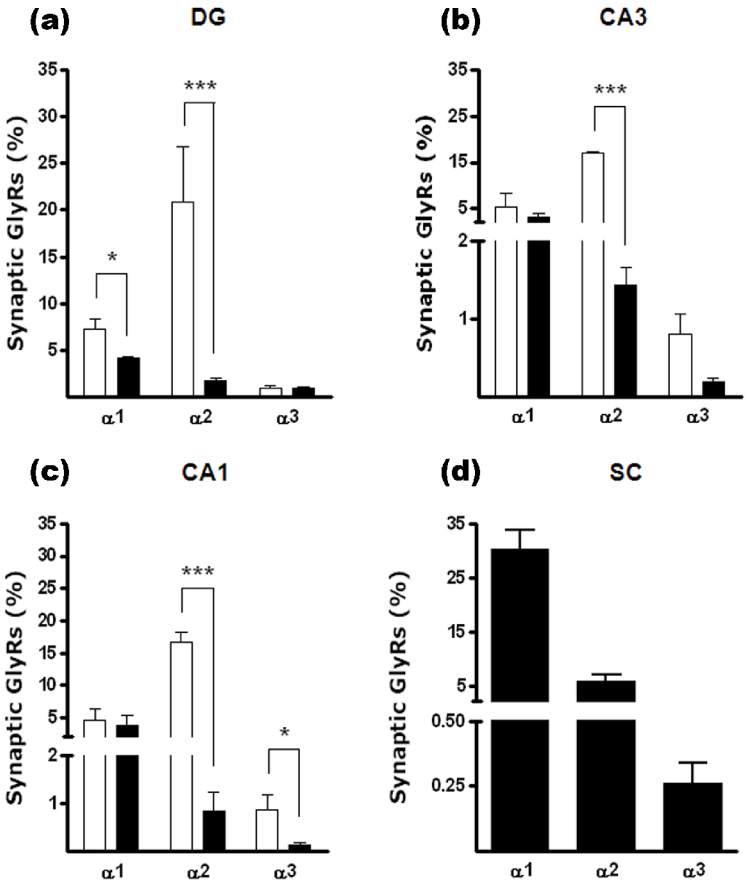


**Figure 5.12. - Quantitative analysis of synaptic GlyRα subunits in immature (▭ P7) and mature (▬ P21) neurons of Dentate Gyrus (a), *Cornus Ammonis* 3 (b), *Cornus Ammonis* 1 (c) and spinal cord (d).** Synaptic GlyR α1, α2 and α3 were quantified upon double staining with mouse monoclonal mAb2b antibody anti-GlyRα1, rabbit polyclonal antibody anti-GlyRα2, rabbit polyclonal antibody anti-GlyRα3, respectively, and rabbit polyclonal or mouse monoclonal antibodies anti-gephyrin. All values are mean ± SEM, *p<0.05, ***p<0.001 (unpaired t-test between P7 and P21). The total number (n) of counted GlyR were 15000<n<25000 for each rat hippocampal area and 27000<n<37000 for spinal cord. Analyzed regions are indicated on top of each graph.

**Table 5.2. -** Localization and relative expression of GlyR subunits in immature and mature rat hippocampus.

| GlyR subunit | Localizaton | Immature stage | | Mature stage | |
|---|---|---|---|---|---|
| | | Somatic | Dendritic | Somatic | Dendritic |
| **GlyRα1** | Synaptic | + | + | - | ++ |
| | Extrasynaptic | + | + | + | ++ |
| **GlyRα2** | Synaptic | +++ | ++ | + | - |
| | Extrasynaptic | + | + | ++ | +++ |
| **GlyRα3** | Synaptic | - | - | - | - |
| | Extrasynaptic | ++ | + | +++ | ++ |

Relative expression levels were estimated by comparison of confocal images: (-), not detected; (+), low expression; (++), moderate expression; (+++), high expression. Somatic localization indicates that glycine receptor (GlyR) surround the cell body. Dendritic localization points to GlyR expression in dendrites.

### 5.1.7. Subcellular localization of GlyR and vGluT1 in rat hippocampus

To evaluate whether GlyR were present in glutamatergic boutons, as described for a particular splice variant of GlyRα3 (Eichler *et al.* 2009), it was carried out a double staining with mAb4a and vGluT1 antibodies at P21 in all hippocampal areas (Figure 5.13A) and, for comparison, in mature spinal cord neurons (Figure 5.14.C). vGluT1 immunoreactivity was found, as expected, mainly in DG *stratum moleculare* and CA1/CA3 *stratum radiatum* areas of the hippocampus but few GlyR co-localized with vGluT1 (asterisks in Figure 5.13.A1-A3). GlyR quantification confirmed the negligible expression (< 3.5%) of GlyR in glutamatergic nerve endings in both hippocampal and spinal cord mature neurons (Figure 5.13.B).

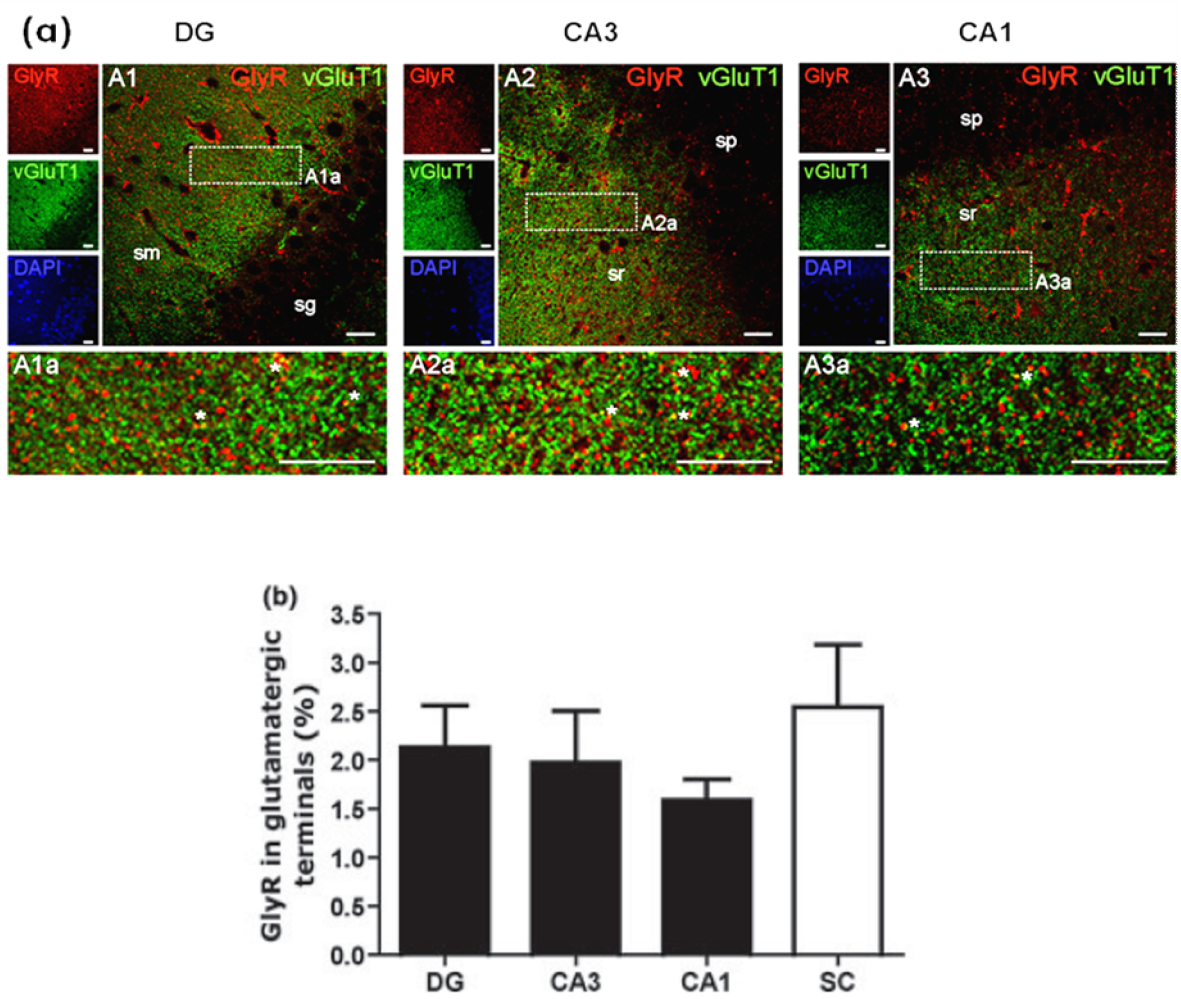


**Figure 5.13. - GlyR occurence in glutamatergic terminals. (A)** Double detection of GlyR and vGluT1 in rat hippocampus by confocal microscopy in Dentate Gyrus (DG) and *Cornus Ammonis* 1 and 3 (CA1 and CA3) regions at P21 (A1-A3). Panels (A1a-A3a) are magnifications of the boxed windows. The primary antibodies used were mouse monoclonal mab4a antibody anti-GlyR and rabbit polyclonal antibody anti-vGluT1. Small left panels represent each labelling alone: GlyR immunoreactivity is red and glutamatergic terminals are green. Nuclei were stained with DAPI. Asterisks indicate GlyR presence in glutamatergic terminals. Confocal images were acquired with a 63X oil-immersion objective. Scale bars, 20 µm. sg, *stratum granulosum*; sm, *stratum moleculare*; so, *stratum oriens*; sp, *stratum pyramidale*; sr, *stratum radiatum*. **(B)** Quantitative analysis of GlyR in glutamatergic terminals. All values are mean ± SEM. The total number (n) of counted GlyR were 10000<n<15000 for each hippocampal area and 48000 for spinal cord (SC).

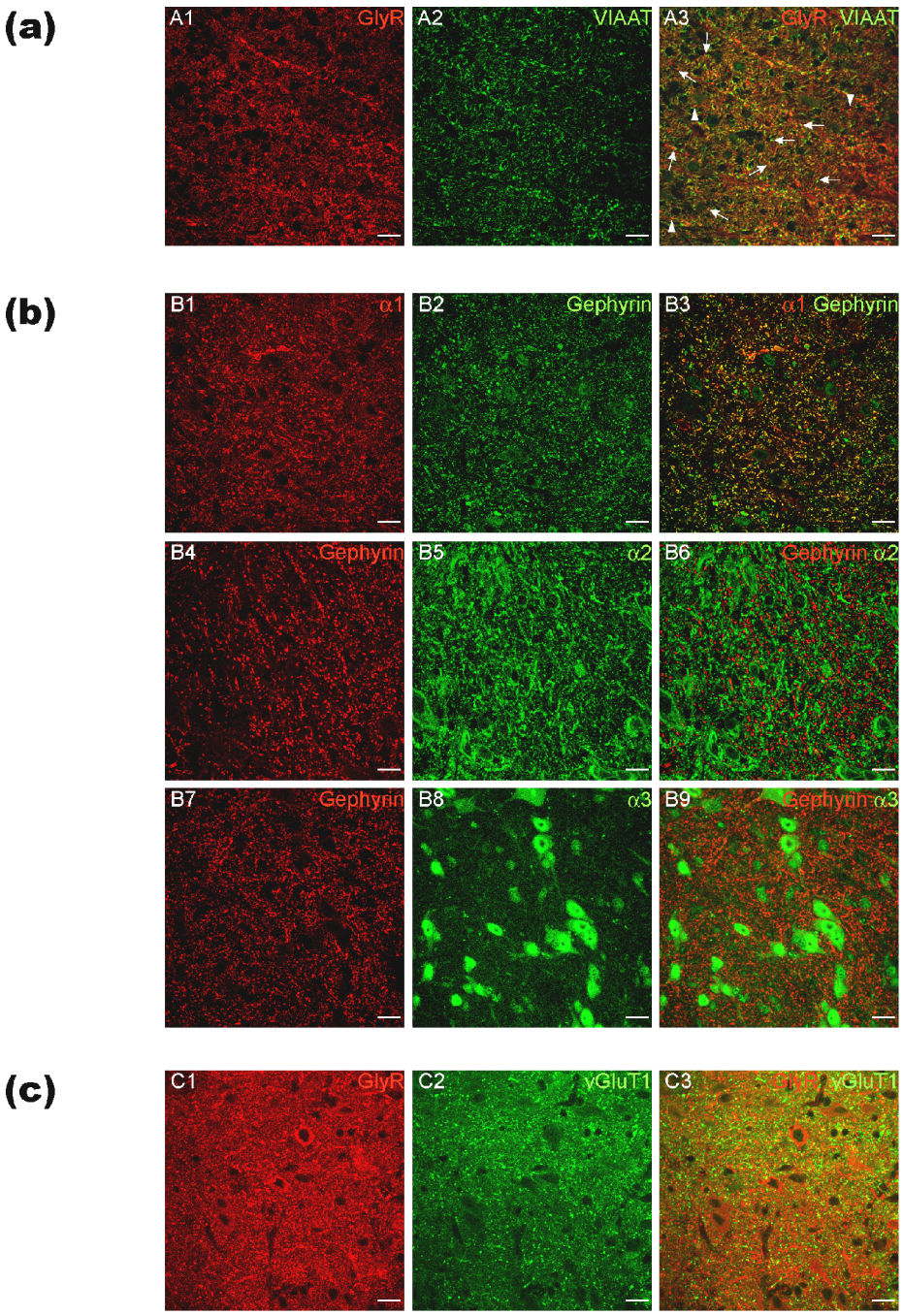


**Figure 5.14. - Immunohistochemistry in rat spinal cord sections, laminae II of the ventral horn, by confocal microscopy.** Detection of GlyR and VIAAT (A), GlyRα1 and gephyrin (B1-B3), GlyRα2 and gephyrin (B4-B6), GlyRα3 and gephyrin (B7-B9) and GlyR and vGluT1 (C). The primary antibodies used were: **(A)** mouse monoclonal mab4a antibody anti-GlyR and rabbit polyclonal antibody anti-VIAAT, **(B)** mouse monoclonal antibody anti-GlyRα1, rabbit polyclonal antibody anti-GlyRα2, rabbit polyclonal antibody anti-GlyRα3, rabbit polyclonal antibody anti-gephyrin and mouse monoclonal antibody anti-gephyrin and **(C)** mouse monoclonal mab4a antibody anti-GlyR and rabbit polyclonal antibody anti-vGluT1. In each row the first two panels represent each labelling alone. Arrows indicate GlyR-containing synapses. Arrowheads point to GlyR extrasynaptic homomeric clusters. Confocal images were acquired with a 63X oil-immersion objective. Scale bars, 20 µm.

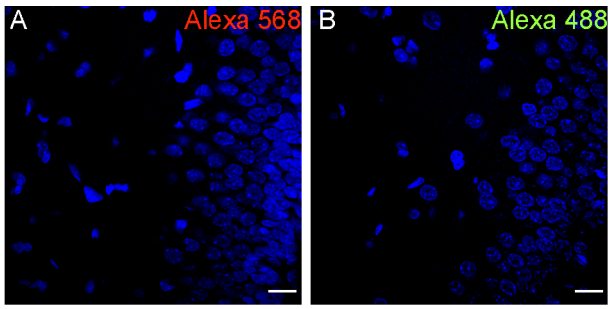


**Figure 5.15. - Negative controls for immunohistochemistry in rat hippocampus (P21) sections by confocal microscopy.** No primary antibodies were added. The secondary fluorescent-labelled antibodies used were: goat anti-mouse-Alexa 568 **(A)** and goat anti-rabbit-Alexa 488 **(B)**. Confocal images were acquired with a 63X oil-immersion objective. Scale bars, 20 µm.

### 5.1.8. Discussion

These data clearly show that GlyR in the rat hippocampus are present from the embryo to the adult, and that their distribution in synaptic and extrasynaptic sites changes over development. GlyR expression reaches its maximum at seven days postnatal (P7), where its expression is increased 3-5 fold as compared with a late embryonic stage (E18). In all developmental stages the majority of GlyR are extrasynaptic and the highest density of synaptic GlyR are found at P7-P14.

Interestingly, there is a temporal correlation between the increase in GlyR expression detected in the first postnatal week with the well known changes in the expression pattern of the ion transporters that determine the direction of $Cl^-$ electrochemichal gradient, NKCC1 and KCC2. During the first postnatal week, the $Cl^-$ loader, NKCC1, is highly expressed (Plotkin *et al.* 1997), while the $Cl^-$ extruder, KCC2 is weakly expressed (Clayton *et al.* 1998), so that glycine and GABA, through activation of the corresponding ligand-gated ion channel, cause membrane depolarization due to $Cl^-$ efflux. Thus, according to these results, GlyR seem to have a higher expression while mediating depolarization. As pointed out (Ben-Ari 2002), membrane depolarization due to activation of $Cl^-$ permeable ionotropic receptors in immature neurons is enough to remove $Mg^{2+}$ ions that are blocking NMDA receptors. At mature stages, the excitatory transmission via NMDA receptors surpasses the progressively declining depolarization mediated by $Cl^-$ permeable ionotropic receptors (Ben-Ari 2002) and, as these results show, at these stages the expression of

hippocampal GlyR decreases. Therefore it can be hypothesized that GlyR are mostly required to provide a reinforcement of $Cl^-$ mediated depolarization in early stages of development and when that is no longer required, GlyR expression decreases by a still unknown mechanism. Interestingly, in newborn neurons (P0), GlyR (containing either α1, α2 or α3 subunits) perfectly delineate the cell bodies of granular cells of the *stratum granulosum* of DG and pyramidal cells of the *stratum pyramidale* of CA1/CA3 regions, being therefore in the appropriate position to reinforce excitatory inputs to glutamatergic neurons, allowing NMDA signaling, which is crucial for neuronal maturation (Ben-Ari 2002). These GlyR have a predominance of α2 and α3 over α1 and β subunits, since the expression of the α2 and α3 subunits was found to be much higher than that of α1 and β subunits. Synaptic GlyR include the β subunit, which directly binds to gephyrin, a cytosolic protein required for a regulated aggregation and postsynaptic clustering of these receptors (Kirsch *et al.* 1991, Meyer *et al.* 1995, Legendre 2001, Levi *et al.* 2004, Meier & Grantyn 2004). At P0, β subunit expression is probably not enough to ensure gephyrin binding and therefore impairs GlyR synaptic targeting. At P7 it was found that GlyR expression increases in *stratum moleculare* and *stratum radiatum* of DG and CA1/CA3 regions, areas where axons and dendrites are abundantly established. It was also observed an increase in β subunit expression. Altogether these data correlate with a boost of synaptic, mostly heteromeric GlyRα2β, in the vicinity of inhibitory nerve endings positive for VIAAT, confirming a postsynaptic location, as described elsewhere for spinal cord neurons (Dumoulin *et al.* 1999). The presynaptic boutons are instructive for postsynaptic receptor accumulation (Dumoulin *et al.* 2000) and so, the now reported GlyR clustering facing a VIAAT positive bouton is indicative of the occurrence of a glycine releasing terminal. Nevertheless, it has to be pointed out that, at least in mature hypoglossal motoneurons, GlyR and $GABA_AR$ were found to co-aggregate in the same postsynaptic density, even though the ability of presynaptic terminals to release both neurotransmitters is lost during development (Muller *et al.* 2006). Whether some of the postsynaptic GlyR, here identified by VIAAT apposition, correspond to a functional glycinergic synapse that may have lost the ability to presynaptically release glycine, cannot be answered in the present work. In the hippocampus, however, it has to be emphasized that synaptic GlyR represent a less significant population than extrasynaptic ones, even at early developmental stages.

In mature hippocampus (P21 on) there is a further decrease in total synaptic GlyR, and even a more pronounced decrease in synaptic GlyRα2. These findings, together with the

occurrence of many extrasynaptic GlyR clusters, suggest that mature hippocampus contains a few synaptic GlyRα1β in the dendrites and many extrasynaptic α2/α3-containing GlyR that occur both in the dendrites and around the cell body of granular and pyramidal cells, as well as in interneurons.

The predominance of α2/α3-containing GlyR in mature hippocampus is in accordance with previous results obtained from *in situ* hybridization studies, which used sequence specific oligonucleotide probes for GlyR subunits (Malosio *et al.* 1991b), and it contrasts with the prevalence of GlyRα1 in spinal cord (Malosio *et al.* 1991b) and brain stem motoneurons (Singer *et al.* 1998). Indeed, in immature caudal CNS neurons, extrasynaptic α2 homomeric GlyR are progressively replaced by synaptic α2β heteromeric GlyR and finally by synaptic α1β and α3β heteromeric GlyR in mature neurons (Muller *et al.* 2008). GlyR are known to be able to move to postsynaptic loci (Meier *et al.* 2001, Dahan *et al.* 2003), which allows their role in fast phasic inhibition, whereas extrasynaptic receptors are probably tonically activated by spillover of neurotransmitter from the synaptic cleft or by non-synaptic glycine release, thus contributing to tonic inhibition (Muller *et al.* 2008, Zhang *et al.* 2008, Legendre *et al.* 2009). Thus, it can be proposed that GlyR-mediated transmission in mature hippocampus contribute to tonic inhibition via extrasynaptic α2/α3 containing homomeric receptors, being probably more relevant than the low expressed synaptic GlyRα1β. The molecular mechanisms responsible for the stabilization of extrasynaptic GlyR, or the mechanisms which allow them to diffuse to synaptic locus, are still unknown and require further studies.

Embryonic cortical neurons from GlyRα2 knockout mice are devoid of glycinergic transmission (Young-Pearse *et al.* 2006). As these results show, at early developmental stages most synaptic GlyR are heteromeric GlyRα2β. Interestingly, at later developmental stages (P7) GlyRα2 lacking neurons already respond to glycine, suggestive of a compensatory influence from other GlyR subunits (Young-Pearse *et al.* 2006). Indeed, these data corroborate these electrophysiological findings, showing an increase in the expression of other GlyR subunits, namely α1, from P7 onwards.

As expected, from P14 on, VIAAT labelling was found in the somatic layers, namely *stratum granulosum* of DG and *stratum pyramidale* of CA1/CA3 regions. This expression is related to the occurrence of axo-somatic inhibitory synapses, which are important to control the excitatory output of granular and pyramidal glutamatergic neurons, and start to be established during the second and third postnatal weeks, in accordance with previous data (Ben-Ari *et al.* 1989).

Although GlyR expression is detected in all hippocampal subregions, there is a higher expression within the *stratum granulosum* and the *stratum moleculare* of DG in all postnatal developmental stages analysed, which is in agreement with prior immunohistochemistry studies using adult rat hippocampus (Danglot *et al.* 2004, Eichler *et al.* 2009). DG is a vulnerable region to epileptic activity (Parent & Lowenstein 2002) and GABAergic transmission impairment in DG might be a cause of epilepsy (Dalby & Mody 2001). Earlier reports (Chattipakorn & McMahon 2003) stated that upon GABAergic transmission impairment, GlyR activation is able to inhibit bursting activity elicited in DG slices, unravelling a role for GlyR in epilepsy. In this work it was showed that synaptic GlyR expression is higher in DG in all developmental stages, which might be related to the requirement of an additional or alternative inhibitory mechanism, such as GlyR-mediated inhibitory transmission, that might prove particularly relevant when GABAergic transmission fails.

In mature rat hippocampal slices functional GlyR were found in CA1 pyramidal cells in GABAergic interneurons and in DG neurons, where they are able to suppress excitability (Chattipakorn & McMahon 2002, Chattipakorn & McMahon 2003, Song *et al.* 2006). However, the role of GlyR in hippocampal synaptic transmission remains a controversial subject (Xu & Gong 2010).

This work explored the GlyR expression in rat hippocampus and identified spatial-temporal changes in GlyR distribution at the main hippocampal areas. Developmental changes in subunit composition of somatic, synaptic and extrasynaptic GlyR were also shown. Summarizing, at birth, GlyR expression is low, GlyR have mainly a somatic localization and are composed of α2 and α3 subunits, which could provide evidence for a potential role of GlyR in modulating hippocampal excitability at early postnatal stages. At P7, GlyR expression is higher and a few synaptic GlyR, mainly GlyRα2β, can be found. In mature hippocampus synaptic GlyRα2β decrease. At this stage, a few synaptic GlyRα1β and plenty of extrasynaptic GlyR α2/α3 can be detected which points towards a role of slow tonic activation of extrasynaptic GlyR α2/α3 in mature hippocampus.

## 5.2. GlyT1 and GlyT2 are functionally expressed in brain astrocytes

*Rita Aroeira has written the draft and performed all the experimental work.*
*The work presented in this section was recently published (Aroeira et al. 2014).*

### 5.2.1. Rationale

At glycinergic synapses, termination of glycine-mediated synaptic activity occurs through removal of the neurotransmitter from the synaptic cleft, by specific GlyT (Eulenburg *et al.* 2005), namely, GlyT1 (Guastella *et al.* 1992) and GlyT2 (Liu *et al.* 1992). Both GlyT are present in several isoforms generated by alternative splicing and the use of alternative promoters (Adams *et al.* 1995, Ebihara *et al.* 2004). By *in situ* hybridization, GlyT1 expression was detected in most brain areas, while GlyT2 was observed in spinal cord and brainstem (Borowsky *et al.* 1993). Furthermore, GlyT2 is present in a lesser extent in the brain than GlyT1 (Jursky & Nelson 1996).

It is widely accepted that GlyT1 is mainly expressed in astrocytes, while GlyT2 is predominantly expressed in glycinergic nerve terminals (Eulenburg *et al.* 2005). However, recent studies (Raiteri *et al.* 2008), which described the presence of GlyT2 in purified preparations of mouse spinal cord astrocyte-derived subcellular particles, named gliosomes, challenged this knowledge. Whether GlyT2 is also present in brain astrocytes, where glycinergic transmission represents a minor proportion of the inhibitory transmission, is still unknown.

Alterations in glycine-mediated neurotransmission were also reported in several pathologies including neuropathic pain, schizophrenia (Dohi *et al.* 2009), hyperekplexia (Rees *et al.* 2006) and hyperexcitability-related diseases (Eichler *et al.* 2008, Harvey *et al.* 2008). Several authors point out the physiological relevance of the regulation of glycine concentration in the synaptic cleft and consider GlyT as an alternative therapeutic target for the treatment of these disorders (Eulenburg *et al.* 2005). Furthermore, astrocytes are no longer regarded as simple supportive cells for neurons, being considered as the third element of a structure known as “tripartite synapse” (Araque *et al.* 1999, Perea *et al.* 2009). Thus, impairments in astrocytic function are increasingly being recognized as an important contributor to neuronal dysfunction.

Therefore, the expression and function of GlyT in brain astrocytes were evaluated.

### 5.2.2. GlyT1 and GlyT2 are expressed in rat cultured cortical astrocytes

Using astrocytes at different maturation stages in culture, namely 10, 18 and 24 DIV, GlyT1 and GlyT2 transcripts were evaluated by qPCR. The results showed that both GlyT1 and GlyT2 mRNA are present in astrocytes from 10 to 24 DIV. Relative quantification in comparison with 10 DIV transcripts (Pfaffl 2001), using β-actin as the reference control gene, indicated that both transcripts were preserved throughout the considered time culture (Figure 5.16.). No signal amplification was detected in the negative controls, which indicated signal specificity. Reaction specificity was further evaluated in all assays by a melting curve (Figure 5.17.).

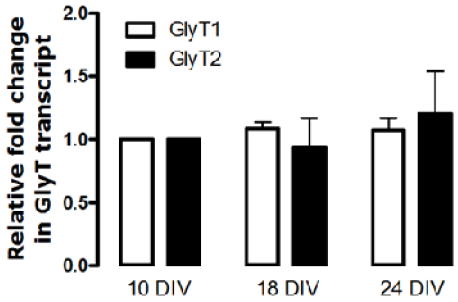


**Figure 5.16. - Changes in the expression level of GlyT1 and GlyT2 transcripts in rat cortical astrocytes over several maturation stages (10, 18 and 24 DIV) by relative qPCR.** β-actin was used as the reference control gene. Values are mean ± SEM, no significative differences ($p>0.05$) were found when comparing the expression of each transcript with 10 DIV (n=6, one way ANOVA followed by Bonferroni's Multiple Comparison Test).

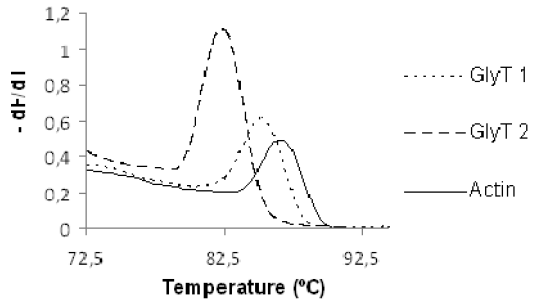


**Figure 5.17. - Melting curves of GlyT1, GlyT2 and β-actin transcripts analyzed by qPCR.** Y axis represents the first derivate of raw fluorescence and X axis corresponds to an increase in temperature. Each curve has a single melting peak, which indicates that a single PCR product is being amplified.

Next, protein expression in primary cortical astrocytes throughout the same culture time was assessed. For this, a western blot procedure was used and the membranes were probed with antibodies that specifically recognized GlyT1, GlyT2 or the endogenous loading control β-actin (Figure 5.18.). The immunoblot obtained for GlyT1 revealed the presence of two bands, one with a molecular weight of approximately 75 kDa and a heavier band with around 90 kDa. This pattern is in agreement with the presence of several GlyT isoforms. In the case of GlyT1, the 75 kDa band indicates the expression of GlyT1a and GlyT1b isoforms, while the 90 kDa band might correspond to GlyT1c (Vargas-Medrano *et al.* 2011). The antibody against GlyT2 detected three bands in the 50-75 kDa range, which is also consistent with the occurrence of GlyT2 isoforms (Eulenburg *et al.* 2005). Furthermore, both GlyT are described to have multiple N-glycosylation sites (Olivares *et al.* 1995, Martinez-Maza *et al.* 2001), which could also explain the intermediate bands observed in GlyT immunoblots. All bands were present at all DIV, being the expression pattern very similar to the one detected for spinal cord homogenates. For the GlyT1 90 kDa isoform a minor intensity decrease over time was noticeable, whereas the 75 kDa isoform of GlyT2 was almost absent in mature astrocytes.

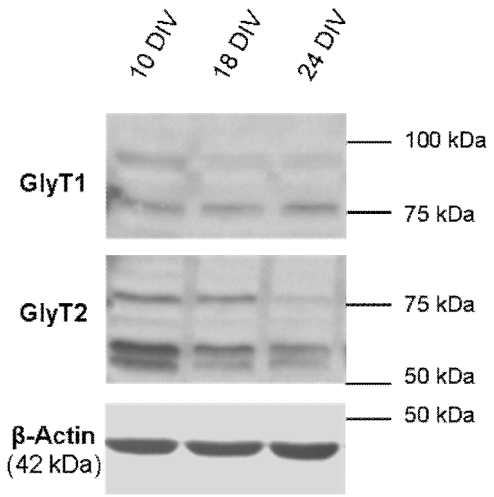


**Figure 5.18. - Expression of GlyT1 and GlyT2 protein in rat cortical astrocytes over several maturation stages (10, 18 and 24 DIV).** Western blot analysis of GlyT1, GlyT2 and β-actin (42 kDa) in rat cultured cortical astrocytes. β-actin was used as a loading control. The immunoreactive bands were detected on a 12% sodium dodecyl sulfate–polyacrylamide gel electrophoresis using GlyT1, GlyT2 and β-actin antibodies.

### 5.2.3. GlyT1 and GlyT2 have a different subcellular localization in rat cortical astrocytes

To assess GlyT1 and GlyT2 localization in cultured astrocytes a double immunofluorescence assay was performed during the course of the culture. This procedure identified differentiated astrocytes, by GFAP staining, together with GlyT and DAPI stained nucleus.

The high incidence of GFAP positive cells in Figure 5.19. and Figure 5.20. confirmed that the cultures were enriched in astrocytes, which demonstrated that the microglia removal protocol was efficient. Additionally, an increase in cellular development and in culture confluence over time was noticed. Images of astrocytes at 10 DIV depicted isolated immature astrocytes with small processes and low GFAP expression, while from 18 DIV on GFAP expression was strongly detected in cell bodies and delineated all processes, indicating the predominance of mature astrocytes.

Confocal images revealed developmental regulated changes in subcellular localization of both GlyT1 (Figure 5.19.) and GlyT2 (Figure 5.20.). At 10 DIV (Figure 5.19., A1-A5), GlyT1 was predominantly detected in the cytoplasm outer layer (arrowheads in Figure 5.19., A5). However, it was already possible to observe GlyT1 expression in some small astrocytic processes (arrows in Figure 5.19., A5). From 18 DIV on (Figure 5.19., A6-A15), besides cytoplasm labelling (arrowheads in Figure 5.19., A10 and A15), GlyT1 was found in long spread processes (arrows in Figure 5.19., A10 and A15). At 10 DIV, GlyT2 (Figure 5.20., A1-A5) was expressed in the cytoplasm (arrowheads in Figure 5.20., A5) and in small astrocytic processes (arrows in Figure 5.20., A5), alike GlyT1. From 18 DIV onwards (Figure 5.20., A6-A15), several GlyT2 clusters can be distinguished over the cytoplasm (arrowheads in Figure 5.20., A10 and A15), in the small non-spread processes (arrows in Figure 5.20., A10) and also in some mature processes of astrocytes (arrows in Figure 5.20., A15).

### 5.2.4. GlyT1 and GlyT2 are expressed in rat brain astrocytes

Due to the unexpected presence of GlyT2 in rat cultured cortical astrocytes, GlyT2 expression in astrocytes was also investigated in brain slices. To this end, GlyT localization in the rat brain was explored by confocal immunohistochemistry analysis of paraffinized coronal brain slices (5 μm). A double staining of GFAP and GlyT, as well as

DAPI, reveals if and where GlyT1 and GlyT2 were expressed in the astrocytes of mature brains (P21). In order to have a broader characterization of GlyT expression in the forebrain, images were taken in a cortical region and in the DG of the hippocampus. P21 astrocytes strongly express GFAP and establish elongated processes in both cortical and hippocampal regions (Figure 5.21., GFAP panels).

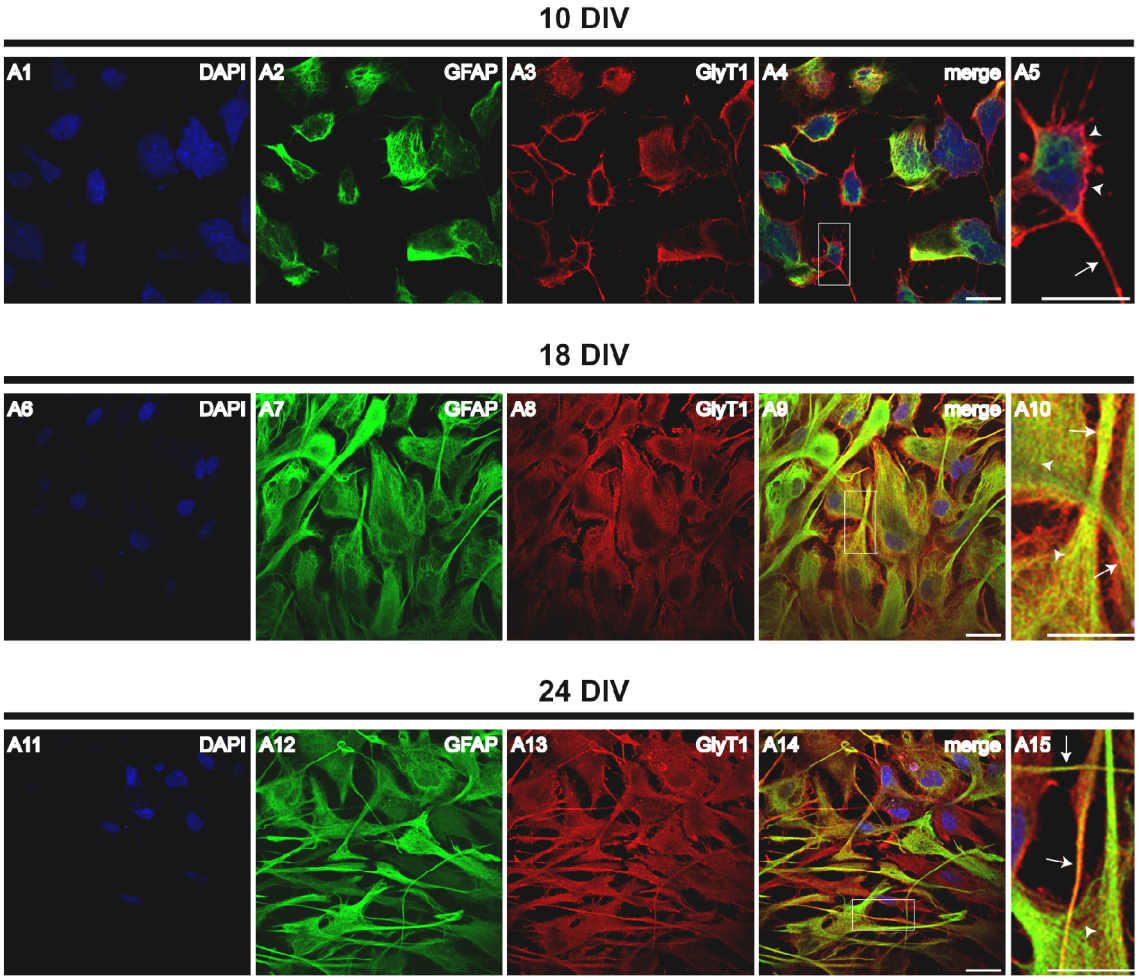


**Figure 5.19. - Double detection of GlyT1 and GFAP in rat cultured cortical astrocytes over several maturation stages (10, 18 and 24 DIV) were assessed by confocal microscopy.** Examples of GlyT1 in cytoplasm (arrowheads) and GlyT1 in astrocytic processes (arrows) are indicated. In every row, the first three panels represent each labelling alone (DAPI stained nuclei, green for GFAP and red for GlyT1) and the last one is a magnification of the boxed window. Confocal images were acquired with a 63X oil-immersion objective. Scale bars, 20 µm.

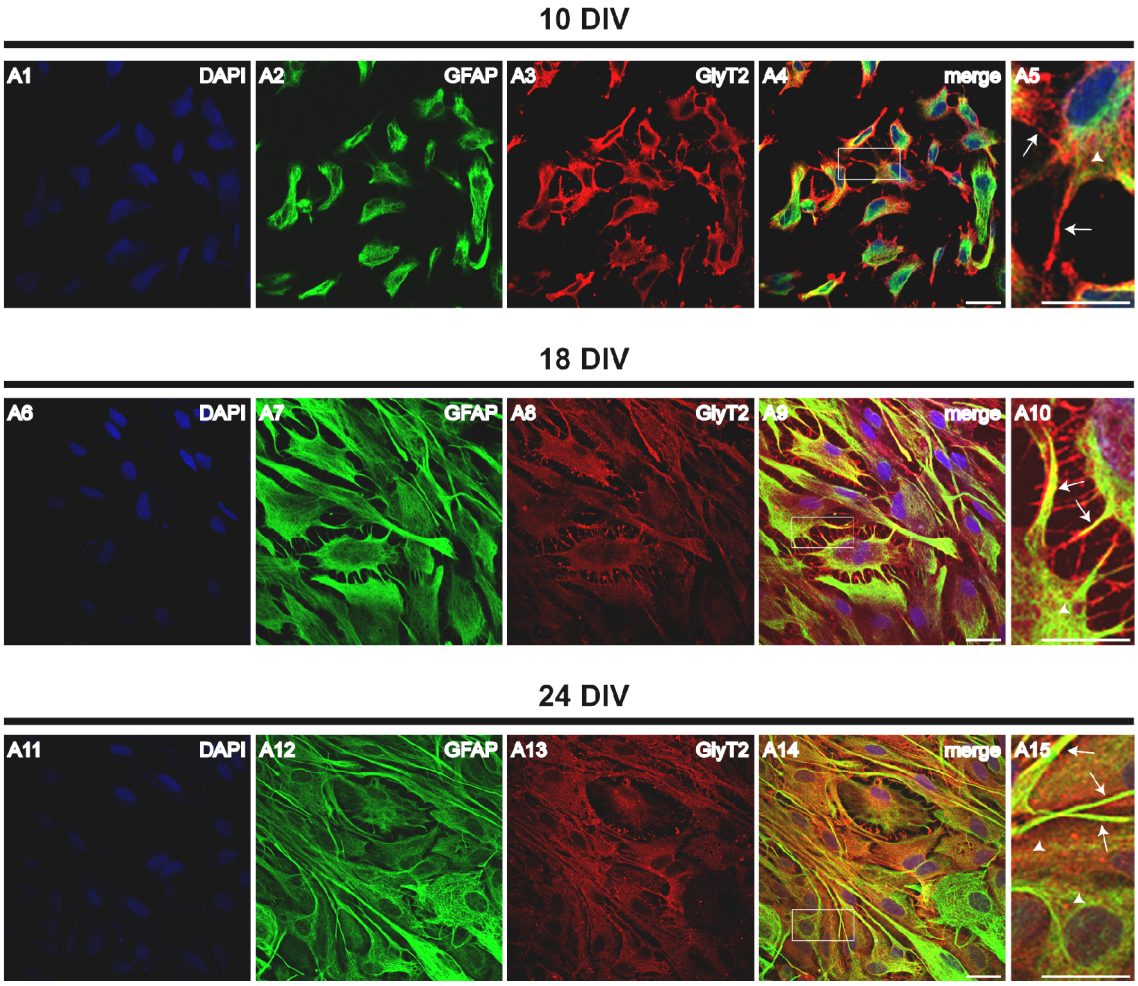


**Figure 5.20. - Double detection of GlyT2 and GFAP in rat cultured cortical astrocytes over several maturation stages (10, 18 and 24 DIV) were assessed by confocal microscopy.** Examples of GlyT2 in cytoplasm (arrowheads) and GlyT2 in astrocytic processes (arrows) are indicated. In every row, the first three panels represent each labelling alone (DAPI stained nuclei, green for GFAP and red for GlyT2) and the last one is a magnification of the boxed window. Confocal images were acquired with a 63X oil-immersion objective. Scale bars, 20 µm.

GlyT1 expression was detected in both regions of the mature rat brain (Figure 5.21.). In the cortical area (Figure 5.21., A1-A5), GlyT1 immunolabelling was present in the astrocytic processes (arrows in Figure 5.21., A5). GlyT1 was also observed over the cytoplasm of many GFAP-negative cells (arrowheads in Figure 5.21., A4) and presented a punctate distribution throughout the whole cortical region (open arrowheads in Figure 5.21., A5). In the DG (Figure 5.21., A6-A10) GlyT1 expression was found to be localized in astrocytic processes (arrows in Figure 5.21., A10), but also extensively spread through the whole

dendritic layer (open arrowheads in Figure 5.21., A10). In the granular layer of DG, GlyT1 was also found to surround many GFAP-negative cells (arrowheads in Figure 5.21., A9).
Similarly, GlyT2 was present in cortical and hippocampal regions (Figure 5.21., B1-B10). In the cortical area (Figure 5.21., B1-B5), GlyT2 immunolabelling was present in the processes of many astrocytes (arrows in Figure 5.21., B5). As observed for GlyT1, GlyT2 was also localized in some GFAP-negative cell bodies (arrowheads in Figure 5.21., B4) and widespread throughout the cortical space (open arrowheads in Figure 5.21., B5). In the DG (Figure 5.21., B6-B10), GlyT2 was expressed in some astrocytes, mostly in small processes very close to the nucleus (arrows in Figure 5.21., B10). As in the cortex, GlyT2 immunolabeling was extensively spread over the dendritic layer (open arrowheads in Figure 5.21., B10) and detected in cell bodies (arrowheads in Figure 5.21., B9) that do not express GFAP.
In summary, the results obtained in brain slices revealed an expression pattern similar to the one obtained for cultured astrocytes, thus corroborating the presence of GlyT1 and GlyT2 in brain astrocytes.
Furthermore, a double immunostaining of GFAP and GlyT in spinal cord slices (Figure 5.22.) confirmed the presence of GlyT1 (Figure 5.22., A1-A5) and GlyT2 (Figure 5.22., B1-B5) in spinal cord astrocytes (arrows in Figure 5.22., A5 and B5), as concluded by the yellow labeling indicative of the co-localization between GlyT1/GlyT2 and GFAP. In spinal cord negative controls, carried out in the absence of the primary antibodies, no staining was detected.

### 5.2.5. GlyT1 and GlyT2 are expressed in neurons

To confirm that the GFAP-negative cell bodies, which express GlyT, are of neuronal nature, a double staining with GlyT1 or GlyT2 and MAP2, a neuronal marker, together with DAPI, was performed and confocal images from cortex and DG were obtained (Figure 5.23.).
In cortical regions, GlyT1 immunolabelling (Figure 5.23., A1-A5) was detected over cell bodies (arrowheads in Figure 5.23., A4) and also in neuronal processes (open arrowheads in Figure 5.23., A5), since it was possible to detect the co-localization between GlyT1 and MAP2. This pattern was also observed in the dendritic region of the hippocampus (open arrowheads in Figure 5.23., A10). GlyT1 was also found to surround the neuronal cell

bodies localized in the DG granular layer, which are known to correspond to glutamatergic neurons (Andersen 2007).

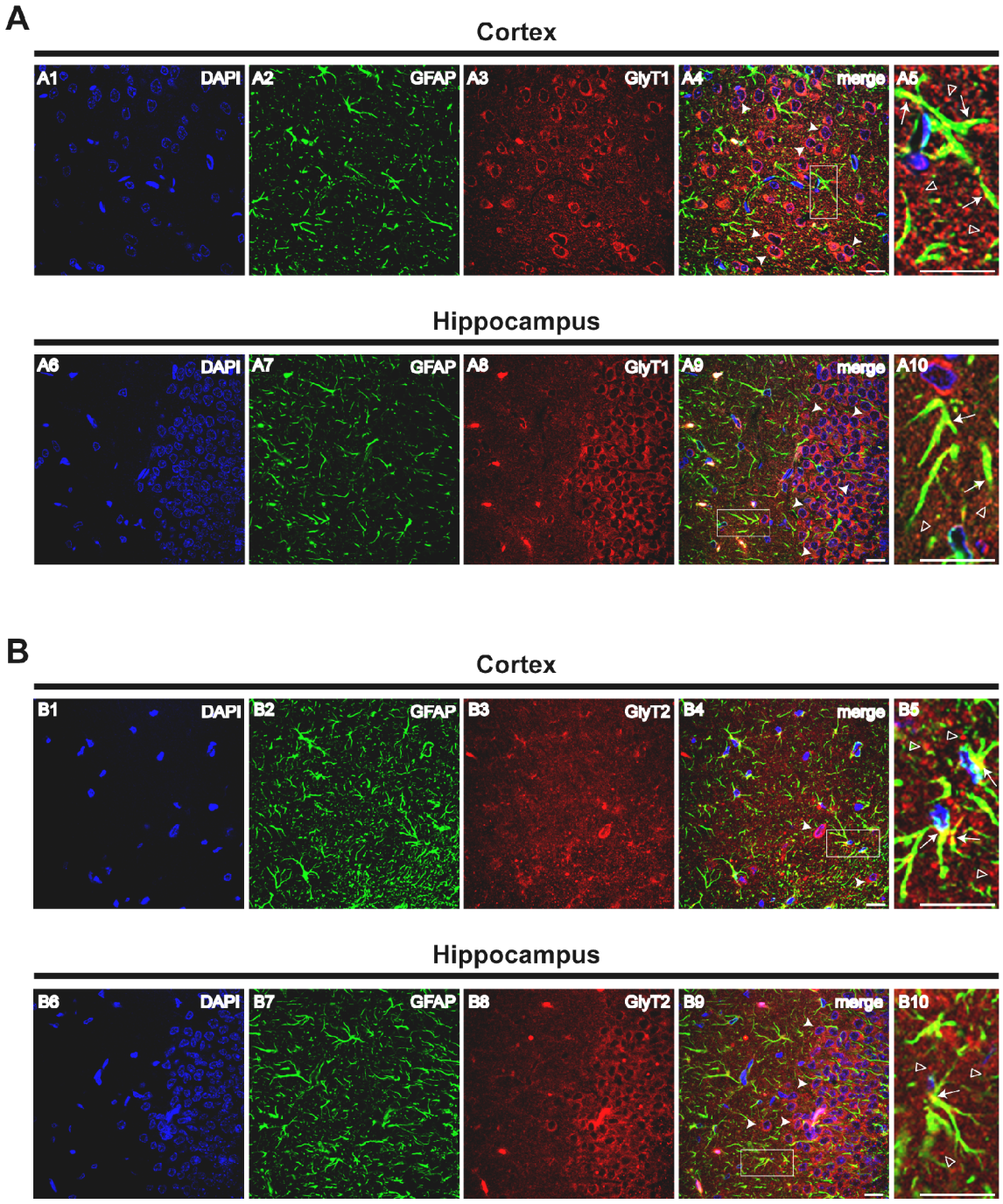


**Figure 5.21. - Localization of GlyT1 and GlyT2 in P21 rat brain astrocytes assessed by confocal microscopy.** Double immunolabeling of GFAP and GlyT1 **(A)** / GlyT2 **(B)** in cortex and dentate gyrus of the hippocampus. In every row, the first three panels represent each labelling alone (DAPI stained nuclei, green for GFAP and red for GlyT1/GlyT2) and the last one is a magnification of the boxed window. Examples of astrocytic GlyT are indicated by arrows, while GlyT occurrence in GFAP-negative cell bodies and processes is pointed by arrowheads and open arrowheads, respectively. Confocal images were acquired with a 63X oil-immersion objective. Scale bars, 20 μm.

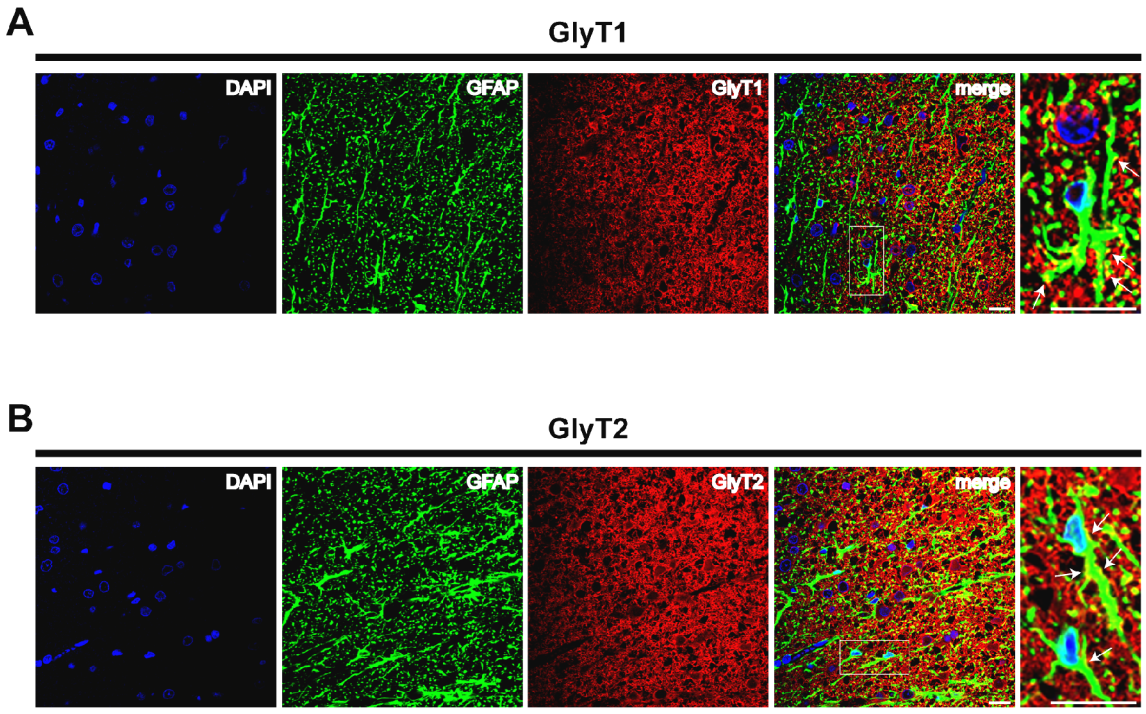


**Figure 5.22. - Localization of GlyT1 and GlyT2 in rat spinal cord slices, laminae II of the ventral horn, by confocal microscopy.** Double detection of GFAP and GlyT1 **(A)** / GlyT2 **(B)** in rat spinal cord. In every row, the first three panels represent each labelling alone (DAPI stained nuclei, green for GFAP and red for GlyT1/GlyT2) and the last one is a magnification of the boxed window. Examples of astrocytic GlyT are indicated by arrows in the magnified panels. Confocal images were acquired with a 63X oil-immersion objective. Scale bars, 20 µm.

Regarding GlyT2 (Figure 5.23., B1-B10), it was possible to detect GlyT2 expression in many neuronal cell bodies spread throughout the cortex (arrowheads in Figure 5.23., B4), probably of interneurons, and in neuronal processes (open arrowheads in Figure 5.23., B5). In the hippocampus (Figure 5.23., B6-B10) the presence of GlyT2 was also detected in some neurons localized in the granular layer (arrowheads in Figure 5.23., B9). As in the cortex, GlyT2 was detected in neuronal processes spread throughout the dendritic layer (open arrowheads in Figure 5.23., B10).

Furthermore, in both regions, the presence of GlyT in MAP2-negative cell bodies and processes (arrows in Figure 5.23., A5, A10, B5 and B10) was detected, which are in accordance with the results showed in the previous subsection, with GlyT detection in astrocytes.

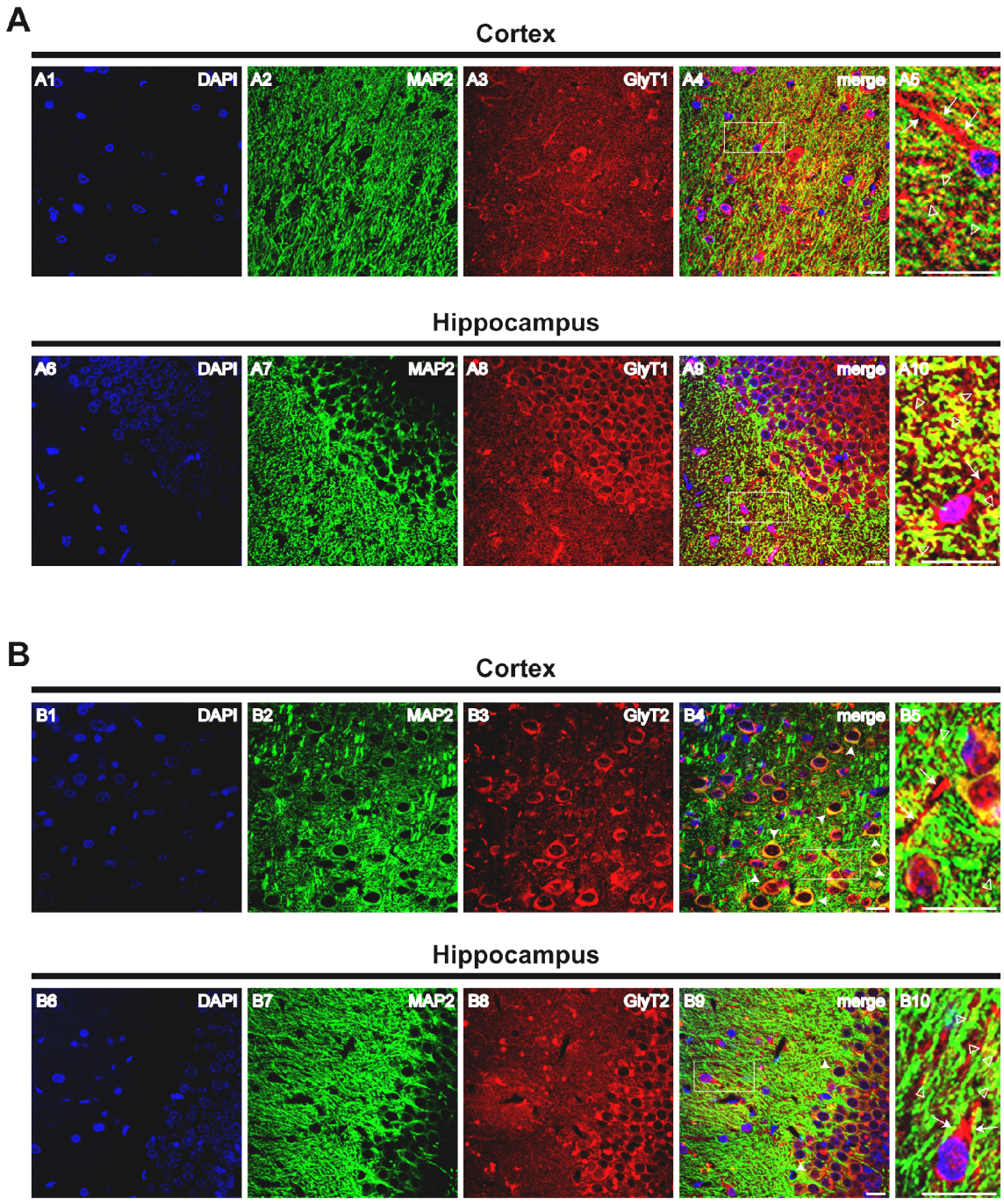


**Figure 5.23. - Localization of GlyT1 and GlyT2 in P21 rat brain neurons assessed by confocal microscopy.** Double immunolabeling of MAP2 and GlyT1 **(A)** / GlyT2 **(B)** in cortex and dentate gyrus of the hippocampus. In every row, the first three panels represent each labelling alone (DAPI stained nuclei, green for GFAP and red for GlyT1/GlyT2) and the last one is a magnification of the boxed window. GlyT1 and GlyT2 presence in neuronal cell bodies and processes are indicated by arrowheads and open arrowheads, respectively. Arrows illustrate non-neuronal GlyT. Confocal images were acquired with a 63X oil-immersion objective. Scale bars, 20 μm.

### 5.2.6. GlyT1 and GlyT2 are functionally expressed in rat cultured cortical astrocytes

To evaluate if astrocytic GlyT1 and GlyT2 are able to transport glycine, [$^3$H]glycine uptake assays in cultured astrocytes were performed. Optimization assays were carried out to define the incubation time with [$^3$H]glycine, as well as the concentration of inhibitors to be used to calculate the transport mediated by GlyT1 or GlyT2. Two concentrations of glycine were used, 50 µM to study high affinity transport (Figure 5.24.A) and 1500 µM to study low affinity transport (Figure 5.24.B). In both cases the uptake of [$^3$H]glycine increased linearly with time of incubation from 30s to 240s (Figure 5.24.A-B), therefore a 2 min incubation time was chosen for the remaining experiments.

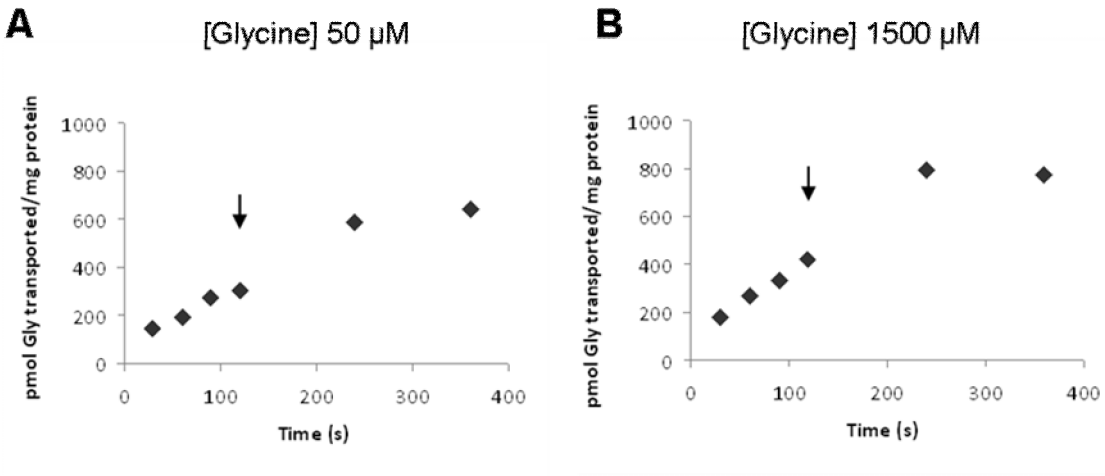


**Figure 5.24. - Transport progression curves using two concentrations of glycine, 50 µM to study GlyT1 (A) and 1500 µM to study GlyT2 (B).** Incubation time ranging from 30s to 360s was tested. Arrows point to the incubation time used in the subsequent experiments.

Transport assays with increasing concentrations (1-30 µM) of Org 24598 (a selective GlyT1 blocker) and a constant [$^3$H]glycine (50 µM) concentration (Figure 5.25.A) revealed that maximal transport inhibition was achieved with 10 µM Org 24598. So, non-GlyT1 mediated transport was defined as the uptake occurring in the presence of 10 µM Org 24598, a concentration about 100 times higher than the IC50 value for GlyT1 inhibition and well below the IC50 value for GlyT2 inhibition (Brown *et al.* 2001).

Uptake assays with 1500 µM [$^3$H]glycine at increasing concentrations of the GlyT2 inhibitors, ALX 1393 (Luccini & Raiteri 2007) or amoxapine (Nunez *et al.* 2000) showed that an inhibition plateau was reached at 50-500 nM of ALX 1393 (Figure 5.25.B) or 0.5-2

μM of amoxapine (Figure 5.25.C). Higher concentrations of these inhibitors further inhibit glycine transport, but were not chosen to define non-GlyT2 mediated transport to avoid the use of concentrations not selective for GlyT2.

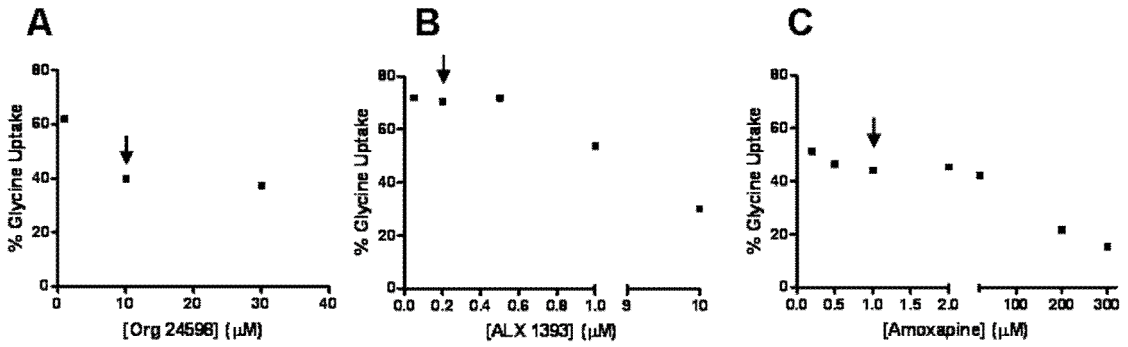


**Figure 5.25. - Concentration-dependent uptake of glycine in rat cultured cortical astrocytes by GlyT inhibitors.** GlyT1-specific inhibitor Org 24598 **(A)**, GlyT2-blockers ALX 1393 **(B)** and amoxapine **(C)** were used in several concentrations. Note the differences in X axis scale between graphs. Y axis represents [$^3$H]glycine uptake as percentage of the control value (absence of inhibitors) in the same experiment. Arrows point to the concentration of inhibitor used in the subsequent experiments to isolate GlyT1 and GlyT2 specific transport.

In order to estimate the relative influence of GlyT1 and GlyT2 for total glycine transport, assays were performed in the presence or absence of the selective inhibitors. Non-GlyT mediated uptake was defined as the uptake in the presence of excess (10 mM) of cold glycine (calculated as about 20% of total glycine transport in control conditions) and was subtracted in all experiments. Uptake of [$^3$H]glycine (50 μM) was reduced to 30.50 ± 1.183 % (n=4) by Org 24598 (10μM) (Figure 5.26.A), suggesting that GlyT1 ensured 70% of GlyT-mediated transport. ALX 1393 (200 nM) blocked the Org 24598-resistant [$^3$H]glycine (50 μM) uptake (Figure 5.26.A) suggesting that even at micromolar concentrations of glycine, GlyT2 is responsible for about 30% of the GlyT-mediated uptake. Similar results were obtained while using a higher concentration of [$^3$H]glycine (Figure 5.26.B). ALX 1393 (200 nM) inhibited [$^3$H]glycine (1500 μM) transport to 61.99 ± 3.76 % (n=4) and the ALX 1393-resistant component of the transport was fully blocked by Org 24598 (10 μM), suggesting that GlyT2 is responsible by near 40% of [$^3$H]glycine (1500 μM) uptake into astrocytes, while GlyT1 accounts for about 60% of the transport.

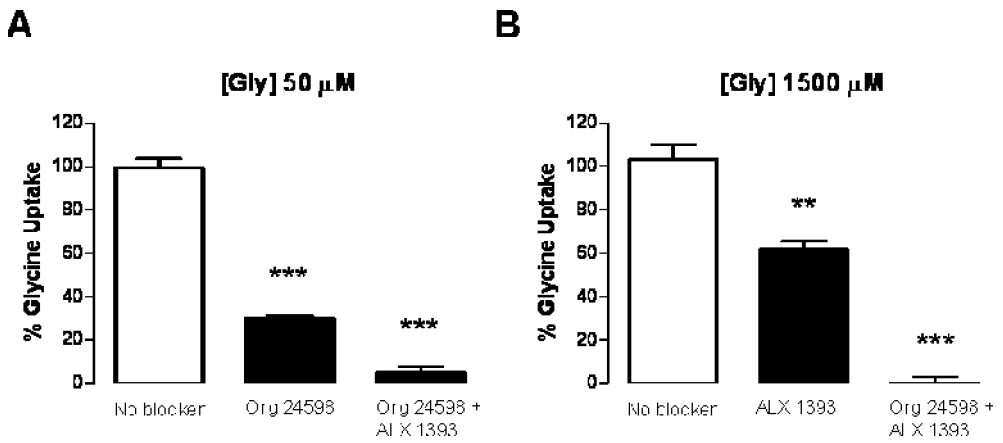


**Figure 5.26. - Characterization of the relative contribution of each glycine transporter in rat cultured cortical astrocytes.** Transport of 50 µM **(A)** or 1500 µM **(B)** glycine in the absence or presence of GlyT1 and GlyT2 selective inhibitors, Org 24598 (10 µM) and ALX 1393 (200 nM), respectively. Drugs used are indicated below each bar. In each experiment, the non GlyT-mediated transport, assessed by the presence of excess of glycine (10 mM), was subtracted and corresponded to about 20% of total uptake in control conditions. 100% in the Y axis represents GlyT-mediated [$^3$H]glycine uptake in the absence of GlyT inhibitors (control GlyT-mediated uptake). All values are mean ± SEM. **p<0.01, ***p<0.001 (n=4, t-test).

Kinetic analysis revealed an apparent $K_m$ of 51± 5.0 µM of glycine for GlyT1, with a maximal velocity ($V_{max}$) of 379.30 ± 10.3 pmol of [$^3$H]glycine per min per mg of protein (Figure 5.27.A). On the other hand, the apparent $K_m$ of glycine for GlyT2 was 1801 ± 149 µM, with a $V_{max}$ of 5730 ± 200 pmol of [$^3$H]glycine per min per mg (Figure 5.27.B). The kinetic constants obtained for GlyT2-mediated transport were similar when non-GlyT2 mediated transport was defined either by ALX 1393 (200 nM) (Figure 5.27.B, full line) or amoxapine (1 µM) (Figure 5.27.B, dashed line). However, although functionally expressed in astrocytes, GlyT2 was found to have a much lower affinity for glycine than GlyT1, 51.15 ± 4.96 µM for GlyT1 *vs* 1801 ± 149 µM for GlyT2.

### 5.2.7. Discussion

The major outcome from these data is the identification and characterization of GlyT2 in cortical astrocytes. The results show that both GlyT1 and GlyT2 are expressed in astrocytes, at mRNA and protein levels, both in primary cultures and brain slices. The experiments carried out in cultured astrocytes show that GlyT1 and GlyT2 localization is

developmentally regulated. The double detection of GFAP and GlyT revealed that GlyT1 is expressed in the cytoplasm and small astrocytic processes of immature astrocytes (10 DIV) and progresses to a more spread expression in the elongated processes of mature cells (18 and 21 DIV). Similarly, GlyT2 expression was found in the cell cytoplasm and processes of astrocytes. In P21 brains, in both cortical and hippocampal regions, GlyT1 was broadly found in extended astrocytic processes, while GlyT2 was mostly detected in the vicinity of the nucleus.

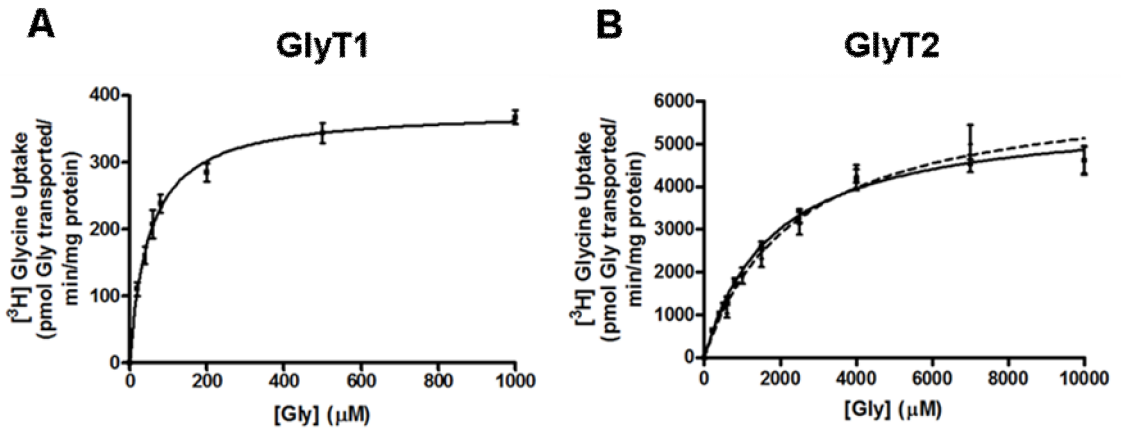


| Drug used to define specific transport | Kinetic Parameters | |
|---|---|---|
| | $K_m$ (μM) | $V_{max}$ (pmol/min/mg) |
| Org 24598 | 51.15±4.96 | 379.30±10.3 |

| Drug used to define specific transport | Kinetic Parameters | |
|---|---|---|
| | $K_m$ (μM) | $V_{max}$ (pmol/min/mg) |
| ALX 1393 ( - ) | 1801±148.9 | 5730±200.2 |
| Amoxapine ( - - ) | 2383±482.4 | 6344±467.0 |

**Figure 5.27. - Saturation curves obtained in rat cultured cortical astrocytes, depicting the amount of glycine taken up by GlyT as a function of the glycine concentration.** GlyT1 **(A)** and GlyT2-mediated **(B)** transport was calculated as the difference between the [$^3$H]glycine uptake in the absence (total transport) and in the presence (unspecific transport) of the GlyT specific inhibitors. Y axis represents the amount of [$^3$H]glycine taken up in control conditions after subtraction of the unspecific mediated transport. Note the differences in scale between graphs. Tables indicate the averaged $K_m$ and $V_{max}$ calculated, for the different GlyT inhibitors by non-linear regression analysis, using GraphPad Prism software. All values are mean ± SEM (5<n<15).

Both GlyT also occur in GFAP-negative cells. The neuronal nature of these cells was confirmed by double immunolabeling of GlyT and a neuronal marker, MAP2. Not surprisingly both transporters were found to surround many neurons, but also to occur in

areas devoid of cell bodies where MAP2 staining was quite spread. GlyT1 has a relevant role at excitatory glutamatergic synapses to control the glycine concentration in the vicinity of ionotropic NMDA receptors, where glycine acts as a co-agonist of glutamate receptors (Supplisson & Bergman 1997, Cubelos *et al.* 2005, Eulenburg *et al.* 2005, Betz *et al.* 2006). Additionally, analysis of GlyT2 expression (Jursky & Nelson 1995) and function (Gomeza *et al.* 2003a, Gomeza *et al.* 2003b, Rousseau *et al.* 2008) has indicated that this transporter is involved in the re-uptake of glycine into glycinergic nerve terminals, enhancing the glycine concentration in the cytosolic space and enabling the reloading of glycinergic synaptic vesicles at inhibitory synapses. As these results show, GlyT2 are also expressed in astrocytes, therefore most probably contributing, together with astrocytic GlyT1, to shape glycinergic transmission.

In addition, evidences that GlyT1 and GlyT2 are functional in astrocytes were presented, since both have the capability to take up glycine from the surrounding environment. It was showed that GlyT1 is responsible for 60-70% of the GlyT-mediated glycine transport. Unexpectedly, and although having a much lower affinity for glycine than GlyT1, GlyT2 was found to ensure 30-40% of GlyT-mediated glycine uptake, being able to take up glycine even when the extracellular glycine concentrations are in the micromolar range. The calculated GlyT1 $K_m$ value (51 μM) is similar to the values previously reported by others in QT-6 cells (Atkinson *et al.* 2001), in oocytes (Guastella *et al.* 1992), in cultured cortical neurons (Wu *et al.* 2008) or in brain synaptosomal preparations (Yee *et al.* 2006). The $K_m$ value now calculated for GlyT2 in brain astrocytes (1801 μM) is higher than the value calculated by others using spinal cord synaptosomes (Geerlings *et al.* 2001) and in brainstem primary neurons (Fornes *et al.* 2008). The reason for diversity in the estimated $K_m$ values in different preparations remains unknown. Nevertheless, low affinity transporters should play a relevant role in glycinergic transmission, since synaptic levels of glycine may transiently increase to the millimolar range (Dohi *et al.* 2009).

The presence of GlyT2 in glial cells has been already noted in slices from the cerebellum (Zafra *et al.* 1995), in cortical oligodendrocyte progenitor cells (Belachew *et al.* 2000) and in astrocyte-derived subcellular particles purified from spinal cord, named gliosomes (Raiteri *et al.* 2008). However, it has been always assumed that cerebral astrocytes lack GlyT2. To my knowledge, this is the first report unequivocally showing that GlyT2 is expressed and is functional in brain astrocytes, being able to transport considerable amounts of glycine either at micromolar or low milimolar concentrations. Nevertheless, the hypothesis that glial GlyT2 could have a compensatory effect upon a glial GlyT1 function

impairment was recently raised by Eulenburg and co-workers (Eulenburg *et al.* 2010), who addressed the role of neuronal and glial GlyT1 by generating conditional knock-out mice in neurons or astrocytes. These authors observed that the majority of glial GlyT1 knock-out mice develop severe neuromotor deficits, which resulted in premature death, but around 20% of the animals survive the critical period, did not develop any detectable deficits and exhibited a normal lifespan. It was therefore postulated that GlyT2 activation could be able to restore GlyT1 loss of function.

It also has to be pointed out that non-GlyT mediated uptake suggests that astrocytes express other types of low affinity glycine transporters, namely the ASC system or the L system (Su *et al.* 1995, Nagaraja & Brookes 1996, Castagna *et al.* 1997, Weiss *et al.* 2001). Additionally, due to its biochemical properties, some glycine can simply cross the membrane by passive diffusion (Tunnicliff 2003).

In conclusion, these results demonstrate that brain astrocytes express GlyT1 and GlyT2, though with a different subcellular localization. Glial GlyT1 is expressed in the long widespread astrocytic process, while glial GlyT2 is predominantly found in the cytoplasm and in the small astrocytic processes. Furthermore, it was assessed that both glial GlyT1 and GlyT2 are functional although, as expected, GlyT1 has a much higher affinity for glycine that GlyT2. Finally, these results can renew the current perception of glycine-mediated neurotransmission in the brain.

## 5.3. GlyT1 and GlyT2 are modulated by BDNF in brain astrocytes

*Rita Aroeira has written the draft and performed all the experimental work.*
*The work presented in this section is under review.*

### 5.3.1. Rationale

GlyT1 (Guastella *et al.* 1992) and GlyT2 (Liu *et al.* 1992) uptake glycine from the extracellular space to the cytoplasm, decreasing glycine levels in the extracellular region, and consequently, the amount of glycine free to activate GlyR, being considered the main responsible for the termination of glycinergic neurotransmission (Eulenburg *et al.* 2005). It was described that GlyT1 is mostly expressed in astrocytes while GlyT2 is mainly restricted to glycinergic nerve terminals (Eulenburg *et al.* 2005). However, reports on the expression of both GlyT1 and GlyT2 in spinal cord gliosomes (Raiteri *et al.* 2008) and in brain astrocytes (Aroeira *et al.* 2014) changed this perception.

BDNF is a neurotrophin that modulates synaptic transmission and plasticity being an important regulator of neuronal differentiation, maturation and survival (Blum & Konnerth 2005, Sebastiao *et al.* 2011).

There are two families of neurotrophins receptors, the Trk receptors and the p75 NTR (Blum & Konnerth 2005). BDNF has a high affinity for TrkB receptors, which include TrkB-FL and TrkB-T isoforms obtained by alternative splicing (Klein *et al.* 1990, Stoilov *et al.* 2002). BDNF-binding to TrkB-FL receptors induces receptor dimerization and autophosphorylation of tyrosine residues in the intracellular kinase domain, which activates the PLCγ, PI3K/Akt and Erk/MAPK pathways. The TrkB-T isoforms lack this intracellular kinase domain (Blum & Konnerth 2005), thus cannot undergo autophosphorylation. Recently, the potential role of truncated TrkB receptor in mediating the neurotrophic effects of BDNF has been reviewed (Fenner 2012). It was also described that TrkB-T receptors are able to mediate PLC-dependent BDNF-evoked $Ca^{2+}$ signalling in glia cells (Rose *et al.* 2003).

GlyT activity modification was shown to be involved in some human disorders, including neuromotor deficiencies (startle disease, myoclonus), pain and epilepsy (Gomeza *et al.* 2003a, Gomeza *et al.* 2003b, Aragon & Lopez-Corcuera 2005). Nevertheless, how GlyT are modulated in astrocytes is still unknown. BDNF was considered a good candidate since it was described to have several actions in astrocytes (Rose *et al.* 2003, Vaz *et al.* 2011),

and thus contribute to the control of neuronal excitability. Hence, the modulation of both GlyT1 and GlyT2 by BDNF in brain astrocytes was analysed.

### 5.3.2. BDNF decreases GlyT-mediated glycine uptake, by decreasing $V_{max}$

In section 5.2. it was showed that brain astrocytes express functional GlyT1 and GlyT2.
To evaluate the BDNF effect upon glycine uptake, mediated by GlyT1 or GlyT2 in astrocytes (21 DIV), [$^3$H]glycine uptake assays were performed with a specific GlyT1 inhibitor, Org 24598 (10 µM), and a specific GlyT2 inhibitor, ALX 1393 (200 nM), as previously reported.
Optimization assays were implemented to discriminate the BDNF incubation time and optimal concentration to be used in the subsequent assays. BDNF (10-200 ng/ml) caused a concentration-dependent decrease in GlyT1 (Figure 5.28.A) and GlyT2 (Figure 5.28.B)-mediated glycine transport into astrocytes. This effect of BDNF occurred within minutes after its application (Figure 5.28. A, B). In the subsequent experiments, a 5-min incubation period with BDNF (30 ng/ml) was used.

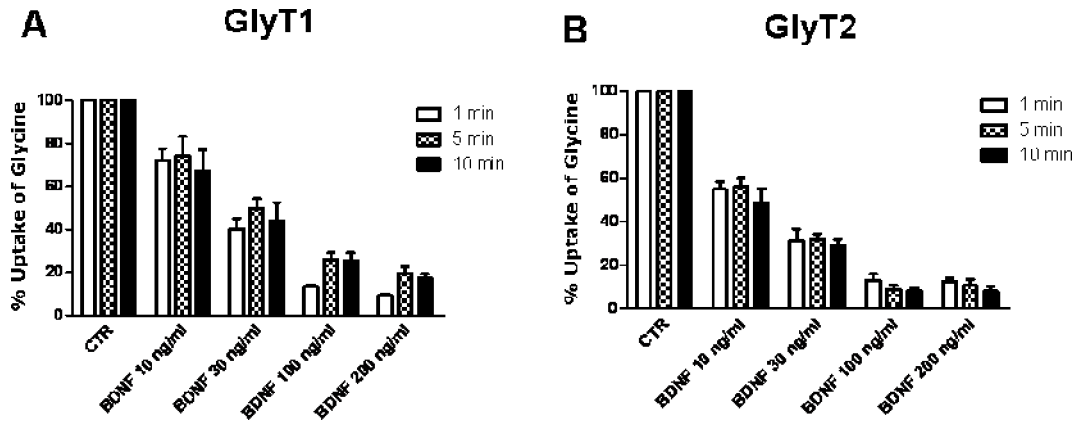


**Figure 5.28. - Concentration-response and time-course curves of BDNF effect upon glycine uptake.** GlyT1- **(A)** and GlyT2- **(B)** mediated glycine transport in primary cultured of astrocytes were analysed. Y axis represents [$^3$H]glycine uptake as percentage of the control value in the same experiment. All values are mean ± SEM. (N=4).

GlyT1 saturation curves obtained in the presence of BDNF (30 ng/ml) (Figure 5.29.A, closed squares) showed a significant decrease in $V_{max}$ (***$p<0.001$, n=4) when compared with untreated cells (Figure 5.29.A, open squares). $K_m$ values were not statistically affected ($p>0.05$, n=4) by BDNF (Figure 5.29.A, table inset).

A similar kinetic analysis was performed for GlyT2-mediated glycine uptake in the absence (Figure 5.29.B, open squares) and in the presence of BDNF (Figure 5.29.B, closed squares). GlyT2-mediated glycine uptake was also significantly decreased by BDNF (30 ng/ml), being the inhibition also in $V_{max}$ (**$p<0.01$, n=6), whereas $K_m$ values for GlyT2 remained statistically unaffected ($p>0.05$, n=6) (Figure 5.29.B, table inset).

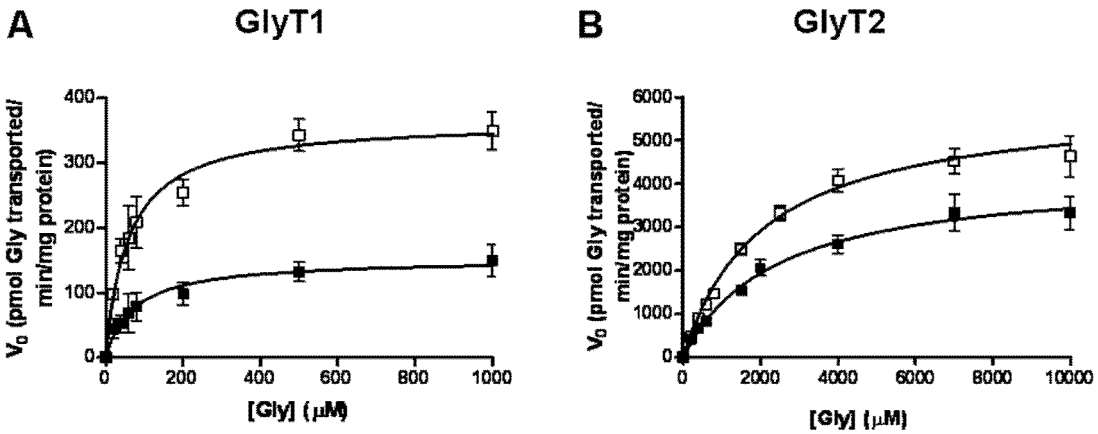


| | Km (μM) | Vmax (pmol/min/mg) |
|---|---|---|
| Control ( □ ) | 58.9 ± 13.3 | 365.5 ± 24.1 |
| BDNF ( ■ ) (30 ng/ml) | 73.1 ± 13.9 | 152.2 ± 9.0 *** |

| | Km (μM) | Vmax (pmol/min/mg) |
|---|---|---|
| Control (□ ) | 2063 ± 254.2 | 5930 ± 299.8 |
| BDNF (■ ) (30 ng/ml) | 2389 ± 485.5 | 4252 ± 345.6 ** |

**Figure 5.29. - Saturation curves depicting the amount of glycine taken up by GlyT1 and GlyT2, with and without BDNF (30 ng/ml), in rat cultured cortical astrocytes.** GlyT1 **(A)** and GlyT2 **(B)**-mediated transport was calculated as the difference between the [$^3$H]glycine uptake in the absence (total transport) and in the presence (unspecific transport) of the GlyT specific inhibitors. The kinetic parameters, $K_m$ and $V_{max}$, were determined by means of non-linear regression analysis and are indicated in the respective table. All values are mean ± SEM. **$p<0.01$, ***$p<0.001$ (N=4, t-test).

### 5.3.3. BDNF modulation of GlyT-mediated glycine transport occurs through TrkB-T1

#### 5.3.3.1. Molecular evidences

It is known that BDNF acts through its high affinity receptor tyrosine kinase B, TrkB, which can exist in two isoforms, TrkB-FL and TrkB-T, obtained by alternative splicing (Klein *et al.* 1990).

In order to investigate which TrkB transcript was present in rat primary cultures of cortical astrocytes and if its expression changed with BDNF incubation (30 ng/ml), a qPCR assay was performed. The results (Figure 5.30.A) showed that TrkB-FL, TrkB-T1 and TrkB-T2 mRNAs were present in primary cultures of astrocytes. Using β-actin as a reference control gene, the relative quantification (Pfaffl 2001) indicated that in the presence of BDNF there were no statistically significant differences ($p>0.05$, as compared with control) in the expression of TrkB transcripts in astrocytes.

An analysis of the Ct values obtained by qPCR reveals that the predominant TrkB isoform in the astrocytes is the TrkB-T1, whereas the TrkB-FL and TrkB-T2 isoforms have a negligible expression (Figure 5.30.B). No signal amplification was detected in the negative controls, which point to signal specificity. Reaction specificity was further evaluated in all assays by a melting curve (Figure 5.31.).

To confirm the results obtained by qPCR, TrkB protein expression was evaluated by using a western blot procedure, in which the membranes were probed with an antibody that recognizes all the TrkB isoforms. The results (Figure 5.30.C) indicated that cultured astrocytes express mainly the TrkB-T isoforms of the receptor, in absence or presence of BDNF (30 ng/ml). Indeed, the antibody recognized a strong band of approximately 95 kDa which corresponds to the TrkB-T and did not identify any band corresponding to the molecular mass of the TrkB-FL isoform (145 kDa). As a positive control, lysates derived from cultured astrocytes were analyzed in parallel with homogenates from cultured hippocampal neurons, non-treated and treated with BDNF (30 ng/ml). In neurons, the antibody was able to detect the presence of both TrkB isoforms, TrkB-FL (145 kDa) and TrkB-T (95 kDa).

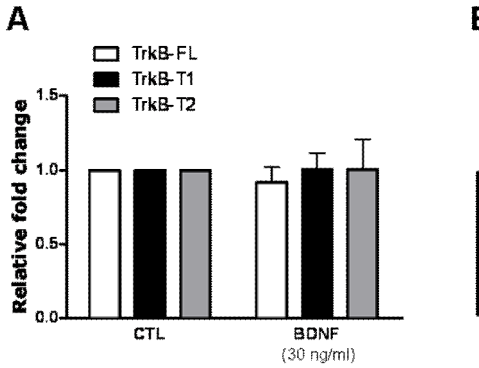


B

| | TrkB-FL | TrkB-T1 | TrkB-T2 |
|---|---|---|---|
| Control | 29.13 ± 0.39 | 20.34 ± 0.36 | 31.97 ± 0.47 |
| BDNF (30 ng/ml) | 29.40 ± 0.46 | 20.38 ± 0.24 | 32.27 ± 0.31 |

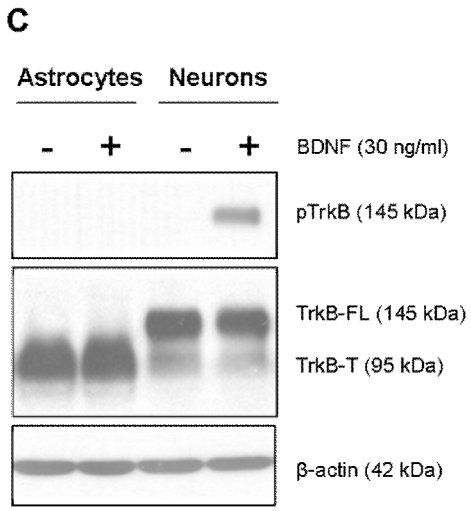


**Figure 5.30. - Expression of TrkB receptor isoforms, in absence and presence of BDNF (30 ng/ml), in 21 DIV astrocytes. (A)** Changes of TrkB-FL, TrkB-T1 and TrkB-T2 mRNAs by relative qPCR. **(B)** The threshold cycle (Ct) values obtained for TrkB-FL, TrkB-T1 and TrkB-T2 in the presence or absence of BDNF (30 ng/ml). **(C)** Analysis of TrkB and pTrkB immunoreactivity in total lysates of astrocytes and neurons. β-actin was used as a control. All values are mean ± SEM. $p>0.05$, as compared with BDNF absence (N=6, one way ANOVA followed by Bonferroni's Comparison Test).

Since BDNF activation of TrkB-FL receptors causes their autophosphorylation, the levels of phosphorylated TrkB (pTrkB) in astrocytes and neurons, in the absence or presence of BDNF (30 ng/ml), were also assessed by western blot. An antibody, which specifically recognizes the phosphorylation site of TrkB, indicated that the pTrkB was detected in neurons, but not in astrocytes (Figure 5.30.C), which corroborates the finding that astrocytes express mainly the TrkB-T receptors (Rose *et al.* 2003).

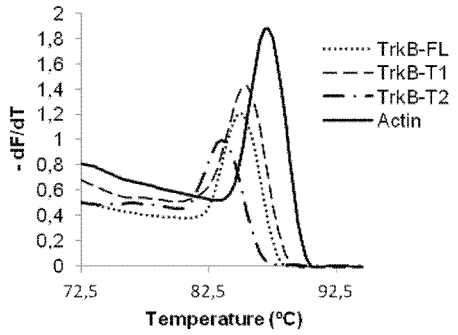


**Figure 5.31. - Melting curves obtained by qPCR of TrkB-FL, TrkB-T1, TrkB-T2 and β-actin transcripts.** Y axis represents the first derivate of raw fluorescence and X axis corresponds to temperature. Each curve has a single melting peak, which indicates that a single PCR product is being amplified.

#### 5.3.3.2. Pharmacological approach

Since only TrkB-FL isoforms have the intracellular catalytic kinase domain, tyrosine kinase inhibitors, such as k252a (Tapley *et al.* 1992), can be used to distinguish between BDNF actions upon TrkB-FL or TrkB-T. Therefore, to assess if the effect of BDNF upon glycine uptake involves the activation of a tyrosine phosphorylation signalling pathway through TrkB-FL, astrocytes were incubated with k252a (0.1 μM).

The results showed (Figure 5.32.) that BDNF (30 ng/ml) significantly inhibits glycine uptake mediated by GlyT1 (Figure 5.32.A, ***$p<0.001$) and by GlyT2 (Figure 5.32.B, ***$p<0.001$). k252a (0.1 μM) *per se* significantly repressed glycine uptake mediated by GlyT1 (Figure 5.32.A, ***$p<0.001$) and GlyT2 (Figure 5.32.B, ***$p<0.001$), which might result from the inhibition of different tyrosine kinases by k252a and the fact that GlyT activation is regulated by phosphorylation (Eulenburg *et al.* 2005). Nevertheless, in the presence of k252a (0.1 μM), BDNF is still able to significantly decrease glycine uptake by both GlyT1 (Figure 5.32.A, *$p<0.05$) and GlyT2 (Figure 5.32.B, *$p<0.05$). These uptake results, together with the molecular evidences, indicate that the effect of BDNF does not require the activation of the tyrosine kinase domain present in TrkB-FL.

To exclude the BDNF activation of low affinity P75NTR receptors, also expressed in astrocytes (Cragnolini *et al.* 2009), an antibody against p75NTR (REX), which block the p75NTR function (Weskamp & Reichardt 1991) was used.

The results revealed (Figure 5.32.) that REX (50 µg/ml, 2h) by itself does not significantly affect the glycine uptake mediated by GlyT1 (Figure 5.32.A) and GlyT2 (Figure 5.32.B). However, BDNF (30 ng/ml) addition to astrocytes, previously incubated with REX (50 µg/ml, 2h), is able to significantly decrease GlyT1- (Figure 5.32.A, ***p<0.001) and GlyT2- (Figure 5.32.B, ***p<0.001) mediated glycine uptake. These results indicated that the BDNF action upon glycine uptake mediated by GlyT1 and GlyT2 in astrocytes is not mediated by the p75NTR receptors.

Altogether, these results point to an involvement of TrkB-T1 isoform in the observed BDNF effect upon GlyT1- and GlyT2-mediated glycine uptake.

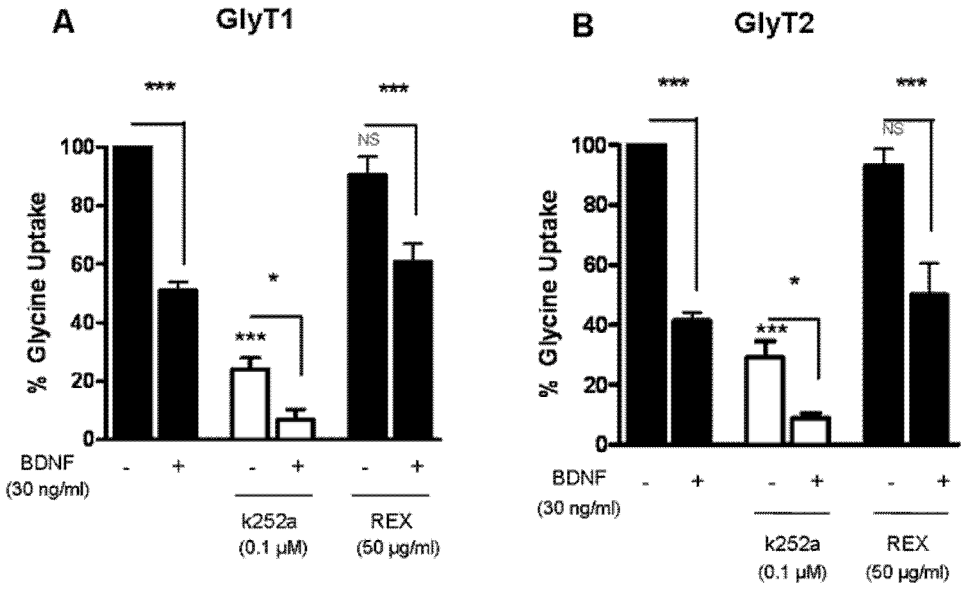


**Figure 5.32. - Influence of BDNF (30 ng/ml) in [$^3$H]glycine uptake.** Glycine transport mediated by GlyT1 **(A)** and GlyT2 **(B)** in the presence and absence of k252a (0.1 µM) and of the p75NTR antibody (REX) (50 µg/ml, 2h) was analysed. Y axis represents [$^3$H]glycine uptake as percentage of the control value in the same experiment. All values are mean ± SEM, NS, not statistically significant (p>0.05), *p<0.05, ***p<0.001, (N=4, one way ANOVA followed by Bonferroni's Comparison Test). Statistical tests were performed in comparison with control conditions, except if otherwise indicated by the connecting lines above the bars. These lines indicate a statistical analysis between BDNF presence and absence under the same drug condition.

### 5.3.4. Glycine uptake is not modulated by the canonical BDNF pathways or by intracellular $Ca^{2+}$ release

To further disclosure the signaling pathways involved in the BDNF effect, inhibitors of the TrkB canonical pathways were used in glycine uptake assays, and the effect of BDNF in the presence and absence of each inhibitor compared. Neither the PLCγ inhibitor U73122 (3μM), the MAPK inhibitor U0126 (10μM) or the PI3K inhibitor LY294002 (10μM), prevented the inhibitory action of BDNF (30 ng/ml) upon glycine uptake (Figure 5.33., *p<0.05, **p<0.01, ***p<0.001), suggesting that the effect of BDNF is not mediated by the TrkB classical pathways. Incubations with each of the inhibitors alone, U73122 (3μM), U0126 (10μM) and LY294002 (10μM) significantly decreased glycine uptake mediated by GlyT1 (Figure 5.33.A, ***p<0.001) and GlyT2 (Figure 5.33.B, ***p<0.001). Again, as happens for k252a, this can be explained by the post-translation modifications of GlyT, since the activity, expression and localization of these transporters can be mediated by phosphorylation and interactions with other proteins (Eulenburg *et al.* 2005).

To complement the data obtained in the uptake experiments, astrocytic lysates incubated with or without BDNF (30 ng/ml) were analyzed by western blot using antibodies that specifically recognized the PLCγ, Akt and MAPK phosphorylated and unphosphorylated forms. The immunoblots depicted in Figure 5.34. show that in astrocytes, BDNF (30 ng/ml) incubation did not modify the phosphorylation levels of PLCγ (Figure 5.34.A), Akt (Figure 5.34.B) or MAPK (Figure 5.34.C). Moreover, the densitometry analysis indicates that the BDNF presence (30 ng/ml) did not statistically change the ratios of pPLCγ/PLCγ, pAkt/Akt and pMAPK/MAPK, when compared to control conditions. As a positive control, experiments were carried out in primary hippocampal neurons where BDNF is known to act through the TrkB-FL isoforms. As expected (Figure 5.34.), in hippocampal neurons BDNF (30 ng/ml) leads to an increase of the phosphorylation states of PLCγ, Akt and MAPK.

Taking together, the results suggest that the GlyT-modulation mediated by BDNF is not caused by the activation of PLCγ, PI3K/Akt or Erk/MAPK, the three main pathways involved in BDNF signaling.

It is known that TrkB-T activation in astrocytes leads to $Ca^{2+}$ release from the endoplasmic reticulum (Rose *et al.* 2003). Thus, to further analyze if the BDNF effect was due to $Ca^{2+}$ signaling events, an intracellular $Ca^{2+}$ chelator, BAPTA-AM, was used. Incubation with

BAPTA-AM (10µM) by itself, slightly decreased the glycine uptake mediated by GlyT1 (Figure 5.33.A) and significantly decreased glycine uptake mediated by GlyT2 (Figure 5.33.B, ***p<0.001). This effect was expected since $Ca^{2+}$ has a crucial role in many cellular events (Fenner 2012). However, BAPTA-AM (10µM) was not able to prevent the inhibitory effect of BDNF (30 ng/ml) on glycine uptake mediated by GlyT1 (Figure 5.33.A, ***p<0.001) and GlyT2 (Figure 5.33.B, ***p<0.001), which excludes a dependence upon intracellular $Ca^{2+}$ release.

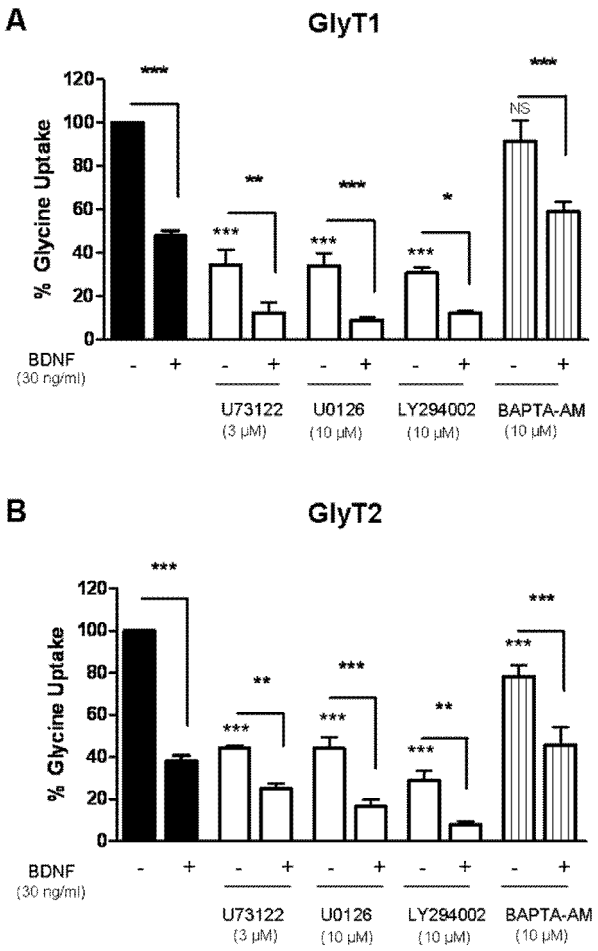


**Figure 5.33. - Effect of BDNF (30 ng/ml) upon [$^3$H]glycine uptake mediated by GlyT1 and GlyT2 in astrocytes.** Glycine transport mediated by GlyT1 **(A)** and GlyT2 **(B)** in the presence of the inhibitors of different signaling pathways of TrkB receptors, namely U73122 (3 µM), LY294002 (10 µM) and U0126 (10 µM), and the intracellular $Ca^{2+}$ chelator BAPTA-AM (10 µM) was analyzed. Y axis represents [$^3$H]glycine uptake as percentage of the control value in the same experiment. All values are mean ± SEM. NS, not statistically significant (p>0.05), *p<0.05, **p<0.01, ***p<0.001, (N=4, one way ANOVA followed by Bonferroni's Comparison Test). Statistical tests were performed in comparison with control conditions, except if otherwise indicated by the connecting lines above the bars. These lines indicate a statistical analysis between BDNF presence and absence under the same drug condition.

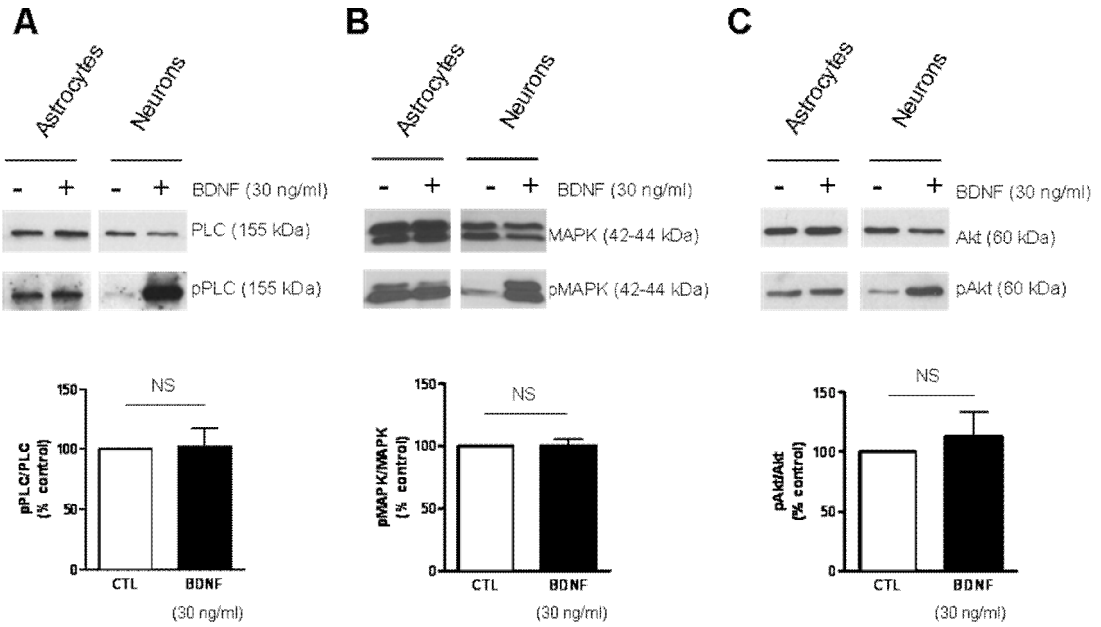


**Figure 5.34. - Western blot analysis of PLC/pPLC (A), Akt/pAkt (B) and MAPK/pMAPK (C) immunoreactivity, in total lysates of astrocytes and neurons, with and without BDNF (30 ng/ml).** The upper panels show representative immunoblots, while the graphs illustrate the phosphorylation ratio obtained by densitometry analysis, performed with ImageJ software. All values are mean ± SEM. NS, not statistically significant ($p>0.05$), as compared with BDNF absence under the same drug condition (N=4, t-test).

### 5.3.5. Glycine uptake is modulated by a RhoGTPase pathway

It is described that the TrkB-T isoforms can regulate cytoskeletal alterations of brain astrocytes and can control the activity of Rho-GTPases (Ohira *et al.* 2005a, Fenner 2012). To test if a Rho-GTPase signaling mechanism could be involved in the BDNF effect herein described, astrocytes were incubated with toxin B (10 ng/ml, 3h) from *Clostridium difficile*, which is described as a glucosyltransferase that inhibits the Rho family of GTPases (Just *et al.* 1994a, Just *et al.* 1994b).

Toxin B (10 ng/ml, 3h) *per se* significantly affected the GlyT1- (Figure 5.35.A, $*p<0.05$) and GlyT2- (Figure 5.35.B, $**p<0.01$) mediated glycine uptake, probably because of the modifications of cytoskeletal proteins that could be interacting with GlyT (Eulenburg *et al.* 2005). Interestingly, toxin B (10 ng/ml, 3h) was able to prevent the BDNF (30 ng/ml) inhibitory effect upon GlyT (Figure 5.35.), since no statistical differences in glycine uptake were observed in the absence and presence of BDNF in astrocytes pre-incubated with toxin B.

These data suggest that the BDNF (30 ng/ml) action in glycine uptake mediated by GlyT involves a Rho-GTPase dependent mechanism, but without activation of TrkB canonical pathways.

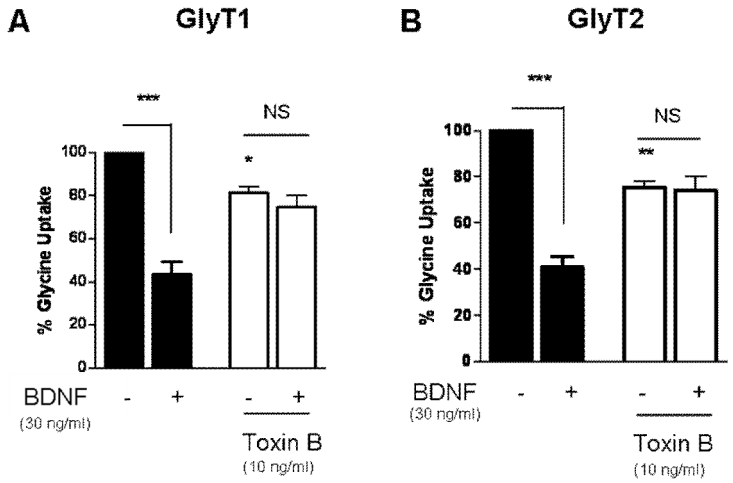


**Figure 5.35. - Effect of BDNF (30 ng/ml) upon [$^3$H]glycine uptake.** Glycine transport mediated by GlyT1 **(A)** and GlyT2 **(B)** in the presence of a Rho GTPase inhibitor, toxin B (10 ng/ml) from Clostridium difficile was analysed. Y axis represents [$^3$H]glycine uptake as percentage of the control value in the same experiment. All values are mean ± SEM. NS, not statistically significant ($p>0.05$), *$p<0.05$, **$p<0.01$, ***$p<0.001$, (N=5, one way ANOVA followed by Bonferroni's Comparison Test). Statistical tests were performed in comparison with control conditions, except if otherwise indicated by the connecting lines above the bars. These lines indicate a statistical analysis between BDNF presence and absence under the same drug condition.

### 5.3.6. BDNF decreases glycine uptake by promoting GlyT endocytosis

Experiments described above showed that BDNF is able to significantly reduce GlyT-mediated glycine uptake, by decreasing $V_{max}$ values. Changes in this kinetic parameter are frequently associated to changes in the number of transporters due to their translocation to and from the plasma membrane. Impairment in the insertion pathway of new transporters in the membrane or increase in GlyT degradation pathways, could both lead to decreases in $V_{max}$ of the transporters.

To test if BDNF was affecting insertion or removal of GlyT from the membrane, astrocytes were incubated with monensin (25 µM, 1h), a transporter recycling inhibitor, or with dynasore (70 µM), a dynamin/clathrin-dependent endocytosis inhibitor. Both monensin (25 µM, 1h) and dynasore (70 µM) *per se* significantly decreased the glycine uptake in

astrocytes through GlyT1 (Figure 5.36.A, ***p<0.001) and GlyT2 (Figure 5.36.B, **p<0.01, ***p<0.001), which can be indicative of a constitutive recycling of GlyT in astrocytes.

In the presence of monensin (25 µM, 1h), BDNF (30 ng/ml) significantly decreased glycine uptake mediated by GlyT1 (Figure 5.36.A, *p<0.05) and GlyT2 (Figure 5.36.B, *p<0.05). By other hand, the effect of BDNF was fully prevented on both GlyT1 and GlyT2 when astrocytes were pre-incubated with dynasore (70 µM) (Figure 5.36.). These results suggest that BDNF acts by promoting GlyT internalization through a dynamin/clathrin-dependent pathway, without directly influencing GlyT insertion pathways.

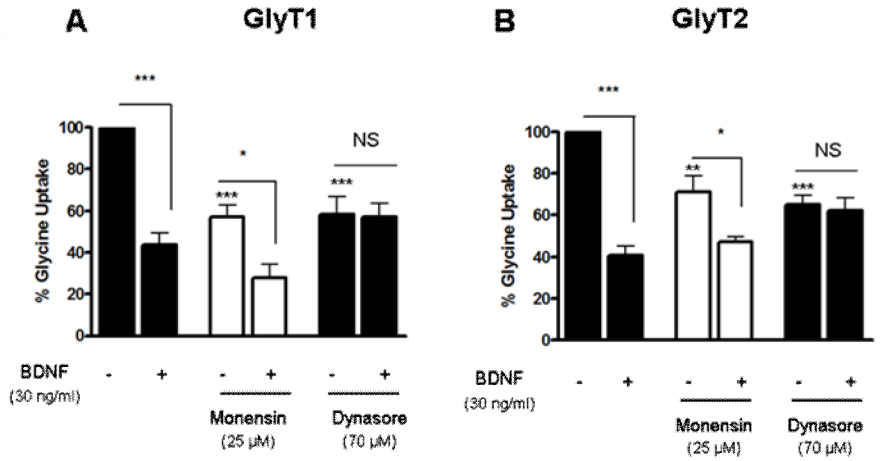


**Figure 5.36. - Influence of monensin (25 µM) and dynasore (70 µM) upon the effect of BDNF (30 ng/ml) on [$^3$H]glycine uptake mediated by GlyT1 (A) and GlyT2 (B).** Y axis represents [$^3$H]glycine uptake as percentage of the control value in the same experiment. All values are mean ± SEM. NS, not statistically significant (p>0.05), *p<0.05, **p<0.01, ***p<0.001, (N=4, one way ANOVA followed by Bonferroni's Comparison Test). Statistical tests were performed in comparison with control conditions, except if otherwise indicated by the connecting lines above the bars. These lines indicate a statistical analysis between BDNF presence and absence under the same drug condition.

To confirm the above conclusions, a double immunofluorescence assay was performed, using an antibody that specifically recognizes early endosomes antigen (EEA1), together with GlyT antibody. The confocal images showed the presence of both GlyT1 (Figure 5.37.A) and GlyT2 (Figure 5.37.B) in primary cultures of astrocytes as previously reported in the section 5.2.. GlyT1 is expressed in the cell cytoplasm and in long spread processes

(red panels in Figure 5.37.A), while GlyT2 was detected in the cytoplasm and in a few small processes (red panels in Figure 5.37.B).
Moreover, in control conditions (Figure 5.37.A) and in the presence of BDNF (30 ng/ml) (Figure 5.37.B) it was possible to identify GlyT1 (arrows in Figure 5.37.-A5 and A10) and GlyT2 (arrows in Figure 5.37.-B5 and B10) that co-localized with EEA1, which suggests GlyT presence in the endosomes and thus undergoing degradation. The same qualitative observation was made when cultured astrocytes were treated with dynasore (70 μM) (Figure 5.38.).

### 5.3.7. BDNF-induced GlyT endocytosis is blocked by toxin B

To test if toxin B was able to block BDNF-induced GlyT endocytosis, a double immunofluorescence assay with EEA1 and GlyT was performed (Figure 5.39.), as described in the previous subsection, in 21 DIV cultured astrocytes treated with toxin B (10 ng/ml, 3h), alone or in the presence of BDNF (30 ng/ml).

### 5.3.8 Quantitative analysis

To investigate if the number of GlyT undertaking internalization changed with BDNF, an in-house mask was used to quantify the number of GlyT1 and GlyT2 which co-localize with EEA1, in control conditions and in BDNF presence (Figure 5.40.). Additionally, this mask was used to determine if dynasore (70 μM) could prevent the BDNF action, as occurred in the uptake experiments. BDNF (30 ng/ml) induced a statistically significant increase in the number of internalized GlyT1 (Figure 5.40.A, *$p<0.05$) and GlyT2 (Figure 5.40.B, **$p<0.01$). However, in the experiments where astrocytes were pre-incubated with dynasore (70 μM), BDNF (30 ng/ml) inhibitory effect was absent, since no statistical differences were detected in the percentage of GlyT1 (Figure 5.40.A, $p>0.05$) and GlyT2 (Figure 5.40.B, $p>0.05$) co-localizing with EEA1, when compared to BDNF absence, in similar conditions.
Altogether, these data attests that BDNF is able to decrease the number of GlyT in the astrocytic membrane by increasing GlyT internalization through a dynamin/clathrin-dependent mechanism.

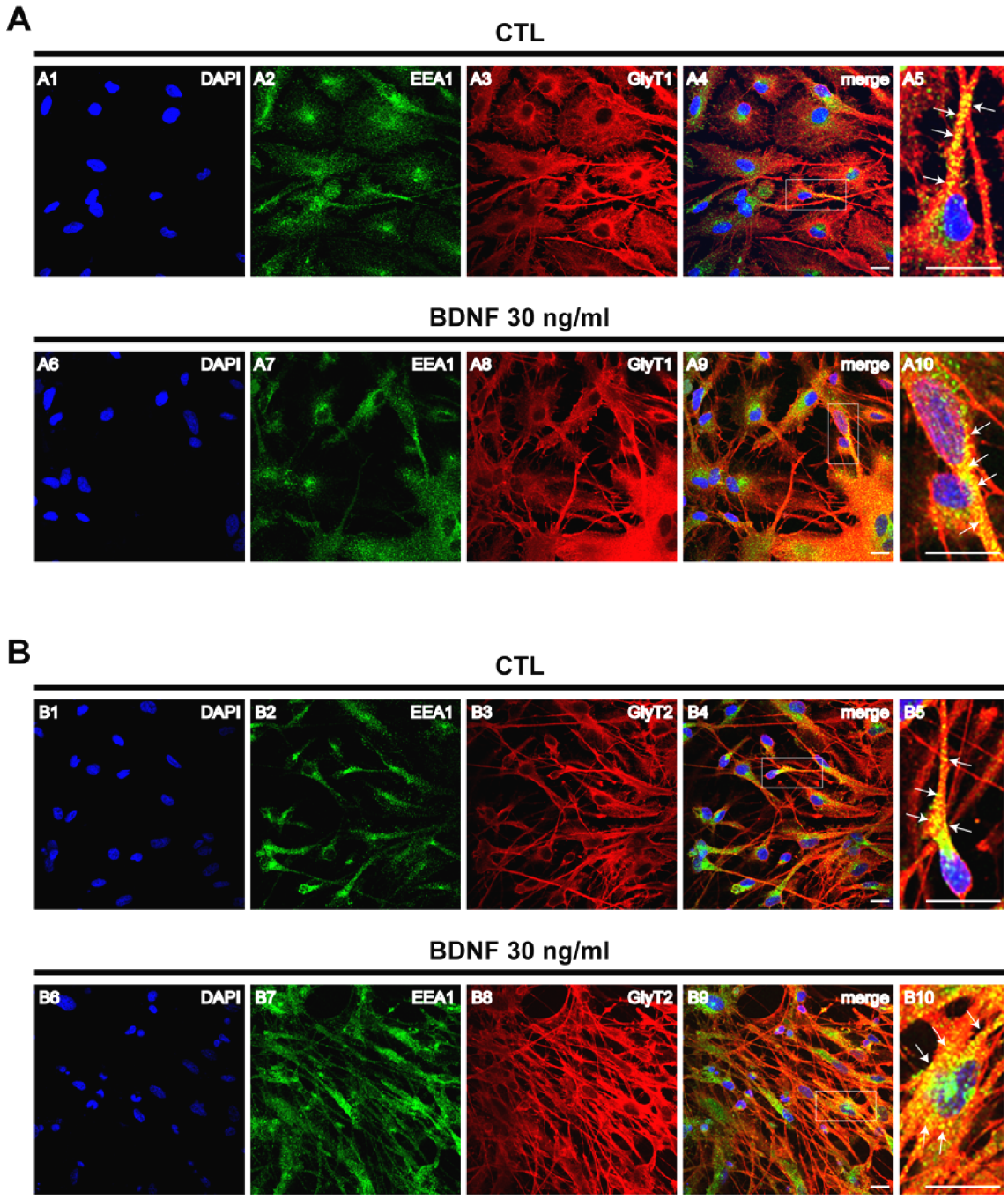


**Figure 5.37. - Double detection of GlyT1 (A) or GlyT2 (B) and EEA1 in rat cultured cortical astrocytes in the absence and presence of BDNF (30 ng/ml).** The first panels in every row represent each labeling alone: DAPI stained nuclei, green for EEA1 and red for GlyT1/GlyT2. GlyT1/GlyT2 presence in endosomes is indicated by arrows. Images were acquired on a confocal laser microscope (Zeiss LSM 510 META) with a 63X oil-immersion objective. Scale bars, 20 µm.

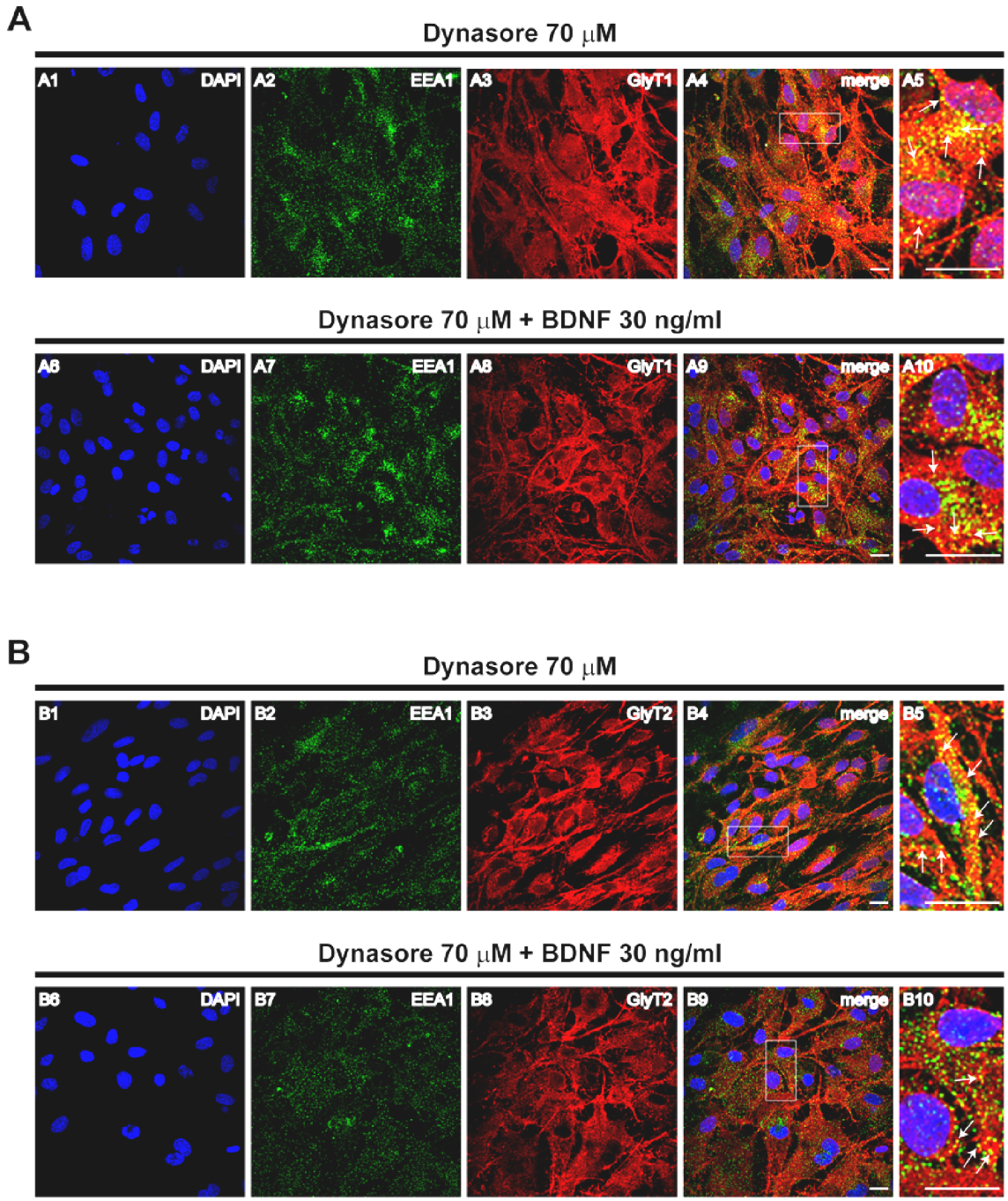


**Figure 5.38. - Double detection of GlyT1 (A) or GlyT2 (B) and EEA1 in rat cultured cortical astrocytes with a pre-incubation with dynasore (70 μM) alone or in the presence of BDNF (30 ng/ml).** The first panels in every row represent each labeling alone: DAPI stained nuclei, green for EEA1 and red for GlyT1/GlyT2. GlyT1/GlyT2 presence in endosomes is shown by arrows. Images were acquired on a confocal laser microscope (Zeiss LSM 510 META) with a 63X oil-immersion objective. Scale bars, 20 μm.

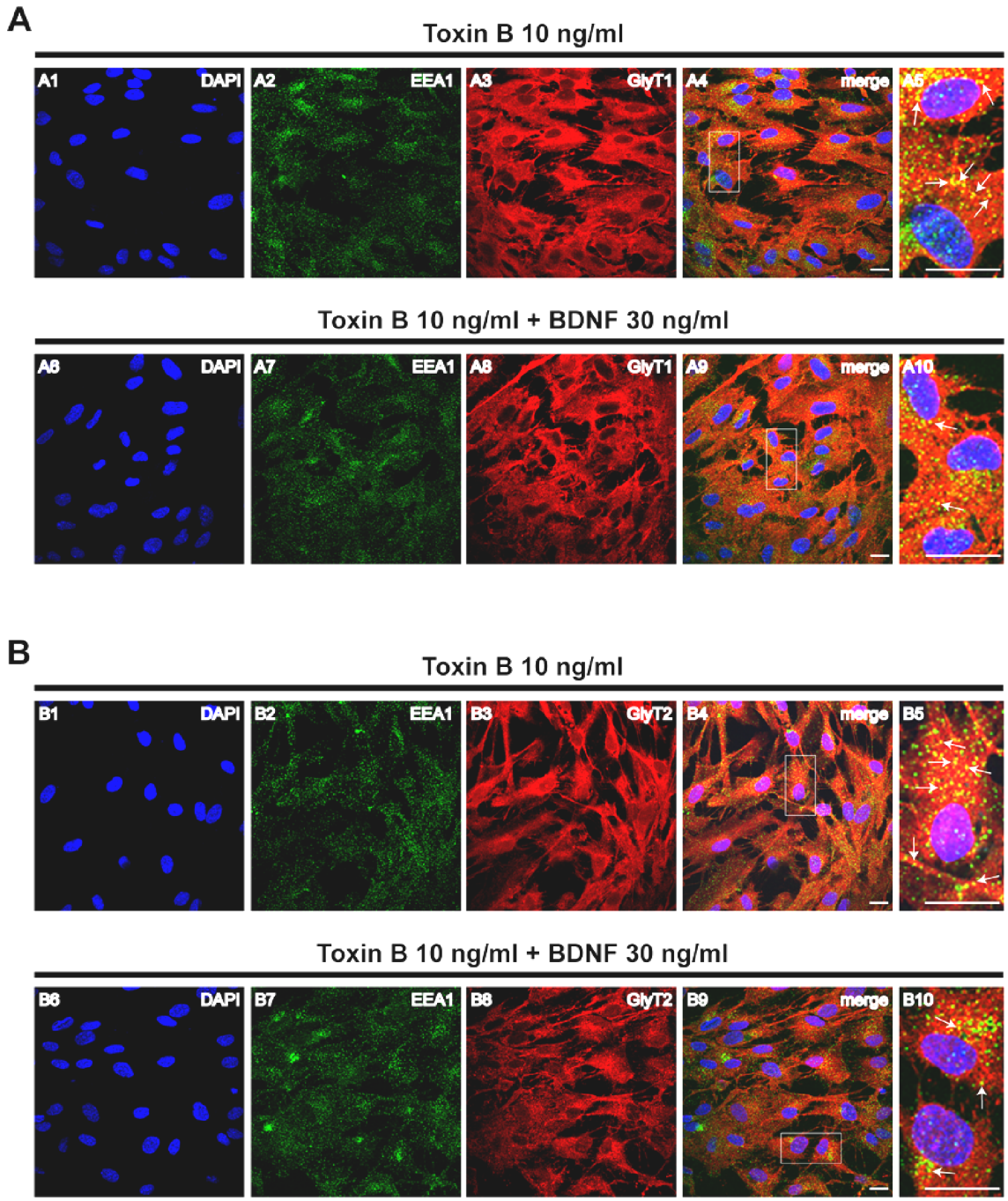


**Figure 5.39. - Double detection of GlyT1 (A) or GlyT2 (B) and EEA1 in rat cultured cortical astrocytes with a pre-incubation with toxin B (10 ng/ml) alone or in the presence of BDNF (30 ng/ml).** The first panels in every row represent each labeling alone: DAPI stained nuclei, green for EEA1 and red for GlyT1/GlyT2. GlyT1/GlyT2 presence in endosomes is indicated by arrows. Images were acquired on a confocal laser microscope (Zeiss LSM 510 META) with a 63X oil-immersion objective. Scale bars, 20 µm.

The same in-house mask was used to evaluate if toxin B (10 ng/ml, 3h) could prevent the effect of BDNF (30 ng/ml) in GlyT endocytosis, as occurred in the uptake experiments (Figure 5.40.). Indeed, BDNF action was prevented by toxin B, since no statistical differences were obtained in the number of endossomatic GlyT in the presence of toxin B, either with or without BDNF (Figure 5.40 A and B.).

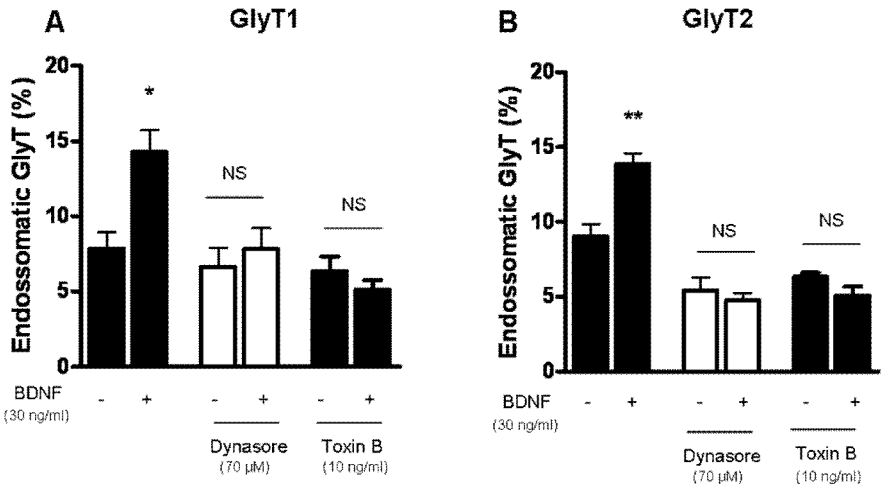


**Figure 5.40. - Quantitative analysis of endossomatic GlyT1 (A) and GlyT2 (B) performed in ImageJ software using a binary in house-mask.** All values are mean ± SEM, NS, not statistically significant ($p>0.05$), *$p<0.05$, **$p<0.01$, as compared with control conditions, except if otherwise indicated by the connecting lines above the bars. These lines indicate a statistical analysis between BDNF presence and absence under the same drug condition. (N=4-5, one way ANOVA followed by Bonferroni's Comparison Test).

### 5.3.9. Discussion

The results herein presented describe, for the first time, an association between BDNF and glycine uptake in astrocytes. It was shown that BDNF inhibits glycine uptake mediated by GlyT1 and GlyT2, through TrkB-T1 receptor activation, and that this impairment occurs by a decrease in GlyT $V_{max}$. The observed BDNF effect does not occur via the classical transduction pathways. Instead, it is proposed that it occurs through a Rho-GTPase activity dependent mechanism, which in turn is responsible for cytoskeleton changes that induce GlyT internalization through a dynamin/clathrin-dependent mechanism (Figure 5.41.).

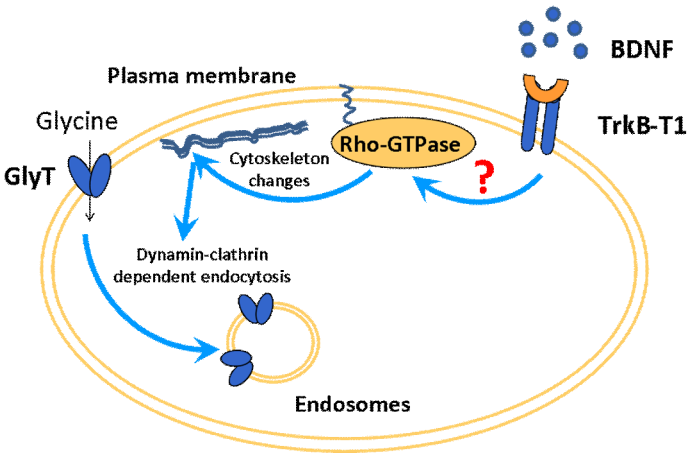


**Figure 5.41. - Model of the mechanism of BDNF-induced GlyT internalization pathway, through TrkB-T1, in primary cultures of astrocytes.** Upon BDNF binding, TrkB-T1 activates a Rho-GTPase pathway which will induce cytoskeleton changes and consequently GlyT internalization through a dynamin/clathrin-dependent mechanism.

The TrkB receptor expression in astrocytes was formerly analyzed and discussed (Rose *et al.* 2003, Ohira *et al.* 2005b, Vaz *et al.* 2011). The qPCR results herein described corroborate the findings that TrkB-T1 transcript is the most expressed TrkB isoform in astrocytes, thus prone to account for the BDNF effect in glycine uptake. Additionally, in cultured astrocytes only TrkB-T receptors immunoreactivity was detected, instead of TrkB-FL isoform. pTrkB was also absent in cultured astrocytes, which reinforces the absence of TrkB-FL since only full length receptors have the intracellular catalytic kinase domain. In fact, in the presence of k252a, a tyrosine kinase inhibitor, and in the presence of the TrkB canonical pathways inhibitors, the BDNF effect upon glycine uptake persists. Western blot assays corroborated these results by showing that, in astrocytes, BDNF does not induce phosphorylation of canonical targets of the TrkB-FL receptor, such as PLC, Akt or MAPK. Moreover, upon blockade of p75NTR receptor, the BDNF action in glycine uptake is maintained. Altogether, these results suggest that the BDNF effect herein observed is not mediated by TrkB-FL or p75NTR receptors.

Until recently, it was thought that TrkB-FL receptors were the only signaling isoform, due to the presence of the intracellular catalytic domain (Patapoutian & Reichardt 2001). However, the existence of several truncated isoforms of TrkB receptor, with higher predominance of TrkB-T1, which lack intrinsic tyrosine kinase activity, suggests the

occurrence of additional mechanisms for TrkB-T induced signaling, either BDNF-dependent or BDNF-independent (Fenner 2012). Although discovered over 20 years ago, little is known about TrkB-T1 physiological function. Nevertheless, many studies have depicted several actions of TrkB-T1, namely, dominant-negative actions over TrkB-FL signaling, regulation of extracellular BDNF levels, induction of cellular morphological alterations and ability to activate intracellular signaling cascades (Fenner 2012). It was also shown that TrkB-T1 binds to Rho GDP Dissociation Inhibitor (RhoGDI1) (Ohira *et al.* 2005a, Fenner 2012). The Rho family GTPases are important regulators of the actin cytoskeleton and are able to control dendritic spine formation and cell motility and morphology (Luo 2002, Tashiro & Yuste 2004). As a Rho-GTPAse inhibitor, RhoGDI1 interaction with TrkB-T1 would activate a Rho-GTPAse pathway and induce cytoskeletal changes, which could be of great relevance in many pathophysiological conditions. It was shown that in the presence of toxin B from *Clostridium difficile*, a well-studied and common Rho family GTPases inhibitor (Just *et al.* 1994a, Just *et al.* 1994b), the BDNF action upon glycine uptake is lost, which indicates an involvement of a Rho-GTPase, a known target of truncated TrkB receptors as described above, in the reported BDNF effect.
This work reports that BDNF decreases glycine uptake mediated by GlyT1 and GlyT2 in astrocytes, through a decrease in $V_{max}$, but without significantly changing the $K_m$ value. This indicates that in the presence of BDNF, the number of transporters in the plasma membrane is reduced. This decrease can be attributed to either the impairment of GlyT insertion pathways in the plasma membrane or the enhancement of the endocytic cell machinery. To clarify this, well known pharmacological tools were used: monensin, that blocks GlyT recycling back to the membrane without influencing endocytosis (Mollenhauer *et al.* 1990) and dynasore, which inhibits the dynamin/clathrin-dependent endocytosis (Macia *et al.* 2006). The results indicate that monensin does not prevent the BDNF effect in glycine uptake and concomitantly, does not influence the number of GlyT in the astrocytic membrane. By other hand, in the presence of dynasore, the BDNF effect upon glycine uptake is lost. Dynasore only inhibits the dynamin/clathrin-dependent endocytosis, but other types of endocytosis have already been described in astrocytes, namely an endocytic pathway independent of clathrin and dynamin but tightly regulated by intracellular $Ca^{2+}$ (Jiang & Chen 2009). However, the use of the intracellular $Ca^{2+}$ chelator, BAPTA-AM, which affected $Ca^{2+}$ signaling, did not prevent the BDNF effect. Since only dynasore was able to prevent the BDNF effect, it can be suggested that the BDNF-

dependent decrease in glycine uptake results from an increase in GlyT internalization through a dynamin/clathrin-dependent pathway.

Thus, the results regarding GlyT expression in the membrane showed that: 1) BDNF causes a striking decrease in $V_{max}$, which is known to be related to the amount of transporters in the membrane; 2) the BDNF effect upon glycine uptake was prevented by an endocytosis inhibitor, dynasore; 3) immunofluorescence assays revealed a BDNF-induced increase in the amount of endosomal GlyT, which is evident by visual assessment and by quantitative analysis, and that is lost in the presence of dynasore and of the Rho-GTPase exogenous inhibitor, toxin B.

The use of most inhibitors *per se* has an effect upon glycine uptake. However, it has to be highlighted the absence of relationship between the degree of effect of the inhibitors *per se* upon glycine transport and their ability to affect the action of BDNF. As an example, pharmacological inhibitors can have a similar effect *per se*, as is the case of monensin and dynasore, but have different effects upon the BDNF action. In this case, only dinasore was able to prevent the inhibitory effect of BDNF upon GlyT- mediated glycine uptake. Other example is the use of the PLCγ inhibitor U73122, the MAPK inhibitor U0126 and the PI3K inhibitor LY294002, which have a marked inhibitory action *per se* upon glycine uptake, but did not impair the BDNF effect.

BDNF actions are already described in GABA uptake. BDNF is able to increase GABA uptake in astrocytes through an enrichment of GABA transporter 1 (GAT-1) in the plasma membrane, but does not modulate GABA transporter 3 (GAT-3) (Vaz *et al.* 2011). GlyT, as GAT, belong to the $Na^+$- and $Cl^-$-dependent family of transporters. However, GAT-1 is known to mainly influence tonic inhibition (Kirmse *et al.* 2008), while GAT-3 can guarantee a successful phasic inhibition (Kirmse *et al.* 2009), which suggests that the facilitatory effect of BDNF upon GAT-1 predominantly modulates the tonic inhibition, promoting a decrease in GABA levels in the extracellular space (Vaz *et al.* 2011). If GlyT1 or GlyT2 affect mainly tonic or phasic neurotransmission cannot be answered with the present work. The inhibitory BDNF effect upon GlyT will increase glycine levels in the extracellular space prone to act upon GlyR. However, considering that GlyR are predominantly extrasynaptic as shown in section 5.1., it is possible to hypothesise a potentiation of glycinergic tonic inhibition. This can be very useful in situations of hyperexcitability (Harvey *et al.* 2008), and BDNF can be seen as a potential candidate for novel therapeutic studies in this field.

In summary, these data describe, for the first time, the BDNF modulation of glycine uptake mediated by GlyT1 and GlyT2, in astrocytes. It is proposed that BDNF acts through TrkB-T1 receptors, promoting GlyT internalization and causing a reduction of GlyT expression in cell surface, by an unknown Rho-GTPase activity dependent mechanism.

## 5.4. GlyT2 is modulated by BDNF in brain synaptosomes

*Rita Aroeira has written the draft and performed all the experimental work.*
*The work presented in this section is under review.*

### 5.4.1. Rationale

GlyT2 is mostly localized in the presynaptic terminals of glycinergic neurons (Zafra *et al.* 1995), and has a crucial role in glycine uptake into the neurons, thus ensuring the refilling of glycinergic presynaptic vesicles (Gomeza *et al.* 2003b) and being considered a marker for glycinergic neurons (Poyatos *et al.* 1997).

BDNF belongs to the neurotrophin family (Binder & Scharfman 2004) and has important functions in neuronal differentiation, maturation and survival, as well as in synaptic transmission and plasticity (Blum & Konnerth 2005).

The signal transducing systems which mediate the BDNF actions are initiated by their interaction with two categories of cell surface receptors, the Trk receptor and the p75 NTR receptor (Patapoutian & Reichardt 2001, Roux & Barker 2002). Most of the BDNF actions are mediated by TrkB receptors that triggers, through the autophosphorylation of tyrosine residues in the intracellular kinase domain, the well-characterized Erk/MAPK, PI3K/Akt, and PLC-γ signalling pathways (Blum & Konnerth 2005, Arevalo & Wu 2006, Sebastiao *et al.* 2011).

TrkB receptors can originate, by alternative splicing, several isoforms, namely the full length receptor, TrkB-FL, and the truncated ones, TrkB-T1, TrkB-T2 and TrkB-T-Shc, which lack the intracellular kinase domain (Klein *et al.* 1990, Stoilov *et al.* 2002).

Alterations in GlyT activity can be related to the development of some pathologies, like startle disease, epilepsy and pain (Gomeza *et al.* 2003a, Gomeza *et al.* 2003b, Aragon & Lopez-Corcuera 2005). Hence, understanding the mechanisms that modulate GlyT2 function could uncover potential therapeutic targets for the treatment of these conditions. In this section the potential role of BDNF upon GlyT2 activity in nerve terminals of the rat hippocampus was explored.

### 5.4.2. GlyT2 is expressed in hippocampal synaptosomes

It was already demonstrated that GlyT2 is associated with membrane rafts in the plasma membrane of brainstem terminals and neurons (Nunez *et al.* 2008). Thus, GlyT2 expression in plated hippocampal nerve terminals was evaluated, through an immunofluorescence protocol.

The synaptosomes-enriched fraction used in this work was characterized by immunostaining with MAP2, a neuronal marker, and GFAP, a marker of differentiated astrocytes. Plated synaptosomes look as dots, either isolated or clustered together, positive for MAP2 (Figure 5.42.A, green panel). Furthermore, the quantitative analysis indicated that GFAP-positive clusters accounted for only 7.1 ± 2.6 % of the total labelled clusters (Figure 5.42.A), confirming that the preparations used in this work were enriched in synaptosomes.

To assess GlyT2 expression in hippocampal synaptosomes, a second double immunolabelling was carried out (Figure 5.42.B). This assay identified nerve terminals, by MAP2 staining (in green), together with GlyT2 (in red). The confocal images showed that hippocampal synaptosomes express GlyT2, as can be observed by the co-localization of MAP2 and GlyT2 (arrows in merge panel, Figure 5.42.B). However, GlyT2 immunostaining was also detected in some MAP2 negative clusters (arrowheads in merge panel, Figure 5.42.B), which most probably correspond to gliosomes (Raiteri *et al.* 2008). This observation is in accordance with the recent findings that astrocytes do express GlyT2 (section 5.2.).

It is also possible to observe (open arrowheads in merge panel, Figure 5.42.B) several MAP2 positive clusters which do not express GlyT2, which might correspond to nerve endings that do not release glycine.

### 5.4.3. BDNF decreases glycine uptake mediated by GlyT2 through a reduction in $V_{max}$

As in previous section, GlyT2 function in brain synaptosomes was assessed by [$^3$H]glycine uptake assays with a specific GlyT2 inhibitor, ALX 1393 (200 nM) (Luccini & Raiteri 2007).

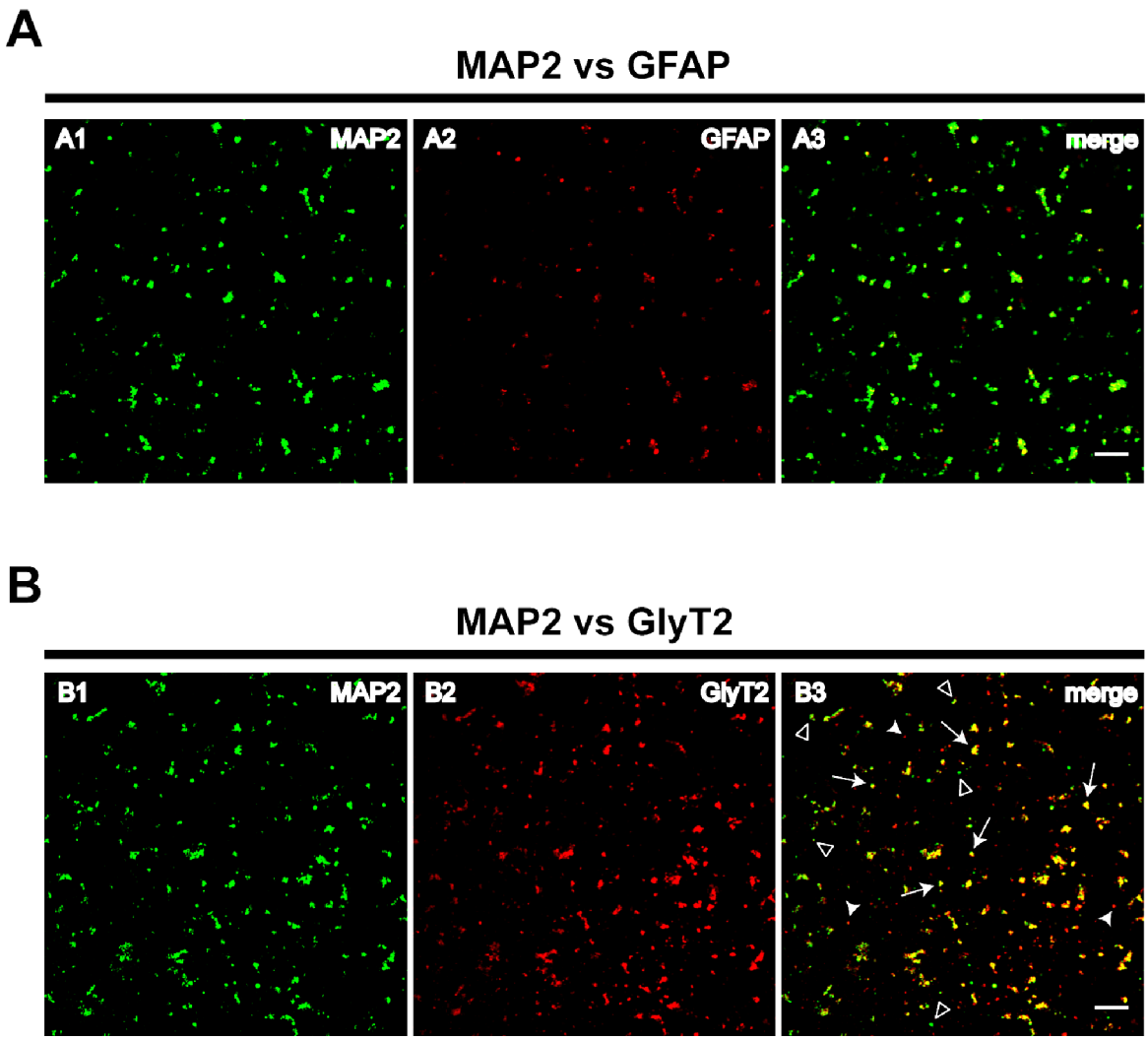


**Figure 5.42. - Characterization of rat hippocampal synaptosomes. (A)** Double immunolabelling of MAP2 (in green) and GFAP (in red). **(B)** Double immunolabelling of MAP2 (in green) and GlyT2 (in red). Arrows illustrate GlyT2-expressing synaptosomes, arrowheads point to GlyT2-expressing gliosomes and open arrowheads indicate synaptosomes that do not express GlyT2. Images were acquired on a confocal laser microscope (Zeiss LSM 510 META) with a 63X oil-immersion objective. Scale bars, 20 µm.

Initial optimization assays were performed to define the [$^3$H]glycine incubation time and the optimal concentration of GlyT2 inhibitor to be used in subsequent experiments. The [$^3$H]glycine uptake increased linearly with the incubation time from 30s to 120s (Figure 5.43.), thus an incubation time of 1 min was chosen for the following experiments. Since higher concentrations of GlyT2 inhibitor (Figure 5.44.) did not reflect an increase in GlyT2 inhibition, a concentration of 200 nM was chosen.

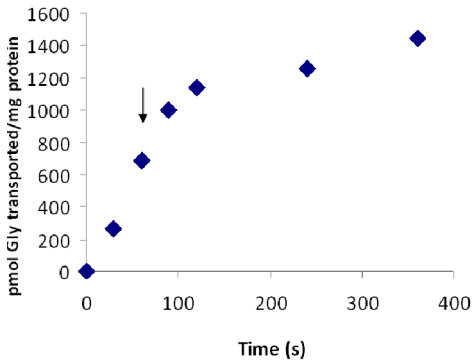


**Figure 5.43. - Transport progression curve using 1.0 mM of glycine to study GlyT2.** Incubation time ranging from 30s to 360s was tested. Arrow points to the incubation time used in the subsequent experiments.

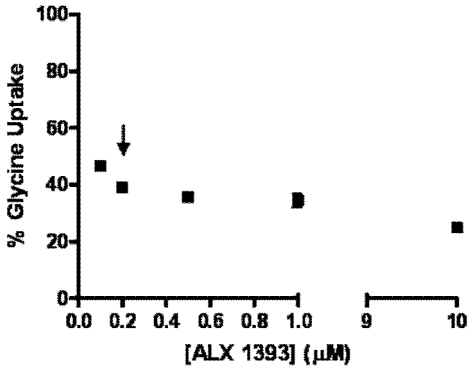


**Figure 5.44. - ALX 1393, a GlyT2 specific inhibitor depicts a concentration-dependent uptake of glycine in rat hippocampal synaptosomes.** Y axis represents [$^3$H]glycine uptake as percentage of the control value (absence of inhibitors) in the same experiment. Arrow points to the concentration of inhibitor used in the subsequent experiments to isolate GlyT2 specific transporter.

To determine if BDNF is able to modify the glycine uptake through GlyT2 in synaptosomes, experiments were performed in the presence of BDNF (10-200 ng/ml), which caused a concentration-dependent decrease in GlyT2-mediated glycine transport within minutes after its application (Figure 5.45.). In the following experiments, synaptosomes were incubated with BDNF (30 ng/ml) for 5 min.

A kinetic analysis of the saturation curves revealed that BDNF (30 ng/ml) significantly decreased $V_{max}$ (**$p<0.01$, $n=6$) when compared with untreated synaptosomes from 8254 ± 466.7 pmol of [$^3$H]glycine per min per mg of protein under control conditions (Figure 5.46., open squares) to 5322 ± 670 pmol of [$^3$H]glycine per min per mg of protein (Figure

5.46., close squares). $K_m$ value was not significantly altered ($p>0.05$, n=6) in the presence of BDNF (30 ng/ml) (Figure 5.46., table).

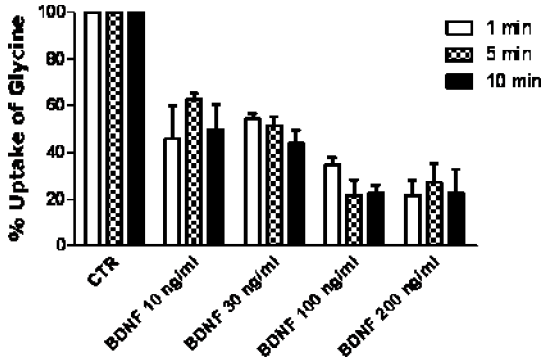


**Figure 5.45. - Concentration-response curve and time-course of BDNF effect upon GlyT2-mediated glycine transport in rat hippocampal synaptosomes.** Y axis represents [$^3$H]glycine uptake as percentage of the control value in the same experiment. All values are mean ± SEM. (N=3).

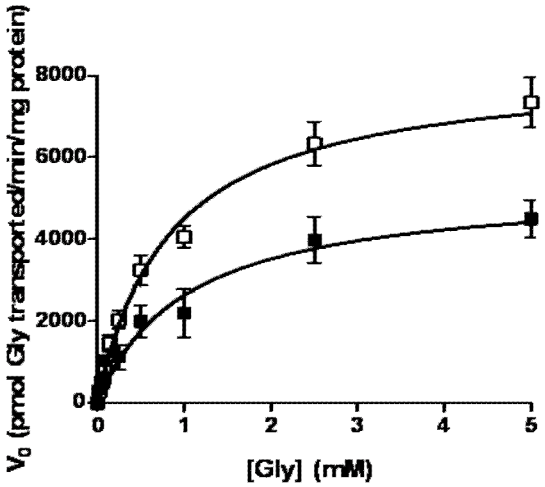


| | Km (μM) | Vmax (pmol/min/mg) |
|---|---|---|
| Control (□) | 836.9 ± 107.2 | 8254 ± 466.7 |
| BDNF (■) (30 ng/ml) | 1030 ± 330.3 | 5322 ± 670** |

**Figure 5.46. - Saturation curves depicting the amount of glycine taken up by GlyT2, with and without BDNF (30 ng/ml), in rat hippocampal synaptosomes.** GlyT2-mediated transport was calculated as the difference between the [$^3$H]glycine uptake in the absence (total transport) and in the presence (unspecific transport) of the GlyT2 specific inhibitor (ALX 1393). The kinetic parameters, $K_m$ and $V_{max}$, were determined by means of nonlinear regression analysis and are indicated in the respective table. All values are mean ± SEM. **$p<0.01$, (N=6, t-test).

### 5.4.4. Synaptosomes express both TrkB-FL and TrkB-T isoforms

BDNF activates its high affinity receptors TrkB, which includes TrkB-FL and TrkB-T, which expression is achieved by alternative splicing (Klein *et al.* 1990). To study which of the TrkB receptor isoform is present in hippocampal synaptosomes and if their expression changed in the presence of BDNF (30 ng/ml), a western blot protocol was performed with an antibody that recognized the TrkB-FL and TrkB-T isoforms. The results obtained (Figure 5.47.A) revealed that BDNF (30 ng/ml) does not modify TrkB isoforms expression in synaptosomes, since two bands were detected in the immunoblot: one band with 145 kDa, which corresponds to the TrkB-FL receptor, and a lower one with about 95 kDa, that matches the molecular mass of TrkB-T isoforms.

The densitometry analysis showed that the TrkB-FL and TrkB-T levels did not significantly change in the presence of BDNF when compared to control conditions (Figure 5.47.B).

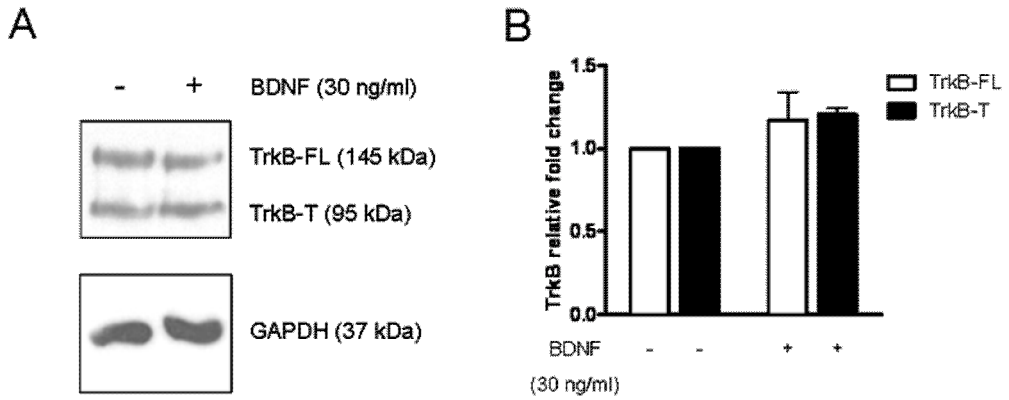


**Figure 5.47. - Expression of TrkB receptors in the absence and presence of BDNF (30 ng/ml). (A)** Representative immunoblots of TrkB receptors in total lysates of rat hippocampal synaptosomes. GAPDH was used as a loading control. **(B)** Densitometry analysis of western blots. The graph shows TrkB-FL and TrkB-T immunoreactivity normalized to GAPDH. All values are mean ± SEM. (N=4).

### 5.4.5. BDNF canonical pathways modulates GlyT2-mediated glycine uptake

The TrkB-FL isoforms have an intracellular catalytic kinase domain, which activates intracellular pathways, namely PLC, Akt and MAPK (Blum & Konnerth 2005, Sebastiao *et al.* 2011). Due to the fact that only the TrkB-FL possess this intracellular catalytic kinase

domain, tyrosine kinase inhibitors, like K252a (Tapley *et al.* 1992), are often used to distinguish between the BDNF-mediated activation of TrkB-FL or TrkB-T receptors and consequently identify which TrkB receptor isoform is responsible for the BDNF effect.
Therefore, synaptosomes were incubated with k252a (0.1 μM) in the absence and in the presence of BDNF (30 ng/ml).
It is shown (Figure 5.48.) that in synaptosomes pre-incubated with BDNF (30 ng/ml), the glycine uptake mediated by GlyT2 is significantly decreased (Figure 5.48., ***$p<0.001$), as compared with BDNF absence. The k252a (0.1 μM) incubation *per se* significantly decreased the GlyT2-mediated glycine uptake (Figure 5.48., *$p<0.05$), when compared to control conditions. This probably arises from the inhibition of different tyrosine kinases by k252a and also from phosphorylation-mediated GlyT activation (Eulenburg *et al.* 2005). However, in the presence of both k252a (0.1 μM) and BDNF (30 ng/ml), k252a was able to prevent (Figure 5.48., $p>0.5$) a further BDNF inhibitory effect upon GlyT2-mediated glycine uptake.

To further clarify what are the signalling pathways involved in the reported BDNF effect, specific inhibitors of the three main TrkB-FL classical pathways, namely the PLC inhibitor U73122 (3μM), the MAPK inhibitor U0126 (10μM) and the PI3K inhibitor LY294002 (10μM) were used. The BDNF (30 ng/ml) action in the presence of each of these inhibitors was compared to BDNF absence exactly in the same experimental conditions.
Synaptosomes pre-incubation with each inhibitor, U73122 (3μM), LY294002 (10μM) and U0126 (10μM) alone, significantly decreased the GlyT2-mediated glycine uptake (Figure 5.48., *$p<0.05$, **$p<0.01$). This is in accordance with GlyT2 susceptibility to post-transduction modifications, since the phosphorylation and interactions with other proteins can regulate GlyT2 activity, expression and localization (Eulenburg *et al.* 2005).
However, as shown in Figure 5.48., the presence of either the PLC inhibitor U73122 (3μM), the MAPK inhibitor U0126 (10μM) or the PI3K inhibitor LY294002 (10μM), prevented the BDNF inhibitory action upon glycine uptake (Figure 5.48., $p>0.05$), when compared to BDNF absence in similar experimental conditions. Hence, the BDNF effect upon GlyT2-mediated glycine uptake in synaptosomes requires the activation of the PLC, MAPK and Akt pathways.

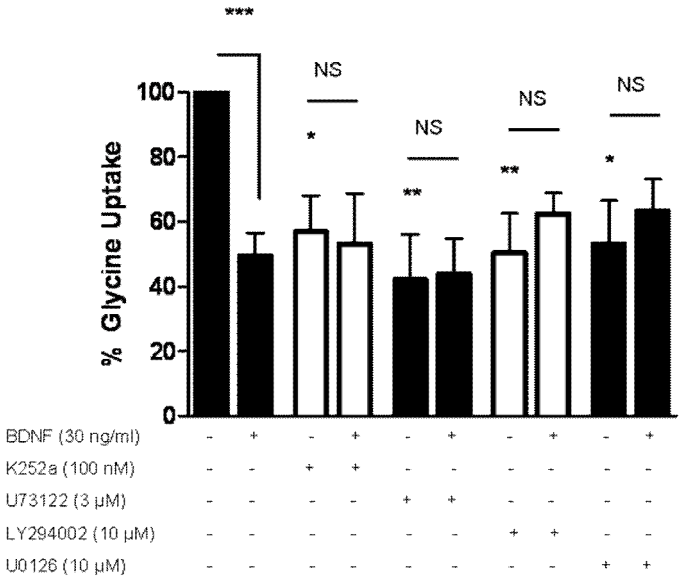


**Figure 5.48. - Effect of BDNF (30 ng/ml) in [$^3$H]glycine uptake mediated by GlyT2 in the presence of k252a (0.1 µM) and of the inhibitors of different signaling pathways of TrkB receptors: U73122 (3 µM), LY294002 (10 µM) and U0126 (10 µM).** Y axis represents [$^3$H]glycine uptake as percentage of the control value in the same experiment. All values are mean ± SEM. NS, not statistically significant ($p>0.05$), *$p<0.05$, **$p<0.01$, ***$p<0.001$, (N=5, one way ANOVA followed by Bonferroni's Comparison Test). Statistical tests were performed in comparison with control conditions, except where otherwise indicated by the connecting lines above the bars, which indicated a statistical analysis between BDNF presence and absence under the same drug condition.

### 5.4.6. BDNF modulation of GlyT2-mediated glycine uptake is not TrkB-T dependent

It is known that, in astrocytes, TrkB-T isoforms regulate cytoskeletal alterations, control Rho GTPases activity (Ohira *et al.* 2005a), stimulate PLC (Rose *et al.* 2003) and PKC (Cheng *et al.* 2007) through G protein activation. It was also described (section 5.3.) that it modulates GlyT-mediated glycine uptake in astrocytes. Since synaptosomes express both TrkB-FL and TrkB-T isoforms, the involvement of TrkB-T isoforms in the observed BDNF effect upon glycine uptake was evaluated.

Therefore, synaptosomes were incubated with toxin B (10 ng/ml) from *Clostridium difficile*, which is a glucosyltranferase known to inhibit the Rho family of GTPases (Just *et al.* 1994a, Just *et al.* 1994b).

The toxin B (10 ng/ml) pre-incubation *per se* significantly decreased the GlyT2-mediated glycine uptake (Figure 5.49., ***$p<0.001$). Once again, these results can be explained by

the modifications in cytoskeletal proteins that could be interacting with GlyT (Eulenburg *et al.* 2005). Still, the pre-incubation of synaptosomes with toxin B (10 ng/ml) and BDNF (30 ng/ml) further decreases GlyT2-mediated glycine uptake (Figure 5.49., *p<0.05), proving that Rho-GTPases activity is not required for the BDNF inhibitory action upon GlyT2-mediated glycine uptake.

Besides revealing that TrkB-T is not involved in the effect of BDNF upon GlyT2 activity, this set of experiments also constituted a control. They show that the level of BDNF effect in the presence of k252a and the others inhibitors, depicted in Figure 5.48., does not result from a ceiling effect. Indeed, toxin B, as the other inhibitors, decreased glycine uptake *per se* but did not prevent a further inhibition of glycine uptake caused by BDNF.

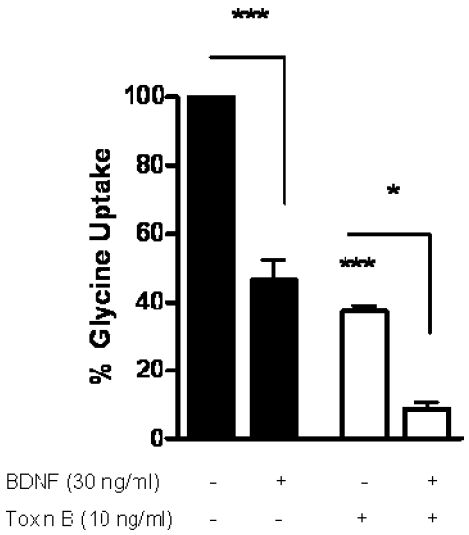


**Figure 5.49. - Effect of BDNF (30 ng/ml) upon [$^3$H]glycine uptake mediated by GlyT2 in the presence of a Rho GTPase inhibitor, toxin B (10 ng/ml) from *Clostridium difficile*.** Y axis represents [$^3$H]glycine uptake as percentage of the control value in the same experiment. All values are mean ± SEM. *p<0.05, ***p<0.001, (N=4, one way ANOVA followed by Bonferroni's Comparison Test). Statistical tests were performed in comparison with control conditions, except where otherwise indicated by the connecting lines above the bars, which indicated a statistical analysis between BDNF presence and absence under the same drug condition.

### 5.4.7. BDNF decreases glycine uptake by reducing GlyT2 insertion in the membrane

It was demonstrated that BDNF is able to significantly inhibit GlyT2-mediated glycine uptake, by decreasing $V_{max}$. Alterations in $V_{max}$ are usually related to changes in the

number of transporters, because of their translocation to and from the plasmatic membrane. Hence, the BDNF-mediated reduction of GlyT2 number in the membrane can be the consequence of either an impairment of the membrane insertion pathways or an activation of the degradation pathways. As carried out in subsection 5.3.6., in order to investigate if BDNF was affecting insertion or removal of GlyT2 from the membrane, synaptosomes were incubated with monensin (25 µM, 1h), a transporter recycling inhibitor, and dynasore (70 µM), a dynamin/clathrin-dependent endocytosis inhibitor.

Both monensin (25 µM) and dynasore (70 µM) pre-incubation alone significantly decreased the GlyT2-mediated glycine uptake (Figure 5.50., **p<0.01, ***p<0.001), which can be indicative of the need of a constitutive recycling of GlyT2 in synaptosomes to keep it functional.

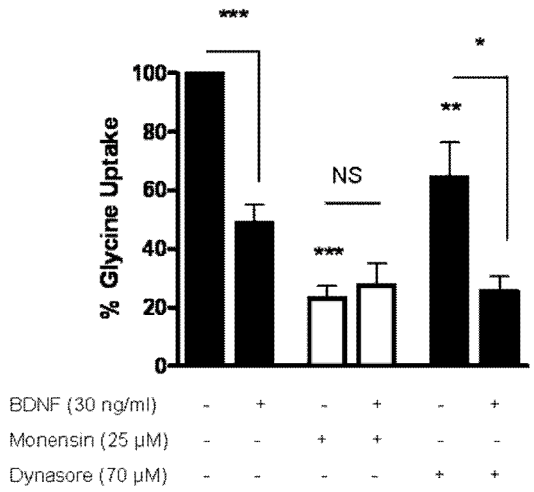


**Figure 5.50. - Influence of monensin (25 µM) and dynasore (70 µM) upon the effect of BDNF (30 ng/ml) on [$^3$H]glycine uptake mediated by GlyT2.** Y axis represents [$^3$H]glycine uptake as percentage of the control value in the same experiment. All values are mean ± SEM. NS, not statistically significant (p>0.05), *p<0.05, **p<0.01, ***p<0.001, (N=4, one way ANOVA followed by Bonferroni's Comparison Test). Statistical tests were performed in comparison with control conditions, except where otherwise indicated by the connecting lines above the bars, which indicated a statistical analysis between BDNF presence and absence under the same drug condition.

In the presence of monensin (25 µM), the BDNF action was prevented, since no statistically differences in glycine uptake mediated by GlyT2 (Figure 5.50., p>0.05) were registered when compared to BDNF absence. On the other hand, when the synaptosomes

were pre-incubated with dynasore (70 μM), BDNF (30 ng/ml) decreased significantly glycine uptake mediated by GlyT2 (Figure 5.50., *p<0.05). This result indicates that, in synaptosomes, BDNF acts upon membrane inclusion pathways, reducing GlyT2 insertion in the plasma membrane.

### 5.4.8. Discussion

The main finding of this work is that BDNF modulates glycine uptake mediated by GlyT2 in synaptosomes obtained from rat hippocampus. Overall, it was showed that BDNF, acting through TrkB-FL receptors and triggering PLCγ, PI3K and MAPK pathways, decreases GlyT2 $V_{max}$ value and consequently inhibits GlyT2-mediated glycine uptake.

The results indicate that synaptosomes, despite being isolated nerve endings that lack the gene level regulation, express both TrkB-FL and TrkB-T isoforms. However, the BDNF-dependent inhibition of glycine uptake here described was proven to be a consequence of the TrkB-FL receptors activation. This is sustained by three lines of evidence. First, BDNF effect was prevented when a tyrosine kinase inhibitor, k252a, was used. Second, BDNF action upon glycine uptake mediated by GlyT2 required the stimulation of the PLCγ/PKC, PI3K/Akt and MAPK pathways. Third, the blockade of Rho-GTPase pathways, potential targets of TrkB-T (Ohira *et al.* 2005a), did not revert the BDNF action.

The main function of GlyT2 is to transport glycine from the extracellular space to the pre-synaptic nerve terminals, which assures the refilling of glycinergic vesicles (Gomeza *et al.* 2003b). Thus, an inhibition of GlyT2-mediated glycine uptake to the pre-synaptic nerve terminals may lead to a decrease in the cytosolic glycine concentration and consequently, to a progressive reduction of glycine incorporation into synaptic vesicles. The recent publication of Eckle and co-workers (Eckle & Antkowiak 2013) states that GlyT2 inhibition, by ALX 1393, in the ventral horn area of organotypic spinal cultures induces a tonic current that was significantly reversed by the GlyR antagonist, strychnine, whereas the phasic glycinergic transmission is not enhanced. On other hand, it is also known that GlyT2 can have an extrasynaptic localization, outside the glycine-releasing active areas (Spike *et al.* 1997), which together with the previous findings that GlyR have mainly an extrasynaptic location (section 5.1.), prompt to the speculation that glycine mainly acts in tonic inhibition. Thus, it can be hypothesize that in the hippocampus, BDNF-dependent GlyT2 inhibition also acts towards the potentiation of the glycinergic tonic inhibition.

The BDNF-mediated GlyT2 inhibition is due to a decrease in $V_{max}$ values. This decrease points to a reduction of the GlyT2 number in the plasma membrane, which can be the consequence of the inhibition of GlyT2 insertion pathways in the membrane or the enhancement of the endocytic cell machinery. To elucidate this question, monensin, that blocks GlyT recycling back to the membrane without influencing endocytosis (Mollenhauer *et al.* 1990) and dynasore, which inhibits the dynamin/clathrin-dependent endocytosis (Macia *et al.* 2006), were used. BDNF action in GlyT2-mediated glycine uptake was prevented by monensin, but not by dynasore, which indicates that the BDNF-dependent decrease in glycine uptake herein described is a consequence of the impairment of the GlyT2 insertion mechanisms and is not related to GlyT2 internalization.

In conclusion, these results describe, for the first time, how BDNF modulates GlyT2 function in glycinergic nerve terminals. It was proven that BDNF, acting through its high affinity receptors TrkB-FL, leads to deficits in the mechanisms of GlyT2 insertion into the plasma membrane and thus promotes a decrease in glycine uptake by nerve terminals. Furthermore, BDNF was also shown to inhibit GlyT-mediated glycine uptake into astrocytes. Overall, BDNF inhibitory action upon GlyT, both in nerve terminals and astrocytes, may induce an increase in extracellular glycine levels and can therefore potentiate the tonic glycinergic currents. However, since glycine is a co-agonist of NMDA receptors, an increase in extracellular glycine can also potentiate NMDA currents.

# 6. General discussion and conclusions

Glycine and GABA are the main inhibitory neurotransmitters in the CNS. GABAergic neurotransmission predominates in all brain regions through the activation of ionotropic $GABA_A$ receptors. Glycinergic synapses are predominantly important in the spinal cord and brainstem (Bowery & Smart 2006) but their relevance in the hippocampus has been poorly explored. Therefore, the main goal of this work was to characterize the main intervenients of glycinergic synapses in rat hippocampus, in the three components that comprise the tripartite synapse. In detail, GlyR localization and subunit composition in the post-synaptic neurons was studied, GlyT1 and GlyT2 expression, localization and function in astrocytes was characterized and the GlyT2 expression and function in the pre-synaptic nerve terminals was described. Furthermore, the effect of BDNF, a crucial neurotrophic factor with numerous functions in the CNS, upon glycine uptake mediated by GlyT in astrocytes and in pre-synaptic nerve terminals was evaluated.

This work clearly shows the presence of GlyR in the rat hippocampus, in a development dependent manner. At P7, when the GlyR expression is higher, the post-synaptic GlyR is mainly composed by α2/β subunits, while in mature hippocampus (P21 on) the number of synaptic GlyR decreases and is mostly composed by α1/β subunits. Contrarily, extrasynaptic GlyR, composed by α2/α3 subunits, emerge and suggest a role for homomeric GlyR in the slow tonic neurotransmission.

Regarding the GlyT expression in astrocytes, the presence of both GlyT1 and GlyT2 over the development of cultured astrocytes, at mRNA and protein levels, was proven. These results were corroborated by fluorescence immunohistochemistry in brain slices.

The GlyT function is to uptake glycine from the extracellular space to the intracellular one, which will lead to a decrease of extracellular glycine concentration and to an increase of intracellular glycine levels, reducing the GlyR-mediated neurotransmission. However, although the presence of GlyT2 in cerebellum glial cells (Zafra *et al.* 1995), in cortical oligodendrocyte progenitor cells (Belachew *et al.* 2000) and in spinal cord gliosomes (Raiteri *et al.* 2008) has been shown, it was still presumed that brain glial cells only express GlyT1, while GlyT2 is localized in the pre-synaptic neurons (Eulenburg *et al.* 2005). Thus, the discovery that both GlyT1 and GlyT2 are able to uptake glycine from the surrounding environment to brain astrocytes changed the present awareness of glycinergic

synapses in the brain. This works reveals that GlyT1 and GlyT2 have very different kinetic parameters in brain astrocytes, which suggest that in situations where glycine levels reach the millimolar range, like happens in the synaptic cleft, GlyT1 is saturated and GlyT2 is able to uptake glycine. Besides this physiological role of GlyT2 in astrocytes it is also possible to propose a function for GlyT2 in pathological conditions when other inhibitory amino acid transporters, like GAT or GlyT1, are impaired. Actually, it was porposed that GlyT2 activation has a compensatory role in GlyT1 knock out animals (Eulenburg *et al.* 2010).

The data here reported also describe the GlyT modulation by BDNF. It was shown that BDNF decreases glycine uptake mediated by both GlyT1 and GlyT2 in astrocytes, which will increase the glycine concentration in the extracellular region. This effect is due to the activation of TrkB-T1, which will lead to an increase in Rho-GTPase activity, and GlyT internalization.

The predominance of TrkB-T1 in astrocytes is not novel (Rose *et al.* 2003). Despite the identification of some molecules that can be modulated by TrkB-T1, namely PLC (Rose *et al.* 2003), PKC (Cheng *et al.* 2007) and Rho GTPases (Ohira *et al.* 2005a) or proteins that can interact with TrkB-T1 like TTIP (Kryl & Barker 2000), the importance of TrkB-T signalling is not well understood. The TrkB-T mediated regulation of GlyT in astrocytes, as shown here, represents one more contribution for this field.

Finally, this work shows that hippocampal nerve terminals express GlyT2. As described for astrocytes, BDNF is also able to modulate GlyT2 in nerve endings. However, contrarily to what was described for astrocytes, the inhibitory role of BDNF upon GlyT2-mediated glycine uptake in nerve terminals is TrkB-FL dependent. BDNF action requires the activation of TrkB-FL receptors and the subsequent canonical intracellular cascades namely PLC, Akt and MAPK pathways. In this case, BDNF inhibits the GlyT2 insertion in the plasma membrane.

The major role of GlyT2 in pre-synaptic terminals is to uptake glycine from the extracellular space to the intracellular one, ensuring that glycine is available to refill the synaptic vesicles (Gomeza *et al.* 2003b). Therefore, BDNF-mediated glycine uptake inhibition causes a gradually decrease of the cytosolic glycine levels and subsequently, a reduction of glycine inclusion in pre-synaptic vesicles, glycine release and glycinergic neurotransmission. Still, both in the nerve endings and astrocytes, BDNF decreases glycine uptake, which will increase glycine levels at the synaptic space and cause glycine leakage to extracellular areas, thus potentiating glycinergic neurotransmission. If the BDNF-

mediated GlyT inhibition will influence either the tonic or the phasic neurotransmission cannot be totally answered by this work. Moreover, it was recently revealed that GlyT2 inhibition, by ALX 1393, in the ventral horn area of organotypic spinal cultures induces a glycinergic tonic current, whereas the phasic glycinergic transmission is not affected (Eckle & Antkowiak 2013), which is in accordance to the GlyT2 distribution in extrasynaptic areas (Spike *et al.* 1997). Therefore, the BDNF inhibitory effect upon GlyT, together with GlyR localization in extrasynaptic regions, points to a potentiation of glycinergic tonic currents by BDNF.

The physiological relevance of these results is still unknown. However, through an impairment of glycine uptake, it can be postulated that BDNF increases the glycinergic tonic neurotransmission, which can be advantageous in situations of hyperexcitability, as epilepsy. This suggests that BDNF can be a possible candidate to new therapeutic approaches in this area. However, the role of BDNF *per se* in epilepsy is still unclear (Binder *et al.* 2001, Paradiso *et al.* 2009) and thus, the BDNF-dependent modulation of the glycinergic system in pathological conditions has to be carefully hypothesized and further studies are needed to clarify this relationship.

In conclusion, the results here presented confirm the occurrence of glycinergic synapses in the rat brain. A complete characterization of the key players of glycinergic neurotransmission in the three components which comprise the tripartite synapse was performed (Figure 6.1.). Overall, this work provides a new awareness of glycinergic neurotransmission in the brain.

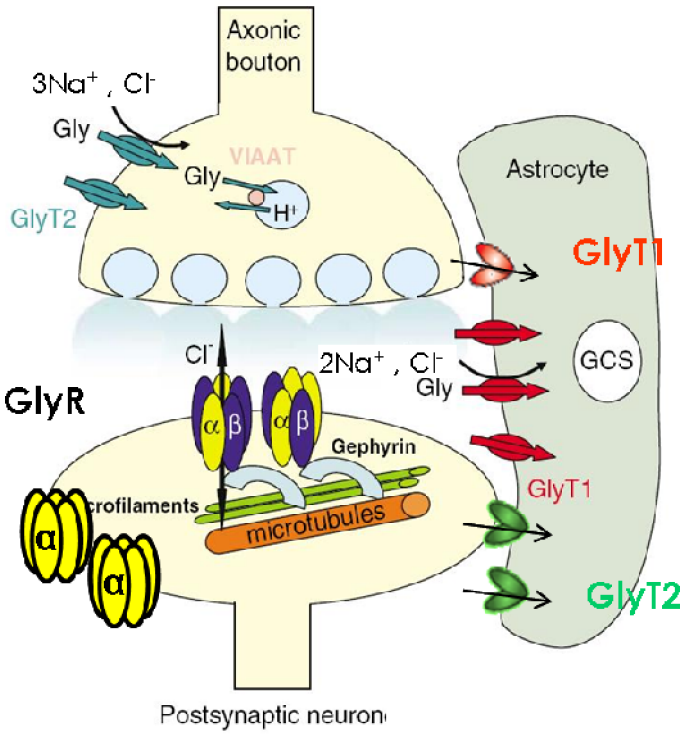


**Figure 6.1. – Proposed model for a representation of a glycinergic synapse in the hippocampus.** Glycine receptor (GlyR) is represented as heteromeric pentamers in the synaptic sites and as homomeric receptors expressed in the extrasynaptic regions. Glycine (Gly) can be transported by both glycine transporter 1 (GlyT1) and glycine transporter 2 (GlyT2) to astrocytes, where it will be hydrolysed by the glycine cleavage system (GCS), or by GlyT2 to the pre-synaptic nerve terminal being available to refill the synaptic vesicles, through vesicular inhibitory amino acid transporter (VIAAT) (Adapted from Bowery & Smart 2006).

# 7. Future perspectives

The work herein described corroborates the presence of glycinergic synapses in the brain and gives detailed information about the main components of glycinergic synapses, namely GlyR, GlyT1 and GlyT2.

Several evidences point to an association between epilepsy and glycinergic neurotransmission. It was already described, in hippocampus, that GlyR agonists and GlyT1 inhibitors are able to decrease neuronal hyperexcitability, controlling the excitatory pattern and thus having an anti-epileptic mechanism (Chattipakorn & McMahon 2003, Kirchner *et al.* 2003, Zhang *et al.* 2008). However, the role of glycinergic transmission in this pathology remains unknown. The work depicted in this thesis has truly contributed to a deeper knowledge of glycinergic transmission players in the brain and thus might help to disclosure a way to use glycinergic transmission as a potential therapeutic target for the treatment of epilepsy.

Alterations in glycinergic transmission at the molecular and functional levels in an epilepsy model will be interesting to address, since a detailed and extensive characterization at these levels can potentially provide valuable information for research within the context of a future therapy. These studies can be pursued in either *in vivo* or *in vitro* epilepsy models, and used to understand the physiological and pathological mechanisms associated with epilepsy thus helping to the development and discovery of new antiepileptic drugs and treatment strategies (Cavalheiro 1995, Sarkisian 2001).

# 8. References


Adams, R. H., Sato, K., Shimada, S., Tohyama, M., Puschel, A. W. and Betz, H. (1995) Gene structure and glial expression of the glycine transporter GlyT1 in embryonic and adult rodents. *J Neurosci,* **15,** 2524-2532.

Ahmadi, S., Muth-Selbach, U., Lauterbach, A., Lipfert, P., Neuhuber, W. L. and Zeilhofer, H. U. (2003) Facilitation of spinal NMDA receptor currents by spillover of synaptically released glycine. *Science,* **300,** 2094-2097.

Allaman, I., Belanger, M. and Magistretti, P. J. (2011) Astrocyte-neuron metabolic relationships: for better and for worse. *Trends Neurosci,* **34,** 76-87.

Allen, N. J. and Barres, B. A. (2009) Neuroscience: Glia - more than just brain glue. *Nature,* **457,** 675-677.

Andersen, P., Morris, R., Amaral, D., Bliss, T. and O'Keefe, J. (Editors) (2007) *The Hippocampus Book*. Oxford University Press, U.S.A.

Andriezen, W. L. (1893) The Neuroglia Elements in the Human Brain. *Br Med J,* **2,** 227-230.

Aragon, C. and Lopez-Corcuera, B. (2005) Glycine transporters: crucial roles of pharmacological interest revealed by gene deletion. *Trends Pharmacol Sci,* **26,** 283-286.

Araque, A., Parpura, V., Sanzgiri, R. P. and Haydon, P. G. (1999) Tripartite synapses: glia, the unacknowledged partner. *Trends Neurosci,* **22,** 208-215.

Arevalo, J. C. and Wu, S. H. (2006) Neurotrophin signaling: many exciting surprises! *Cell Mol Life Sci,* **63,** 1523-1537.

Aroeira, R. I., Ribeiro, J. A., Sebastiao, A. M. and Valente, C. A. (2011) Age-related changes of glycine receptor at the rat hippocampus: from the embryo to the adult. *J Neurochem,* **118,** 339-353.

Aroeira, R. I., Sebastiao, A. M. and Valente, C. A. (2014) GlyT1 and GlyT2 in brain astrocytes: expression, distribution and function. *Brain Struct Funct,* **219,** 817-830.

Atkinson, B. N., Bell, S. C., De Vivo, M. et al. (2001) ALX 5407: a potent, selective inhibitor of the hGlyT1 glycine transporter. *Mol Pharmacol,* **60,** 1414-1420.

Avila, A., Nguyen, L. and Rigo, J. M. (2013a) Glycine receptors and brain development. *Front Cell Neurosci,* **7,** 184.

Avila, A., Vidal, P. M., Dear, T. N., Harvey, R. J., Rigo, J. M. and Nguyen, L. (2013b) Glycine receptor alpha2 subunit activation promotes cortical interneuron migration. *Cell Rep,* **4,** 738-750.

Bai, F. and Witzmann, F. A. (2007) Synaptosome proteomics. *Subcell Biochem,* **43,** 77-98.

Barde, Y. A., Edgar, D. and Thoenen, H. (1982) Purification of a new neurotrophic factor from mammalian brain. *EMBO J,* **1,** 549-553.

Bartkowska, K., Turlejski, K. and Djavadian, R. L. (2010) Neurotrophins and their receptors in early development of the mammalian nervous system. *Acta Neurobiol Exp (Wars),* **70,** 454-467.

Becker, C. M., Hoch, W. and Betz, H. (1988) Glycine receptor heterogeneity in rat spinal cord during postnatal development. *EMBO J,* **7,** 3717-3726.

Belachew, S., Malgrange, B., Rigo, J. M., Rogister, B., Leprince, P., Hans, G., Nguyen, L. and Moonen, G. (2000) Glycine triggers an intracellular calcium influx in oligodendrocyte progenitor cells which is

mediated by the activation of both the ionotropic glycine receptor and Na+-dependent transporters. *Eur J Neurosci,* **12,** 1924-1930.

Ben-Ari, Y., Cherubini, E., Corradetti, R. and Gaiarsa, J. L. (1989) Giant synaptic potentials in immature rat CA3 hippocampal neurones. *J Physiol,* **416,** 303-325.

Ben-Ari, Y. (2002) Excitatory actions of gaba during development: the nature of the nurture. *Nat Rev Neurosci,* **3,** 728-739.

Benitez-Diaz, P., Miranda-Contreras, L., Mendoza-Briceno, R. V., Pena-Contreras, Z. and Palacios-Pru, E. (2003) Prenatal and postnatal contents of amino acid neurotransmitters in mouse parietal cortex. *Dev Neurosci,* **25,** 366-374.

Betz, H., Gomeza, J., Armsen, W., Scholze, P. and Eulenburg, V. (2006) Glycine transporters: essential regulators of synaptic transmission. *Biochem Soc Trans,* **34,** 55-58.

Betz, H. and Laube, B. (2006) Glycine receptors: recent insights into their structural organization and functional diversity. *J Neurochem,* **97,** 1600-1610.

Biber, K., Klotz, K. N., Berger, M., Gebicke-Harter, P. J. and van Calker, D. (1997) Adenosine A1 receptor-mediated activation of phospholipase C in cultured astrocytes depends on the level of receptor expression. *J Neurosci,* **17,** 4956-4964.

Biffo, S., Offenhauser, N., Carter, B. D. and Barde, Y. A. (1995) Selective binding and internalisation by truncated receptors restrict the availability of BDNF during development. *Development,* **121,** 2461-2470.

Binder, D. K., Routbort, M. J. and McNamara, J. O. (1999a) Immunohistochemical evidence of seizure-induced activation of trk receptors in the mossy fiber pathway of adult rat hippocampus. *J Neurosci,* **19,** 4616-4626.

Binder, D. K., Routbort, M. J., Ryan, T. E., Yancopoulos, G. D. and McNamara, J. O. (1999b) Selective inhibition of kindling development by intraventricular administration of TrkB receptor body. *J Neurosci,* **19,** 1424-1436.

Binder, D. K., Croll, S. D., Gall, C. M. and Scharfman, H. E. (2001) BDNF and epilepsy: too much of a good thing? *Trends Neurosci,* **24,** 47-53.

Binder, D. K. and Scharfman, H. E. (2004) Brain-derived neurotrophic factor. *Growth Factors,* **22,** 123-131.

Blum, R. and Konnerth, A. (2005) Neurotrophin-mediated rapid signaling in the central nervous system: mechanisms and functions. *Physiology (Bethesda),* **20,** 70-78.

Booher, J. and Sensenbrenner, M. (1972) Growth and cultivation of dissociated neurons and glial cells from embryonic chick, rat and human brain in flask cultures. *Neurobiology,* **2,** 97-105.

Borowsky, B., Mezey, E. and Hoffman, B. J. (1993) Two glycine transporter variants with distinct localization in the CNS and peripheral tissues are encoded by a common gene. *Neuron,* **10,** 851-863.

Bowery, N. G. and Smart, T. G. (2006) GABA and glycine as neurotransmitters: a brief history. *Br J Pharmacol,* **147 Suppl 1,** S109-119.

Brackmann, M., Zhao, C., Schmieden, V. and Braunewell, K. H. (2004) Cellular and subcellular localization of the inhibitory glycine receptor in hippocampal neurons. *Biochem Biophys Res Commun,* **324,** 1137-1142.

Bradaia, A., Schlichter, R. and Trouslard, J. (2004) Role of glial and neuronal glycine transporters in the control of glycinergic and glutamatergic synaptic transmission in lamina X of the rat spinal cord. *J Physiol,* **559,** 169-186.

Bradford, M. M. (1976) A rapid and sensitive method for the quantitation of microgram quantities of protein utilizing the principle of protein-dye binding. *Anal Biochem,* **72,** 248-254.

Brown, A., Carlyle, I., Clark, J. et al. (2001) Discovery and SAR of org 24598-a selective glycine uptake inhibitor. *Bioorg Med Chem Lett,* **11,** 2007-2009.

Burnette, W. N. (1981) "Western blotting": electrophoretic transfer of proteins from sodium dodecyl sulfate--polyacrylamide gels to unmodified nitrocellulose and radiographic detection with antibody and radioiodinated protein A. *Anal Biochem,* **112,** 195-203.

Caldeira, M. V., Melo, C. V., Pereira, D. B., Carvalho, R., Correia, S. S., Backos, D. S., Carvalho, A. L., Esteban, J. A. and Duarte, C. B. (2007a) Brain-derived neurotrophic factor regulates the expression and synaptic delivery of alpha-amino-3-hydroxy-5-methyl-4-isoxazole propionic acid receptor subunits in hippocampal neurons. *J Biol Chem,* **282,** 12619-12628.

Caldeira, M. V., Melo, C. V., Pereira, D. B., Carvalho, R. F., Carvalho, A. L. and Duarte, C. B. (2007b) BDNF regulates the expression and traffic of NMDA receptors in cultured hippocampal neurons. *Mol Cell Neurosci,* **35,** 208-219.

Canas, N., Pereira, I. T., Ribeiro, J. A. and Sebastiao, A. M. (2004) Brain-derived neurotrophic factor facilitates glutamate and inhibits GABA release from hippocampal synaptosomes through different mechanisms. *Brain Res,* **1016,** 72-78.

Caraiscos, V. B., Mihic, S. J., MacDonald, J. F. and Orser, B. A. (2002) Tyrosine kinases enhance the function of glycine receptors in rat hippocampal neurons and human alpha(1)beta glycine receptors. *J Physiol,* **539,** 495-502.

Castagna, M., Shayakul, C., Trotti, D., Sacchi, V. F., Harvey, W. R. and Hediger, M. A. (1997) Molecular characteristics of mammalian and insect amino acid transporters: implications for amino acid homeostasis. *J Exp Biol,* **200,** 269-286.

Cavalheiro, E. A. (1995) The pilocarpine model of epilepsy. *Ital J Neurol Sci,* **16,** 33-37.

Chao, M. V. and Hempstead, B. L. (1995) p75 and Trk: a two-receptor system. *Trends Neurosci,* **18,** 321-326.

Chattipakorn, S. C. and McMahon, L. L. (2002) Pharmacological characterization of glycine-gated chloride currents recorded in rat hippocampal slices. *J Neurophysiol,* **87,** 1515-1525.

Chattipakorn, S. C. and McMahon, L. L. (2003) Strychnine-sensitive glycine receptors depress hyperexcitability in rat dentate gyrus. *J Neurophysiol,* **89,** 1339-1342.

Cheng, A., Coksaygan, T., Tang, H., Khatri, R., Balice-Gordon, R. J., Rao, M. S. and Mattson, M. P. (2007) Truncated tyrosine kinase B brain-derived neurotrophic factor receptor directs cortical neural stem cells to a glial cell fate by a novel signaling mechanism. *J Neurochem,* **100,** 1515-1530.

Cherubini, E., Bernardi, G., Stanzione, P., Marciani, M. G. and Mercuri, N. (1981) The action of glycine on rat epileptic foci. *Neurosci Lett,* **21,** 93-97.

Clayton, G. H., Owens, G. C., Wolff, J. S. and Smith, R. L. (1998) Ontogeny of cation-Cl- cotransporter expression in rat neocortex. *Brain Res Dev Brain Res,* **109,** 281-292.

Climent, E., Sancho-Tello, M., Minana, R., Barettino, D. and Guerri, C. (2000) Astrocytes in culture express the full-length Trk-B receptor and respond to brain derived neurotrophic factor by changing intracellular calcium levels: effect of ethanol exposure in rats. *Neurosci Lett,* **288,** 53-56.

Cohen, S., Levi-Montalcini, R. and Hamburger, V. (1954) A Nerve Growth-Stimulating Factor Isolated from Sarcom as 37 and 180. *Proc Natl Acad Sci U S A,* **40,** 1014-1018.

Conner, J. M., Lauterborn, J. C., Yan, Q., Gall, C. M. and Varon, S. (1997) Distribution of brain-derived neurotrophic factor (BDNF) protein and mRNA in the normal adult rat CNS: evidence for anterograde axonal transport. *J Neurosci,* **17,** 2295-2313.

Coons, A. H. and Kaplan, M. H. (1950) Localization of antigen in tissue cells; improvements in a method for the detection of antigen by means of fluorescent antibody. *J Exp Med,* **91,** 1-13.

Cragnolini, A. B., Huang, Y., Gokina, P. and Friedman, W. J. (2009) Nerve growth factor attenuates proliferation of astrocytes via the p75 neurotrophin receptor. *Glia,* **57,** 1386-1392.

Cragnolini, A. B., Volosin, M., Huang, Y. and Friedman, W. J. (2012) Nerve growth factor induces cell cycle arrest of astrocytes. *Dev Neurobiol,* **72,** 766-776.

Croll, S. D., Suri, C., Compton, D. L., Simmons, M. V., Yancopoulos, G. D., Lindsay, R. M., Wiegand, S. J., Rudge, J. S. and Scharfman, H. E. (1999) Brain-derived neurotrophic factor transgenic mice exhibit passive avoidance deficits, increased seizure severity and in vitro hyperexcitability in the hippocampus and entorhinal cortex. *Neuroscience,* **93,** 1491-1506.

Cubelos, B., Gimenez, C. and Zafra, F. (2005) Localization of the GLYT1 glycine transporter at glutamatergic synapses in the rat brain. *Cereb Cortex,* **15,** 448-459.

Curtis, D. R., Hosli, L., Johnston, G. A. and Johnston, I. H. (1968) The hyperpolarization of spinal motoneurones by glycine and related amino acids. *Exp Brain Res,* **5,** 235-258.

Dahan, M., Levi, S., Luccardini, C., Rostaing, P., Riveau, B. and Triller, A. (2003) Diffusion dynamics of glycine receptors revealed by single-quantum dot tracking. *Science,* **302,** 442-445.

Dalby, N. O. and Mody, I. (2001) The process of epileptogenesis: a pathophysiological approach. *Curr Opin Neurol,* **14,** 187-192.

Danglot, L., Rostaing, P., Triller, A. and Bessis, A. (2004) Morphologically identified glycinergic synapses in the hippocampus. *Mol Cell Neurosci,* **27,** 394-403.

Davies, J. S., Chung, S. K., Thomas, R. H. et al. (2010) The glycinergic system in human startle disease: a genetic screening approach. *Front Mol Neurosci,* **3,** 8.

del Pino, I., Paarmann, I., Karas, M., Kilimann, M. W. and Betz, H. (2011) The trafficking proteins Vacuolar Protein Sorting 35 and Neurobeachin interact with the glycine receptor beta-subunit. *Biochem Biophys Res Commun,* **412,** 435-440.

Delpire, E. (2000) Cation-Chloride Cotransporters in Neuronal Communication. *News Physiol Sci,* **15,** 309-312.

Diogenes, M. J., Fernandes, C. C., Sebastiao, A. M. and Ribeiro, J. A. (2004) Activation of adenosine A2A receptor facilitates brain-derived neurotrophic factor modulation of synaptic transmission in hippocampal slices. *J Neurosci,* **24,** 2905-2913.

Dohi, T., Morita, K., Kitayama, T., Motoyama, N. and Morioka, N. (2009) Glycine transporter inhibitors as a novel drug discovery strategy for neuropathic pain. *Pharmacol Ther,* **123,** 54-79.

Du, F., Qian, Z. M., Zhu, L., Wu, X. M., Qian, C., Chan, R. and Ke, Y. (2010) Purity, cell viability, expression of GFAP and bystin in astrocytes cultured by different procedures. *J Cell Biochem,* **109,** 30-37.

Dumoulin, A., Rostaing, P., Bedet, C., Levi, S., Isambert, M. F., Henry, J. P., Triller, A. and Gasnier, B. (1999) Presence of the vesicular inhibitory amino acid transporter in GABAergic and glycinergic synaptic terminal boutons. *J Cell Sci,* **112 ( Pt 6),** 811-823.

Dumoulin, A., Levi, S., Riveau, B., Gasnier, B. and Triller, A. (2000) Formation of mixed glycine and GABAergic synapses in cultured spinal cord neurons. *Eur J Neurosci,* **12,** 3883-3892.

Dutertre, S., Becker, C. M. and Betz, H. (2012) Inhibitory glycine receptors: an update. *J Biol Chem,* **287,** 40216-40223.

Ebihara, S., Yamamoto, T., Obata, K. and Yanagawa, Y. (2004) Gene structure and alternative splicing of the mouse glycine transporter type-2. *Biochem Biophys Res Commun,* **317,** 857-864.

Eckle, V. S. and Antkowiak, B. (2013) ALX 1393 inhibits spontaneous network activity by inducing glycinergic tonic currents in the spinal ventral horn. *Neuroscience,* **253,** 165-171.

Eichler, S. A., Kirischuk, S., Juttner, R., Schaefermeier, P. K., Legendre, P., Lehmann, T. N., Gloveli, T., Grantyn, R. and Meier, J. C. (2008) Glycinergic tonic inhibition of hippocampal neurons with depolarizing GABAergic transmission elicits histopathological signs of temporal lobe epilepsy. *J Cell Mol Med,* **12,** 2848-2866.

Eichler, S. A., Forstera, B., Smolinsky, B., Juttner, R., Lehmann, T. N., Fahling, M., Schwarz, G., Legendre, P. and Meier, J. C. (2009) Splice-specific roles of glycine receptor alpha3 in the hippocampus. *Eur J Neurosci,* **30,** 1077-1091.

Eide, F. F., Vining, E. R., Eide, B. L., Zang, K., Wang, X. Y. and Reichardt, L. F. (1996) Naturally occurring truncated trkB receptors have dominant inhibitory effects on brain-derived neurotrophic factor signaling. *J Neurosci,* **16,** 3123-3129.

Eulenburg, V., Armsen, W., Betz, H. and Gomeza, J. (2005) Glycine transporters: essential regulators of neurotransmission. *Trends Biochem Sci,* **30,** 325-333.

Eulenburg, V., Retiounskaia, M., Papadopoulos, T., Gomeza, J. and Betz, H. (2010) Glial glycine transporter 1 function is essential for early postnatal survival but dispensable in adult mice. *Glia,* **58,** 1066-1073.

Fenner, B. M. (2012) Truncated TrkB: beyond a dominant negative receptor. *Cytokine Growth Factor Rev,* **23,** 15-24.

Flint, A. C., Liu, X. and Kriegstein, A. R. (1998) Nonsynaptic glycine receptor activation during early neocortical development. *Neuron,* **20,** 43-53.

Fornes, A., Nunez, E., Aragon, C. and Lopez-Corcuera, B. (2004) The second intracellular loop of the glycine transporter 2 contains crucial residues for glycine transport and phorbol ester-induced regulation. *J Biol Chem,* **279,** 22934-22943.

Fornes, A., Nunez, E., Alonso-Torres, P., Aragon, C. and Lopez-Corcuera, B. (2008) Trafficking properties and activity regulation of the neuronal glycine transporter GLYT2 by protein kinase C. *Biochem J,* **412,** 495-506.

Frank, L., Ventimiglia, R., Anderson, K., Lindsay, R. M. and Rudge, J. S. (1996) BDNF down-regulates neurotrophin responsiveness, TrkB protein and TrkB mRNA levels in cultured rat hippocampal neurons. *Eur J Neurosci,* **8,** 1220-1230.

Fritschy, J. M., Harvey, R. J. and Schwarz, G. (2008) Gephyrin: where do we stand, where do we go? *Trends Neurosci,* **31,** 257-264.

Gabryel, B., Adamczyk, J., Huzarska, M., Pudelko, A. and Trzeciak, H. I. (2002) Aniracetam attenuates apoptosis of astrocytes subjected to simulated ischemia in vitro. *Neurotoxicology,* **23,** 385-395.

Gahwiler, B. H. (1999) Nerve cells in culture: the extraordinary discovery by Ross Granville Harrison. *Brain Res Bull,* **50,** 343-344.

Ganong, W. (2012) *Review of Medical Physiology*. McGraw Hill.

Geerlings, A., Nunez, E., Lopez-Corcuera, B. and Aragon, C. (2001) Calcium- and syntaxin 1-mediated trafficking of the neuronal glycine transporter GLYT2. *J Biol Chem,* **276,** 17584-17590.

Gingras, M., Gagnon, V., Minotti, S., Durham, H. D. and Berthod, F. (2007) Optimized protocols for isolation of primary motor neurons, astrocytes and microglia from embryonic mouse spinal cord. *J Neurosci Methods,* **163,** 111-118.

Gomeza, J., Hulsmann, S., Ohno, K., Eulenburg, V., Szoke, K., Richter, D. and Betz, H. (2003a) Inactivation of the glycine transporter 1 gene discloses vital role of glial glycine uptake in glycinergic inhibition. *Neuron,* **40,** 785-796.

Gomeza, J., Ohno, K., Hulsmann, S., Armsen, W., Eulenburg, V., Richter, D. W., Laube, B. and Betz, H. (2003b) Deletion of the mouse glycine transporter 2 results in a hyperekplexia phenotype and postnatal lethality. *Neuron,* **40,** 797-806.

Gomeza, J., Armsen, W., Betz, H. and Eulenburg, V. (2006) Lessons from the knocked-out glycine transporters. *Handb Exp Pharmacol***,** 457-483.

Graham, D., Pfeiffer, F. and Betz, H. (1983) Photoaffinity-labelling of the glycine receptor of rat spinal cord. *Eur J Biochem,* **131,** 519-525.

Gray, E. G. and Whittaker, V. P. (1962) The isolation of nerve endings from brain: an electron-microscopic study of cell fragments derived by homogenization and centrifugation. *J Anat,* **96,** 79-88.

Grenningloh, G., Pribilla, I., Prior, P., Multhaup, G., Beyreuther, K., Taleb, O. and Betz, H. (1990) Cloning and expression of the 58 kd beta subunit of the inhibitory glycine receptor. *Neuron,* **4,** 963-970.

Grudzinska, J., Schemm, R., Haeger, S., Nicke, A., Schmalzing, G., Betz, H. and Laube, B. (2005) The beta subunit determines the ligand binding properties of synaptic glycine receptors. *Neuron,* **45,** 727-739.

Guastella, J., Brecha, N., Weigmann, C., Lester, H. A. and Davidson, N. (1992) Cloning, expression, and localization of a rat brain high-affinity glycine transporter. *Proc Natl Acad Sci U S A,* **89,** 7189-7193.

Haglid, K. G., Wang, S., Qiner, Y. and Hamberger, A. (1994) Excitotoxicity. Experimental correlates to human epilepsy. *Mol Neurobiol,* **9,** 259-263.

Hallbook, F. (1999) Evolution of the vertebrate neurotrophin and Trk receptor gene families. *Curr Opin Neurobiol,* **9,** 616-621.

Hamilton, N. B. and Attwell, D. (2010) Do astrocytes really exocytose neurotransmitters? *Nat Rev Neurosci,* **11,** 227-238.

Harlow, E., and Lane, D. (1999) *Using Antibodies - A Laboratory Manual*. 1st Ed., Cold Spring Harbor Laboratory Press, U.S.A.

Harrison, R. G. (1912) The cultivation of tissues in extraneous media as a method of morphogenetic study. *Anat Rec,* **6,** 181-193.

Harsing, L. G., Jr. and Matyus, P. (2013) Mechanisms of glycine release, which build up synaptic and extrasynaptic glycine levels: the role of synaptic and non-synaptic glycine transporters. *Brain Res Bull,* **93,** 110-119.

Harvey, R. J., Depner, U. B., Wassle, H. et al. (2004) GlyR alpha3: an essential target for spinal PGE2-mediated inflammatory pain sensitization. *Science,* **304,** 884-887.

Harvey, R. J., Carta, E., Pearce, B. R., Chung, S. K., Supplisson, S., Rees, M. I. and Harvey, K. (2008) A critical role for glycine transporters in hyperexcitability disorders. *Front Mol Neurosci,* **1,** 1.

He, X. P., Kotloski, R., Nef, S., Luikart, B. W., Parada, L. F. and McNamara, J. O. (2004) Conditional deletion of TrkB but not BDNF prevents epileptogenesis in the kindling model. *Neuron,* **43,** 31-42.

Hebb, C. O. and Whittaker, V. P. (1958) Intracellular distributions of acetylcholine and choline acetylase. *J Physiol,* **142,** 187-196.

Heinrich, C., Lahteinen, S., Suzuki, F. et al. (2011) Increase in BDNF-mediated TrkB signaling promotes epileptogenesis in a mouse model of mesial temporal lobe epilepsy. *Neurobiol Dis,* **42,** 35-47.

Hondermarck, H. (2012) Neurotrophins and their receptors in breast cancer. *Cytokine Growth Factor Rev,* **23,** 357-365.

Horiuchi, M., Loebrich, S., Brandstaetter, J. H., Kneussel, M. and Betz, H. (2005) Cellular localization and subcellular distribution of Unc-33-like protein 6, a brain-specific protein of the collapsin response mediator protein family that interacts with the neuronal glycine transporter 2. *J Neurochem,* **94,** 307-315.

Hruskova, B., Trojanova, J., Kulik, A., Kralikova, M., Pysanenko, K., Bures, Z., Syka, J., Trussell, L. O. and Turecek, R. (2012) Differential distribution of glycine receptor subtypes at the rat calyx of held synapse. *J Neurosci,* **32,** 17012-17024.

Huang, E. J. and Reichardt, L. F. (2003) Trk receptors: roles in neuronal signal transduction. *Annu Rev Biochem,* **72,** 609-642.

Ibanez, C. F., Ernfors, P., Timmusk, T., Ip, N. Y., Arenas, E., Yancopoulos, G. D. and Persson, H. (1993) Neurotrophin-4 is a target-derived neurotrophic factor for neurons of the trigeminal ganglion. *Development,* **117,** 1345-1353.

Ito, S. and Cherubini, E. (1991) Strychnine-sensitive glycine responses of neonatal rat hippocampal neurones. *J Physiol,* **440,** 67-83.

James, V. M., Bode, A., Chung, S. K. et al. (2013) Novel missense mutations in the glycine receptor beta subunit gene (GLRB) in startle disease. *Neurobiol Dis,* **52,** 137-149.

Jensen, M. L., Schousboe, A. and Ahring, P. K. (2005) Charge selectivity of the Cys-loop family of ligand-gated ion channels. *J Neurochem,* **92,** 217-225.

Jeong, H. J., Jang, I. S., Moorhouse, A. J. and Akaike, N. (2003) Activation of presynaptic glycine receptors facilitates glycine release from presynaptic terminals synapsing onto rat spinal sacral dorsal commissural nucleus neurons. *J Physiol,* **550,** 373-383.

Jiang, M. and Chen, G. (2009) Ca2+ regulation of dynamin-independent endocytosis in cortical astrocytes. *J Neurosci,* **29,** 8063-8074.

Johnson, J. W. and Ascher, P. (1987) Glycine potentiates the NMDA response in cultured mouse brain neurons. *Nature,* **325,** 529-531.

Jonas, P., Bischofberger, J. and Sandkuhler, J. (1998) Corelease of two fast neurotransmitters at a central synapse. *Science,* **281,** 419-424.

Jursky, F., Tamura, S., Tamura, A., Mandiyan, S., Nelson, H. and Nelson, N. (1994) Structure, function and brain localization of neurotransmitter transporters. *J Exp Biol,* **196,** 283-295.

Jursky, F. and Nelson, N. (1995) Localization of glycine neurotransmitter transporter (GLYT2) reveals correlation with the distribution of glycine receptor. *J Neurochem,* **64,** 1026-1033.

Jursky, F. and Nelson, N. (1996) Developmental expression of the glycine transporters GLYT1 and GLYT2 in mouse brain. *J Neurochem,* **67,** 336-344.

Just, I., Fritz, G., Aktories, K., Giry, M., Popoff, M. R., Boquet, P., Hegenbarth, S. and von Eichel-Streiber, C. (1994a) Clostridium difficile toxin B acts on the GTP-binding protein Rho. *J Biol Chem,* **269,** 10706-10712.

Just, I., Richter, H. P., Prepens, U., von Eichel-Streiber, C. and Aktories, K. (1994b) Probing the action of Clostridium difficile toxin B in Xenopus laevis oocytes. *J Cell Sci,* **107 ( Pt 6),** 1653-1659.

Kirchner, A., Breustedt, J., Rosche, B., Heinemann, U. F. and Schmieden, V. (2003) Effects of taurine and glycine on epileptiform activity induced by removal of Mg2+ in combined rat entorhinal cortex-hippocampal slices. *Epilepsia,* **44,** 1145-1152.

Kirmse, K., Dvorzhak, A., Kirischuk, S. and Grantyn, R. (2008) GABA transporter 1 tunes GABAergic synaptic transmission at output neurons of the mouse neostriatum. *J Physiol,* **586,** 5665-5678.

Kirmse, K., Kirischuk, S. and Grantyn, R. (2009) Role of GABA transporter 3 in GABAergic synaptic transmission at striatal output neurons. *Synapse,* **63,** 921-929.

Kirsch, J., Langosch, D., Prior, P., Littauer, U. Z., Schmitt, B. and Betz, H. (1991) The 93-kDa glycine receptor-associated protein binds to tubulin. *J Biol Chem,* **266,** 22242-22245.

Kirsch, J., Malosio, M. L., Wolters, I. and Betz, H. (1993) Distribution of gephyrin transcripts in the adult and developing rat brain. *Eur J Neurosci,* **5,** 1109-1117.

Kirsch, J. (2006) Glycinergic transmission. *Cell Tissue Res,* **326,** 535-540.

Klein, R., Conway, D., Parada, L. F. and Barbacid, M. (1990) The trkB tyrosine protein kinase gene codes for a second neurogenic receptor that lacks the catalytic kinase domain. *Cell,* **61,** 647-656.

Kokaia, M., Ernfors, P., Kokaia, Z., Elmer, E., Jaenisch, R. and Lindvall, O. (1995) Suppressed epileptogenesis in BDNF mutant mice. *Exp Neurol,* **133,** 215-224.

Kryl, D. and Barker, P. A. (2000) TTIP is a novel protein that interacts with the truncated T1 TrkB neurotrophin receptor. *Biochem Biophys Res Commun,* **279,** 925-930.

Kubota, H., Alle, H., Betz, H. and Geiger, J. R. (2010) Presynaptic glycine receptors on hippocampal mossy fibers. *Biochem Biophys Res Commun,* **393,** 587-591.

Kuhse, J., Kuryatov, A., Maulet, Y., Malosio, M. L., Schmieden, V. and Betz, H. (1991) Alternative splicing generates two isoforms of the alpha 2 subunit of the inhibitory glycine receptor. *FEBS Lett,* **283,** 73-77.

Kuhse, J., Laube, B., Magalei, D. and Betz, H. (1993) Assembly of the inhibitory glycine receptor: identification of amino acid sequence motifs governing subunit stoichiometry. *Neuron,* **11,** 1049-1056.

Lahteinen, S., Pitkanen, A., Saarelainen, T., Nissinen, J., Koponen, E. and Castren, E. (2002) Decreased BDNF signalling in transgenic mice reduces epileptogenesis. *Eur J Neurosci,* **15,** 721-734.

Lall, D., Armbruster, A., Ruffert, K., Betz, H. and Eulenburg, V. (2012) Transport activities and expression patterns of glycine transporters 1 and 2 in the developing murine brain stem and spinal cord. *Biochem Biophys Res Commun,* **423,** 661-666.

Lange, S. C., Bak, L. K., Waagepetersen, H. S., Schousboe, A. and Norenberg, M. D. (2012) Primary cultures of astrocytes: their value in understanding astrocytes in health and disease. *Neurochem Res,* **37,** 2569-2588.

Langosch, D., Thomas, L. and Betz, H. (1988) Conserved quaternary structure of ligand-gated ion channels: the postsynaptic glycine receptor is a pentamer. *Proc Natl Acad Sci U S A,* **85,** 7394-7398.

Larmet, Y., Reibel, S., Carnahan, J., Nawa, H., Marescaux, C. and Depaulis, A. (1995) Protective effects of brain-derived neurotrophic factor on the development of hippocampal kindling in the rat. *Neuroreport,* **6,** 1937-1941.

Lee, E. A., Cho, J. H., Choi, I. S., Nakamura, M., Park, H. M., Lee, J. J., Lee, M. G., Choi, B. J. and Jang, I. S. (2009) Presynaptic glycine receptors facilitate spontaneous glutamate release onto hilar neurons in the rat hippocampus. *J Neurochem,* **109,** 275-286.

Lee, R., Kermani, P., Teng, K. K. and Hempstead, B. L. (2001) Regulation of cell survival by secreted proneurotrophins. *Science,* **294,** 1945-1948.

Legendre, P. (2001) The glycinergic inhibitory synapse. *Cell Mol Life Sci,* **58,** 760-793.

Legendre, P., Forstera, B., Juttner, R. and Meier, J. C. (2009) Glycine Receptors Caught between Genome and Proteome - Functional Implications of RNA Editing and Splicing. *Front Mol Neurosci,* **2,** 23.

Lessmann, V. and Heumann, R. (1998) Modulation of unitary glutamatergic synapses by neurotrophin-4/5 or brain-derived neurotrophic factor in hippocampal microcultures: presynaptic enhancement depends on pre-established paired-pulse facilitation. *Neuroscience,* **86,** 399-413.

Levi-Montalcini, R. and Hamburger, V. (1951) Selective growth stimulating effects of mouse sarcoma on the sensory and sympathetic nervous system of the chick embryo. *J Exp Zool,* **116,** 321-361.

Levi, S., Logan, S. M., Tovar, K. R. and Craig, A. M. (2004) Gephyrin is critical for glycine receptor clustering but not for the formation of functional GABAergic synapses in hippocampal neurons. *J Neurosci,* **24,** 207-217.

Levi, S., Schweizer, C., Bannai, H., Pascual, O., Charrier, C. and Triller, A. (2008) Homeostatic regulation of synaptic GlyR numbers driven by lateral diffusion. *Neuron,* **59,** 261-273.

Lewis, T. M., Schofield, P. R. and McClellan, A. M. (2003) Kinetic determinants of agonist action at the recombinant human glycine receptor. *J Physiol,* **549,** 361-374.

Liu, Q. R., Nelson, H., Mandiyan, S., Lopez-Corcuera, B. and Nelson, N. (1992) Cloning and expression of a glycine transporter from mouse brain. *FEBS Lett,* **305,** 110-114.

Lu, T., Rubio, M. E. and Trussell, L. O. (2008) Glycinergic transmission shaped by the corelease of GABA in a mammalian auditory synapse. *Neuron,* **57,** 524-535.

Luccini, E. and Raiteri, L. (2007) Mechanisms of [(3)H]glycine release from mouse spinal cord synaptosomes selectively labeled through GLYT2 transporters. *J Neurochem,* **103,** 2439-2448.

Luo, L. (2002) Actin cytoskeleton regulation in neuronal morphogenesis and structural plasticity. *Annu Rev Cell Dev Biol,* **18,** 601-635.

Lynch, J. W. (2004) Molecular structure and function of the glycine receptor chloride channel. *Physiol Rev,* **84,** 1051-1095.

Lynch, J. W. (2009) Native glycine receptor subtypes and their physiological roles. *Neuropharmacology,* **56,** 303-309.

Macia, E., Ehrlich, M., Massol, R., Boucrot, E., Brunner, C. and Kirchhausen, T. (2006) Dynasore, a cell-permeable inhibitor of dynamin. *Dev Cell,* **10,** 839-850.

Malosio, M. L., Grenningloh, G., Kuhse, J., Schmieden, V., Schmitt, B., Prior, P. and Betz, H. (1991a) Alternative splicing generates two variants of the alpha 1 subunit of the inhibitory glycine receptor. *J Biol Chem,* **266,** 2048-2053.

Malosio, M. L., Marqueze-Pouey, B., Kuhse, J. and Betz, H. (1991b) Widespread expression of glycine receptor subunit mRNAs in the adult and developing rat brain. *EMBO J,* **10,** 2401-2409.

Martina, M., Gorfinkel, Y., Halman, S., Lowe, J. A., Periyalwar, P., Schmidt, C. J. and Bergeron, R. (2004) Glycine transporter type 1 blockade changes NMDA receptor-mediated responses and LTP in hippocampal CA1 pyramidal cells by altering extracellular glycine levels. *J Physiol,* **557,** 489-500.

Martinez-Maza, R., Poyatos, I., Lopez-Corcuera, B., E, N. u., Gimenez, C., Zafra, F. and Aragon, C. (2001) The role of N-glycosylation in transport to the plasma membrane and sorting of the neuronal glycine transporter GLYT2. *J Biol Chem,* **276,** 2168-2173.

McCarthy, K. D. and de Vellis, J. (1980) Preparation of separate astroglial and oligodendroglial cell cultures from rat cerebral tissue. *J Cell Biol,* **85,** 890-902.

McNamara, J. O. and Scharfman, H. E. (2012) Temporal Lobe Epilepsy and the BDNF Receptor, TrkB.

Meier, J., Meunier-Durmort, C., Forest, C., Triller, A. and Vannier, C. (2000) Formation of glycine receptor clusters and their accumulation at synapses. *J Cell Sci,* **113 ( Pt 15),** 2783-2795.

Meier, J., Vannier, C., Serge, A., Triller, A. and Choquet, D. (2001) Fast and reversible trapping of surface glycine receptors by gephyrin. *Nat Neurosci,* **4,** 253-260.

Meier, J. and Grantyn, R. (2004) A gephyrin-related mechanism restraining glycine receptor anchoring at GABAergic synapses. *J Neurosci,* **24,** 1398-1405.

Meier, J. C., Henneberger, C., Melnick, I., Racca, C., Harvey, R. J., Heinemann, U., Schmieden, V. and Grantyn, R. (2005) RNA editing produces glycine receptor alpha3(P185L), resulting in high agonist potency. *Nat Neurosci,* **8,** 736-744.

Meyer, G., Kirsch, J., Betz, H. and Langosch, D. (1995) Identification of a gephyrin binding motif on the glycine receptor beta subunit. *Neuron,* **15,** 563-572.

Middlemas, D. S., Lindberg, R. A. and Hunter, T. (1991) trkB, a neural receptor protein-tyrosine kinase: evidence for a full-length and two truncated receptors. *Mol Cell Biol,* **11,** 143-153.

Miller, P. S., Harvey, R. J. and Smart, T. G. (2004) Differential agonist sensitivity of glycine receptor alpha2 subunit splice variants. *Br J Pharmacol,* **143,** 19-26.

Minichiello, L. (2009) TrkB signalling pathways in LTP and learning. *Nat Rev Neurosci,* **10,** 850-860.

Mollenhauer, H. H., Morre, D. J. and Rowe, L. D. (1990) Alteration of intracellular traffic by monensin; mechanism, specificity and relationship to toxicity. *Biochim Biophys Acta,* **1031,** 225-246.

Mori, M., Gahwiler, B. H. and Gerber, U. (2002) Beta-alanine and taurine as endogenous agonists at glycine receptors in rat hippocampus in vitro. *J Physiol,* **539,** 191-200.

Mudo, G., Jiang, X. H., Timmusk, T., Bindoni, M. and Belluardo, N. (1996) Change in neurotrophins and their receptor mRNAs in the rat forebrain after status epilepticus induced by pilocarpine. *Epilepsia,* **37,** 198-207.

Muller, E., Le Corronc, H., Triller, A. and Legendre, P. (2006) Developmental dissociation of presynaptic inhibitory neurotransmitter and postsynaptic receptor clustering in the hypoglossal nucleus. *Mol Cell Neurosci,* **32,** 254-273.

Muller, E., Le-Corronc, H. and Legendre, P. (2008) Extrasynaptic and postsynaptic receptors in glycinergic and GABAergic neurotransmission: a division of labor? *Front Mol Neurosci,* **1,** 3.

Mullis, K. B. (1990) The unusual origin of the polymerase chain reaction. *Sci Am,* **262,** 56-61, 64-55.

Nagaraja, T. N. and Brookes, N. (1996) Glutamine transport in mouse cerebral astrocytes. *J Neurochem,* **66,** 1665-1674.

Nagy, K., Marko, B., Zsilla, G. et al. (2010) Alterations in brain extracellular dopamine and glycine levels following combined administration of the glycine transporter type-1 inhibitor Org-24461 and risperidone. *Neurochem Res,* **35,** 2096-2106.

Nelson, D. L., Cox, M.M. (2000) *Lehninger Principles of Biochemistry*. 3rd Ed, Worth Publishers, U.S.A.

Nicholls, D. G. (2010) Stochastic aspects of transmitter release and bioenergetic dysfunction in isolated nerve terminals. *Biochem Soc Trans,* **38,** 457-459.

Nikolic, Z., Laube, B., Weber, R. G., Lichter, P., Kioschis, P., Poustka, A., Mulhardt, C. and Becker, C. M. (1998) The human glycine receptor subunit alpha3. Glra3 gene structure, chromosomal localization, and functional characterization of alternative transcripts. *J Biol Chem,* **273,** 19708-19714.

Noebels, J. L. (2003) The biology of epilepsy genes. *Annu Rev Neurosci,* **26,** 599-625.

Nong, Y., Huang, Y. Q., Ju, W., Kalia, L. V., Ahmadian, G., Wang, Y. T. and Salter, M. W. (2003) Glycine binding primes NMDA receptor internalization. *Nature,* **422,** 302-307.

Nunez, E., Lopez-Corcuera, B., Vazquez, J., Gimenez, C. and Aragon, C. (2000) Differential effects of the tricyclic antidepressant amoxapine on glycine uptake mediated by the recombinant GLYT1 and GLYT2 glycine transporters. *Br J Pharmacol,* **129,** 200-206.

Nunez, E., Alonso-Torres, P., Fornes, A., Aragon, C. and Lopez-Corcuera, B. (2008) The neuronal glycine transporter GLYT2 associates with membrane rafts: functional modulation by lipid environment. *J Neurochem,* **105,** 2080-2090.

Ohira, K., Shimizu, K. and Hayashi, M. (2001) TrkB dimerization during development of the prefrontal cortex of the macaque. *J Neurosci Res,* **65,** 463-469.

Ohira, K., Kumanogoh, H., Sahara, Y., Homma, K. J., Hirai, H., Nakamura, S. and Hayashi, M. (2005a) A truncated tropomyosin-related kinase B receptor, T1, regulates glial cell morphology via Rho GDP dissociation inhibitor 1. *J Neurosci,* **25,** 1343-1353.

Ohira, K., Shimizu, K., Yamashita, A. and Hayashi, M. (2005b) Differential expression of the truncated TrkB receptor, T1, in the primary motor and prefrontal cortices of the adult macaque monkey. *Neurosci Lett,* **385,** 105-109.

Ohira, K., Homma, K. J., Hirai, H., Nakamura, S. and Hayashi, M. (2006) TrkB-T1 regulates the RhoA signaling and actin cytoskeleton in glioma cells. *Biochem Biophys Res Commun,* **342,** 867-874.

Ohira, K., Funatsu, N., Homma, K. J., Sahara, Y., Hayashi, M., Kaneko, T. and Nakamura, S. (2007) Truncated TrkB-T1 regulates the morphology of neocortical layer I astrocytes in adult rat brain slices. *Eur J Neurosci,* **25,** 406-416.

Olivares, L., Aragon, C., Gimenez, C. and Zafra, F. (1995) The role of N-glycosylation in the targeting and activity of the GLYT1 glycine transporter. *J Biol Chem,* **270,** 9437-9442.

Palkovits, M., and Brownstein, M.J. (1983) *Microdissection of brain areas by the punch technique in: Brain Microdissection Techniques*. 1st Ed., Cuello A. C. MeElsevier, U.S.A.

Palkovits, M., Brownstein, M.J. (1988) *Maps and Guide to Microdissection of the Rat Brain*. 1st Ed., Elsevier Science Publishing, U.S.A.

Pang, P. T., Teng, H. K., Zaitsev, E. et al. (2004) Cleavage of proBDNF by tPA/plasmin is essential for long-term hippocampal plasticity. *Science,* **306,** 487-491.

Paradiso, B., Marconi, P., Zucchini, S. et al. (2009) Localized delivery of fibroblast growth factor-2 and brain-derived neurotrophic factor reduces spontaneous seizures in an epilepsy model. *Proc Natl Acad Sci U S A,* **106,** 7191-7196.

Parent, J. M. and Lowenstein, D. H. (2002) Seizure-induced neurogenesis: are more new neurons good for an adult brain? *Prog Brain Res,* **135,** 121-131.

Patapoutian, A. and Reichardt, L. F. (2001) Trk receptors: mediators of neurotrophin action. *Curr Opin Neurobiol,* **11,** 272-280.

Patterson, S. L., Grover, L. M., Schwartzkroin, P. A. and Bothwell, M. (1992) Neurotrophin expression in rat hippocampal slices: a stimulus paradigm inducing LTP in CA1 evokes increases in BDNF and NT-3 mRNAs. *Neuron,* **9,** 1081-1088.

Paxinos, G., and Watson, C. (1998) *The Rat Brain in Stereotaxic Coordinates*. 4th Ed., Academic Press, U.S.A.

Perea, G., Navarrete, M. and Araque, A. (2009) Tripartite synapses: astrocytes process and control synaptic information. *Trends Neurosci,* **32,** 421-431.

Peterson, G. L. (1979) Review of the Folin phenol protein quantitation method of Lowry, Rosebrough, Farr and Randall. *Anal Biochem,* **100,** 201-220.

Pfaffl, M. W. (2001) A new mathematical model for relative quantification in real-time RT-PCR. *Nucleic Acids Res,* **29,** e45.

Pfeiffer, F., Simler, R., Grenningloh, G. and Betz, H. (1984) Monoclonal antibodies and peptide mapping reveal structural similarities between the subunits of the glycine receptor of rat spinal cord. *Proc Natl Acad Sci U S A,* **81,** 7224-7227.

Phillips, H. S., Hains, J. M., Laramee, G. R., Rosenthal, A. and Winslow, J. W. (1990) Widespread expression of BDNF but not NT3 by target areas of basal forebrain cholinergic neurons. *Science,* **250,** 290-294.

Piechotta, K., Weth, F., Harvey, R. J. and Friauf, E. (2001) Localization of rat glycine receptor alpha1 and alpha2 subunit transcripts in the developing auditory brainstem. *J Comp Neurol,* **438,** 336-352.

Plotkin, M. D., Snyder, E. Y., Hebert, S. C. and Delpire, E. (1997) Expression of the Na-K-2Cl cotransporter is developmentally regulated in postnatal rat brains: a possible mechanism underlying GABA's excitatory role in immature brain. *J Neurobiol,* **33,** 781-795.

Polak, J. M., and Van Noorden, S. (1997) *Introduction to Immunocytochemistry*. Introduction to Immunocytochemistry, 2nd Ed., Bios Scientific Publishers, U.S.A.

Poyatos, I., Ponce, J., Aragon, C., Gimenez, C. and Zafra, F. (1997) The glycine transporter GLYT2 is a reliable marker for glycine-immunoreactive neurons. *Brain Res Mol Brain Res,* **49,** 63-70.

Pribilla, I., Takagi, T., Langosch, D., Bormann, J. and Betz, H. (1992) The atypical M2 segment of the beta subunit confers picrotoxinin resistance to inhibitory glycine receptor channels. *EMBO J,* **11,** 4305-4311.

Purves, D., Augustine, G.J., Fitzpatrick, D., Hall, W.C., LaMantia, A.S., McNamara, J.O. and White, L.E. (Editors) (2008) *Neuroscience*. 4th Ed, Sinauer Associates, Inc., U.S.A.

Raiteri, L., Stigliani, S., Usai, C., Diaspro, A., Paluzzi, S., Milanese, M., Raiteri, M. and Bonanno, G. (2008) Functional expression of release-regulating glycine transporters GLYT1 on GABAergic neurons and GLYT2 on astrocytes in mouse spinal cord. *Neurochem Int,* **52,** 103-112.

Rajendra, S., Lynch, J. W., Pierce, K. D., French, C. R., Barry, P. H. and Schofield, P. R. (1994) Startle disease mutations reduce the agonist sensitivity of the human inhibitory glycine receptor. *J Biol Chem,* **269,** 18739-18742.

Rees, M. I., Lewis, T. M., Kwok, J. B., Mortier, G. R., Govaert, P., Snell, R. G., Schofield, P. R. and Owen, M. J. (2002) Hyperekplexia associated with compound heterozygote mutations in the beta-subunit of the human inhibitory glycine receptor (GLRB). *Hum Mol Genet,* **11,** 853-860.

Rees, M. I., Harvey, K., Ward, H. et al. (2003) Isoform heterogeneity of the human gephyrin gene (GPHN), binding domains to the glycine receptor, and mutation analysis in hyperekplexia. *J Biol Chem,* **278,** 24688-24696.

Rees, M. I., Harvey, K., Pearce, B. R. et al. (2006) Mutations in the gene encoding GlyT2 (SLC6A5) define a presynaptic component of human startle disease. *Nat Genet,* **38,** 801-806.

Reichardt, L. F. (2006) Neurotrophin-regulated signalling pathways. *Philos Trans R Soc Lond B Biol Sci,* **361,** 1545-1564.

Romei, C., Di Prisco, S., Raiteri, M. and Raiteri, L. (2011) Glycine release provoked by disturbed Na(+), Na(+) and Ca(2)(+) homeostasis in cerebellar nerve endings: roles of Ca(2)(+) channels, Na(+)/Ca(2)(+) exchangers and GlyT2 transporter reversal. *J Neurochem,* **119,** 50-63.

Rose, C. R., Blum, R., Pichler, B., Lepier, A., Kafitz, K. W. and Konnerth, A. (2003) Truncated TrkB-T1 mediates neurotrophin-evoked calcium signalling in glia cells. *Nature,* **426,** 74-78.

Rousseau, F., Aubrey, K. R. and Supplisson, S. (2008) The glycine transporter GlyT2 controls the dynamics of synaptic vesicle refilling in inhibitory spinal cord neurons. *J Neurosci,* **28,** 9755-9768.

Roux, M. J. and Supplisson, S. (2000) Neuronal and glial glycine transporters have different stoichiometries. *Neuron,* **25,** 373-383.

Roux, P. P. and Barker, P. A. (2002) Neurotrophin signaling through the p75 neurotrophin receptor. *Prog Neurobiol,* **67,** 203-233.

Rudge, J. S., Mather, P. E., Pasnikowski, E. M., Cai, N., Corcoran, T., Acheson, A., Anderson, K., Lindsay, R. M. and Wiegand, S. J. (1998) Endogenous BDNF protein is increased in adult rat hippocampus after a kainic acid induced excitotoxic insult but exogenous BDNF is not neuroprotective. *Exp Neurol,* **149,** 398-410.

Ruiz-Gomez, A., Morato, E., Garcia-Calvo, M., Valdivieso, F. and Mayor, F., Jr. (1990) Localization of the strychnine binding site on the 48-kilodalton subunit of the glycine receptor. *Biochemistry,* **29,** 7033-7040.

Sagne, C., El Mestikawy, S., Isambert, M. F., Hamon, M., Henry, J. P., Giros, B. and Gasnier, B. (1997) Cloning of a functional vesicular GABA and glycine transporter by screening of genome databases. *FEBS Lett,* **417,** 177-183.

Sambrook, J., and Russell, D. (2001) *Molecular Cloning - a Laboratory Manual*. Cold Spring Harbor Laboratory Press, U.S.A.

Sarkisian, M. R. (2001) Overview of the Current Animal Models for Human Seizure and Epileptic Disorders. *Epilepsy Behav,* **2,** 201-216.

Sato, K., Yoshida, S., Fujiwara, K., Tada, K. and Tohyama, M. (1991) Glycine cleavage system in astrocytes. *Brain Res,* **567,** 64-70.

Saura, J. (2007) Microglial cells in astroglial cultures: a cautionary note. *J Neuroinflammation,* **4,** 26.

Scharfman, H. E., Goodman, J. H., Sollas, A. L. and Croll, S. D. (2002) Spontaneous limbic seizures after intrahippocampal infusion of brain-derived neurotrophic factor. *Exp Neurol,* **174,** 201-214.

Schnell, S. A., Staines, W. A. and Wessendorf, M. W. (1999) Reduction of lipofuscin-like autofluorescence in fluorescently labeled tissue. *J Histochem Cytochem,* **47,** 719-730.

Schonrock, B. and Bormann, J. (1995) Modulation of hippocampal glycine receptor channels by protein kinase C. *Neuroreport,* **6,** 301-304.

Sebastiao, A. M., Assaife-Lopes, N., Diogenes, M. J., Vaz, S. H. and Ribeiro, J. A. (2011) Modulation of brain-derived neurotrophic factor (BDNF) actions in the nervous system by adenosine A(2A) receptors and the role of lipid rafts. *Biochim Biophys Acta,* **1808,** 1340-1349.

Seidah, N. G., Benjannet, S., Pareek, S. et al. (1996) Cellular processing of the nerve growth factor precursor by the mammalian pro-protein convertases. *Biochem J,* **314 ( Pt 3),** 951-960.

Seiler, N. and Sarhan, S. (1984) Synergistic anticonvulsant effects of a GABA agonist and glycine. *Gen Pharmacol,* **15,** 367-369.

Shahar, A., Vellis, J., Vernadakis, A., and Haber, B. (Editors) (1989) *A Dissection and Tissue Culture Manual of the Nervous System*. 1st Ed., Alan R. Liss, Inc, U.S.A.

Shelton, D. L., Sutherland, J., Gripp, J., Camerato, T., Armanini, M. P., Phillips, H. S., Carroll, K., Spencer, S. D. and Levinson, A. D. (1995) Human trks: molecular cloning, tissue distribution, and expression of extracellular domain immunoadhesins. *J Neurosci,* **15,** 477-491.

Siegel, R., Agranoff, B., Albers, R.W. and Molinoff, P. (Editors) (1989) *Basic Neurochemistry – Molecular, Cellular and Medical Aspects*. 4th Ed., Raven Press, U.S.A.

Simonato, M., Tongiorgi, E. and Kokaia, M. (2006) Angels and demons: neurotrophic factors and epilepsy. *Trends Pharmacol Sci,* **27,** 631-638.

Singer, J. H., Talley, E. M., Bayliss, D. A. and Berger, A. J. (1998) Development of glycinergic synaptic transmission to rat brain stem motoneurons. *J Neurophysiol,* **80,** 2608-2620.

Smith, K. E., Borden, L. A., Hartig, P. R., Branchek, T. and Weinshank, R. L. (1992) Cloning and expression of a glycine transporter reveal colocalization with NMDA receptors. *Neuron,* **8,** 927-935.

Sofroniew, M. V. and Vinters, H. V. (2010) Astrocytes: biology and pathology. *Acta Neuropathol,* **119,** 7-35.

Sola, M., Bavro, V. N., Timmins, J. et al. (2004) Structural basis of dynamic glycine receptor clustering by gephyrin. *EMBO J,* **23,** 2510-2519.

Song, W., Chattipakorn, S. C. and McMahon, L. L. (2006) Glycine-gated chloride channels depress synaptic transmission in rat hippocampus. *J Neurophysiol,* **95,** 2366-2379.

Specht, C. G., Grunewald, N., Pascual, O., Rostgaard, N., Schwarz, G. and Triller, A. (2011) Regulation of glycine receptor diffusion properties and gephyrin interactions by protein kinase C. *EMBO J,* **30,** 3842-3853.

Spike, R. C., Watt, C., Zafra, F. and Todd, A. J. (1997) An ultrastructural study of the glycine transporter GLYT2 and its association with glycine in the superficial laminae of the rat spinal dorsal horn. *Neuroscience,* **77,** 543-551.

Stoilov, P., Castren, E. and Stamm, S. (2002) Analysis of the human TrkB gene genomic organization reveals novel TrkB isoforms, unusual gene length, and splicing mechanism. *Biochem Biophys Res Commun,* **290,** 1054-1065.

Strachan, T., and Read, A.P. (2004) *Human Molecular Genetics 3*. 3rd Ed., Garland Science Publishing, U.S.A.

Su, T. Z., Lunney, E., Campbell, G. and Oxender, D. L. (1995) Transport of gabapentin, a gamma-amino acid drug, by system l alpha-amino acid transporters: a comparative study in astrocytes, synaptosomes, and CHO cells. *J Neurochem,* **64,** 2125-2131.

Supplisson, S. and Bergman, C. (1997) Control of NMDA receptor activation by a glycine transporter co-expressed in Xenopus oocytes. *J Neurosci,* **17,** 4580-4590.

Takahashi, T., Momiyama, A., Hirai, K., Hishinuma, F. and Akagi, H. (1992) Functional correlation of fetal and adult forms of glycine receptors with developmental changes in inhibitory synaptic receptor channels. *Neuron,* **9,** 1155-1161.

Tanaka, T., Saito, H. and Matsuki, N. (1997) Inhibition of GABAA synaptic responses by brain-derived neurotrophic factor (BDNF) in rat hippocampus. *J Neurosci,* **17,** 2959-2966.

Tapley, P., Lamballe, F. and Barbacid, M. (1992) K252a is a selective inhibitor of the tyrosine protein kinase activity of the trk family of oncogenes and neurotrophin receptors. *Oncogene,* **7,** 371-381.

Tashiro, A. and Yuste, R. (2004) Regulation of dendritic spine motility and stability by Rac1 and Rho kinase: evidence for two forms of spine motility. *Mol Cell Neurosci,* **26,** 429-440.

Towbin, H., Staehelin, T. and Gordon, J. (1979) Electrophoretic transfer of proteins from polyacrylamide gels to nitrocellulose sheets: procedure and some applications. *Proc Natl Acad Sci U S A,* **76,** 4350-4354.

Triller, A., Cluzeaud, F., Pfeiffer, F., Betz, H. and Korn, H. (1985) Distribution of glycine receptors at central synapses: an immunoelectron microscopy study. *J Cell Biol,* **101,** 683-688.

Triller, A., Cluzeaud, F. and Korn, H. (1987) gamma-Aminobutyric acid-containing terminals can be apposed to glycine receptors at central synapses. *J Cell Biol,* **104,** 947-956.

Tsai, G., Lane, H. Y., Yang, P., Chong, M. Y. and Lange, N. (2004) Glycine transporter I inhibitor, N-methylglycine (sarcosine), added to antipsychotics for the treatment of schizophrenia. *Biol Psychiatry,* **55,** 452-456.

Tunnicliff, G. (2003) Membrane glycine transport proteins. *J Biomed Sci,* **10,** 30-36.

Turecek, R. and Trussell, L. O. (2001) Presynaptic glycine receptors enhance transmitter release at a mammalian central synapse. *Nature,* **411,** 587-590.

Ulbricht, W. (1998) Effects of veratridine on sodium currents and fluxes. *Rev Physiol Biochem Pharmacol,* **133,** 1-54.

Vandenberg, R. J., Shaddick, K. and Ju, P. (2007) Molecular basis for substrate discrimination by glycine transporters. *J Biol Chem,* **282,** 14447-14453.

Vargas-Medrano, J., Castrejon-Tellez, V., Plenge, F., Ramirez, I. and Miranda, M. (2011) PKCbeta-dependent phosphorylation of the glycine transporter 1. *Neurochem Int,* **59,** 1123-1132.

Vaz, S. H., Cristovao-Ferreira, S., Ribeiro, J. A. and Sebastiao, A. M. (2008) Brain-derived neurotrophic factor inhibits GABA uptake by the rat hippocampal nerve terminals. *Brain Res,* **1219,** 19-25.

Vaz, S. H., Jorgensen, T. N., Cristovao-Ferreira, S., Duflot, S., Ribeiro, J. A., Gether, U. and Sebastiao, A. M. (2011) Brain-derived neurotrophic factor (BDNF) enhances GABA transport by modulating the trafficking of GABA transporter-1 (GAT-1) from the plasma membrane of rat cortical astrocytes. *J Biol Chem,* **286,** 40464-40476.

Weiss, M. D., Derazi, S., Kilberg, M. S. and Anderson, K. J. (2001) Ontogeny and localization of the neutral amino acid transporter ASCT1 in rat brain. *Brain Res Dev Brain Res,* **130,** 183-190.

Weskamp, G. and Reichardt, L. F. (1991) Evidence that biological activity of NGF is mediated through a novel subclass of high affinity receptors. *Neuron,* **6,** 649-663.

Whittaker, V. P., Michaelson, I. A. and Kirkland, R. J. (1964) The separation of synaptic vesicles from nerve-ending particles ('synaptosomes'). *Biochem J,* **90,** 293-303.

Wilson, K., and Walker, J. (Editors) (2005) *Principles and Techniques of Biochemistry and Molecular Biology*. 6th Ed., Cambridge University Press, U.S.A.

Wu, Z. L., O'Kane, T. M., Connors, T. J., Marino, M. J. and Schaffhauser, H. (2008) The phosphatidylinositol 3-kinase inhibitor LY 294002 inhibits GlyT1-mediated glycine uptake. *Brain Res,* **1227,** 42-51.

Xu, T. L. and Gong, N. (2010) Glycine and glycine receptor signaling in hippocampal neurons: diversity, function and regulation. *Prog Neurobiol,* **91,** 349-361.

Xu, T. X., Gong, N. and Xu, T. L. (2005) Inhibitors of GlyT1 and GlyT2 differentially modulate inhibitory transmission. *Neuroreport,* **16,** 1227-1231.

Yacoubian, T. A. and Lo, D. C. (2000) Truncated and full-length TrkB receptors regulate distinct modes of dendritic growth. *Nat Neurosci,* **3,** 342-349.

Yang, Z., Taran, E., Webb, T. I. and Lynch, J. W. (2012) Stoichiometry and subunit arrangement of alpha1beta glycine receptors as determined by atomic force microscopy. *Biochemistry,* **51,** 5229-5231.

Yee, B. K., Balic, E., Singer, P. et al. (2006) Disruption of glycine transporter 1 restricted to forebrain neurons is associated with a procognitive and antipsychotic phenotypic profile. *J Neurosci,* **26,** 3169-3181.

Young-Pearse, T. L., Ivic, L., Kriegstein, A. R. and Cepko, C. L. (2006) Characterization of mice with targeted deletion of glycine receptor alpha 2. *Mol Cell Biol,* **26,** 5728-5734.

Young, A. B. and Snyder, S. H. (1973) Strychnine binding associated with glycine receptors of the central nervous system. *Proc Natl Acad Sci U S A,* **70,** 2832-2836.

Zafra, F., Aragon, C., Olivares, L., Danbolt, N. C., Gimenez, C. and Storm-Mathisen, J. (1995) Glycine transporters are differentially expressed among CNS cells. *J Neurosci,* **15,** 3952-3969.

Zhang, L. H., Gong, N., Fei, D., Xu, L. and Xu, T. L. (2008) Glycine uptake regulates hippocampal network activity via glycine receptor-mediated tonic inhibition. *Neuropsychopharmacology,* **33,** 701-711.

Zigmond, M. J., Bloom, F.E., Landis, S.C., Roberts, J.L. and Squire, L.R. (Editors) (1999) *Fundamental Neuroscience*. 1st Ed, Academic Press, U.S.A.

# 9. Appendix

Journal of Neurochemistry JNC

JOURNAL OF NEUROCHEMISTRY | 2011 doi: 10.1111/j.1471-4159.2011.07197.x

## Age-related changes of glycine receptor at the rat hippocampus: from the embryo to the adult

Rita I. Aroeira, Joaquim A. Ribeiro, Ana M. Sebastião and Cláudia A. Valente

*Institute of Pharmacology and Neurosciences, Faculty of Medicine, and Unit of Neurosciences, Institute of Molecular Medicine, University of Lisbon, Portugal*

**Abstract**

Glycinergic inhibitory transmission has been described in spinal cord, but rather disregarded in the brain. The spatial-temporal characterization of glycine receptors (GlyR) in the hippocampus over development is herein reported. GlyR expression increases from late embryonic stage (E18) to 7 days postnatal (P7) and decreases from P7 on. Quantitative real-time PCR showed that GlyR subunit expression changes over neuronal maturation with a preponderance of α2 and α3, over α1 and β. In immature stages, GlyR delineate the cell body of neurons at the Dentate Gyrus and Cornus Ammonis 1 and 3 (CA1/CA3) and are composed of α2 and α3 subunits. At P7, synaptic GlyRα2β can already be observed in the dendritic areas of Dentate Gyrus and of CA1/CA3. In the mature hippocampus, synaptic GlyR decrease and, although a few synaptic GlyRα1β can still be detected in the dendritic layers, extrasynaptic α2/α3-containing GlyR and somatic localized GlyRα3 are the most abundant. Our results point towards an important function of a slow tonic activation of extrasynaptic GlyR, over a fast phasic activation of synaptic GlyRα1β. We clearly show that GlyR are widely expressed in hippocampus and that their subcellular localization and subunit composition change over development.

**Keywords:** glycine receptor, rat hippocampus, subcellular localization, subunit composition.

*J. Neurochem.* (2011) 10.1111/j.1471-4159.2011.07197.x

In the CNS, GABA and glycine act as inhibitory neurotransmitters. Fast GABAergic neurotransmission predominates in all brain regions through activation of ionotropic $GABA_A$ receptors ($GABA_AR$). Glycine also mediates fast inhibitory transmission via ionotropic glycine receptors (GlyR), which predominate in the spinal cord and brainstem (Bowery and Smart 2006). GlyR form pentameric channels, composed by two different subunits, α and β (Langosch *et al.* 1988), permeable to $Cl^-$ ions. Several variants of α subunits (α1, α2, α3 and α4) have been described (Bowery and Smart 2006). In immature spinal cord neurons, it is consensual that α2 (49 kDa) is the abundant isoform, and GlyR are mostly α2 homomeric. The α1 (48 kDa) subunit dominates in the mature spinal cord neurons in association with β (58 kDa) subunit forming αβ heteromeric receptors (Becker *et al.* 1988). The β subunit is essential for the anchoring to gephyrin (Bowery and Smart 2006), a cytoplasmic protein necessary for synaptic localization of GlyR (Kirsch *et al.* 1991).

Glycine receptors expression in the hippocampus has been recognized by using electrophysiological (Chattipakorn and McMahon 2002), immunocytochemical (Brackmann *et al.* 2004; Lévi *et al.* 2004; Meier and Grantyn 2004), immunohistochemical (Danglot *et al.* 2004) and *in situ* hybridization approaches (Malosio *et al.* 1991). Work *in vivo* also demonstrated that intravenously injected glycine can depress seizure activity in an animal model of epilepsy (Cherubini *et al.* 1981), and can potentiate the anti-epileptic effects of $GABA_AR$ agonists (Seiler and Sarhan 1984). These observations, together with the recent discovery that patients with temporal lobe epilepsy show an altered GlyR expression in hippocampus (Eichler *et al.* 2008, 2009), suggest that these receptors could have a role in neurotransmission at the hippocampus. However, detailed information on the expres-

Received September 10, 2010; revised manuscript received/accepted January 19, 2011.

Address correspondence and reprint requests to Cláudia A. Valente, Unit of Neurosciences, Institute of Molecular Medicine, University of Lisbon, Av. Prof. Egas Moniz, 1649-028 Lisbon, Portugal.
E-mail: cvalentecastro@fm.ul.pt

*Abbreviations used*: CA, Cornus Ammonis; Ct, threshold cycle; DAPI, 4′,6-diamidino-2-phenylindole; DG, Dentate Gyrus; $GABA_AR$, $GABA_A$ receptors; GlyR, glycine receptors; P, postnatal day; PBS, phosphate buffered saline; PFA, paraformaldehyde; qPCR, quantitative real-time PCR; vGluT1, vesicular glutamate transporter 1; VIAAT, vesicular inhibitory amino acid transporter.

sion of these receptors, their subunit composition and subcellular localization in the hippocampus is still missing.

In the present study, we performed a spatial characterization of GlyR in the rat hippocampus over several developmental stages, late embryonic stage (E18) to 9 weeks after birth. To address this issue we evaluated total GlyR expression by western blot and assessed mRNA expression of α1, α2, α3 and β subunits by quantitative real-time PCR (qPCR). GlyR localization in the two main hippocampal areas, Dentate Gyrus (DG) and Cornus Ammonis (CA) was identified by confocal fluorescence immunohistochemistry.

We report here a 3- to 5-fold-increase in GlyR expression from E18 to 7 days postnatal (P7), followed by an age dependent decrease from P7 on, so that GlyR levels in adults are about those detected at E18. We also show that GlyR subcellular localization and subunit composition change over development. In immature stages (P7), extrasynaptic α1/α2/α3-containing GlyR are present in cell bodies rich layers surrounding the cell body, while synaptic and extrasynaptic α1/α2-containing GlyR were found in the dendritic layers. At this stage, many heteromeric GlyRα2β are localized in the dendrites and have a post-synaptic location, facing boutons positive for the vesicular inhibitory amino acid transporter (VIAAT), an inhibitory pre-synaptic marker. In the mature hippocampus, synaptic GlyRα2β decrease and more synaptic GlyRα1β emerge. However, extrasynaptic α2/α3-containing GlyR are the most abundant.

## Materials and methods

### Animals and tissue fixation

Sprague–Dawley rats, either male or female, were obtained from Harlan (Barcelona, Spain). All protocols complied with the current Portuguese Laws and with the European Union Directive 86/609/EEC on the protection of Animals used for Experimental and other scientific purposes.

Except otherwise indicated, pregnant females with 18 days of gestation (E18 embryos), P0–P21 (P0, P3, P7, P14 and P21) rats and adult rats (9 weeks old) were deeply anesthetized with 30% isoflurane in propylene glycol and decapitated. In all stages, the brain was quickly removed in ice cold phosphate buffered saline (PBS) (137 mM NaCl, 2.7 mM KCl, 8 mM $Na_2HPO_4.2H_2O$ and 1.5 mM $KH_2PO_4$, pH 7.4). The spinal cord from P21 rats was also isolated and kept in cold PBS.

For immunohistochemistry studies E18, P0 and P7 brains, as well as P21 spinal cords, were isolated as described above and fixed in 4% paraformaldehyde (PFA) in PBS for 1 week at room temperature (20–25°C). A shorter (48 h) fixation time was assayed but it did not allow proper fixation of non-superficial brain areas, including the hippocampus. For P14 onwards, brain immersion in 4% PFA for 1 week was not enough for proper fixation of deep brain structures, and therefore a fixation step by perfusion was carried out. Rats were deeply anesthetized with pentobarbital (Hikma, London, UK) (60 mg/kg body weight, i.p.) and intracardially perfused with PBS, then with 0.5% heparin in PBS (5000 U.I./mL) (B. Braun, Melsungen, Germany), and finally fixed with 4% PFA in PBS as described by others (Danglot *et al.* 2004; Muller *et al.* 2006). After perfusion brains were removed and further post-fixed by immersion in 4% PFA for 1 week at 20–25°C. Thus, fixation time was made comparable between all developmental stages and possible discrepancies (antibodies reactivity, and consequently, labelling pattern) which might arise from different fixation protocols, were minimised.

### Antibodies

For western blot experiments the primary antibodies used were: mouse monoclonal mAb4a anti-GlyR (Synaptic Systems, Goettingen, Germany, 1 mg/mL, 1 : 250), specific to all GlyR subunits and previously characterized (Pfeiffer *et al.* 1984), and rabbit polyclonal anti-alpha-tubulin (Abcam, Cambridge, UK, 0.5 mg/mL, 1 : 5000). The secondary antibodies used were goat anti-mouse and goat anti-rabbit, both IgG-horseradish peroxidase conjugated (Santa Cruz, Santa Cruz, CA, USA, 200 µg/0.5 mL, 1 : 5000).

For immunohistochemistry assays we also used monoclonal mAb4a anti-GlyR (Synaptic Systems, 1 mg/mL, 1 : 500). For specific detection of each GlyRα subunits, mouse monoclonal mAb2b anti-GlyRα1 (Synaptic Systems, 1 mg/mL, 1 : 250), rabbit polyclonal H-50 anti-GlyRα2 (Santa Cruz, 200 µg/mL, 1 : 250) and rabbit polyclonal anti-GlyRα3 (Millipore, Billerica, MA, USA, 0.5 mg/mL, 1 : 250) were used. Pre-synaptic inhibitory terminals were labelled with rabbit polyclonal anti-VIAAT (kindly provided by Dr. B. Gasnier, Paris, France, 1 : 200) and previously described (Dumoulin *et al.* 1999). For double staining of GlyRα subunits and the cytoplasmic post-synaptic protein gephyrin, two different antibodies against gephyrin were used. For double staining with GlyRα1, a rabbit polyclonal antibody (Synaptic Systems, 1 : 250, 1 mg/mL) against gephyrin was used. For double staining with GlyRα2 and GlyRα3, a mouse monoclonal mAb7a antibody against gephyrin (300 µL of hybridoma supernatant, lyophilized/300 µL, Synaptic Systems, 1 : 250) was employed. Pre-synaptic glutamatergic terminals were identified by immunolabelling with rabbit polyclonal anti-vesicular glutamate transporter 1 (vGluT1) (Synaptic Systems, 1 : 1000, 1 mg/mL). Microtubule associated protein was stained with mouse monoclonal AP20 anti-MAP2 (Chemicon, Temecula, CA, USA, 1 mg/mL, 1 : 500). Detection was performed with goat anti-mouse and goat anti-rabbit (Invitrogen, Grand Island, NY, USA, 2 mg/mL, 1 : 400) labelled with Alexa Fluor 568 and Alexa Fluor 488, respectively.

### Western blot

Hippocampi and spinal cords were isolated and washed in cold PBS, homogenized and solubilised in ristocetin-induced platelet agglutination buffer (50 mM Tris base pH 8, 1 mM EDTA, 0.1% sodium dodecyl sulfate, 150 mM NaCl and 1% NP40; Fluka Biochemika, Buchs, Switzerland), supplemented with protease inhibitors (Complete Mini-EDTA free from Roche, Mannheim, Germany), using a Potter homogenizer. The unsolubilized material was removed by centrifugation (11 000 *g*, 10 min, 4°C).

Soluble protein was quantified with Bio-Rad DC reagent (Peterson 1979). Proteins (70 µg/lane and 5 µg/lane for hippocampus and spinal cord homogenates, respectively) and protein size markers (Precision Plus Protein Standards from Bio-Rad) were separated by sodium dodecyl sulfate–polyacrylamide gel electrophoresis. After electrophoresis, samples were transferred to a

nitrocellulose membrane by electroblotting and blocked with 5% non-fat powder milk in TBS-T (20 mM Tris base, 137 mM NaCl and 0.1% Tween-20). Membranes were incubated with the primary antibodies and with the horseradish peroxidase-conjugated secondary antibodies. Immunoreactions were visualized with the ECL chemiluminescence detection system (Amersham-ECL Western Blotting Detection Reagents from GE Healthcare, Buckinghamshire, UK). The integrated intensity of each band was calculated using computer assisted-densitometry with ImageJ software 1.44b (http://rsbweb.nih.gov/ij/). The results were presented as the ratio (mean ± SEM) of GlyR immunoreactivity and α-tubulin normalized to E18. The statistical analysis was performed using ANOVA followed by Bonferroni's Multiple Comparison Test.

### Immunohistochemistry

Fixed tissues were dehydrated before paraffin embedding and coronal sections of spinal cord and brain (5 μm thickness) were cut using a microtome (Leica RM 2145, Wetzlar, Germany). Brain slices were obtained in an area corresponding to the stereotaxic coordinates (relative to bregma) between −5.20 and −5.60 mm (Paxinos and Watson 1998). Slices were deparaffined and the antigen recovery was performed with boric acid (0.02 M $H_3BO_3$ in 2 mM NaOH, pH 7) for 15 min at 95–100°C. Slices were then permeabilized (1% Triton X-100, 0.1% gelatin in PBS) for 10 min. For GlyR labelling with mAb4a, sections were subsequently immersed in methanol for 10 min at −20°C and washed with PBS. After blocking (0.25% gelatin in PBS for mAb4a, VIAAT, vGluT1 and MAP2 labelling and 10% fetal bovine serum in PBS for GlyR α1, α2 and α3 and gephyrin labelling) slices were incubated with the primary antibodies, 4°C overnight, and with the fluorescent-labelled secondary antibodies for 2 h at 20–25°C. Nuclei were stained with 4′,6-diamidino-2-phenylindole (DAPI) (Sigma, St. Louis, MO, USA, 1 : 15 000) and the sections were mounted in Mowiol (Sigma). In all experiments, specificity and absence of antibody cross-reaction were confirmed by omission of the primary antibodies.

### Quantitative analysis

The images were acquired with a frame size of 2048 × 2048 pixels on an inverted confocal laser scanning microscope (Zeiss LSM 510 META; Carl Zeiss AG, Weimar, Germany) using a PlanApochromat 63× oil-immersion objective (Carl Zeiss AG) with a numerical aperture of 1.40 (pixel size: 100 × 100 nm). DAPI fluorescence was detected with a 405 nm diode laser (30 mW nominal output) and a BP 420–480 nm filter. Alexa Fluor 488 fluorescence was detected using the 488 nm line of an Argon laser (45 mW nominal output) and a BP 500–550 nm filter. Alexa Fluor 568 was detected using a 561 nm DPSS laser (15 mW nominal output) and a LP 615 nm filter. The pinhole aperture was adjusted in each channel to achieve the same optical slice thickness for all channels (0.7 μm). For each group of triple labelling, all images were taken using the same excitation and acquisition settings for each channel. Fluorochromes were excited sequentially with multi-track frame imaging to eliminate any potential bleed-through. Images were obtain in DG, CA3 and CA1 hippocampal regions corresponding to the following stereotaxic coordinates (relative to the bregma): for DG lateral 2.5–3 mm and depth 3.8 mm; for CA3 lateral 4 mm and depth 7 mm and finally, for CA1 lateral 4 mm and depth 3 mm (Paxinos and Watson 1998).

Quantitative analysis was performed using in-house developed masks written for ImageJ software. For quantification of synaptic GlyR from immunohistochemistry images of mAb4a and VIAAT double staining (Figs 4 and 5), binary masks were created for both GlyR (red) and VIAAT (green) images using the same cut-off intensity threshold value for each staining, defined as the minimum intensity corresponding to specific staining above background values. GlyR and VIAAT were identified in each binary mask image using the Particle Analyzer function of ImageJ. For VIAAT apposition quantification, GlyR binary mask was dilated by 1 pixel (∼ 100 nm) all around. This value was chosen since distance between pre- and post-synaptic cell membranes is 20–40 nm (Kandel *et al.* 2000). GlyR clusters were considered synaptic if there was at least one pixel corresponding to a VIAAT puncta in the dilated GlyR mask. The percentage of synaptic GlyR clusters was then calculated from the total number of detected GlyR clusters.

Since mAb4a antibody recognizes all α subunits, another quantitative analysis was performed in immunohistochemistry images obtained from double staining of GlyR subunit specific antibody and gephyrin (Figs 6–8). The purpose was to evaluate co-localization rather than apposition so the GlyR binary mask dilation step was skipped in this analysis. Each staining in a double labelling image (GlyR subunit and gephyrin) was therefore subjected to the same intensity threshold cut-off, binary mask generation and particle analysis detection to identify clusters of GlyR and gephyrin. GlyR clusters were now considered synaptic if they had at least one pixel co-localized with gephyrin clusters. The results were presented as a percentage of synaptic GlyR from the total number of detected GlyR clusters. The same mask was used to evaluate co-localization between GlyR and glutamatergic nerve endings in immunohistochemistry images obtained from double staining of GlyR and vGluT1 (Fig. 10a). In this case, GlyR was considered present in a glutamatergic bouton if it had at least one pixel co-localizing with vGluT1. The results were presented as the percentage of GlyR-containing glutamatergic boutons over GlyR total number. All values (mean ± SEM) were statistically compared using Student's *t*-Test.

Images were prepared for printing using Illustrator (Adobe Systems, San Jose, CA, USA).

### RNA preparation

RNA was isolated from rat hippocampus and spinal cord homogenates (GE Healthcare RNAspin Mini RNA Isolation Kit). The integrity of total RNA was confirmed by gel electrophoresis. Synthesis of first-strand cDNA from 3 μg (for qPCR) of total RNA (in 20 μL) was carried out with the SuperScript II Reverse Transcriptase (EC 2.7.7.49, Invitrogen) according to the manufacturer's recommendations (SuperScript First Strand Synthesis Systems for RT-PCR from Invitrogen).

### RT–PCR

cDNA was amplified in a PCR reaction containing 0.8 μM of each oligonucleotide primer (Invitrogen), 0.05 mM of each dNTP (Promega, Madison, WI, USA), 1 mM $MgCl_2$ (Promega) and 0.2 units of Taq DNA polymerase (EC 2.7.7.7, Promega). The thermocycler (MyCycler – Bio-Rad, Hercules, CA, USA) profile was 2 min at 94°C, 25–40 cycles with 30 s at 94°C, 90 s at 60°C and 60 s at 72°C followed by a final elongation step of 15 min at

72°C. PCR products and DNA size markers (Hipperladder I from Bioline, London, UK) were separated in a 2% agarose gel with 0.4 μL/mL ethidium bromide and specific bands were detected with a digital camera (Kodak, Stuttgart, Germany).

To ensure that product amplification did not arise from genomic DNA, PCR reactions using cDNA synthesized in the absence of reverse transcriptase were also prepared.

### Quantitative real-time PCR

cDNA amplification was performed in a Rotor-Gene 6000 real-time rotary analyzer thermocycler (Corbett Life Science, Hilden, Germany) in the presence of SYBR Green Master Mix (Applied Biosystems, Foster City, CA, USA) and 0.2 μM of each specific gene primer. The PCR conditions included an initial denaturation for 2 min at 94°C, 50 cycles with 30 s at 94°C, 90 s at 60°C and 60 s at 72°C, followed by a melting curve to assess the specificity of the reactions. The threshold cycle (Ct) and the melting curves (Figure S1) were acquired with Rotor-Gene 6000 Software 1.7 (Corbett Life Science). To determine the relationship between Ct and mRNA levels, we performed calibration curves with 5-fold sequential dilutions of a cDNA with known concentration per each gene. The calibration curves were created by plotting Ct vs. the log concentration of cDNA, i.e. Ct vs. log cDNA (ng/μL), which allowed the calculation of cDNA initial concentration for each gene at each developmental stage. These curves also permit to determine PCR efficiency needed for the relative quantification by comparative Pfaffl method (Pfaffl 2001). The relative qPCR establishes the cDNA expression level by normalization with an internal control gene. Normalization of target gene expression is useful in order to compensate sample-to-sample and run-to-run variations and to ensure the experimental reliability. β-actin was used as a reference gene for normalization. For each gene, replica reactions were performed and the mean of the two reactions was used to calculate the corresponding expression level. Two types of negative controls, 'no reverse transcription' and 'no template', were run with samples.

In the case of the relative quantification, the statistical comparison was carried out using ANOVA followed by Bonferroni's Multiple Comparison Test.

### Oligonucleotides

The oligonucleotide primers used were: 5′-ACTCTGCGATTCTA-CCTTTGG-3′ and 5′-ATATTCATTGTAGGCGAGACGG-3′ for α1 subunit (Invitrogen); 5′-CAGAGTTCAGGTTCCAGGG-3′ and 5′-TCCACAAACTTCTTCTTGATAG-3′ for α2 subunit (Invitrogen) (Heck *et al.* 1996); 5′-GTGAGACACTTTCGGACACTAC-3′ and 5′-GATGGGTCGAGGTCTAATGAATC-3′ for α3 subunit (Invitrogen); 5′-CTGTTCATATCAAGCACTTTGC-3′ and 5′-GGGATG-ACAGGCTTGGCAG-3′ for β subunit (Invitrogen) (Heck *et al.* 1996); 5′-AGCCATGTACGTAGCCATCC-3′ and 5′-CTCTCAGC-TGTGGTGGTGAA-3′ for beta-actin (Invitrogen) (kindly provided by Dr. Tiago Outeiro, IMM, Lisbon, Portugal). The primers for GlyR α1 and α3 subunits were designed as follows: from the GenBank sequence database of the National Center for Biotechnology Information (http://www.ncbi.nlm.nih.gov/), mRNA sequence for GlyR α1 and α3 subunits from *Rattus norvegicus*, was obtained and used to create sequencing primers with OligoAnalyzer 3.1, provided by Integrated DNA Technologies (Coralville, IA, USA).

## Results

### GlyR expression in rat hippocampus

To evaluate total GlyR protein expression in rat hippocampus at different stages of development, a GlyR specific antibody (mAb4a), which has been fully characterized (Pfeiffer *et al.* 1984), was used for western blot analysis. GlyR expression in the hippocampus was evaluated at a late embryonic stage (E18), at P0 up to weaning (P3, P7, P14 and P21) and in adult (9 weeks old) rats. In all ages studied, mAb4a antibody identified a single band of 48–49 kDa, which corresponds to the molecular weight of GlyRα subunits (Fig. 1a). For comparison and internal control, spinal cord homogenates were also analysed. In this case, 14 times less protein was loaded and a very intense band was detected with mAb4a

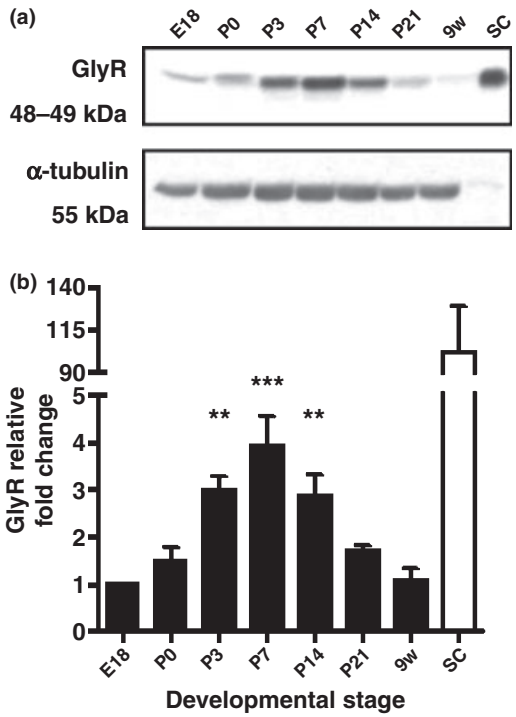


**Fig. 1** Expression of GlyR in rat hippocampus at different developmental stages. (a) Western blot analysis of GlyR (48–49 kDa) and α-tubulin (55 kDa) in rat hippocampal (70 μg) and spinal cord homogenates (5 μg). α-Tubulin was used as a loading control. The immunoreactive bands were detected on a 12% sodium dodecyl sulfate–polyacrylamide gel electrophoresis using mAb4a GlyR antibody. Homogenates were obtained from embryonic to 9-week-old rat hippocampus (E18, P0, P3, P7, P14, P21 and 9 weeks) and P21 spinal cord (SC). (b) Densitometry analysis of western blots ($n = 5$). The graph shows the ratio of GlyR immunoreactivity and α-tubulin normalized to E18. All values are mean ± SEM. $^{**}p < 0.01$, $^{***}p < 0.001$ as compared with E18 (one way ANOVA followed by Bonferroni's Multiple Comparison Test).

(Fig. 1a), which is in agreement with GlyR high expression in caudal regions of the CNS. No other band was detected indicating high mAb4a specificity for GlyRα subunits.

Densitometry analysis of western blots (Fig. 1b) revealed a 3- to 5-fold-increase in the expression of GlyR from the embryonic stage (E18) to 7 days postnatal (P7) ($n = 5$, $p < 0.01$). From P14 on, GlyR expression levels started to decrease, although at P14, expression was kept significantly higher than that detected at E18 ($n = 5$, $p < 0.01$). However, and as expected, GlyR expression in hippocampus is much lower than in spinal cord. These data reveal a clear developmentally regulated expression of GlyR in rat hippocampus and is in agreement with the expression pattern reported recently for pre-synaptic GlyR in hippocampal mossy fibers, using electrophysiological recordings (Kubota *et al.* 2010).

mRNA expression of the principal GlyR subunits namely, α1, α2, α3 and β, in rat hippocampus from E18 to postnatal stages, was studied by Reverse Transcriptase-PCR (Fig. 2a) with specific oligonucleotide primers. No PCR products were detected using cDNA synthesized in the absence of reverse transcriptase (−RT wells), which ensured that amplification did not arise from contaminating genomic DNA. These primers were also used in qPCR and no signal amplification was detected in the negative controls (data not shown), which indicated absence of genomic DNA, external contamination or other factors that could originate a non-specific increase in the fluorescence signal. The initial concentration of each transcript (GlyR subunits mRNA α1, α2, α3 and β) at each developmental stage is showed in Fig. 2(b) and the relative changes of each GlyR subunit mRNA, evaluated by relative qPCR, are shown in Fig. 3. It is clear that the proportion of GlyR subunits mRNA in hippocampus changes over development, but there is always a predominance of α2 and α3 over α1 and β subunits (Fig. 2b). Thus, GlyR in hippocampal neurons might be mainly composed of GlyR α2 and α3 subunits, while spinal cord neurons have a prevalence of GlyRα1, as reported by others (Malosio *et al.* 1991).

Glycine receptor α1 mRNA expression was very low at E18, but progressively increased during the first postnatal weeks (up to 20- to 30-fold), reaching a plateau level from P14 onwards (Fig. 3a). β mRNA subunit expression pattern (Fig. 3d) was similar to that of α1, but the increase in expression over development (about 10-fold from E18 to P14) was lower than the one observed in GlyRα1 mRNA expression. GlyRα2 expression was high in samples from early postnatal stages (P0 and P7); at P7, α2 mRNA levels increased by 1.8-fold from those detected at E18. From P14 on, GlyRα2 expression slightly decreased but even in adult rats (9 weeks old), α2 levels were not significantly lower ($p > 0.05$) than those detectable at E18 (Fig. 3b), in clear contrast with what has been reported for adult spinal cord neurons (Malosio *et al.* 1991). GlyRα3 mRNA levels were low at E18 and greatly increased (up to 20- to 30-fold) from E18 to P7 (Fig. 3c). From P14 onwards, GlyRα3 mRNA expression decreased as happens for GlyRα2 mRNA. However, in adult rats, GlyRα3 mRNA expression was still 8-fold higher than at E18, being about the same as detected at P0.

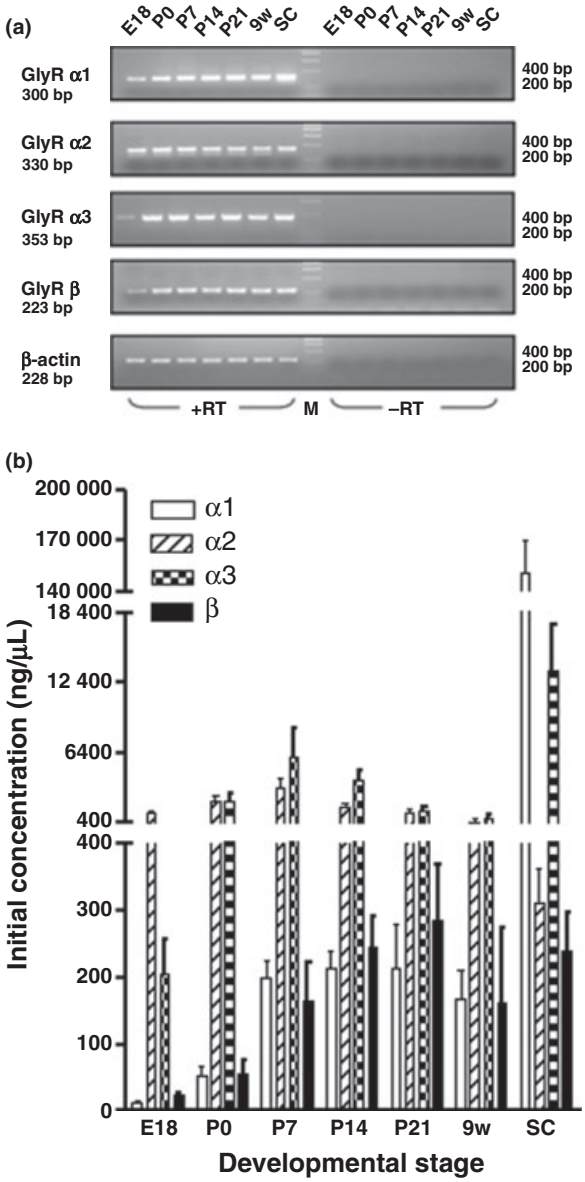


**Fig. 2** Expression of GlyR subunit mRNAs in rat hippocampus at different developmental stages (E18, P0, P7, P14, P21 and 9 weeks) and spinal cord (SC). (a) RT-PCR analysis of GlyR subunits (α1, α2, α3 and β) and β-actin in rat hippocampus. PCR products were detected on a 2% agarose gel. β-actin was used as a loading control. No PCR products were obtained using cDNA synthesized in the absence of RT (−RT wells). (b) Changes in initial concentration of GlyR subunits transcripts (α1, α2, α3 and β) in rat hippocampus.

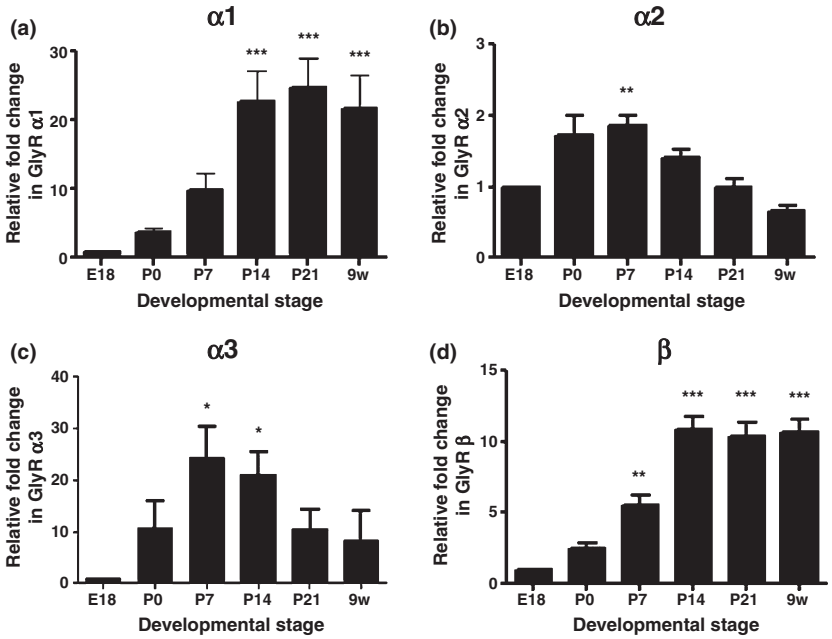


**Fig. 3** Composition analysis of GlyR subunit mRNAs in rat hippocampus at different developmental stages (E18, P0, P7, P14, P21 and 9 weeks) by relative qPCR. (a–d) Changes in GlyR subunits (α1, α2, α3 and β) mRNA expression levels. All values are mean ± SEM. $^{*}p < 0.05$, $^{**}p < 0.01$, $^{***}p < 0.001$ comparing with E18 ($n = 4$, one way ANOVA followed by Bonferroni's Multiple Comparison Test). Genes are indicated on top of each graph. Note the differences in scale between panels.

## Subcellular localization of GlyR and VIAAT in rat hippocampus

Analyses of coronal brain slices (5 μm) labelled with the nuclear marker DAPI revealed that at E18 it is not yet possible to distinguish between the main hippocampal areas and only the Ammon's horn is macroscopically delineated (Figure S2). At P7, it is already possible to completely identify the major hippocampal areas, namely DG and CA1/CA3. At this stage, it is possible to distinguish pyramidal cell nuclei in the *stratum pyramidale* of CA1/CA3 as well as granular cells distributed in *stratum granulosum* of DG. Interneurons in the *stratum radiatum* of CA1/CA3 areas and in the *stratum moleculare* of DG can also be visualized.

Glycine receptors subcellular localization in the rat hippocampus was investigated by confocal immunohistochemistry analysis of coronal brain slices (5 μm). Presynaptic glycine and/or GABA are packaged into synaptic vesicles via the common neurotransmitter transporter VIAAT, which is therefore located in both GABAergic and glycinergic terminals and can be used as a marker of all inhibitory pre-synaptic boutons, either GABAergic, glycinergic or mixed (Dumoulin *et al.* 1999). Therefore, a double staining with mAb4a and VIAAT antibodies, together with DAPI, allowed us to identify synaptic and extrasynaptic GlyR (Figs 4 and 5) localized in dendritic or cell bodies rich layers. A positive control was performed in slices from mature spinal cord in the same conditions (Figure S3). In the absence of the primary antibodies, no staining was observed (Figure S4) and therefore no autofluorescence signaling had to be taken into account.

The confocal images of each hippocampal area (DG, CA1 and CA3) were obtained from the delineated regions indicated in Fig. 4(a). In order to have a full characterization of GlyR expression within each area, each image covered two layers, one layer rich in cell bodies of pyramidal cells (*stratum granulosum* of DG and *stratum pyramidale* of CA1/CA3), and one layer rich in dendrites and cell bodies of interneurons (*stratum moleculare* of DG and *stratum radiatum* of CA1/CA3).

In the embryonic stage (E18), both mAb4a and VIAAT antibodies perfectly delineate the cell body (Fig. 4b). At this stage, we did not observe any juxtaposed mAb4a and VIAAT immunolabelling, which is an indicator of no synapse formation. At the neonatal stage (P0), GlyR clusters immunolabelling is mainly surrounding the cell body of granular and pyramidal cells, as well as the cell bodies of some interneurons (Fig. 4C1–C3), while VIAAT is restricted to the dendritic layers, namely *stratum moleculare* of DG and *stratum radiatum* of CA1/CA3, being strongly expressed close to the cell bodies of interneurons. However, at this stage a few synaptic GlyR are already detected in all hippocampal areas (Table 1), but with a higher proportion in DG.

At P7, somatic GlyR expression, in granular and pyramidal cells, decreases and immunolabelling start to be detected in the dendritic layers of the hippocampus (Fig. 4C4–C6). At this stage, GlyR clusters also delineate the soma of interneurons in *stratum moleculare* and *stratum radiatum* areas of the hippocampus, as indicated by arrowheads in Fig. 4(C4a–C6a). Several inhibitory GlyR-containing synapses could be detected at P7 (arrows in Fig. 4C4a–C6a), with a prevalence in DG (Table 1). These synapses, identified by the close apposition of GlyR and VIAAT labelling were found in dendrites and facing the soma of some

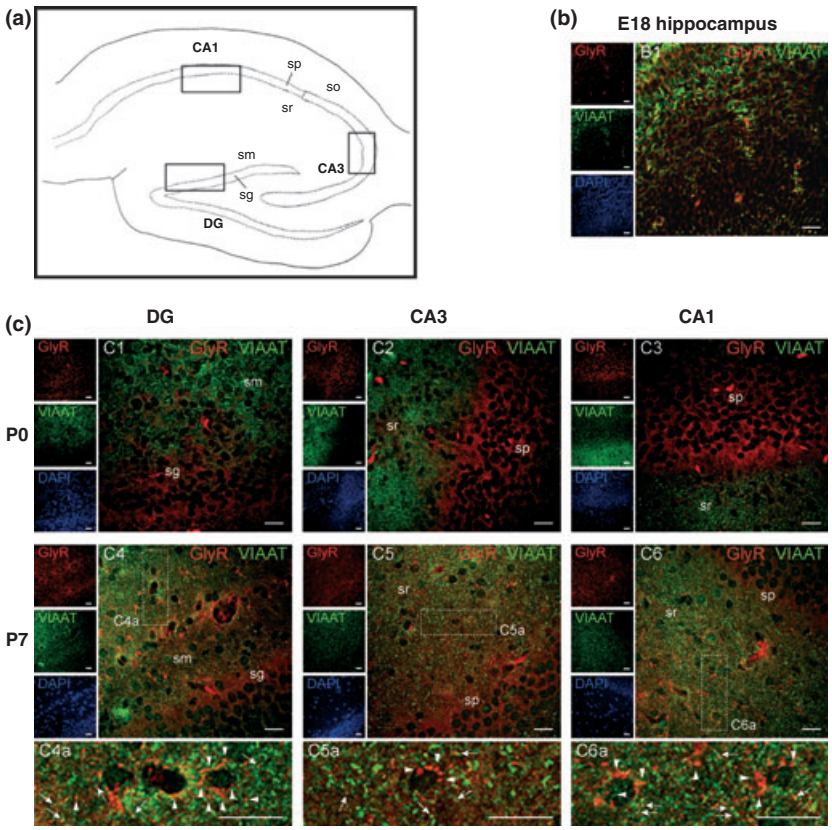


**Fig. 4** Synaptic and extrasynaptic localization of GlyR at early developmental stages. (a) Representation of the hippocampus (adapted from Andersen *et al.* 2007). The areas enclosed by the boxes show the regions where the confocal images were taken, namely Dentate Gyrus (DG) and Cornus Ammonis 1 and 3 (CA1 and CA3). Double detection of GlyR and VIAAT in rat hippocampus by confocal microscopy: (b) E18, (c) DG, CA3 and CA1 regions at P0 (C1–C3) and P7 (C4–C6). Panels (C4a–C6a) are magnifications of the boxed windows. The primary antibodies used were mouse monoclonal mab4a antibody anti-GlyR and rabbit polyclonal antibody anti-VIAAT. Small left panels represent each labelling alone: GlyR immunoreactivity is red and VIAAT containing terminals are green. Nuclei were stained with DAPI. Post-synaptic GlyR apposed to VIAAT positive terminals are indicated by arrows. Arrowheads point to GlyR extrasynaptic homomeric clusters. Confocal images were acquired with a 63× oil-immersion objective. Scale bars, 20 μm. sg, *stratum granulosum*; sm, *stratum moleculare*; so, *stratum oriens*; sp, *stratum pyramidale*; sr, *stratum radiatum*.

interneurons. Synaptic GlyR were restricted to the post-synaptic densities, since we did not observe a full co-localization between GlyR and VIAAT. Instead, we noticed a typical pre/post-synaptic apposition between VIAAT and GlyR clusters, as previously observed in the spinal cord (Dumoulin *et al.* 1999).

At P14, we detected less mAb4a labelling around the cell body of pyramidal cells in *stratum granulosum* of DG and *stratum pyramidale* of CA1/CA3, than in the previous developmental stages. On the other hand, at this stage, the number of GlyR-containing synapses was high (Table 1), being possible to distinguish many GlyR immunoreactive clusters apposed to VIAAT-positive boutons (arrows in Fig. 5A1a–A3a). Some GlyR clusters were spread along all dendritic regions, but not apposed to VIAAT-positive terminals therefore representing extrasynaptic GlyR (arrowheads in Fig. 5A1a–A3a). At this stage, VIAAT immunoreactivity was found in the cell body layers of DG and CA1/CA3 regions, as well as in the dendrites rich layers of these regions.

At P21 and 9-week-old rats (Fig. 5A4–A9), the DG *stratum moleculare* and the CA1/CA3 *stratum radiatum* are full with extrasynaptic GlyR clusters (arrowheads in Fig. 5A4a–A9a). In fact, the amount of synaptic GlyR (arrows in Fig. 5A4a–A9a) is decreased (Table 1). VIAAT-immunoreactivity is widely spread within all dendritic regions but not predominantly apposed to GlyR clusters. These VIAAT clusters label GABAergic terminals, as reported by others (Dumoulin *et al.* 1999), which are abundant in the adult hippocampus.

## Subcellular localization of GlyR subunits and gephyrin in rat hippocampus

Gephyrin, a cytoplasmic protein, is the core molecule for anchoring and stabilizing GlyR and $GABA_AR$ at inhibitory post-synaptic sites (Kirsch *et al.* 1993; Meier *et al.* 2001;

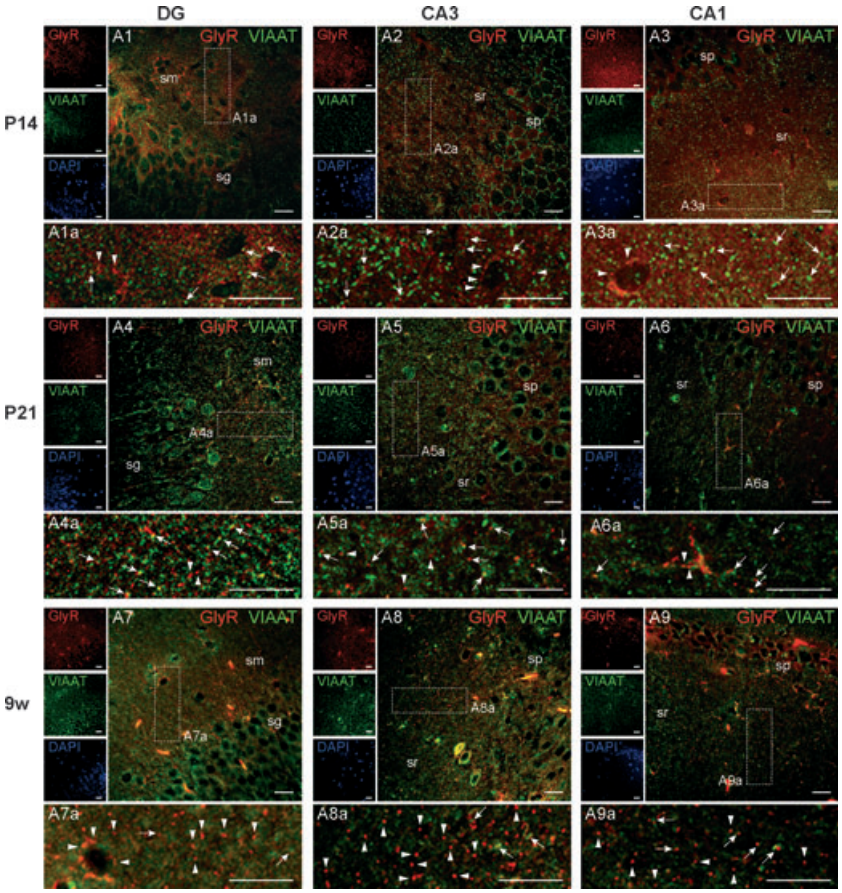


**Fig. 5** Synaptic and extrasynaptic localization of GlyR at late developmental stages. Double detection of GlyR and VIAAT in rat hippocampus by confocal microscopy in Dentate Gyrus (DG) and Cornus Ammonis 1 and 3 (CA1 and CA3) regions at P14 (A1–A3), P21 (A4–A6) and 9 weeks old (A7–A9). Panels (A1a–A9a) are magnifications of the boxed windows. The primary antibodies used were mouse monoclonal mab4a antibody anti-GlyR and rabbit polyclonal antibody anti-VIAAT. Small left panels represent each labelling alone: GlyR immunoreactivity is red and VIAAT containing terminals are green. Nuclei were stained with DAPI. Arrows indicate GlyR-containing synapses. Arrowheads point to GlyR extrasynaptic homomeric clusters. Confocal images were acquired with a 63× oil-immersion objective. Scale bars, 20 μm sg, *stratum granulosum*; sm, *stratum moleculare*; so, *stratum oriens*; sp, *stratum pyramidale*; sr, *stratum radiatum*.

**Table 1** Quantitative analysis of synaptic GlyR in rat hippocampal areas, Dentate Gyrus (DG) and Cornus Ammonis 1 and 3 (CA1 and CA3), and in spinal cord (SC), as achieved by juxtaposition of VIAAT and mAb4a immunolabelling

| | DG | | CA3 | | CA1 | | SC | |
|---|---|---|---|---|---|---|---|---|
| | Synaptic GlyR (%) | *n* | Synaptic GlyR (%) | *n* | Synaptic GlyR (%) | *n* | Synaptic GlyR (%) | *n* |
| P0 | 7.3 ± 1.8 | 17 786 | 2.4 ± 0.9 | 20 943 | 1.9 ± 1.3 | 18 847 | – | – |
| P7 | 15.9 ± 8.1 | 15 222 | 14.8 ± 9.9 | 13 142 | 14.6 ± 7.7 | 23 996 | – | – |
| P14 | 19.1 ± 7.9 | 18 426 | 15.9 ± 6.7 | 17 883 | 14.4 ± 8.1 | 21 552 | – | – |
| P21 | 7.8 ± 3.0 | 17 128 | 7.3 ± 2.1 | 20 269 | 7.1 ± 4.0 | 15 122 | 30.3 ± 1.7 | 37 754 |
| 9w | 6.7 ± 2.4 | 20 481 | 5.8 ± 2.4 | 21 707 | 3.8 ± 1.7 | 18 009 | – | – |

Slices were immunolabelled with mouse monoclonal mab4a antibody anti-GlyR and rabbit polyclonal antibody anti-VIAAT. The results represent the percentage of GlyR (mean ± SEM) with a synaptic localization. In each case, the total number (*n* = 100%) of counted GlyR is indicated.

Fritschy *et al.* 2008). Gephyrin, through binding to the β subunit, recruits GlyR to the post-synaptic membrane and therefore inhibitory GlyR-containing synapses always co-localize with gephyrin (Kirsch *et al.* 1991).

Hence, a double staining of GlyR subunits (GlyRα1, α2 and α3) and gephyrin, together with DAPI, was used to evaluate the subunit composition of synaptic and extrasynaptic GlyR in immature (P7) and mature neurons (P21).

The double staining of each of the GlyRα subunits and the cytoplasmic post-synaptic protein gephyrin show a predominance of extrasynaptic GlyR, which do not co-localize with gephyrin, in rat hippocampus (Figs 6–8, Table 2), in accordance with what was observed with the double labelling of mAb4a and VIAAT antibodies. At early postnatal stages (P7), GlyRα1 (Fig. 6A1–A3) and GlyRα2 (Fig. 7A1–A3) immunoreactivity was found in both dendritic and cell body rich layers. At this stage, it is possible to detect extrasynaptic

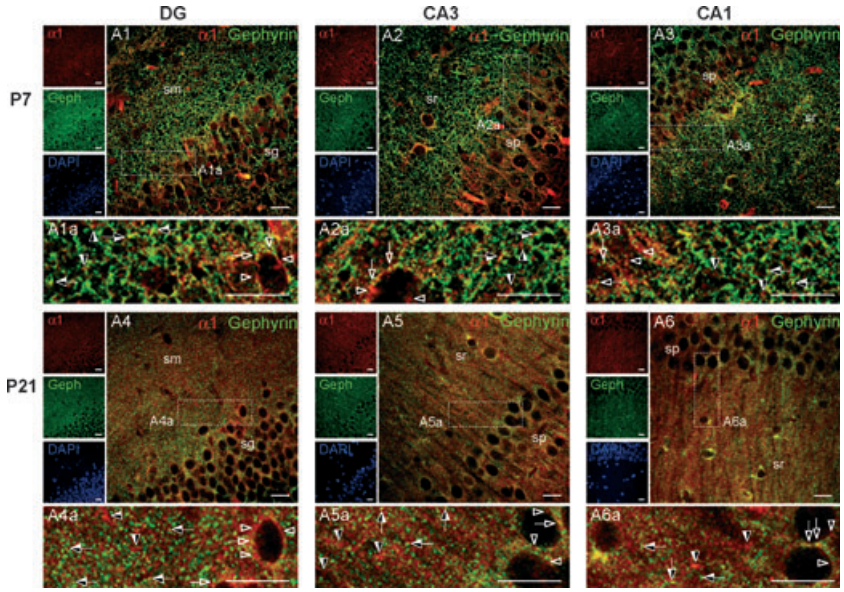


**Fig. 6** Synaptic and extrasynaptic localization of GlyRα1 subunit. Double detection of GlyRα1 and gephyrin in rat hippocampus by confocal microscopy, in Dentate Gyrus (DG) and Cornus Ammonis 1 and 3 (CA1 and CA3) regions, at P7 (A1–A3) and P21 (A4–A6). Panels A1a–A6a are magnifications of the boxed windows. The primary antibodies used were mouse monoclonal mAb2b antibody anti-GlyRα1 and rabbit polyclonal antibody anti-gephyrin. Small left panels represent each labelling alone: red for GlyRα1 and green for gephyrin. Nuclei were stained with DAPI. Examples of extrasynaptic GlyRα1 with a somatic localization (open arrowheads), extrasynaptic GlyRα1 with a dendritic localization (mid-open arrowheads), synaptic GlyRα1 with a somatic localization (open arrows) and synaptic GlyRα1 with a dendritic localization (mid-open arrows) are indicated in the magnified panels. Confocal images were acquired with a 63× oil-immersion objective. Scale bars, 20 μm. sg, *stratum granulosum*; sm, *stratum moleculare*; sp, *stratum pyramidale*; sr, *stratum radiatum*.

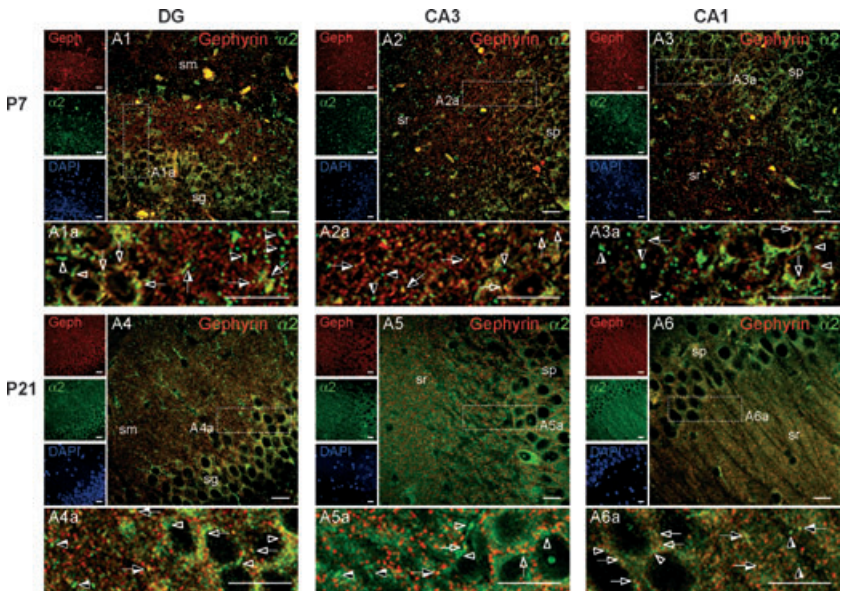


**Fig. 7** Synaptic and extrasynaptic localization of GlyRα2 subunit. Double detection of GlyRα2 and gephyrin in rat hippocampus by confocal microscopy in Dentate Gyrus (DG) and Cornus Ammonis 1 and 3 (CA1 and CA3) regions of the hippocampus at P7 (A1–A3) and P21 (A4–A6). Panels A1a–A6a are magnifications of the boxed windows. The primary antibodies used were rabbit polyclonal antibody anti-GlyRα2 and mouse monoclonal antibody anti-gephyrin. Small left panels represent each labelling alone: red for Gephyrin and green for GlyRα2. Nuclei were stained with DAPI. Examples of extrasynaptic GlyRα2 with a somatic localization (open arrowheads), extrasynaptic GlyRα2 with a dendritic localization (mid-open arrowheads), synaptic GlyRα2 with a somatic localization (open arrows) and synaptic GlyRα2 with a dendritic localization (mid-open arrows) are indicated in the magnified panels. Confocal images were acquired with a 63× oil-immersion objective. Scale bars, 20 μm. sg, *stratum granulosum*; sm, *stratum moleculare*; sp, *stratum pyramidale*; sr, *stratum radiatum*.

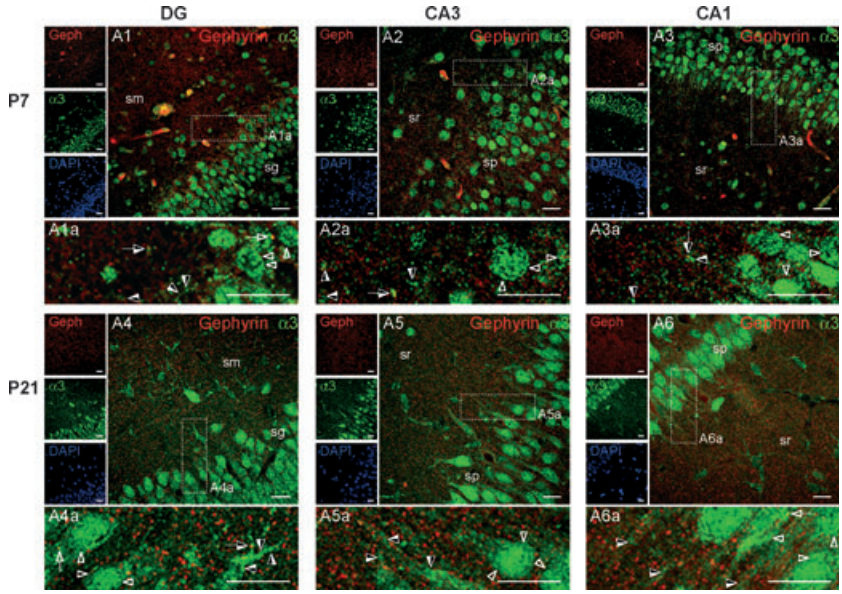


**Fig. 8** Synaptic and extrasynaptic localization of GlyRα3 subunit. Double detection of GlyRα3 and gephyrin in rat hippocampus by confocal microscopy in Dentate Gyrus (DG) and Cornus Ammonis 1 and 3 (CA1 and CA3) regions of the hippocampus at P7 (A1–A3) and P21 (A4–A6). Panels A1a–A6a are magnifications of the boxed windows. The primary antibodies used were rabbit polyclonal antibody anti-GlyRα3 and mouse monoclonal antibody anti-gephyrin. Small left panels represent each labelling alone: red for Gephyrin and green for GlyRα3. Nuclei were stained with DAPI. Examples of extrasynaptic GlyRα3 with a somatic localization (open arrowheads), extrasynaptic GlyRα3 with a dendritic localization (mid-open arrowheads), synaptic GlyRα3 with a somatic localization (open arrows) and synaptic GlyRα3 with a dendritic localization (mid-open arrows) are indicated in the magnified panels. Confocal images were acquired with a 63× oil-immersion objective. Scale bars, 20 μm. sg, *stratum granulosum*; sm, *stratum moleculare*; sp, *stratum pyramidale*; sr, *stratum radiatum*.

**Table 2** Localization and relative expression of GlyR subunits in immature and mature rat hippocampus

| GlyR subunit | Localization | Immature stage | | Mature stage | |
|---|---|---|---|---|---|
| | | Somatic | Dendritic | Somatic | Dendritic |
| GlyRα1 | Synaptic | + | + | – | ++ |
| | Extrasynaptic | + | + | + | ++ |
| GlyRα2 | Synaptic | +++ | ++ | + | – |
| | Extrasynaptic | + | + | ++ | +++ |
| GlyRα3 | Synaptic | – | – | – | – |
| | Extrasynaptic | ++ | + | +++ | ++ |

Relative expression levels were estimated by comparison of confocal images: (–), not detected; (+), low expression; (++), moderate expression; (+++), high expression. Somatic localization indicates that GlyR surround the cell body. Dendritic localization points to GlyR expression in dendrites.

α1/α2-containing GlyR (open/mid-open arrowheads in Fig. 6A1a–A3a and Fig. 7A1a–A3a) that do not co-localize with gephyrin and a few synaptic GlyR that contain mostly α2 subunits (open/mid-open arrows in Fig. 7A1a–A3a). Quantitative analysis of synaptic GlyR confirms a higher proportion of GlyRα2 in all hippocampal subregions (Fig. 9a–c). GlyRα3 (Fig. 8A1–A3) surrounds the cell body of granular cells in *stratum granulosum* of DG and pyramidal cells in *stratum pyramidale* of CA1/CA3, being hardly detected at inhibitory synapses (open/mid-open arrows in Fig. 8A1a–A3a, Table 2).

In the mature hippocampus (P21), GlyRα1 (Fig. 6A4–A6) and GlyRα2 (Fig. 7A4–A6) immunoreactivity is high in the dendritic regions of DG and CA areas, with a preponderance of GlyRα2 in the *stratum moleculare* of DG. In this area, extrasynaptic GlyRα2 perfectly delineates several dendrites (mid-open arrowheads in Fig. 7A4a). Some extrasynaptic GlyRα1 can also be observed (open/mid-open arrowheads in Fig. 6A4a). On the other hand, GlyRα3 (Fig. 8A4–A6) is still confined to the cell body containing layers. Nevertheless, at P21, GlyRα3 immunofluorescence is greatly increased in the dendritic regions of all hippocampal areas (mid-open arrowheads in Fig. 8A4a–A6a) as compared with the one found at P7. In the mature neurons, quantitative analysis (Fig. 9a–c) points to a significant ($p < 0.05$) decrease in synaptic GlyRα2 in all hippocampal areas. Therefore, at this stage the α subunit of the few synaptic GlyR is dominantly α1 (Fig. 9, Table 2). Furthermore, the expression of α2 and α3 transcripts is high (Fig. 2), which is in accordance with the occurrence of many extrasynaptic α2/α3-containing GlyR in the mature hippocampal neurons.

As a control, we also evaluated spinal cord mature neurons and confirmed (Figure S3B3) that synaptic GlyR are mainly GlyRα1 (Fig. 9d).

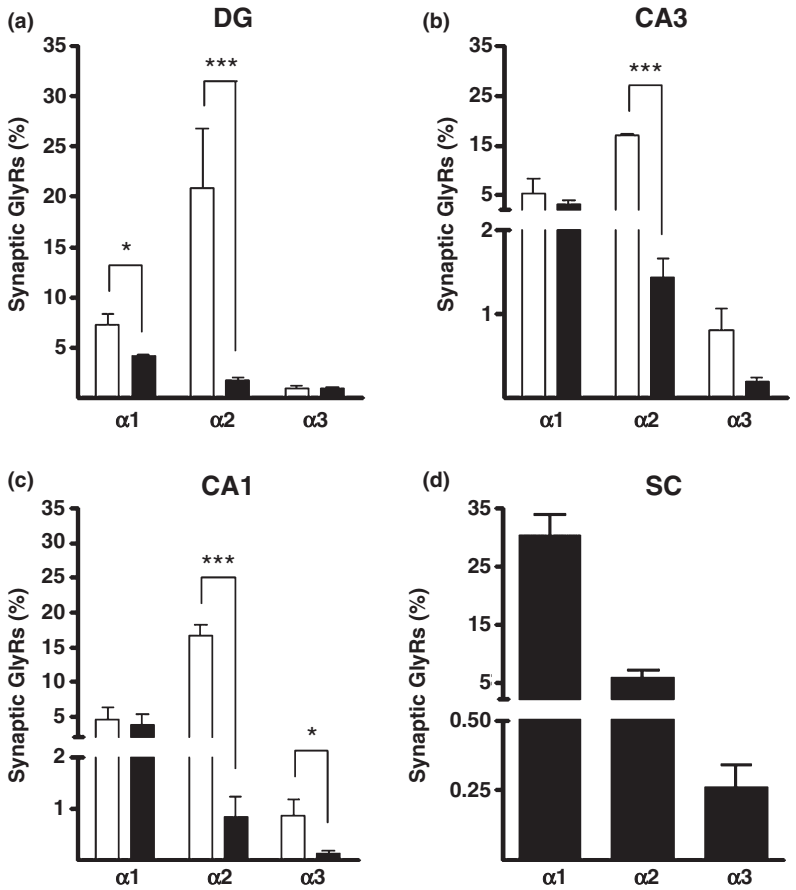


**Fig. 9** Quantitative analysis of synaptic GlyRα subunits in immature (□ P7) and mature (■ P21) neurons of Dentate Gyrus (a), Cornus Ammonis 3 (b), Cornus Ammonis 1 (c) and spinal cord (d). Synaptic GlyR α1, α2 and α3 were quantified upon double staining with mouse monoclonal mAb2b antibody anti-GlyRα1, rabbit polyclonal antibody anti-GlyRα2, rabbit polyclonal antibody anti-GlyRα3, respectively, and rabbit polyclonal or mouse monoclonal antibodies anti-gephyrin. All values are mean ± SEM, $^{*}p < 0.05$, $^{***}p < 0.001$ (unpaired *t*-Test between P7 and P21). The total number (*n*) of counted GlyR was 15 000 < *n* < 25 000 for each rat hippocampal area and 27 000 < *n* < 37 000 for spinal cord. Analyzed regions are indicated on top of each graph.

### Subcellular localization of GlyR and vGluT1 in rat hippocampus

To evaluate whether GlyR were present in glutamatergic boutons, as described recently for a particular splice variant of GlyRα3 (Eichler *et al.* 2009), we carried out a double staining with mAb4a and vGluT1 antibodies at P21 in all hippocampal areas (Fig. 10a) and, for comparison, in the mature spinal cord neurons (Figure S3C). vGluT1 immunoreactivity was found, as expected, mainly in DG *stratum moleculare* and CA1/CA3 *stratum radiatum* areas of the hippocampus but few GlyR co-localized with vGluT1 (asterisks in Fig. 10A1–A3). GlyR quantification confirmed the negligible expression (< 3.5%) of GlyR in glutamatergic nerve endings in both hippocampal and spinal cord mature neurons (Fig. 10b).

## Discussion

The data now reported clearly show that GlyR in the rat hippocampus are present from the embryo to the adult, and that their distribution in synaptic and extrasynaptic sites changes over development. GlyR expression reaches its maximum at 7 days postnatal (P7), where its expression is increased 3- to 5-fold as compared with a late embryonic stage (E18). In all developmental stages, the majority of GlyR are extrasynaptic and the highest density of synaptic GlyR is found at P7–P14.

Interestingly, there is a temporal correlation between the increase in GlyR expression detected in the first postnatal week with the well known changes in the expression pattern of the ion transporters that determine the direction of $Cl^-$ electrochemical gradient, $Na^+$-$K^+$-$2Cl^-$ co-transporter 1 and $K^+$-$Cl^-$ co-transporter 2. During the first postnatal week, the $Cl^-$ loader, $Na^+$-$K^+$-$2Cl^-$ co-transporter 1, is highly expressed (Plotkin *et al.* 1997), while the $Cl^-$ extruder, $K^+$-$Cl^-$ co-transporter 2 is weakly expressed (Clayton *et al.* 1998), so that glycine and GABA, through activation of the corresponding ligand-gated ion channel, cause membrane depolarization because of $Cl^-$ efflux. Thus, according to our results, GlyR seem to have a higher expression while mediating depolarization. As pointed out (Ben-Ari 2002), membrane depolarization because of activation of $Cl^-$ permeable ionotropic receptors in immature neurons is enough to remove $Mg^{2+}$ ions that are blocking NMDA receptors. At mature stages, the excitatory transmission via NMDA receptors surpasses the progressively declining depolarization mediated by $Cl^-$ permeable ionotropic receptors (Ben-Ari 2002) and, as we now show, at these stages the

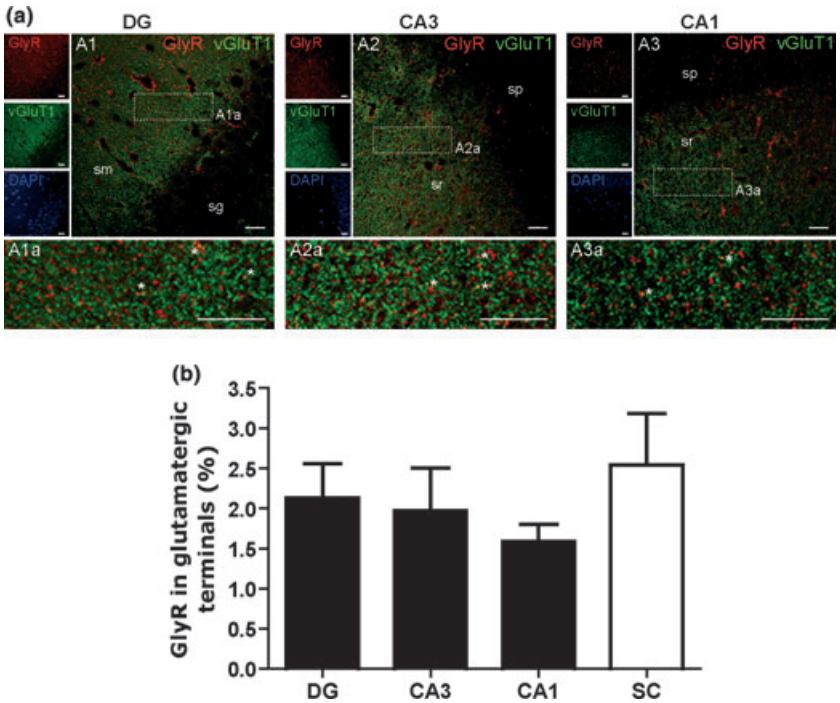


**Fig. 10** GlyR occurence in glutamatergic terminals. (a) Double detection of GlyR and vGluT1 in rat hippocampus by confocal microscopy in Dentate Gyrus (DG) and Cornus Ammonis 1 and 3 (CA1 and CA3) regions at P21 (A1–A3). Panels (A1a–A3a) are magnifications of the boxed windows. The primary antibodies used were mouse monoclonal mab4a antibody anti-GlyR and rabbit polyclonal antibody anti-vGluT1. Small left panels represent each labelling alone: GlyR immunoreactivity is red and glutamatergic terminals are green. Nuclei were stained with DAPI. Asterisks indicate GlyR presence in glutamatergic terminals. Confocal images were acquired with a 63× oil-immersion objective. Scale bars, 20 μm. sg, *stratum granulosum*; sm, *stratum moleculare*; so, *stratum oriens*; sp, *stratum pyramidale*; sr, *stratum radiatum*. (b) Quantitative analysis of GlyR in glutamatergic terminals. All values are mean ± SEM. The total number (*n*) of counted GlyR was 10 000 < *n* < 15 000 for each hippocampal area and 48 000 for spinal cord (SC).

expression of hippocampal GlyR decreases. We therefore hypothesize that GlyR are mostly required to provide a reinforcement of $Cl^-$ mediated depolarization in early stages of development and when that is no longer required, GlyR expression decreases by a still unknown mechanism. Interestingly, in newborn neurons (P0), GlyR (containing either α1, α2 or α3 subunits) perfectly delineate the cell bodies of granular cells of the *stratum granulosum* of DG and pyramidal cells of the *stratum pyramidale* of CA1/CA3 regions, being therefore in the appropriate position to reinforce excitatory inputs to glutamatergic neurons, allowing NMDA signaling, which is crucial for neuronal maturation (Ben-Ari 2002). These GlyR have a predominance of α2 and α3 over α1 and β subunits, since the expression of the α2 and α3 subunits was found to be much higher than that of α1 and β subunits. Synaptic GlyR include the β subunit, which directly binds to gephyrin, a cytosolic protein required for a regulated aggregation and post-synaptic clustering of these receptors (Kirsch *et al.* 1991; Meyer *et al.* 1995; Legendre 2001; Lévi *et al.* 2004; Meier and Grantyn 2004). At P0, β subunit expression is probably not enough to ensure gephyrin binding and therefore impairs GlyR synaptic targeting. At P7, we found that GlyR expression increases in *stratum moleculare* and *stratum radiatum* of DG and CA1/CA3 regions, areas where axons and dendrites are abundantly established. We also observed an increase in β subunit expression. Altogether these data correlate with a boost of synaptic, mostly heteromeric GlyRα2β, in the vicinity of inhibitory nerve endings positive for VIAAT, confirming a post-synaptic location, as described elsewhere for spinal cord neurons (Dumoulin *et al.* 1999). The pre-synaptic boutons are instructive for post-synaptic receptor accumulation (Dumoulin *et al.* 2000) and so, the now reported GlyR clustering facing a $VIAAT^+$ positive bouton is indicative of the occurrence of a glycine releasing terminal. Nevertheless, it has to be pointed out that, at least in the mature hypoglossal motoneurons, GlyR and $GABA_AR$ were found to co-aggregate in the same post-synaptic density, even though the ability of pre-synaptic terminals to release both neurotransmitters is lost during development (Muller *et al.* 2006). Whether some of the post-synaptic GlyR, here identified by VIAAT apposition, correspond to a functional glycinergic synapse that may have lost the ability to pre-synaptically release glycine, cannot be answered in

the present work. In the hippocampus, however, we emphasize that synaptic GlyR represent a less significant population than extrasynaptic ones, even at early developmental stages.

In the mature hippocampus (P21 on), there is a further decrease in total synaptic GlyR, and even a more pronounced decrease in synaptic GlyRα2. These findings, together with the occurrence of many extrasynaptic GlyR clusters, suggest that mature hippocampus contains a few synaptic GlyRα1β in the dendrites and many extrasynaptic α2/α3-containing GlyR that occur both in the dendrites and around the cell body of granular and pyramidal cells, as well as in interneurons.

The predominance of α2/α3-containing GlyR in the mature hippocampus is in accordance with previous results obtained from *in situ* hybridization studies, which used sequence specific oligonucleotide probes for GlyR subunits (Malosio *et al.* 1991), and it contrasts with the prevalence of GlyRα1 in spinal cord (Malosio *et al.* 1991) and brainstem motoneurons (Singer *et al.* 1998). Indeed, in immature caudal CNS neurons, extrasynaptic α2 homomeric GlyR are progressively replaced by synaptic α2β heteromeric GlyR and finally by synaptic α1β and α3β heteromeric GlyR in the mature neurons (Muller *et al.* 2008). GlyR are known to be able to move to post-synaptic loci (Meier *et al.* 2001; Dahan *et al.* 2003), which allows their role in fast phasic inhibition, whereas extrasynaptic receptors are probably tonically activated by spillover of neurotransmitter from the synaptic cleft or by non-synaptic glycine release, thus contributing to tonic inhibition (Muller *et al.* 2008; Zhang *et al.* 2008; Legendre *et al.* 2009). We hence propose that GlyR-mediated transmission in the mature hippocampus contribute to tonic inhibition via extrasynaptic α2/α3 containing homomeric receptors, being probably more relevant than the low expressed synaptic GlyRα1β. The molecular mechanisms responsible for the stabilization of extrasynaptic GlyR, or the mechanisms which allow them to diffuse to synaptic locus, are still unknown and require further studies.

Embryonic cortical neurons from GlyRα2 knockout mice are devoid of glycinergic transmission (Young-Pearse *et al.* 2006). As we show here, at early developmental stages most synaptic GlyR are heteromeric GlyRα2β. Interestingly, at later developmental stages (P7) GlyRα2 lacking neurons already respond to glycine, suggestive of a compensatory influence from other GlyR subunits (Young-Pearse *et al.* 2006). Indeed, our data corroborate these electrophysiological findings, showing an increase in the expression of other GlyR subunits, namely α1, from P7 onwards.

As expected, from P14 on, VIAAT labelling was found in the somatic layers, namely *stratum granulosum* of DG and *stratum pyramidale* of CA1/CA3 regions. This expression is related to the occurrence of axo-somatic inhibitory synapses, which are important to control the excitatory output of granular and pyramidal glutamatergic neurons, and start to be established during the second and third postnatal weeks, in accordance with previous data (Ben-Ari *et al.* 1989).

Although GlyR expression is detected in all hippocampal subregions, there is a higher expression within the *stratum granulosum* and the *stratum moleculare* of DG in all postnatal developmental stages analysed, which is in agreement with prior immunohistochemistry studies using adult rat hippocampus (Danglot *et al.* 2004; Eichler *et al.* 2009). DG is a vulnerable region to epileptic activity (Parent and Lowenstein 2002) and GABAergic transmission impairment in DG might be a cause of epilepsy (Dalby and Mody 2001). Earlier reports (Chattipakorn and McMahon 2003) stated that upon GABAergic transmission impairment, GlyR activation is able to inhibit bursting activity elicited in DG slices, unravelling a role for GlyR in epilepsy. In this work, we show that synaptic GlyR expression is higher in DG in all developmental stages, which might be related to the requirement of an additional or alternative inhibitory mechanism, such as GlyR-mediated inhibitory transmission, that might prove particularly relevant when GABAergic transmission fails.

In the mature rat hippocampal slices, functional GlyR were found in CA1 pyramidal cells in GABAergic interneurons and in DG neurons, where they are able to suppress excitability (Chattipakorn and McMahon 2002, 2003; Song *et al.* 2006). However, the role of GlyR in hippocampal synaptic transmission remains a controversial subject recently reviewed (Xu and Gong 2010).

In the present work, we have explored GlyR expression in rat hippocampus and identified spatial-temporal changes in GlyR distribution at the main hippocampal areas. Developmental changes in subunit composition of somatic, synaptic and extrasynaptic GlyR are also shown. Summarizing, at birth, GlyR expression is low, GlyR have mainly a somatic localization and are composed of α2 and α3 subunits, which could provide evidence for a potential role of GlyR in modulating hippocampal excitability at early postnatal stages. At P7, GlyR expression is higher and a few synaptic GlyR, mainly GlyRα2β, can be found. In the mature hippocampus, synaptic GlyRα2β decrease. At this stage, a few synaptic GlyRα1β and plenty of extrasynaptic GlyR α2/α3 can be detected which points towards a role of slow tonic activation of extrasynaptic GlyR α2/α3 in the mature hippocampus.

## Acknowledgements

The authors thank Dr. Bruno Gasnier (Paris) for generously supplying the antibody against VIAAT, Dr. Tiago Outeiro (Lisbon) for kindly supplying the oligonucleotide primers for β-actin and Dr. José Rino (Lisbon) for the development of the masks used in the quantitative analysis. This work was supported by Fundação para a Ciência e a Tecnologia (FCT), Portugal and by COST B30

(NEREPLAS) concerted action from EU. Rita I Aroeira is in receipt of a fellowship (SFRH/BD/62831/2009) from FCT.

The authors declare that this research was conducted in the absence of any commercial or financial relationships that could be construed as a potential conflict of interest.

## Supporting information

Additional supporting information may be found in the online version of this article:

**Figure S1.** Melting curves of GlyR subunits (α1, α2, α3 and β) and β-actin transcripts analyzed by qPCR.

**Figure S2.** Hippocampal cytoarchitecture changes by confocal microscopy over the developmental stages studied: E18, P0, P7, P14, P21 and 9-week-old rats.

**Figure S3.** Immunohistochemistry in rat spinal cord sections, laminae II of the ventral horn, by confocal microscopy.

**Figure S4.** Negative controls for immunohistochemistry in rat hippocampus (P21) sections by confocal microscopy.

As a service to our authors and readers, this journal provides supporting information supplied by the authors. Such materials are peer-reviewed and may be re-organized for online delivery, but are not copy-edited or typeset. Technical support issues arising from supporting information (other than missing files) should be addressed to the authors.

## References

Andersen P., Morris R., Amaral D., Bliss T. and O'Keefe J., eds (2007) *The Hippocampus Book*. Oxford University Press, USA.

Becker C. M., Hoch W. and Betz H. (1988) Glycine receptor heterogeneity in rat spinal cord during postnatal development. *EMBO J.* **7**, 3717–3726.

Ben-Ari Y. (2002) Excitatory actions of GABA during development: the nature of nurture. *Nat. Rev. Neurosci.* **3**, 728–739.

Ben-Ari Y., Cherubini E., Corradetti R. and Gaiarsa J. L. (1989) Giant synaptic potentials in immature rat CA3 hippocampal neurones. *J. Physiol. (Lond)* **416**, 303–325.

Bowery N. G. and Smart T. G. (2006) GABA and glycine as neurotransmitters: a brief history. *Br. J. Pharmacol.* **147**, S109–S119.

Brackmann M., Zhao C., Schmieden V. and Braunewell K. H. (2004) Cellular and subcellular localization of the inhibitory glycine receptor in hippocampal neurons. *Biochem. Biophys. Res. Commun.* **324**, 1137–1142.

Chattipakorn S. C. and McMahon L. L. (2002) Pharmacological characterization of glycine-gated chloride currents recorded in rat hippocampal slices. *J. Neurophysiol.* **87**, 1515–1525.

Chattipakorn S. C. and McMahon L. L. (2003) Strychnine-sensitive glycine receptors depress hyperexcitability in rat dentate gyrus. *J. Neurophysiol.* **89**, 1339–1342.

Cherubini E., Bernardi G., Stanzione P., Marciani M. G. and Mercuri N. (1981) The action of glycine on rat epileptic foci. *Neuroscience Lett.* **21**, 93–97.

Clayton G. H., Owens G. C., Wolf J. S. and Smith R. L. (1998) Ontogeny of cation-$Cl^-$ cotransporter expression in rat neocortex. *Dev. Brain Res.* **109**, 281–292.

Dahan M., Lévi S., Luccardini C., Rostaing P., Riveau B. and Triller A. (2003) Diffusion dynamics of glycine receptors revealed by single-quantum dot tracking. *Science* **302**, 442–445.

Dalby N. O. and Mody I. (2001) The process of epileptogenesis: a pathophysiological approach. *Curr. Opin. Neurol.* **14**, 187–192.

Danglot L., Rostaing P., Triller A. and Bessis A. (2004) Morphologically identified glycinergic synapses in the hippocampus. *Mol. Cell. Neurosci.* **27**, 394–403.

Dumoulin A., Rostaing P., Bedet C., Lévi S., Isambert M. F., Henry J. P., Triller A. and Gasnier B. (1999) Presence of the vesicular inhibitory amino acid transporter in GABAergic and glycinergic synaptic terminal boutons. *J. Cell Sci.* **112**, 811–823.

Dumoulin A., Lévi S., Riveau B., Gasnier B. and Triller A. (2000) Formation of mixed glycine and GABAergic synapses in cultured spinal cord neurons. *Eur. J. Neurosci.* **12**, 3883–3892.

Eichler S. A., Kirischuk S., Jüttner R., Schäfermeier P. K., Legendre P., Lehmann T. N., Gloveli T., Grantyn R. and Meier J. C. (2008) Glycinergic tonic inhibition of hippocampal neurons with depolarising GABAergic transmission elicits histopathological signs of temporal lobe epilepsy. *J. Cell Mol. Med.* **12**, 2848–2866.

Eichler S. A., Förstera B., Smolinsky B., Jüttner R., Lehmann T. N., Fähling M., Schwarz G., Legendre P. and Meier J. C. (2009) Splice-specific roles of glycine receptor α3 in the hippocampus. *Eur. J. Neurosci.* **30**, 1077–1091.

Fritschy J.-M., Harvey R. J. and Schwarz G. (2008) Gephyrin: where do we stand, where do we go? *Trends Neurosci.* **31**, 257–264.

Heck S., Enz R., Richter-Landsberg C. and Blohm D. H. (1996) Expression and mRNA splicing of glycine receptor subunits and gephyrin during neuronal differentiation of P19 cells in vitro, studied by RT-PCR and immunocytochemistry. *Dev. Brain Res.* **98**, 211–220.

Kandel E. R., Schwartz J. H. and Jessell T. M., eds (2000) *Principles of Neural Science*, 4th edn. McGraw-Hill, USA.

Kirsch J., Langosch D., Prior P., Littauer U. Z., Schmitt B. and Betz H. (1991) The 93-kDa glycine receptor-associated protein binds to tubulin. *J. Biol. Chem.* **266**, 22242–22245.

Kirsch J., Malosio M. L., Wolters I. and Betz H. (1993) Distribution of gephyrin transcripts in the adult and developing rat brain. *Eur. J. Neurosci.* **5**, 1109–1117.

Kubota H., Alle H., Betz H. and Geiger J. R. P. (2010) Presynaptic glycine receptors on hippocampal mossy fibers. *Biochem. Biophys. Res. Commun.* **393**, 587–591.

Langosch D., Thomas L. and Betz H. (1988) Conserved quaternary structure of ligand-gated ion channels: the postsynaptic glycine receptor is a pentamer. *Proc. Natl Acad. Sci. USA* **85**, 7394–7398.

Legendre P. (2001) The glycinergic inhibitory synapse. *Cell. Mol. Life Sci.* **58**, 760–793.

Legendre P., Forstera B., Juttner R. and Meier J. C. (2009) Glycine receptors caught between genome and proteome – functional implications of RNA editing and splicing. *Front. Mol. Neurosci.* **2**, 23.

Lévi S., Logan S. M., Tovar K. R. and Craig A. M. (2004) Gephyrin is critical for glycine receptor clustering but not for the formation of functional GABAergic synapses in hippocampal neurons. *J. Neurosci.* **24**, 207–217.

Malosio M. L., Marqueze-Pouey B., Kuhse J. and Betz H. (1991) Widespread expression of glycine receptor subunit mRNAs in the adult and developing rat brain. *EMBO J.* **10**, 2401–2409.

Meier J. and Grantyn R. (2004) A gephyrin-related mechanism restraining glycine receptor anchoring at GABAergic synapses. *J. Neurosci.* **24**, 1398–1405.

Meier J., Vannier C., Sergé A., Triller A. and Choquet D. (2001) Fast and reversible trapping of surface glycine receptors by gephyrin. *Nat. Neurosci.* **4**, 253–260.

Meyer G., Kirsch J., Betz H. and Langosch D. (1995) Identification of a gephyrin binding motif on the glycine receptor β subunit. *Neuron* **15**, 563–572.

Muller E., Le-Corronc H., Triller A. and Legendre P. (2006) Developmental dissociation of presynaptic inhibitory neurotransmitter and

postsynaptic receptor clustering in the hypoglossal nucleus. *Mol. Cell. Neurosci.* **32**, 254–273.

Muller E., Le-Corronc H. and Legendre P. (2008) Extrasynaptic and postsynaptic receptors in glycinergic and GABAergic neurotransmission: a division of labor? *Front. Mol. Neurosci.* **1**, 3.

Parent J. M. and Lowenstein D. H. (2002) Seizure-induced neurogenesis: are more new neurons good for an adult brain? *Prog. Brain Res.* **135**, 121–131.

Paxinos G. and Watson C. (1998) *The Rat Brain in Stereotaxic Coordinates*, 4th edn. Academic Press, San Diego, USA.

Peterson G. L. (1979) Review of the folin phenol protein quantitation method of Lowry, Rosebrough, Farr and Randall. *Anal. Biochem.* **100**, 201–220.

Pfaffl M. W. (2001) A new mathematical model for relative quantification in real-time RT-PCR. *Nucleic Acids Res.* **29**, 2002–2007.

Pfeiffer F., Simler R., Grenningloh G. and Betz H. (1984) Monoclonal antibodies and peptide mapping reveal structural similarities between the subunits of the glycine receptor of rat spinal cord. *Proc. Natl Acad. Sci. USA* **81**, 7224–7227.

Plotkin M. D., Snyder E. Y., Hebert S. C. and Delpire E. (1997) Expression of the Na-K-2Cl cotransporter is developmentally regulated in postnatal rat brains: a possible mechanism underlying GABA's excitatory role in immature brain. *J. Neurobiol.* **33**, 781–795.

Seiler N. and Sarhan S. (1984) Synergistic anticonvulsant effects of a GABA agonist and glycine. *Gen. Pharmacol.* **15**, 367–369.

Singer J. H., Talley E. M., Bayliss D. A. and Berger A. J. (1998) Development of glycinergic synaptic transmission to rat brain stem motoneurons. *J. Neurophysiol.* **80**, 2608–2620.

Song W., Chattipakorn S. C. and McMahon L. L. (2006) Glycine-gated chloride channels depress synaptic transmission in rat hippocampus. *J. Neurophysiol.* **95**, 2366–2379.

Xu T.-L. and Gong N. (2010) Glycine and glycine receptor signaling in hippocampal neurons: diversity, function and regulation. *Prog. Neurobiol.* **91**, 349–361.

Young-Pearse T. L., Ivic L., Kriegstein A. R. and Cepko C. L. (2006) Characterization of mice with targeted deletion of glycine receptor alpha 2. *Mol. Cell. Biol.* **26**, 5728–5734.

Zhang L. H., Gong N., Fei D., Xu L. and Xu T. L. (2008) Glycine uptake regulates hippocampal network activity via glycine receptor-mediated tonic inhibition. *Neuropsychopharmacology* **33**, 701–711.

Brain Struct Funct
DOI 10.1007/s00429-013-0537-3

ORIGINAL ARTICLE

# GlyT1 and GlyT2 in brain astrocytes: expression, distribution and function

**Rita I. Aroeira · Ana M. Sebastião · Cláudia A. Valente**

Received: 12 December 2012 / Accepted: 2 March 2013


**Abstract** GlyT1 and GlyT2 are the transporters responsible for glycine uptake from the synaptic cleft. The expression and function of these two glycine transporters in rat cortical cultured astrocytes over several maturation stages (10, 18 and 24 days in vitro) were herein investigated. Quantitative PCR and western blot showed that both GlyT1 and GlyT2 transcripts and protein were expressed in astrocytes in the examined maturation stages. Double detection of Glial fibrillary acidic protein (GFAP) and GlyT1/GlyT2 revealed that both transporters were detected in the cell body and in the processes of astrocytes. Furthermore, the double immunofluorescence analysis carried out in P21 rat brain slices corroborated the presence of both transporters in cortical and hippocampal astrocytes. The functional characterization of GlyT1 and GlyT2 in cultured astrocytes performed by [$^3$H]glycine uptake experiments revealed that both transporters take up glycine in a concentration-dependent way, but with a very distinct affinity. Kinetic analysis revealed a $K_m$ of 51.15 ± 4.96 μM and a $V_{max}$ of 379.30 ± 10.31 pmol/min/mg for GlyT1 and a $K_m$ of 1,801 ± 148.9 μM and a $V_{max}$ of 5,730 ± 200.2 pmol/min/mg for GlyT2. It is concluded that astrocytes express functional GlyT2, which challenge previous findings that those cells would express only GlyT1, whereas GlyT2 was supposed to be restricted to the glycinergic nerve terminals. Therefore, the work herein reported provides new insights about glycinergic neurotransmission in the brain.

**Keywords** Glycine transporter 1 · Glycine transporter 2 · Astrocytes · Brain · Glycine uptake · Inhibitory neurotransmission

## Introduction

GABA and glycine are the main inhibitory neurotransmitters in the central nervous system (CNS). GABA predominates in brain inhibitory synapses, while glycine acts as a major inhibitory neurotransmitter in the caudal regions of the CNS, activating the strychnine-sensitive glycine receptors (GlyR) (Bowery and Smart 2006).

At glycinergic synapses, termination of glycine-mediated synaptic activity occurs through removal of the neurotransmitter from the synaptic cleft, by specific $Na^+$/$Cl^-$-dependent glycine transporters (GlyT) present in the plasma membrane of pre-synaptic nerve endings and in astrocytes (Eulenburg et al. 2005). Until now, two GlyT have been identified, GlyT1 (Guastella et al. 1992) and GlyT2 (Liu et al. 1992), sharing about 50 % of amino acid sequence homology but displaying different pharmacology (Dohi et al. 2009). Both GlyT are present in several isoforms generated by alternative splicing and the use of alternative promoters (Adams et al. 1995; Ebihara et al. 2004). By in situ hybridization, GlyT1 expression was detected in most brain areas, while GlyT2 was observed in spinal cord and brainstem (Borowsky et al. 1993). Furthermore, GlyT2 protein distribution reproduces the distribution of GlyR, the postsynaptic component of the glycinergic synapse (Jursky et al. 1994; Jursky and Nelson

**Electronic supplementary material** The online version of this article (doi:10.1007/s00429-013-0537-3) contains supplementary material, which is available to authorized users.

R. I. Aroeira · A. M. Sebastião · C. A. Valente (✉)
Institute of Pharmacology and Neurosciences,
Faculty of Medicine, and Unit of Neurosciences,
Institute of Molecular Medicine, University of Lisbon,
Av. Prof. Egas Moniz, 1649-028 Lisbon, Portugal
e-mail: cvalentecastro@fm.ul.pt

Published online: 26 March 2013

1995; Zafra et al. 1995), being present in a lesser extent in the brain than GlyT1 (Jursky and Nelson 1996).

It is widely accepted that GlyT1 is mainly expressed in astrocytes, while GlyT2 is predominantly expressed in glycinergic nerve terminals (Eulenburg et al. 2005). However, recent studies (Raiteri et al. 2008), which described the presence of GlyT2 in purified preparations of mouse spinal cord astrocyte-derived subcellular particles, named gliosomes, challenged this knowledge. Whether GlyT2 is also present in brain astrocytes, where glycinergic transmission represents a minor proportion of the inhibitory transmission, is still unknown.

It is known that GlyT have distinct functions at glycinergic synapses according to its localization. Glial GlyT1 ensures the removal of glycine from the synaptic cleft leading to the termination of glycine-mediated neurotransmission, while neuronal GlyT2 ensures the refilling of presynaptic vesicles of glycinergic neurons (Gomeza et al. 2003a, b). In addition, GlyT1 is also present in glutamatergic neurons and regulates the concentration of glycine at excitatory synapses containing *N*-methyl-D-aspartate (NMDA) receptors, known to require glycine as a co-agonist (Eulenburg et al. 2005; Betz et al. 2006). Therefore, GlyT1 mediates both the clearance of glycine from the synaptic cleft of inhibitory synapses and participates in the regulation of glycine concentration at excitatory synapses.

Alterations in glycine-mediated neurotransmission were also reported in several pathologies including neuropathic pain, schizophrenia (Dohi et al. 2009), hyperekplexia (Rees et al. 2006) and hyperexcitability-related diseases (Harvey et al. 2008; Eichler et al. 2008). Several authors point out the physiological relevance of the regulation of glycine concentration in the synaptic cleft and consider GlyT as an alternative therapeutic target for the treatment of these disorders (Eulenburg et al. 2005). Furthermore, impairments in astrocytic function are increasingly being recognized as an important contributor to neuronal dysfunction. Astrocytes are no longer regarded as simple supportive cells for neurons, being considered as the third element of a structure known as "tripartite synapse" (Araque et al. 1999; Perea et al. 2009). Astrocytes play a pivotal role in brain homeostasis through several cooperative metabolic processes that they establish with neurons, such as energy supply and neurotransmitter recycling functions (Allaman et al. 2011). At the synapse, astrocytes can be stimulated by released neurotransmitters, which cause intracellular $Ca^{2+}$ elevations and trigger gliotransmitter release (such as ATP, D-serine and glutamate), that in turn regulate synaptic transmission and plasticity (Hamilton and Attwell 2010).

Recently, GlyR characterization in the hippocampus over several developmental stages was carried out (Aroeira et al. 2011). These results together with the previous evidence for the relevance of astrocytes to control neuronal function (Perea et al. 2009; Hamilton and Attwell 2010) lead us to evaluate the expression and function of GlyT in astrocytes. We demonstrate that GlyT2, and not only GlyT1, is expressed and functionally active in brain astrocytes.

## Materials and methods

### Animals

Sprague–Dawley rats were acquired from Harlan (Barcelona, Spain). All experimental procedures were in accordance with the current Portuguese laws and with the European Union Directive (86/609/EEC) on the protection of animals used for experimental and other scientific purposes. All efforts were made to minimize animal suffering and to use the minimum number of animals.

### Reagents and drugs

Unless stated otherwise, all reagents were purchased from Sigma (St. Louis, MO, USA). [$^3$H]glycine (specific activity 44.7 Ci/mmol) was from PerkinElmer (Waltham, MA, USA). Org 24598, a specific GlyT1 inhibitor (Brown et al. 2001), ALX 1393 (Luccini and Raiteri 2007) and amoxapine (Núñez et al. 2000), two specific GlyT2 inhibitors, were also purchased from Sigma.

### Antibodies

For western blot, the primary antibodies used were rabbit polyclonal anti-GlyT1/GlyT2 (kindly provided by Dr. Manuel Miranda-Arango, Texas, USA, 1:1,000) and rabbit polyclonal anti-β-actin (Abcam, Cambridge, UK, 0.32 mg/ml, 1:10,000).

The secondary antibodies used were goat anti-mouse and goat anti-rabbit, both IgG-horseradish peroxidase conjugated (Santa Cruz, Santa Cruz, CA, USA, 200 µg/0.5 ml, 1:5,000).

The primary antibodies used in immunofluorescence were rabbit antibody anti-GlyT1/GlyT2 (Alpha Diagnostic Intl. Inc., San Antonio, TX, USA, 1 mg/ml; 1:20), mouse monoclonal antibody anti-GFAP, clone GA5, a known marker for differentiated astrocytes (Millipore, Billerica, MA, USA, 1:500) and mouse monoclonal AP20 anti-Microtubule Associated Protein 2 (MAP2) (Chemicon, Temecula, CA, USA, 1 mg/ml, 1:500), a neuronal marker.

The secondary fluorescent-labeled antibodies used were goat anti-rabbit-Alexa 568 and goat anti-mouse-Alexa 488 (Invitrogen, Grand Island, NY, USA, 2 mg/ml, 1:400).

## Primary cultures of astrocytes

Astrocytes-enriched cultures were prepared from the cerebral cortex of newborn rat pups (0–2 days old), as previously reported (Biber et al. 1997; Vaz et al. 2011). Briefly, the animals were sacrificed by decapitation and the brain was quickly dissected in ice cold phosphate buffered saline (PBS) (137 mM NaCl, 2.7 mM KCl, 8 mM $Na_2HPO_4.2H_2O$ and 1.5 mM $KH_2PO_4$, pH 7.4). Following meninges and white matter removal, the cerebral cortex was isolated. Cells were vigorously dissociated in 4.5 g/l glucose Dulbecco's modified eagles medium (DMEM) (Gibco, Paisley, UK), medium supplemented with 10 % fetal bovine serum (FBS) (Gibco) and 1 % antibiotic/antimycotic, filtered through a 230-µm cell strainer and centrifuged at 200*g* for 10 min at room temperature (RT). The pellet was ressuspended in 4.5 g/l glucose DMEM, filtered through a 70-µm cell strainer (BD Falcon, NJ, USA) and centrifuged again. Cells were seeded into 60-mm dishes for western blot and quantitative PCR (qPCR). For immunocytochemistry (ICC) assays, cells were plated on poly-D-lysine hydrobromide (PDL) (10 µg/ml)-coated coverslips at a density of 100 000 cells/well. For uptake assays cells were seeded in 24-well plates. Cultures were maintained in an incubator with a humidified atmosphere (5 % $CO_2$) at 37 °C for 3–4 weeks and medium was renewed twice a week.

In order to further purify the cultures from any contaminating microglia cells (McCarthy and de Vellis 1980; Gabryel et al. 2002; Gingras et al. 2007; Du et al. 2010), at 9 DIV the plates were shaken overnight on an orbital shaker at 300 rpm.

## qPCR

RNA was extracted from astrocytes-enriched cultures (GE Healthcare RNAspin Mini RNA Isolation Kit). Total RNA integrity was confirmed by gel electrophoresis and 3 µg of total RNA (in 20 µl) was used to synthesize the first-strand cDNA with the SuperScript II Reverse Transcriptase (EC 2.7.7.49, Invitrogen) according to the manufacturer's guidelines (SuperScript First Strand Synthesis Systems for RT-PCR from Invitrogen).

cDNA amplification was carried out in a Rotor-Gene 6000 real-time rotary analyzer thermocycler (Corbett Life Science, Hilden, Germany) as previously described (Aroeira et al. 2011). In brief, the reactions took place in the presence of SYBR Green Master Mix (Applied Biosystems, Foster City, CA, USA) and 0.2 µM of each specific gene primers. PCR parameters included an initial denaturation step for 2 min at 94 °C and 50 cycles with 30 s at 94 °C, 90 s at 60 °C and 60 s at 72 °C. Reaction specificity was evaluated in all assays by a melting curve.

The threshold cycle (Ct) and the melting curves required for the relative quantification (Pfaffl 2001) were acquired with Rotor-Gene 6000 Software 1.7 (Corbett Life Science). β-actin was used as the reference internal standard. Replica reactions were always performed for each gene and negative controls, such as "no reverse transcription" and "no template", were also carried out. For the relative quantification, the statistical analysis was accomplished using ANOVA followed by Bonferroni's Multiple Comparison Test.

The primers (all from Invitrogen) used were: 5′-CTGG AGGCTGTATGTGCTGA-3′ and 5′-GATGACGAAGCC AGCATAGA-3′ for GlyT1 (Barker et al. 1999); 5′-TCCGT CCTCATAGCCATCTA-3′ and 5′-TCACTCCCGCTGAC AAATG-3′ for GlyT2; 5′-AGCCATGTACGTAGCCA TCC-3′ and 5′-CTCTCAGCTGTGGTGGTGAA-3′ for β-actin. The primers for GlyT2 were designed using the OligoAnalyzer 3.1, provided by Integrated DNA Technologies (Coralville, IA, USA). The GlyT2 mRNA sequence from *Rattus norvegicus* was obtained from the GenBank sequence database of the National Center for Biotechnology Information (http://www.ncbi.nlm.nih.gov/).

## Western blot

Lysates were obtained from astrocytes at 10, 18 and 24 DIV. Total protein was quantified with Bio-Rad DC (Hercules, CA, USA) reagent (Peterson 1979) and separated by sodium dodecyl sulfate-polyacrylamide gel electrophoresis (SDS-PAGE). Subsequently, proteins were transferred to a nitrocellulose membrane, which was blocked with 5 % non-fat powder milk in TBS-T (20 mM Tris base, 137 mM NaCl and 0.1 % Tween-20) and incubated with the primary and with the horseradish peroxidase-conjugated secondary antibodies. Immunoreactions were visualized with the ECL chemiluminescence detection system (Amersham-ECL Western Blotting Detection Reagents from GE Healthcare, Buckinghamshire, UK).

## Immunofluorescence protocols

For immunocytochemistry assays, cultured cells were fixed in 4 % paraformaldehyde (PFA) in PBS for 15 min at room temperature (RT), at 10, 18 and 24 DIV. After fixation, cells were permeabilized (0.1 % Triton X-100 in PBS) for 10 min and blocked (10 % FBS in PBS with 0.05 % Tween-20) for 1 h. After blocking, cells were incubated with the primary antibodies, 4 °C overnight, and subsequently with the fluorescent-labeled secondary antibodies for 1 h at RT. Autofluorescence was removed with 50 mM $CuSO_4$ in 50 mM ammonium acetate buffer, pH 5 (adapted from Schnell et al. 1999) for 30 min. Nuclei were stained with 4′,6-diamidino-2-phenylindole

(DAPI) (1:20,000) and the preparations were mounted in Mowiol.

Tissue samples (brain and spinal cord) were extracted as formerly explained (Aroeira et al. 2011). P21 brains and spinal cords were carefully and quickly removed in ice cold PBS and fixed in 4 % PFA in PBS for 1 week at RT. Before brain extraction, P21 animals were intracardially perfused with 4 % PFA in PBS.

Fixed tissues were dehydrated before paraffin embedding, and coronal sections of spinal cord and brain (5 μm thickness) were cut using a microtome (Leica RM 2145, Wetzlar, Germany). Slices were deparaffined and an incubation in boric acid (0.02 $MH_3BO_3$ in 2 mM NaOH, pH 7), for 15 min at 95–100 °C, was used for antigen recovery.

Brain slices were obtained in a region equivalent to the stereotaxic coordinates (relative to bregma) between −5.20 and −5.60 mm (Paxinos and Watson 1998). Slices were permeabilized (1 % Triton X-100, 10 % FBS in PBS) for 10 min, blocked (10 % FBS in PBS) and incubated with the primary antibodies overnight at 4 °C. Slices were finally incubated with the fluorescent-labeled secondary antibodies during 2 h at RT. Nuclei were stained with DAPI (1:15,000) and sections were mounted in Mowiol (Sigma).

In all immunofluorescence assays, specificity and absence of antibody cross-reaction were confirmed by omission of the primary antibodies.

Images were acquired with a frame size of 2048 × 2048 pixels on an inverted confocal laser scanning microscope (Zeiss LSM 510 META) with a PlanApochromat 63X oil-immersion objective (Zeiss, Germany) with a numerical aperture of 1.40 (pixel size 100 × 100 nm). DAPI fluorescence was detected with a 405 nm diode laser (30 mW nominal output) and a BP 420–480 nm filter. Alexa Fluor 488 fluorescence was detected using the 488 nm line of an Argon laser (45 mW nominal output) and a BP 500–550 nm filter. Alexa Fluor 568 was detected using a 561 nm DPSS laser (15 mW nominal output) and a LP 615 nm filter. Images were prepared for printing using Illustrator (Adobe Systems, San Jose, CA, USA).

### [$^3$H]Glycine uptake assays

Glycine uptake analysis was performed in 21–24 DIV confluent astrocytes. Cells were pre-incubated in serum-free 1 g/l glucose DMEM (Gibco) during 3 h in the optimal atmosphere (5 % $CO_2$, 37 °C). This step was followed by medium exchange to new serum-free 1 g/l glucose DMEM containing GlyT-specific inhibitors and, cells were further incubated for 20 min. In control experiments cells were kept in the presence of serum-free 1 g/l glucose DMEM without any added drug.

The [$^3$H]glycine transport was initiated by the addition of several [$^3$H]glycine concentrations in KHR transport buffer (containing in mM: 137 NaCl, 5.4 KCl, 1.8 $CaCl_2{\cdot}2H_2O$, 1.2 $MgSO_4$ and 10 HEPES, pH 7.40) for 2 min. Uptake was stopped by washing the cells twice with ice cold stop buffer (containing in mM: 137 NaCl and 10 HEPES, pH 7.40). Cells were subsequently solubilized with lysis buffer (100 mM NaOH and 0.1 % SDS) at 37 °C for 1 h and scraped from the plates.

Protein concentration was quantified using Bio-Rad DC protein assay (Peterson 1979). The amount of [$^3$H]glycine taken up by astrocytes was quantified by liquid scintillation counting (PerkinElmer—MicroBeta Trilux).

The specific transport mediated by GlyT1 or GlyT2 was calculated as the difference between the [$^3$H]glycine uptake in the absence (total transport) and in the presence of the GlyT1 inhibitor, Org 24598 (10 μM), or GlyT2 inhibitors, ALX 1393 (200 nM) and amoxapine (1 μM), except when otherwise indicated.

The calculation of the kinetic constants $K_m$ and $V_{max}$ was achieved using GraphPad Prism software (San Diego, CA, USA) by means of non-linear regression analysis.

## Results

### GlyT1 and GlyT2 are expressed in rat cultured cortical astrocytes

Using astrocytes at different maturation stages in culture, namely 10, 18 and 24 DIV, we evaluated GlyT1 and GlyT2 transcripts by qPCR. The results showed that both GlyT1 and GlyT2 mRNA are present in astrocytes from 10 to 24 DIV. Relative quantification in comparison with 10 DIV transcripts (Pfaffl 2001), using β-actin as a reference control gene, indicated that both transcripts were preserved throughout the considered time culture (Fig. 1). No signal amplification was detected in the negative controls (data not shown), which indicated signal specificity. Reaction specificity was further evaluated in all assays by a melting curve (Online Resource 1).

Next, we assessed protein expression in primary cortical astrocytes throughout the same culture time. For this, we used a western blot procedure and probed the membranes with antibodies that specifically recognized GlyT1, GlyT2 and the endogenous loading control β-actin (Fig. 2). The immunoblot obtained for GlyT1 revealed the presence of two bands, one with a molecular weight of approximately 75 kDa and a heavier band with around 90 kDa. This pattern is in agreement with the presence of several GlyT isoforms. In the case of GlyT1, the 75 kDa band indicates the expression of GlyT1a and GlyT1b isoforms, while the 90 kDa band might correspond to GlyT1c

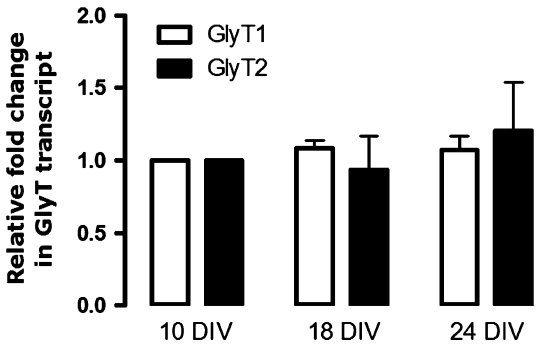


**Fig. 1** Changes in the expression level of GlyT1 and GlyT2 transcripts in rat cortical astrocytes over several maturation stages (10, 18 and 24 DIV) by relative qPCR. β-actin was used as a reference control gene. Values are mean ± SEM, no significative differences ($p > 0.05$) were found when comparing the expression of each transcript with 10 DIV ($n = 6$, one way ANOVA followed by Bonferroni's multiple comparison test)

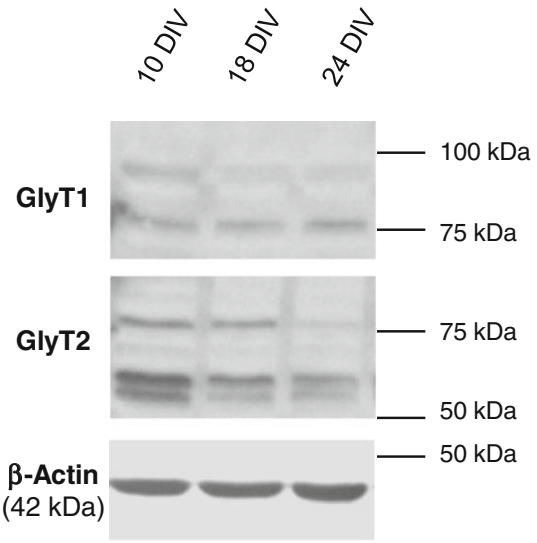


**Fig. 2** Expression of GlyT1 and GlyT2 protein in rat cortical astrocytes over several maturation stages (10, 18 and 24 DIV). Western blot analysis of GlyT1, GlyT2 and β-actin in rat cultured cortical astrocytes. β-actin was used as a loading control. The immunoreactive bands were detected on a 12 % sodium dodecyl sulfate-polyacrylamide gel electrophoresis using GlyT1, GlyT2 and β-actin antibodies

(Vargas-Medrano et al. 2011). The antibody against GlyT2 detected three bands in the 50–75 kDa range, which is also consistent with the occurrence of GlyT2 isoforms (Eulenburg et al. 2005). Furthermore, both GlyT are described to have multiple *N*-glycosylation sites (Olivares et al. 1995; Martinez-Maza et al. 2001), which could also explain the intermediate bands observed in GlyT immunoblots. All bands were present at all DIV, being the expression pattern very similar to the one detected for spinal cord homogenates, which were used as a control (data not shown). For the GlyT1 90 kDa isoform, a minor intensity decrease over time was noticeable, whereas the 75 kDa isoform of GlyT2 was almost absent in mature astrocytes.

## GlyT1 and GlyT2 have a different subcellular localization in rat cortical astrocytes

To assess GlyT1 and GlyT2 localization in cultured astrocytes, we performed a double immunofluorescence assay during the course of the culture. This procedure identified differentiated astrocytes, by GFAP staining, together with GlyT- and DAPI-stained nucleus.

The high incidence of GFAP positive cells in Figs. 3, 4 confirmed that the cultures were enriched in astrocytes, which demonstrated that the microglia removal protocol was efficient. In addition, it was noticed an increase in cellular development and in culture confluence over time. Images of astrocytes at 10 DIV depicted isolated immature astrocytes with small processes and low GFAP expression, while from 18 DIV on GFAP expression was strongly detected in cell bodies and delineated all processes, indicating the predominance of mature astrocytes.

Confocal images revealed developmental regulated changes in subcellular localization of both GlyT1 (Fig. 3) and GlyT2 (Fig. 4). At 10 DIV (Fig. 3, A1-A5), GlyT1 was predominantly detected in the cytoplasm outer layer (arrowheads in Fig. 3, A5). However, it was already possible to observe GlyT1 expression in some small astrocytic processes (arrows in Fig. 3, A5). From 18 DIV on (Fig. 5, A6–A15), besides cytoplasm labeling (arrowheads in Fig. 3, A10 and A15), GlyT1 was found in long spread processes (arrows in Fig. 3, A10 and A15). In what concerns GlyT2, at 10 DIV (Fig. 4, A1–A5), it was expressed in the cytoplasm (arrowheads in Fig. 4, A5) and in small astrocytic processes (arrows in Fig. 4, A5), alike GlyT1. From 18 DIV onwards (Fig. 4, A6–A15), several GlyT2 clusters can be distinguished over the cytoplasm (arrowheads in Fig. 4, A10 and A15), in the small non-spread processes (arrows in Fig. 4, A10) and also in some mature processes of astrocytes (arrows in Fig. 4, A15).

## GlyT1 and GlyT2 are expressed in rat brain astrocytes

Due to the unexpected presence of GlyT2 in rat cultured cortical astrocytes, we decided to investigate whether GlyT2 expression in astrocytes was also observed in brain slices. To this end, GlyT localization in the rat brain was explored by confocal immunohistochemistry analysis of coronal brain slices (5 μm). A double staining of GFAP and GlyT, as well as DAPI, allowed us to uncover if and where GlyT1 and GlyT2 were expressed in the astrocytes of mature brains (P21). In order to have a broader characterization of GlyT expression in the forebrain, images were taken in a cortical region and in the dentate gyrus (DG) of the hippocampus. P21 astrocytes strongly express

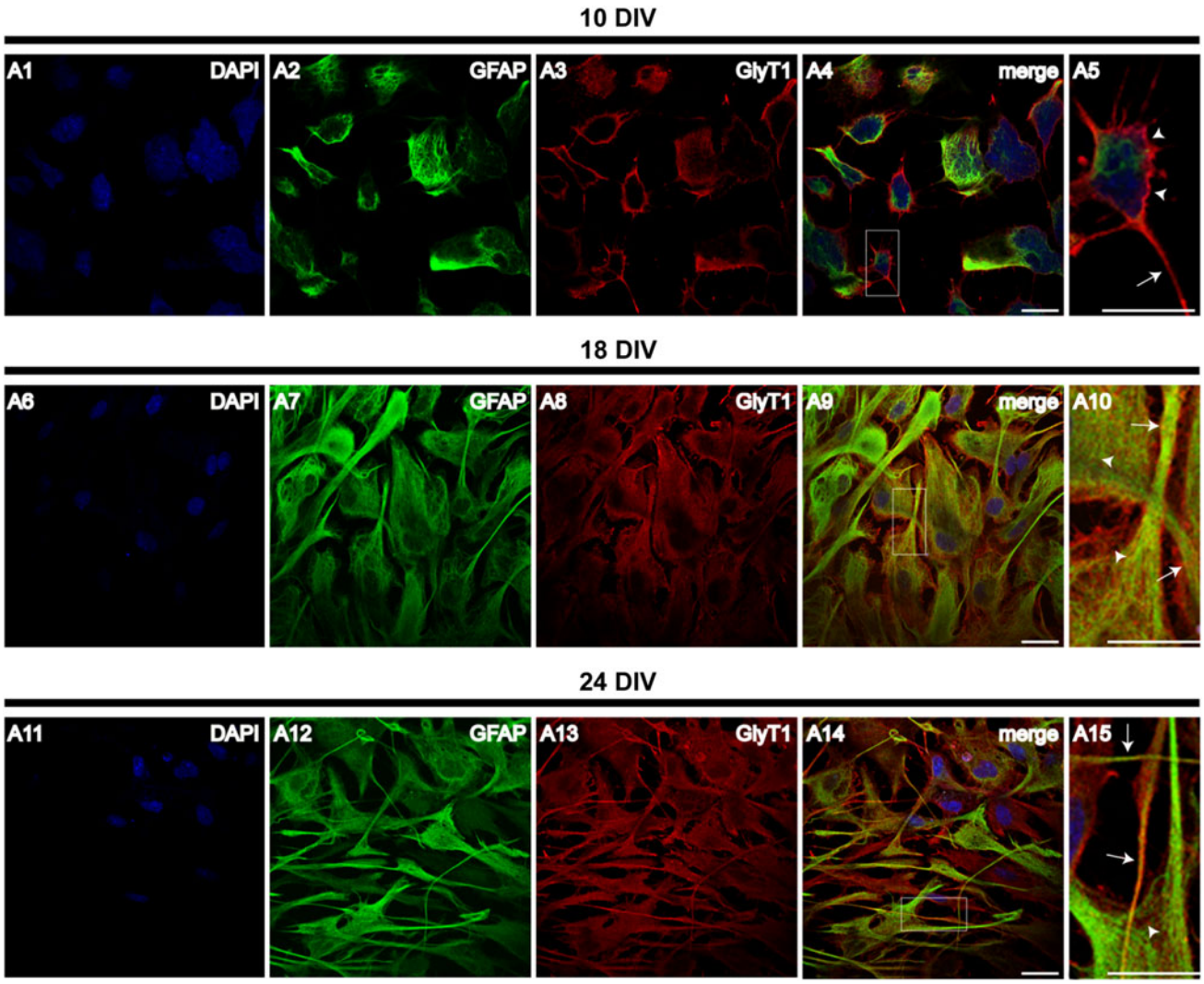


**Fig. 3** Double detection of GlyT1 and GFAP in rat cultured cortical astrocytes over several maturation stages (10, 18 and 24 DIV) was assessed by confocal microscopy. Examples of GlyT1 in cytoplasm (*arrowheads*) and GlyT1 in astrocytic process (*arrows*) are indicated. The first three panels in every row represent each labeling alone: DAPI-stained nuclei, *green* for GFAP and *red* for GlyT1. Confocal images were acquired with a 63× oil-immersion objective. *Scale bars* 20 μm

GFAP and establish elongated processes in both cortical and hippocampal regions (Figs. 5, 6, GFAP panels).

GlyT1 expression was detected in both regions of the mature rat brain (Fig. 5). In the cortical area (Fig. 5, A1–A5), GlyT1 immunolabeling was present in the astrocytic processes (arrows in Fig. 5–A5). GlyT1 was also observed over the cytoplasm of many GFAP-negative cells (arrowheads in Fig. 5, A4) and presented a punctate distribution throughout the whole cortical region (open arrowheads in Fig. 5, A5). In the DG (Fig. 5, A6–A10), GlyT1 expression was found to be localized in astrocytic processes (arrows in Fig. 5, A10), but also extensively spread through the whole dendritic layer (open arrowheads in Fig. 5, A10). In the granular layer of DG, GlyT1 was also found to surround many GFAP-negative cells (arrowheads in Fig. 5, A9).

Similarly, GlyT2 was present in cortical and hippocampal regions (Fig. 5, B1–B10). In the cortical area (Fig. 5, B1–B5), GlyT2 immunolabeling was present in the processes of many astrocytes (arrows in Fig. 5, B5). As observed for GlyT1, GlyT2 was also localized in some GFAP-negative cell bodies (arrowheads in Fig. 5, B4) and widespread throughout the cortical space (open arrowheads in Fig. 5, B5). In the DG (Fig. 5, B6–B10), GlyT2 was expressed in some astrocytes, mostly in small processes very close to the nucleus (arrows in Fig. 5, B10). As in the cortex, GlyT2 immunolabeling was extensively spread over the dendritic layer (open arrowheads in Fig. 5, B10) and detected in cell bodies (arrowheads in Fig. 5, B9) that do not express GFAP. In summary, the results obtained in brain slices revealed an expression pattern similar to the

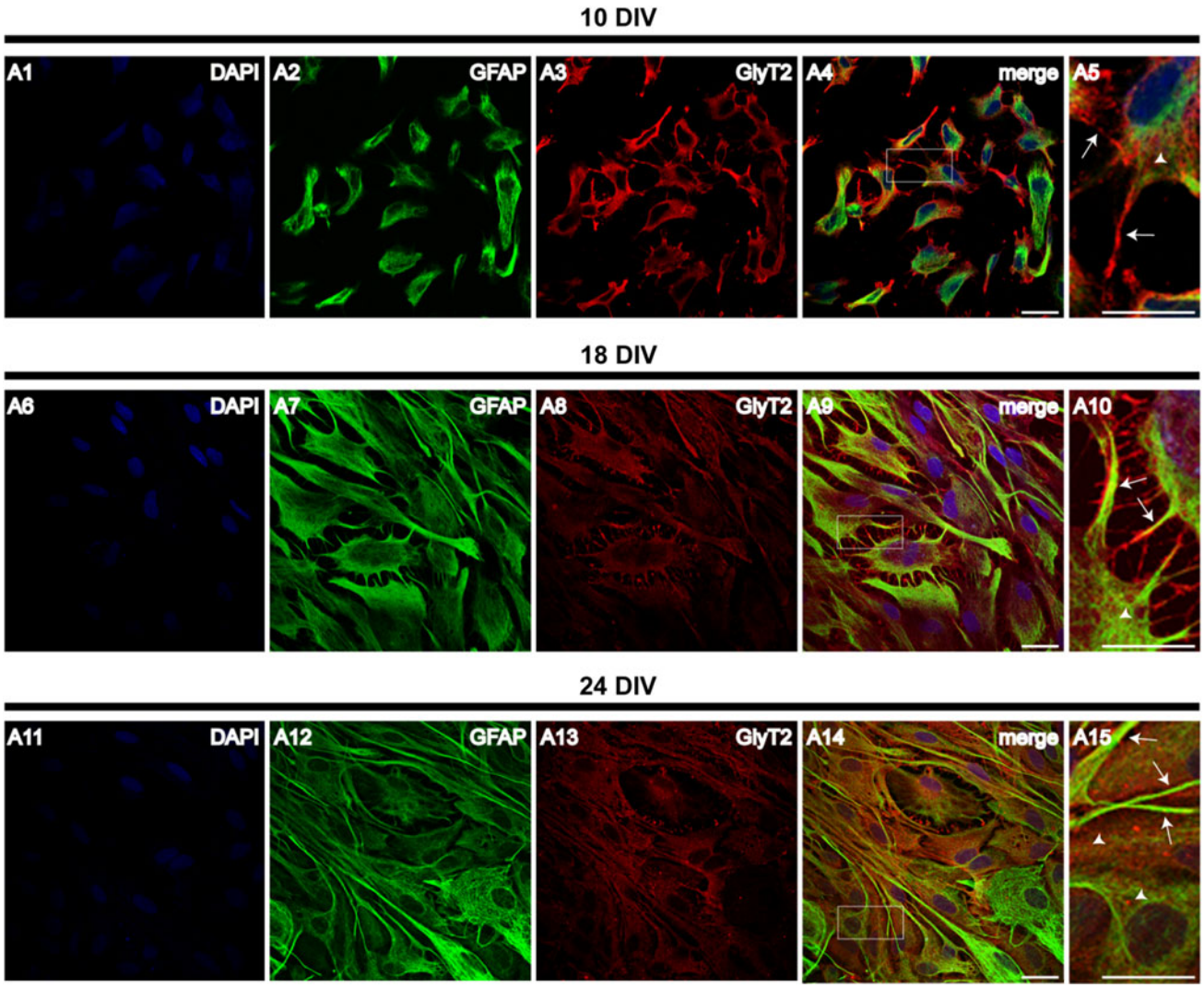


**Fig. 4** Double detection of GlyT2 and GFAP in rat cultured cortical astrocytes over several maturation stages (10, 18 and 24 DIV) was assessed by confocal microscopy. Examples of GlyT2 in cytoplasm (*arrowheads*) and GlyT2 in astrocytic process (*arrows*) are indicated. The first three panels in every row represent each labeling alone: DAPI-stained nuclei, *green* for GFAP and *red* for GlyT2. Confocal images were acquired with a 63× oil-immersion objective. *Scale bars* 20 μm

one obtained for cultured astrocytes, thus corroborating the presence of GlyT1 and GlyT2 in brain astrocytes.

Furthermore, we performed a double immunostaining of GFAP and GlyT in spinal cord slices (Fig. 6), which confirmed the presence of GlyT1 (Fig. 6, A1–A5) and GlyT2 (Fig. 6, B1–B5) in spinal cord astrocytes (arrows in Fig. 6, A5 and B5), as concluded by the yellow labeling indicative of the co-localization between GlyT1/GlyT2 and GFAP. In spinal cord negative controls, carried out in the absence of the primary antibodies, no staining was detected (data not shown).

## GlyT1 and GlyT2 are expressed in neurons

To confirm that the GFAP-negative cell bodies, which express GlyT, are of neuronal nature, we performed a double staining with GlyT1 or GlyT2 and MAP2, a neuronal marker, together with DAPI, and obtained confocal images from cortex and DG (Fig. 7).

In cortical regions, GlyT1 immunolabeling (Fig. 7, A1–A5) was detected over cell bodies (arrowheads in Fig. 7, A4) and also in neuronal processes (open arrowheads in Fig. 7, A5), since it was possible to detect the co-localization between GlyT1 and MAP2. This pattern was also observed in the dendritic region of the hippocampus (open arrowheads in Fig. 7, A10). GlyT1 was also found to surround the neuronal cell bodies localized in the DG granular layer, which are known to correspond to glutamatergic neurons (Andersen et al. 2007).

Regarding GlyT2 (Fig. 7, B1–B10), it was possible to detect GlyT2 expression in many neuronal cell bodies spread throughout the cortex (arrowheads in Fig. 7, B4), probably of interneurons, and in neuronal processes (open

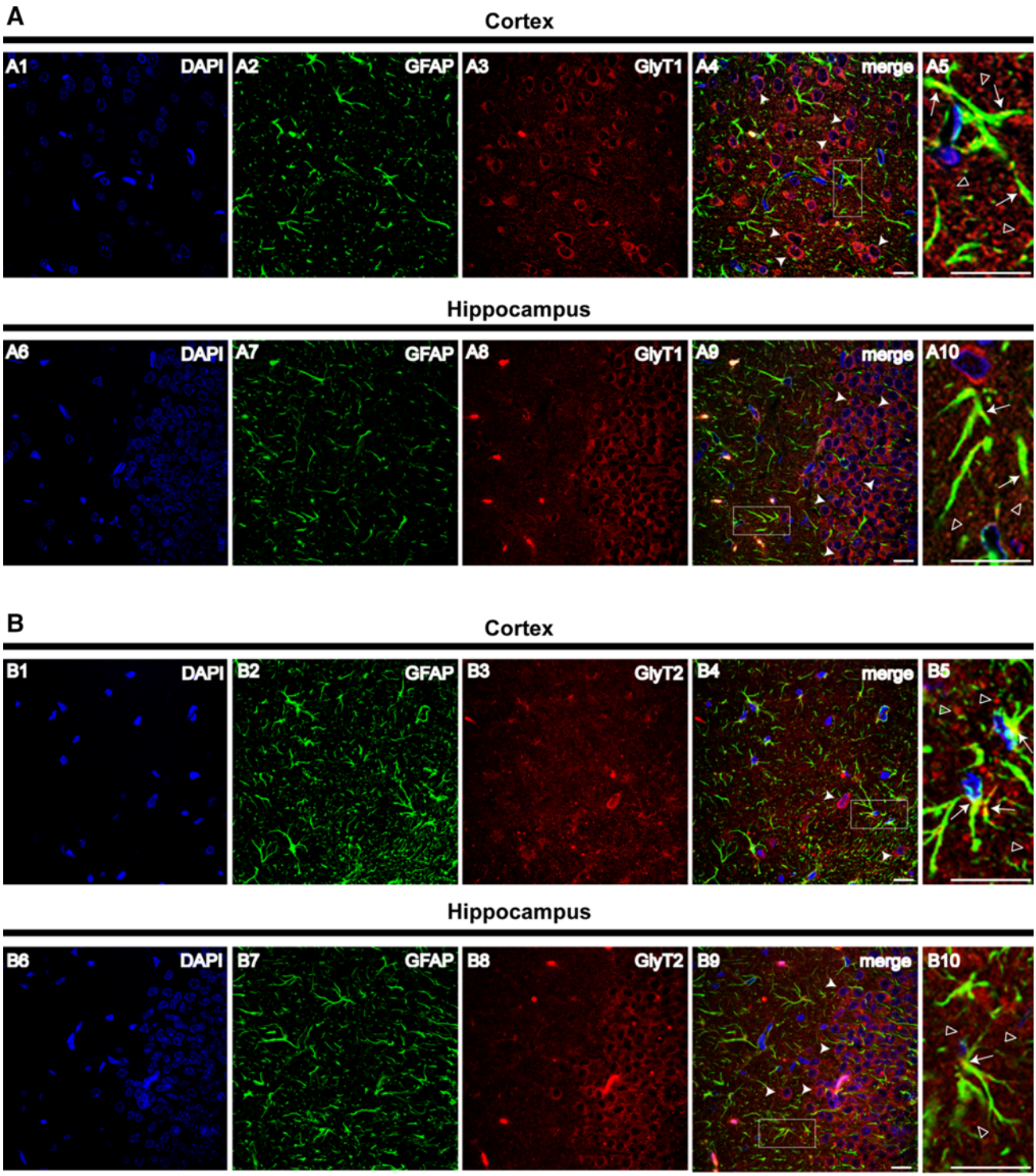


**Fig. 5** Localization of GlyT1 and GlyT2 in P21 rat brain astrocytes assessed by confocal microscopy. Double immunolabeling of GFAP and GlyT1 (**a**)/GlyT2 (**b**) in cortex and dentate gyrus of the hippocampus. The first panels in every row represent each labeling alone: DAPI-stained nuclei, *green* for GFAP and *red* for GlyT1/GlyT2. Examples of astrocytic GlyT are indicated by *arrows*, while GlyT occurrence in GFAP-negative cell bodies and processes is pointed by *arrowheads* and *open arrowheads*, respectively. Confocal images were acquired with a 63× oil-immersion objective. *Scale bars* 20 μm

arrowheads in Fig. 7, B5). In the hippocampus (Fig. 7, B6–B10), the presence of GlyT2 was also detected in some neurons localized in the granular layer (arrowheads in Fig. 7, B9). As in the cortex, GlyT2 was detected in neuronal processes spread throughout the dendritic layer (open arrowheads in Fig. 7, B10).

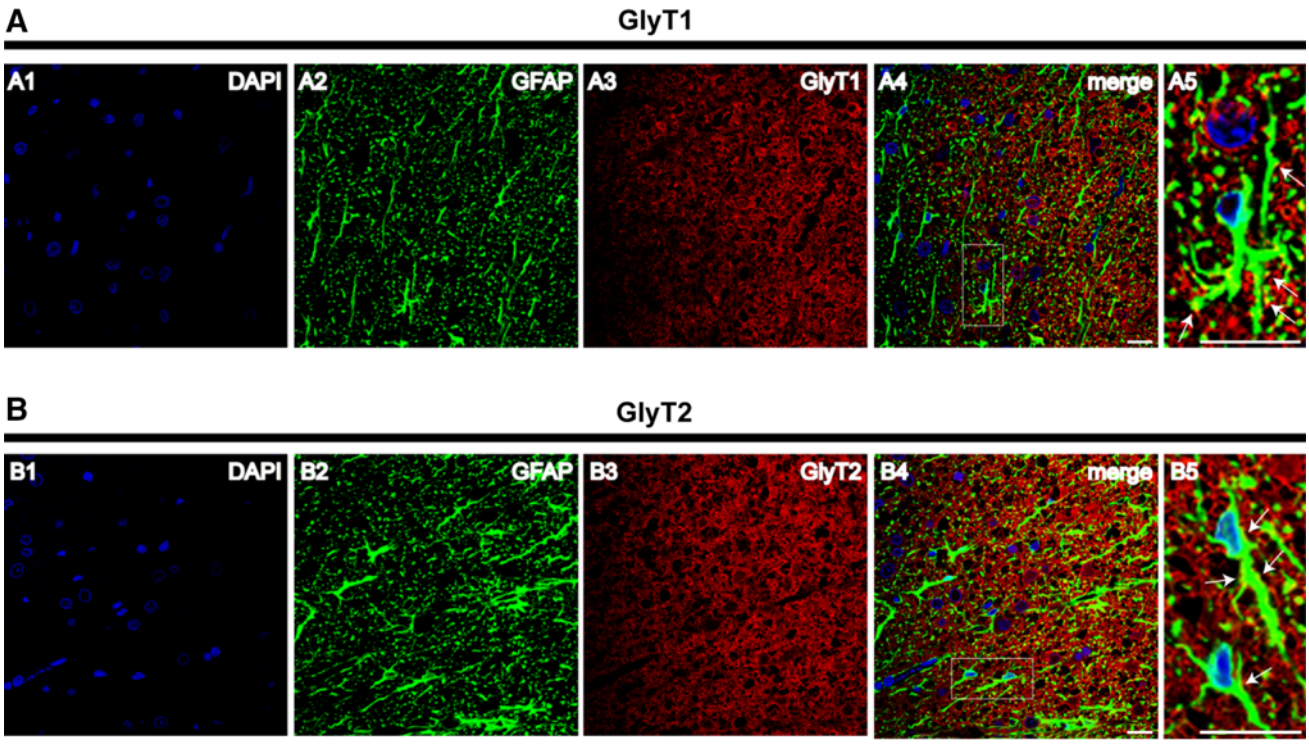


**Fig. 6** Localization of GlyT1 and GlyT2 in rat spinal cord slices, laminae II of the ventral horn, by confocal microscopy. Double detection of GFAP and GlyT1 (**a**) /GlyT2 (**b**) in rat spinal cord. The first three panels in every row represent each labeling alone: DAPI-stained nuclei, *green* for GFAP and *red* for GlyT1/GlyT2. Examples of astrocytic GlyT are indicated by *arrows* in the magnified panels. Confocal images were acquired with a 63× oil-immersion objective. *Scale bars* 20 μm

Furthermore, was detected, in both regions, the presence of GlyT in MAP2-negative cell bodies and processes (arrows in Fig. 7, A5, A10, B5 and B10), which are in accordance with the results showed in the previous section, the GlyT detection in astrocytes.

## GlyT1 and GlyT2 are functionally expressed in rat cultured cortical astrocytes

To evaluate if astrocytic GlyT1 and GlyT2 are able to transport glycine, [$^3$H]glycine uptake assays in cultured astrocytes were performed. Optimization assays were carried out to define the incubation time with [$^3$H]glycine, as well as the concentration of inhibitors to be used to calculate the transport mediated by GlyT1 or GlyT2. Two concentrations of glycine were used, 50 μM to study high affinity transport and 1,500 μM to study low affinity transport. In both cases, the uptake of [$^3$H]glycine increased linearly with time of incubation from 30 to 240 s (Online Resource 2), therefore, a 2-min incubation time was chosen for the remaining experiments.

Transport assays with increasing concentrations (1–30 μM) of Org 24598 (a selective GlyT1 blocker) and a constant [$^3$H]glycine (50 μM) concentration (Online Resource 3A) revealed that maximal transport inhibition was achieved with 10 μM Org 24598. So, non-GlyT1 mediated transport was defined as the uptake occurring in the presence of 10 μM Org 24598, a concentration about 100 times the IC50 value for GlyT1 inhibition and well below the IC50 value for GlyT2 inhibition (Brown et al. 2001).

Uptake assays with 1,500 μM [$^3$H]glycine at increasing concentrations of the GlyT2 inhibitors, ALX 1393 (Luccini and Raiteri 2007) or amoxapine (Núñez et al. 2000) showed that an inhibition plateau was reached at 50–500 nM of ALX 1393 (Online Resource 3B) or 0.5–2 μM of amoxapine (Online Resource 3C). Higher concentrations of those inhibitors further inhibit glycine transport, but were not chosen to define non-GlyT2 mediated transport to avoid the use of concentrations not selective for GlyT2.

To estimate the relative influence of GlyT1 and GlyT2 for total glycine transport, assays were performed in the presence or absence of the selective inhibitors. Non-GlyT-mediated uptake was defined as the uptake in the presence of excess (10 mM) of cold glycine (calculated as about 20 % of total glycine transport in control conditions) and was subtracted in all experiments. Uptake of [$^3$H]glycine (50 μM) was reduced to 30.50 ± 1.183 % ($n = 4$) by Org 24598 (10 μM) (Fig. 8A), suggesting that GlyT1 ensured 70 % of GlyT-mediated transport. ALX 1393 (200 nM)

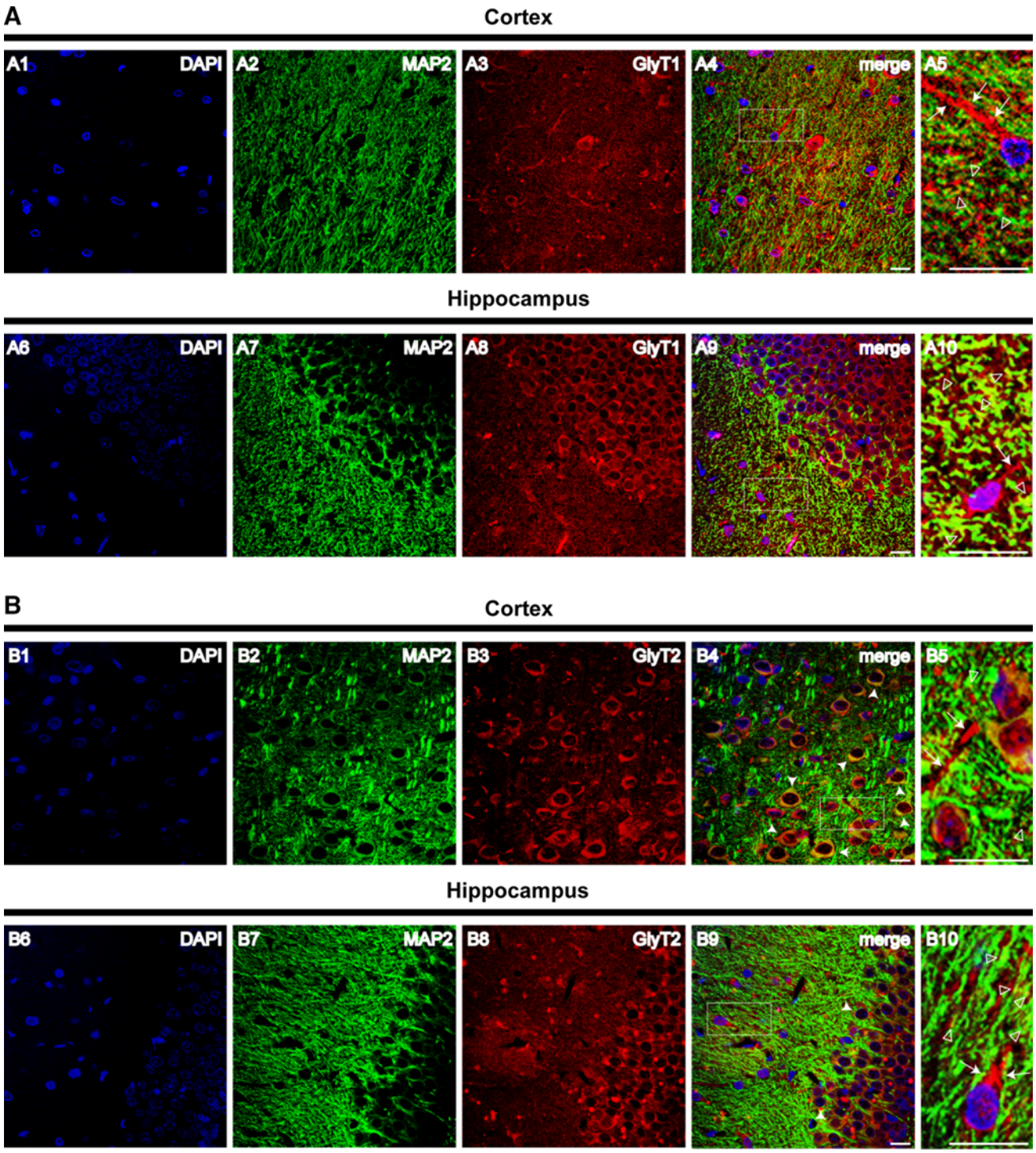


**Fig. 7** Localization of GlyT1 and GlyT2 in P21 rat brain neurons assessed by confocal microscopy. Double immunolabeling of MAP2 and GlyT1 (**a**) /GlyT2 (**b**) in cortex and dentate gyrus of the hippocampus. The first panels in every row represent each labeling alone: DAPI-stained nuclei, *green* for MAP2 and *red* for GlyT1/GlyT2. GlyT1 and GlyT2 presence in neuronal cell bodies and processes are indicated by *arrowheads* and *open arrowheads*, respectively. *Arrows* illustrate non-neuronal GlyT. Confocal images were acquired with a 63× oil-immersion objective. *Scale bars* 20 μm

blocked the Org 24598-resistant [$^3$H]glycine (50 μM) uptake (Fig 8A) suggesting that even at micromolar concentrations of glycine, GlyT2 is responsible for about 30 % of the GlyT-mediated uptake. Similar results were obtained while using a higher concentration of [$^3$H]glycine (Fig. 8B). ALX 1393 (200 nM) inhibited [$^3$H]glycine

(1,500 μM) transport to 61.99 ± 3.76 % ($n = 4$) and the ALX 1393-resistant component of the transport was fully blocked by Org 24598 (10 μM), suggesting that GlyT2 is responsible by near 40 % of [$^3$H]glycine (1,500 μM) uptake into astrocytes, while GlyT1 accounts for about 60 % of the transport.

Kinetic analysis revealed an apparent $K_m$ of 51 ± 5.0 μM of glycine for GlyT1, with a maximal velocity ($V_{max}$) of 379.30 ± 10.3 pmol of [$^3$H]glycine/min/mg of protein (Fig. 9A). On the other hand, the apparent $K_m$ of glycine for GlyT2 was 1,801 ± 149 μM, with a $V_{max}$ of 5,730 ± 200 pmol of [$^3$H]glycine per min per mg (Fig. 9B). The kinetic constants obtained for GlyT2-mediated transport were similar when non-GlyT2 mediated transport was defined either by ALX 1393 (200 nM) (Fig. 9B, full line) or amoxapine (1 μM) (Fig. 9B, dashed line). However, although functionally expressed in astrocytes, GlyT2 was found to have a much lower affinity for glycine than GlyT1, 51.15 ± 4.96 μM for GlyT1 versus 1,801 ± 149 μM for GlyT2.

## Discussion

A major outcome from the present work is the identification and characterization of GlyT2 in cortical astrocytes. We show that both GlyT1 and GlyT2 are expressed in astrocytes, at mRNA and protein levels, both in primary cultures and brain slices. The experiments carried out in cultured astrocytes show that GlyT1 and GlyT2 localization is developmentally regulated. The double detection of GFAP and GlyT revealed that GlyT1 is expressed in the cytoplasm and small astrocytic processes of immature astrocytes (10 DIV) and progresses to a more spread expression in the elongated processes of mature cells (18 and 21 DIV). Similarly, GlyT2 expression was found in the cell cytoplasm and processes of astrocytes. In P21 brains, in both cortical and hippocampal regions, GlyT1 was broadly found in extended astrocytic processes, while GlyT2 was mostly detected in the vicinity of the nucleus.

Both GlyT also occur in GFAP-negative cells. We have confirmed the neuronal nature of these cells by double immunolabeling of GlyT and a neuronal marker, MAP2. Not surprisingly both transporters were found to surround many neurons, but also to occur in areas devoid of cell bodies where MAP2 staining was quite spread. GlyT1 has a relevant role at excitatory glutamatergic synapses to control the glycine concentration in the vicinity of ionotropic NMDA receptors, where glycine acts as a co-agonist of glutamate receptors (Supplisson and Bergman 1997; Cubelos et al. 2005; Eulenburg et al. 2005; Betz et al. 2006). In addition, analysis of GlyT2 expression (Jursky and Nelson 1995) and function (Gomeza et al. 2003a, b; Rousseau et al. 2008) has indicated that this transporter is involved in the re-uptake of glycine into glycinergic nerve terminals, enhancing the glycine concentration in the cytosolic space and enabling the reloading of glycinergic synaptic vesicles at inhibitory synapses. As we now show, GlyT2 are also expressed in astrocytes, therefore, most probably contributing, together with astrocytic GlyT1, to shape glycinergic transmission.

In addition, we show evidences that GlyT1 and GlyT2 are functional in astrocytes, since both have the capability to take up glycine from the surrounding environment. We show that GlyT1 is responsible for 60–70 % of the GlyT-mediated glycine transport. Unexpectedly, and although having a much lower affinity for glycine than GlyT1, GlyT2 was found to ensure 30–40 % of GlyT-mediated glycine uptake, being able to take up glycine even when the extracellular glycine concentrations are in the micromolar

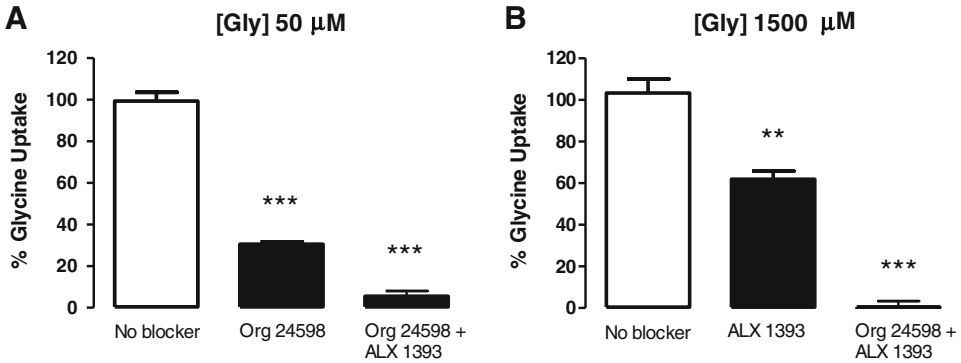


**Fig. 8** Characterization of the relative contribution of each glycine transporter in rat cultured cortical astrocytes. Transport of 50 μM (**a**) or 1,500 μM (**b**) glycine in the absence or presence of GlyT1 and GlyT2 selective inhibitors, Org 24598 (10 μM) and ALX 1393 (200 nM), respectively. Drug presence is indicated below *each bar*. In each experiment, the non-GlyT-mediated transport, assessed by the presence of excess of glycine (10 mM), was subtracted and corresponded to about 20 % of total uptake in control conditions. 100 % in the *Y* axis represents GlyT-mediated [$^3$H]glycine uptake in the absence of GlyT inhibitors (control GlyT-mediated uptake). All values are mean ± SEM. $^{**}p < 0.01$, $^{***}p < 0.001$ ($n = 4$, *t* test)

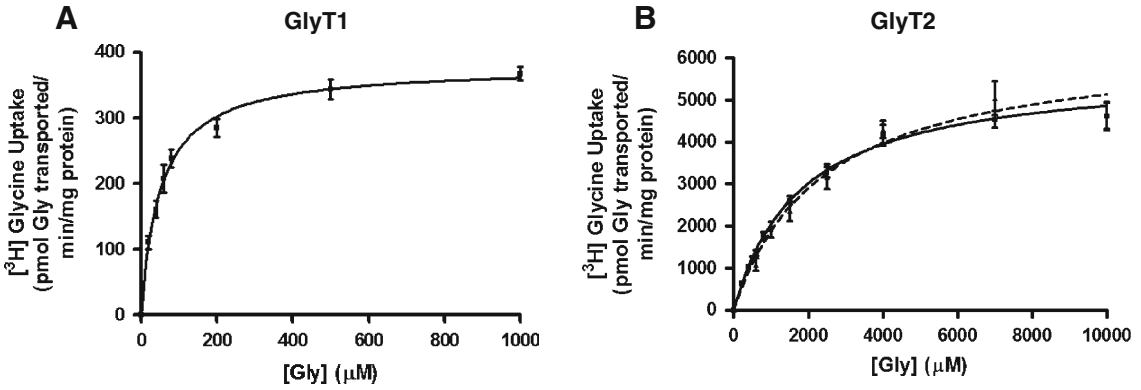


| Drug used to define specific transport | Kinetic Parameters | |
|---|---|---|
| | $K_m$ (μM) | $V_{max}$ (pmol/min/mg) |
| Org 24598 | 51.15±4.96 | 379.30±10.3 |

| Drug used to define specific transport | Kinetic Parameters | |
|---|---|---|
| | $K_m$ (μM) | $V_{max}$ (pmol/min/mg) |
| ALX 1393 (——) | 1801±148.9 | 5730±200.2 |
| Amoxapine (– – –) | 2383±482.4 | 6344±467.0 |

**Fig. 9** Saturation curves obtained in rat cultured cortical astrocytes, depicting the amount of glycine taken up by GlyT as a function of the glycine concentration. GlyT1 (**a**) and GlyT2-mediated (**b**) transport was calculated as the difference between the [$^3$H]glycine uptake in the absence (total transport) and in the presence (unspecific transport) of the GlyT-specific inhibitors. *Y* axis represents the amount of [$^3$H] glycine taken up in control conditions after subtraction of the unspecific mediated transport. Note the differences in scale between graphs. *Tables* indicate the averaged $K_m$ and $V_{max}$ calculated, for the different GlyT inhibitors by non-linear regression analysis, using GraphPad Prism software. All values are mean ± SEM ($5 < n < 15$)

range. The calculated GlyT1 $K_m$ value (51 μM) is similar to the values previously reported by others in QT-6 cells (Atkinson et al. 2001), in oocytes (Guastella et al. 1992), in cultured cortical neurons (Wu et al. 2008) or in brain synaptosomal preparations (Yee et al. 2006). The $K_m$ value now calculated for GlyT2 in brain astrocytes (1,801 μM) is higher than the value calculated by others using spinal cord synaptosomes (Geerlings et al. 2001) and in brainstem primary neurons (Fornés et al. 2008). The reason for diversity in the estimated $K_m$ values in different preparations remains unknown. Nevertheless, low affinity transporters should play a relevant role in glycinergic transmission, since synaptic levels of glycine may transiently increase to the millimolar range (Dohi et al. 2009).

The presence of GlyT2 in glial cells has been already noted in slices from the cerebellum (Zafra et al. 1995), in cortical oligodendrocyte progenitor cells (Belachew et al. 2000) and in astrocyte-derived subcellular particles purified from spinal cord, named gliosomes (Raiteri et al. 2008). However, it has been always assumed that cerebral astrocytes lack GlyT2. To our knowledge, this is the first report unequivocally showing that GlyT2 is expressed and is functional in brain astrocytes, being able to transport considerable amounts of glycine either at micromolar or low milimolar concentrations. Nevertheless, the hypothesis that glial GlyT2 could have a compensatory effect upon a glial GlyT1 function impairment was recently raised by Eulenburg and co-workers (Eulenburg et al. 2010), who addressed the role of neuronal and glial GlyT1 by generating conditional knock-out mice in neurons or astrocytes. These authors observed that the majority of glial GlyT1 knock-out mice develop severe neuromotor deficits, which resulted in premature death, but around 20 % of the animals survive the critical period without developing any detectable deficits and exhibiting a normal lifespan. It was, therefore, postulated that GlyT2 activation could be able to restore GlyT1 loss of function.

We also would like to point out that non-GlyT-mediated uptake suggests that astrocytes express other types of low affinity glycine transporters, namely the ASC system or the L system (Su et al. 1995; Nagaraja and Brookes 1996; Castagna et al. 1997; Weiss et al. 2001). In addition, due to its biochemical properties, some glycine can simply cross the membrane by passive diffusion (Tunnicliff 2003).

In conclusion, our work demonstrates that brain astrocytes express GlyT1 and GlyT2, though with a different subcellular localization. Glial GlyT1 is expressed in the long widespread astrocytic process, while glial GlyT2 is predominantly found in the cytoplasm and in the small astrocytic processes. Furthermore, we assessed that both glial GlyT1 and GlyT2 are functional although, as expected, GlyT1 has a much higher affinity for glycine than

GlyT2. We strongly believe that this work can renew the current perception of glycine-mediated neurotransmission in the brain.

**Acknowledgments** The authors thank Dr. Manuel Miranda-Arango (Texas) for kindly supplying the antibodies against GlyT1 and GlyT2. This work was supported by Fundação para a Ciência e a Tecnologia (FCT), Portugal. Rita I Aroeira is in receipt of a fellowship (SFRH/BD/62831/2009) from FCT. The authors declare that this research was conducted in the absence of any commercial or financial relationships that could be construed as a potential conflict of interest.

## References

Adams RH, Sato K, Shimada S, Tohyama M, Pöschel AW, Betz H (1995) Gene structure and glial expression of the glycine transporter GLYT1 in embryonic and adult rodents. J Neurosci 15:2524–2532

Allaman I, Bélanger M, Magistretti PJ (2011) Astrocyte–neuron metabolic relationships: for better and for worse. Trends Neurosci 34:76–87

Andersen P, Morris R, Amaral D, Bliss T, O'Keefe J (eds) (2007) The hippocampus book. Oxford University Press, USA

Araque A, Parpura V, Sanzgiri RP, Haydon PG (1999) Tripartite synapses: glia, the unacknowledged partner. Trends Neurosci 22:208–215

Aroeira RI, Ribeiro JA, Sebastião AM, Valente CA (2011) Age-related changes of glycine receptor at the rat hippocampus: from the embryo to the adult. J Neurochem 118:339–353

Atkinson BN, Bell SC, De Vivo M, Kowalski LR, Lechner SM, Ognyanov VI, Tham CS, Tsai C, Jia J, Ashton D, Klitenick MA (2001) ALX 5407: a potent, selective inhibitor of the hGlyT1 glycine transporter. Mol Pharmacol 60:1414–1420

Barker GA, Wilkins RJ, Golding S, Ellory JC (1999) Neutral amino acid transport in bovine articular chondrocytes. J Physiol 514(3):795–808

Belachew S, Malgrange B, Rigo JM, Rogister B, Leprince P, Hans G, Nguyen L, Moonen G (2000) Glycine triggers an intracellular calcium influx in oligodendrocyte progenitor cells which is mediated by the activation of both the ionotropic glycine receptor and $Na^+$-dependent transporters. Eur J Neurosci 12:1924–1930

Betz H, Gomeza J, Armsen W, Scholze P, Eulenburg V (2006) Glycine transporters: essential regulators of synaptic transmission. Biochem Soc Trans 34:55–58

Biber K, Klotz KN, Berger M, Gebicke-Härter PJ, van Calker D (1997) Adenosine A1 receptor-mediated activation of phospholipase C in cultured astrocytes depends on the level of receptor expression. J Neurosci 17:4956–4964

Borowsky B, Mezey E, Hoffman BJ (1993) Two glycine transporter variants with distinct localization in the CNS and peripheral tissues are encoded by a common gene. Neuron 10:851–863

Bowery NG, Smart TG (2006) GABA and glycine as neurotransmitters: a brief history. Br J Pharmacol 147:S109–S119

Brown A, Carlyle I, Clark J, Hamilton W, Gibson S, McGarry G, McEachen S, Rae D, Thorn S, Walker G (2001) Discovery and SAR of Org 24598-A selective glycine uptake inhibitor. Bioorg Med Chem Lett 11:2007–2009

Castagna M, Shayakul C, Trotti D, Sacchi VF, Harvey WR, Hediger MA (1997) Molecular Characteristics of mammalian and insect amino acid transporters: implications for amino acid homeostasis. J Exp Biol 200:269–286

Cubelos B, Gimenez C, Zafra F (2005) Localization of the GlyT1 glycine transporter at glutamatergic synapses in the rat brain. Cereb Cortex 15:448–459

Dohi T, Morita K, Kitayama T, Motoyama N, Morioka N (2009) Glycine transporter inhibitors as a novel drug discovery strategy for neuropathic pain. Pharmacol Therap 123:54–79

Du F, Qian ZM, Zhu L, Wu XM, Qian C, Chan R, Ke Y (2010) Purity, cell viability, expression of GFAP and bystin in astrocytes cultured by different procedures. J Cell Biochem 109:30–37

Ebihara S, Yamamoto T, Obata K, Yanagawa Y (2004) Gene structure and alternative splicing of the mouse glycine transporter type-2. Biochem Biophys Res Commun 317:857–864

Eichler SA, Kirischuk S, Jöttner R, Schaäfermeier PK, Legendre P, Lehmann TN, Gloveli T, Grantyn R, Meier JC (2008) Glycinergic tonic inhibition of hippocampal neurons with depolarising GABAergic transmission elicits histopathological signs of temporal lobe epilepsy. J Cell Mol Med 12:2848–2866

Eulenburg V, Armsen W, Betz H, Gomeza J (2005) Glycine transporters: essential regulators of neurotransmission. Trends Biochem Sci 30(6):325–333

Eulenburg V, Retiounskaia M, Papadopoulos T, Gomeza J, Betz H (2010) Glial glycine transporter 1 function is essential for early postnatal survival but dispensable in adult mice. Glia 58:1066–1073

Fornés A, Núñez E, Alonso-Torres P, Aragón C, López-Corcuera B (2008) Trafficking properties and activity regulation of the neuronal glycine transporter GLYT2 by protein kinase C. Biochem J 412:495–506

Gabryel B, Adamczyk J, Huzarska M, Pudełko A, Trzeciak HI (2002) Aniracetam attenuates apoptosis of astrocytes aubjected to simulated ischemia in vitro. Neurotoxic 23:385–395

Geerlings A, Núñez E, López-Corcuera B, Aragón C (2001) Calcium- and syntaxin 1-mediated trafficking of the neuronal glycine transporter GLYT2. J Biol Chem 276:17584–17590

Gingras M, Gagnon V, Minotti S, Durham HD, Berthod F (2007) Optimized protocols for isolation of primary motor neurons, astrocytes and microglia from embryonic mouse spinal cord. J Neurosci Method 163:111–118

Gomeza J, Hulsmann S, Ohno K, Eulenburg V, Szoke K, Richter D, Betz H (2003a) Inactivation of the glycine transporter 1 gene discloses vital role of glial glycine uptake in glycinergic inhibition. Neuron 40:785–796

Gomeza J, Ohno K, Hulsmann S, Armsen W, Eulenburg V, Richter DW, Laube B, Betz H (2003b) Deletion of the mouse glycine transporter 2 results in a hyperekplexia phenotype and postnatal lethality. Neuron 40:797–806

Guastella J, Brecha N, Weigmann C, Lester A, Davidson N (1992) Cloning, expression and localization of a rat brain high-affinity glycine transporter. Proc Natl Acad Sci USA 89:7189–7193

Hamilton NB, Attwell D (2010) Do astrocytes really exocytose neurotransmitters? Nat Rev Neurosci 11(4):227–238

Harvey RJ, Carta E, Pearce BR, Chung SK, Supplisson S, Rees MI, Harvey K (2008) A critical role for glycine transporters in hyperexcitability disorders. Front Mol Neurosci 1:1–6

Jursky F, Nelson N (1995) Localization of glycine neurotransmitter transporter (GLYT2) reveals correlation with the distribution of glycine receptor. J Neurochem 64:1026–1033

Jursky F, Nelson N (1996) Developmental expression of the glycine transporters GLYT1 and GLYT2 in mouse brain. J Neurochem 67(1):336–344

Jursky F, Tamura S, Tamura A, Mandiyan S, Nelson H, Nelson N (1994) Structure, function and brain localization of neurotransmitter transporters. J Exp Biol 196:283–295

Liu QR, Nelson H, Mandiyan S, López-Corcuera B, Nelson N (1992) Cloning and expression of a glycine transporter from mouse brain. FEBS Lett 305:110–114

Luccini E, Raiteri L (2007) Mechanisms of [$^3$H]glycine release from mouse spinal cord synaptosomes selectively labeled through GLYT2 transporters. J Neurochem 103:2439–2448

Martinez-Maza R, Poyatos I, López-Corcuera B, Núñez E, Giménez C, Zafra F, Aragón C (2001) The role of N-glycosylation in transport to the plasma membrane and sorting of the neuronal glycine transporter GLYT2. J Biol Chem 276:2168–2173

McCarthy KD, de Vellis J (1980) Preparation of separate astroglial and ligodendroglial cell cultures from rat cerebral tissue. J Cell Biol 85(3):890–902

Nagaraja TN, Brookes N (1996) Glutamine transport in mouse cerebral astrocytes. J Neurochem 66:1665–1674

Núñez E, López-Corcuera B, Vázquez J, Giménez C, Aragón C (2000) Differential effects of the tricyclic antidepressant amoxapine on glycine uptake mediated by the recombinant GLYT1 and GLYT2 glycine transporters. Br J Pharmacol 129(1):200–206

Olivares L, Aragón C, Giménez C, Zafra F (1995) The role of *N*-glycosylation in the targeting and activity of the GLYT1 glycine transporter. J Biol Chem 270:9437–9442

Paxinos G, Watson C (1998) The rat brain in stereotaxic coordinates, 4th edn. Academic Press, San Diego

Perea G, Navarrete M, Araque A (2009) Tripartite synapses: astrocytes process and control synaptic information. Trends Neurosci 32(8):421–431

Peterson GL (1979) Review of the folin phenol protein quantitation method of Lowry, Rosebrough, Farr and Randall. Anal Biochem 100:201–220

Pfaffl MW (2001) A new mathematical model for relative quantification in real-time RT-PCR. Nucleic Acids Res 29(9): 2002–2007

Raiteri L, Stigliani S, Usai C, Diaspro A, Paluzzi S, Milanese M, Raiteri M, Bonanno G (2008) Functional expression of release-regulating glycine transporters GLYT1 on GABAergic neurons and GLYT2 on astrocytes in mouse spinal cord. Neurochem Int 52:103–112

Rees MI, Harvey K, Pearce BR, Chung SK, Duguid IC, Thomas P, Beatty S, Graham GE, Armstrong L, Shiang R, Abbott KJ, Zuberi SM, Stephenson JBP, Owen MJ, Tijssen MAJ, van den Maagdenberg AMJM, Smart TG, Supplisson S, Harvey RJ (2006) Mutations in the gene encodingGlyT2 (SLC6A5) define a presynaptic component of human startle disease. Nat Genet 38:801–806

Rousseau F, Aubrey KR, Supplisson S (2008) The glycine transporter GlyT2 controls the dynamics of synaptic vesicle refilling in inhibitory spinal cord neurons. J Neurosci 28:9755–9768

Schnell SA, Staines WA, Wessendorf MW (1999) Reduction of lipofuscin-like autofluorescence in fluorescently labeled tissue. J Histochem Cytochem 47:719–730

Su TZ, Lunney E, Cambell G, Oxender DL (1995) Transport of gabapentin, a gamma-amino acid drug, by system L alpha amino acid transporters: a comparative study in astrocytes, synaptosomes and CHO cells. J Neurochem 64:2125–2131

Supplisson S, Bergman C (1997) Control of NMDA receptor activation by a glycine transporter co-expressed in xenopus oocytes. J Neurosci 17:4580–4590

Tunnicliff G (2003) Membrane glycine transport proteins. J Biomed Sci 10:30–36

Vargas-Medrano J, Castrejon-Tellez V, Plenge F, Ramirez I, Miranda M (2011) PKCβ-dependent phosphorylation of the glycine transporter 1. Neurochem Int 59(8):1123–1132

Vaz SH, Jørgensen TN, Cristóvão-Ferreira S, Duflot S, Ribeiro JA, Gether U, Sebastião AM (2011) Brain-derived neurotrophic factor (BDNF) enhances GABA transport by modulating the trafficking of GABA transporter-1 (GAT-1) from the plasma membrane of rat cortical astrocytes. J Biol Chem 286(47): 40464–40476

Weiss MD, Derazi S, Kilberg MS, Anderson KJ (2001) Ontogeny and localization of the neutral amino acid transporter ASCT1 in rat brain. Brain Res Dev Brain Res 130:183–190

Wu ZL, O'Kane TM, Connors TJ, Marina MJ, Schaffhauser H (2008) The phosphatidylinositol 3- kinase inhibitor LY 294002 inhibits GlyT1-mediated glycine uptake. Brain Res 1227:42–51

Yee BK, Balic E, Singer P, Schwerdel C, Grampp T, Gabernet L, Knuesel I, Benke D, Feldon J, Mohler H, Boison D (2006) Disruption of glycine transporter 1 restricted to forebrain neuron is associated with a procognitive and antipsychotic phenotypic profile. J Neurosci 26(12):3169–3181

Zafra F, Aragón C, Olivares L, Danbolt NC, Giménez C, Storm-Mathisen J (1995) Glycine transporters are differentially expressed among CNS cells. J Neurosci 15:3952–3969